

---

The *Lotus japonicus*  
Temperature-Sensitive  
Root Development and Nodulation Mutant  
*brush*

Dissertation  
der Fakultät für Biologie der  
Ludwig-Maximilians-Universität München

vorgelegt von  
Kristina Haage  
am 16. Mai 2012

---

Dissertation eingereicht am: 16. Mai 2012

Tag der mündlichen Prüfung: 20. Juli 2012

1. Gutachter: Prof. Dr. Martin Parniske

2. Gutachter: Prof. Dr. Arthur Schüßler

---

### **Eidesstattliche Versicherung**

Ich versichere hiermit an Eides statt, dass die vorliegende Dissertation von mir selbständig und ohne unerlaubte Hilfe angefertigt ist.

### **Erklärung**

Hiermit erkläre ich, dass die Dissertation nicht ganz oder in wesentlichen Teilen einer anderen Prüfungskommission vorgelegt worden ist. Ich habe nicht versucht, anderweitig eine Dissertation einzureichen oder mich einer Doktorprüfung zu unterziehen.

---

*Für meine Eltern*

**TABLE OF CONTENTS**

<b>1</b>	<b>Introduction.....</b>	<b>1</b>
1.1	The Arbuscular Mycorrhiza .....	1
1.2	The Root Nodule Symbiosis.....	5
1.3	The Common Symbiosis (SYM) Pathway.....	6
1.4	Calcium in Arbuscular Mycorrhiza and Root Nodule Symbiosis Signalling .	8
<b>2</b>	<b>Results.....</b>	<b>10</b>
2.1	A Forward Genetic Screen for Mutants Impaired in Arbuscular Mycorrhiza Development.....	10
2.1.1	The AM Screen .....	11
2.1.2	Putative AM Mutants Impaired in Different Steps during AM .....	12
2.1.3	SL2042-N .....	16
2.1.4	SL1856-N .....	16
2.1.5	SL1755-N .....	17
2.2	The Calcium-Dependent Protein Kinase (CPK) 29 .....	18
2.2.1	CPK29 of <i>Lotus japonicus</i> .....	19
2.2.1.1	Gene Structure of Lj CPK29.....	19
2.2.1.2	Expression Patterns of Lj CPK29a and Lj CPK29b in Roots and Nodules .....	22
2.2.1.3	Subcellular Localization of Lj CPK29a and Lj CPK29b .....	23
2.2.2	CPK29 of <i>Medicago truncatula</i> .....	24
2.2.2.1	<i>M. truncatula</i> CPK29 Gene Structure.....	24
2.2.2.2	<i>Tnt1</i> Insertion Lines of Mt CPK29 .....	25
2.2.3	Phylogeny of CPK29 Homologs.....	25
2.3	The Temperature-Sensitive Nodulation and Root Development Mutant <i>brush</i> .....	31
2.3.1	Phenotypic Characterization of <i>brush</i> Mutants .....	33
2.3.1.1	Temperature Shifts at Early Developmental Stages .....	33
2.3.1.2	Temperature Shift Two Weeks after Germination.....	36
2.3.1.3	Temperature Shift Six Weeks after Germination.....	38
2.3.2	Map-Based Cloning of <i>brush</i> .....	40
2.3.2.1	Screening for Recombinants .....	40
2.3.2.2	Phenotypes and Genotypes of F4 and F5 Progenies .....	43
2.3.3	<i>brush</i> Backcross Mutants Resemble <i>brush</i> Mutants .....	47
2.3.4	Cyclic Nucleotide-Gated Channel 1 of <i>Lotus japonicus</i> .....	51
2.3.4.1	EMS-Induced Mutation in CNGC1 .....	51
2.3.4.2	Complementation of <i>brush</i> with CNGC1 .....	51
2.3.4.3	TILLING Mutants of CNGC1 .....	54
2.3.4.4	ProCNGC1-GUS Analysis.....	56

---

TABLE OF CONTENTS

2.3.4.5 The CNGC Gene Cluster .....	56
2.3.4.6 Phylogenetic Relationships of CNGCs of <i>L. japonicus</i> , <i>M. truncatula</i> and <i>A. thaliana</i> .....	58
<b>3 Discussion.....</b>	<b>60</b>
3.1.1 A Forward Genetic Screen for Mutants Impaired in Arbuscular Mycorrhiza Development .....	60
3.1.2 The Calcium-Dependent Protein Kinase 29 of <i>Lotus japonicus</i> .....	62
3.1.3 The <i>Lotus japonicus</i> Mutant <i>brush</i> .....	67
<b>4 Summary .....</b>	<b>72</b>
<b>5 Materials and Methods .....</b>	<b>73</b>
<b>5.1 Materials.....</b>	<b>73</b>
5.1.1 Plant Material, Fungal and Rhizobial Strains .....	73
5.1.2 Oligonucleotides.....	73
5.1.3 Media and Solutions.....	73
5.1.3.1 Plant Cultivation Media .....	73
5.1.3.1.1 FP-Medium .....	73
5.1.3.1.2 B5-Medium .....	74
5.1.3.2 Media for Bacteria Cultivation .....	74
5.1.3.2.1 LB-Medium .....	74
5.1.3.2.2 TY-Medium .....	74
5.1.3.3 GUS Staining Buffer.....	75
5.1.3.4 RNA Extraction Buffer .....	75
5.1.3.5 Buffers for DNA Extraction .....	75
5.1.3.5.1 DNA Extraction Buffer .....	75
5.1.3.5.2 HB Buffer .....	76
5.1.3.5.3 Wash Buffer .....	76
5.1.3.5.4 CTAB Buffer .....	76
5.1.3.6 DNA Storage Buffer .....	76
<b>5.2 Methods.....</b>	<b>77</b>
5.2.1 Plant Cultivation and Crossings .....	77
5.2.2 AM Inoculation and Staining .....	77
5.2.3 Inoculation with Rhizobia .....	77
5.2.4 GUS-Staining .....	77
5.2.5 Temperature-Shift Experiments .....	78
5.2.5.1 Temperature-Shift Two and Four Days post Germination .....	78
5.2.5.2 Temperature-shift Two Weeks post Germination.....	78
5.2.5.3 Temperature-Shift Six Weeks post Germination.....	78
5.2.6 <i>Lotus japonicus</i> Hairy-Root Transformation.....	78

---

---

TABLE OF CONTENTS

5.2.7 Transient Transformation of <i>N. benthamiana</i> Leaves .....	79
5.2.8 DNA Extraction from Plant Leaves.....	79
5.2.8.1 Small-Scale DNA Extraction .....	79
5.2.8.2 Large-Scale DNA Extraction .....	79
5.2.8.3 Isolation of Nuclear DNA from Plant Leaves.....	80
5.2.9 RNA Extraction.....	80
5.2.10 Nucleic Acid Quantification .....	81
5.2.11 cDNA Synthesis .....	81
5.2.12 Polymerase Chain Reactions.....	81
5.2.12.1 Standard and High-Fidelity PCRs .....	81
5.2.12.2 5'- and 3'-RACEs .....	81
5.2.13 Standardized Gene Mapping and SSR Marker Analysis .....	81
5.2.14 dCAPS Marker Analysis.....	82
5.2.15 SNP Analysis by KASP Assays .....	82
5.2.16 DNA Extraction from Agarose Gels.....	82
5.2.17 Clean-Up of PCR Reactions .....	82
5.2.18 Sequencing .....	83
5.2.19 Cloning .....	83
5.2.20 Plasmid DNA Purification .....	83
5.2.21 Bioinformatics.....	83
5.2.21.1 Databases .....	84
5.2.21.2 Phylogenetic Analyses .....	84
5.2.22 Microscopy .....	84
5.2.23 Statistics .....	84
<b>6 Supplementary Tables .....</b>	<b>86</b>
<b>7 References .....</b>	<b>90</b>
<b>8 Abbreviations.....</b>	<b>107</b>
<b>9 Appendix .....</b>	<b>109</b>
9.1 Sequence Information of Genes Annotated in This Study.....	109
9.1.1 CPK Sequences.....	109
9.1.2 CNGC Sequences.....	114
9.2 List of Figures.....	125
9.3 List of Tables .....	126
<b>Acknowledgements.....</b>	<b>127</b>
<b>Curriculum Vitae.....</b>	<b>128</b>

# 1 Introduction

The term symbiosis originates from the Greek meaning ‘living together’, which was coined by Albert Bernhard Frank and Anton de Bary in the second half of the 19<sup>th</sup> century (Wilkinson, 2001; Smith and Read, 2008). Thereafter according to its basic meaning, symbiosis was used to describe the close non-transient physical contact between two organisms, ranging from pathogenic to mutualistic interactions (Smith and Read, 2008). This study focuses on the investigation of genetic components involved in the development of two mutualistic plant root endosymbioses, namely arbuscular mycorrhiza (AM) and root nodule symbiosis (RNS).

## 1.1 The Arbuscular Mycorrhiza

The discovery that tree roots associate with fungal hyphae prompted A. B. Frank to invent the term mycorrhiza from the Greek meaning fungus-root (Frank, 1885; Frank and Trappe, 2005). The Ectomycorrhiza is characterized by an extraradical hyphal mantle and an intraradical but intercellular Hartig net (Trappe, 2005). In contrast, the arbuscular mycorrhiza is an example for an endosymbiosis, established between AM fungi, which belong to the monophyletic phylum *Glomeromycota*, and the majority of vascular land plants (Schüßler et al., 2001; Smith and Read, 2008). 400 million year-old fossils of land plants already show clear traces of arbuscules, indicating a close association with, and perhaps a mechanistic link between, AM and the colonization of the land by plants (Remy et al., 1994; Redecker et al., 2000). AM fungi are obligate biotrophs and rely on carbon obtained from their photosynthetic partner (Schüßler et al., 2001). In return plants in general benefit from an enhanced phosphate and nitrogen supply and an increased resistance to pathogens and abiotic stresses (Balestrini et al., 1992; Newsham et al., 1995; Smith et al., 2003; Govindarajulu et al., 2005; Liu et al., 2007). Furthermore, AM fungal diversity has a positive impact on plant biodiversity and ecosystem productivity (van der Heijden et al., 1998).

### Arbuscular Mycorrhiza Development

Before physical contact of the two symbiotic partners during the “presymbiotic phase” of AM development, two classes of signaling molecules, namely strigolactones and lipochitooligosaccharides, have recently been identified to play major roles (Xie and Yoneyama, 2010; Gough and Cullimore, 2011). Spores of AM fungi are able to germinate in absence of a host root, but hyphal growth is restricted and ceases after approximately one or two weeks, if AM could not be initiated (Koske, 1981; Bago et al., 2000). After a dormancy phase, the spores are able to germinate again (Bago et al., 2000). In the presence of host roots hyphae start to grow and branch intensively (Mosse and Hepper, 1975; Bécard and Piché, 1989; Giovannetti et al., 1993). Furthermore, if hyphae are treated with host root exudates their number of nuclei as well as their mitochondrial density and respiration is increased (Buee et al., 2000; Tamasloukht et al.,

## INTRODUCTION

---

2003). Interestingly, root exudates of non-host species do not affect fungal morphology (Giovannetti et al., 1993; Buee et al., 2000). So-called branching factors have been isolated from *Lotus japonicus* and *Sorghum* roots and identified as strigolactones (Figure 1; Akiyama et al., 2005; Besserer et al., 2006), which have already been shown to stimulate seed germination of parasitic plants, such as *Striga* or *Orobanche* species (Figure 1; Cook et al., 1966; Cook et al., 1972; Bouwmeester et al., 2003). Apparently, these root parasites take advantage of the plant's strigolactone production to locate potential host roots (Bouwmeester et al., 2007). Furthermore, strigolactones represent a new class of endogenous plant hormones, which is involved in shoot branching (Gomez-Roldan et al., 2008; Umehara et al., 2008). Interestingly, strigolactone-deficient pea mutants are unable to form AM (Gomez-Roldan et al., 2008).

AM fungi also exude signaling molecules (Myc factors) that are able to induce symbiosis-specific host gene expression (Figure 1; Chabaud et al., 2002; Kosuta et al., 2003). The Myc factors have recently been identified as sulfated and non-sulfated simple lipochitooligosaccharides (AMF LCOs) (Maillet et al., 2011). They have been isolated from the AM fungus *Glomus intraradices* (Maillet et al., 2011). Based on phylogenetic analysis using genetic markers, the AM model fungus *G. intraradices* DAOM197198 had to be reclassified and is now called *Rhizophagus irregularis* (Stockinger et al., 2009; Schüßler and Walker, 2010; Sokolski et al., 2010; Krüger et al., 2012).

A putative Myc factor receptor has been discovered in *Parasponia andersonii*, a non-legume belonging to the order of the Rosales, which is able to form nitrogen-fixing nodules after inoculation with rhizobia (Becking, 1979; Op den Camp et al., 2011). This putative ortholog of *NFP*, the Nod factor receptor of the legume *Medicago truncatula*, is called *PaNFP*, and appears to be essential for the intracellular accommodation of the endosymbiont during the development of RNS and AM (Op den Camp et al., 2011). Accordingly, it has been postulated that during the evolution of legumes a *NFP* precursor had been duplicated and one copy developed into a Nod factor receptor, whereas the other copy retained the ability to specifically recognize Myc factors (Op den Camp et al., 2011). This hypothesis is supported by the fact that Nod factors and the Myc factors identified by Maillet and associates (2011) are structurally similar. Already before hyphae contact the root, diffusible fungal molecules activate *MtMSBP1*, encoding a membrane-bound steroid-binding protein, at the anticipated entry sites of the plant root. RNAi of *MtMSBP1* in transgenic roots resulted in septated hyphae and collapsing arbuscules implicating *MtMSBP1* also in later stages of AM development (Kuhn et al., 2010).

Hyphae touching a host root are able to form a hyphopodium on the root surface (Figure 1; Harrison, 1999). Observing *M. truncatula* roots cells in contact with hyphae of *Gigaspora gigantea* or *Gi. rosea*, Genre and associates (2005) discovered the existence of a novel cytoskeleton and endoplasmatic reticulum-containing cytoplasmic bridge-like structure, the prepenetration apparatus (PPA). This work revealed that the epidermal cell underneath a hyphopodium prepares for intracellular accommodation of the fungus. First, its nucleus is repositioned underneath the hyphopodium contact site. From there, the PPA assembly follows the trans-cellular movement of the nucleus. Only after completion of the cytoplasmic bridge the hypha penetrates the cell and the PPA directs it towards the cortical cells. Hence, host roots are actively involved already during

## INTRODUCTION

---

this first step of AM infection (Figure 1; Genre et al., 2005). A fungal effector playing a role during AM formation was discovered by Kloppholz and associates (2011). The effector protein SP7 is secreted as assays in *Magnaporthe oryzae* indicated and it is localized in the plant nucleus (Figure 1). Expression of SP7 in transgenic roots enhanced AM colonization, whereas concomitantly the expression of the pathogen-induced *ERF19* transcription factor was reduced (Kloppholz et al., 2011). After penetration of the root, hyphae proceed to colonize the root cortex intercellularly (Harrison, 1999). There, several AM fungi form vesicles, which are suggested to be lipid storage organs (Smith and Gianinazzi-Pearson, 1988). In addition, hyphae enter cortical cells, where they form arbuscules (from Latin arbuscula, meaning small tree) by repeated dichotomous branching (Harrison, 1999). PPA-like cellular rearrangements are again preceding arbuscule development (Figure 1; Genre et al., 2008). A plant-derived peri-arbuscular membrane enfolds the arbuscules (Smith and Gianinazzi-Pearson, 1988). Arbuscules have long been proposed to represent the interface at which nutrient exchange between the symbiotic partners takes place and several molecular components corroborating this hypothesis have been identified during the last few years. In *M. truncatula*, the phosphate transporter MtPt4 is specifically expressed during AM and colocalizes with the periabruscular membrane (Harrison et al., 2002). Interestingly, phosphate import via MtPt4 seems to be essential for sustaining AM, since in *mtpt4* mutants showed a drastically shortened arbuscule lifespan and further proliferation of the hyphae in the mutant's root cortex ceased (Javot et al., 2007). It is therefore suggested that nutrient supply by arbuscules is monitored by the plant cell and arbuscules that do not deliver are penalized with premature senescence (Javot et al., 2007). Lyso-phosphatidylcholine extracted from roots inoculated with AM fungi was identified to be a signal molecule that induces the expression of mycorrhiza-specific phosphate transporter genes of potato and tomato (Drissner et al., 2007). Two half-ABC transporter genes in *Medicago* called *STR* and *STR2* have been discovered to be involved in arbuscule development, because *str* mutants and transgenic *STR2* RNAi roots inoculated with AM fungi exhibited stunted arbuscules (Zhang et al., 2010). The AM-specific subtilases *SbtM1* and *SbtM3* are also essential for AM development. Both subtilases carry a predicted signal peptide and, in transgenic roots, SbtM1 could be detected at the arbuscule and in the apoplast surrounding infected cells. Cleavage of a hypothetical substrate of these two subtilases present in the periarbuscular space may be important for proper arbuscule development (Takeda et al., 2009). Interestingly, SbtM1 colocalizes with PPA-like structures in roots inoculated with AM fungi (Takeda et al., 2012). The monosaccharide transporter2 (MST2) of *G. intraradices* could be localized to arbuscules and intraradical hyphae, suggesting that carbon uptake by the AM fungi is not only occurring via the arbuscule interface. Furthermore, the expression of *MST2* is closely correlated to that of *MtPT4* and therefore supports a link between carbon and phosphate homeostasis. Host-induced gene silencing of *MST2* resulted in a general reduction of AM colonization and malformed arbuscules. Therefore, MST2 is important for successful AM functioning (Helber et al., 2011).

In summary, several major scientific breakthroughs have been reported recently that contribute to the elucidation of the complex and fine-tuned developmental process of the AM.

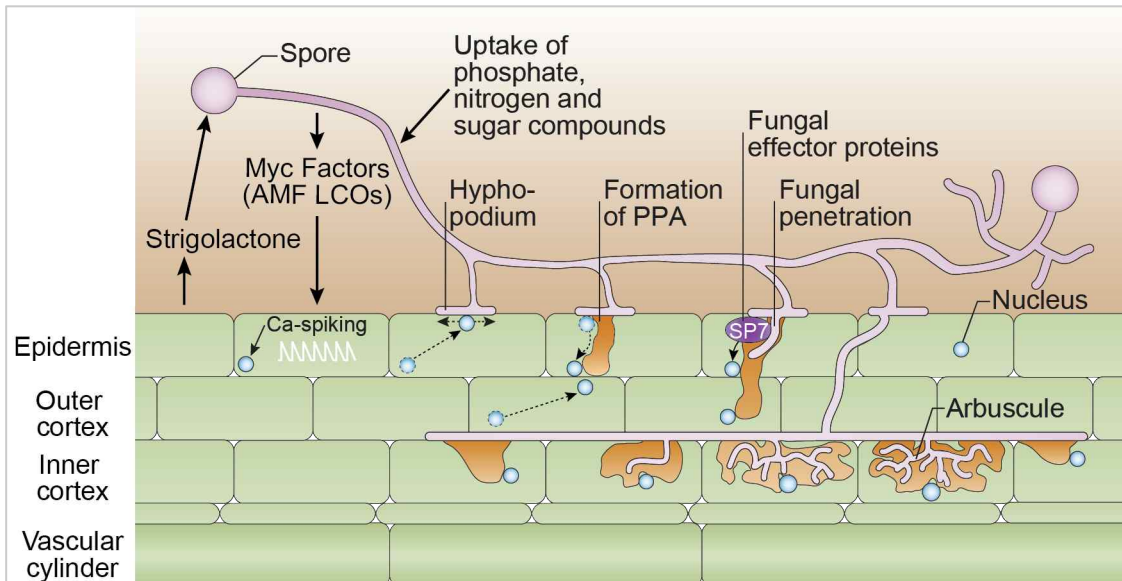


**Figure 1. AM development.**

AM fungi are able to take up phosphate by phosphate transporters in the extraradical mycelium (Harrison and van Buuren, 1995; Maldonado-Mendoza et al., 2001), nitrogen (Hodge et al., 2001; Govindarajulu et al., 2005; Lopez-Pedrosa et al., 2006) and sugar (Helber et al., 2011) compounds from the soil and deliver them to the plant. In turn the plant supplies the fungus with carbohydrates (Bago et al., 2003). Plant root exudates contain strigolactones, which promote on the one hand seed germination of parasitic plants (e. g. *Striga*), on the other hand germination of AM fungal spores and hyphal branching (Cook et al., 1966; Akiyama et al., 2005; Besserer et al., 2006). AM fungi produce lipochitooligosaccharides (AMF LCOs), Myc factors, that are recognized by the plant root (Maillet et al., 2011; Op den Camp et al., 2011). On the root surface, the hypha forms a hyphopodium and perinuclear calcium (Ca) spiking is induced in epidermal cells (Sieberer et al., 2012). The nucleus of the cell underneath moves first towards the site of the hyphopodium before it guides the formation of the prepenetration apparatus (PPA) through the cell (Genre et al., 2005; Genre et al., 2008). The hypha penetrates the cell through the PPA and colonizes the root cortex intercellularly. The fungal effector protein SP7 is secreted by *R. irregularis*, localizes to the plant nucleus and interferes with plant gene expression (Klopholz et al., 2011). Arbuscules are formed in cortical cells by repeated dichotomous branching of the hyphae, again preceded by the formation of a PPA-like structure (Genre et al., 2008). The generation of new spores is completing the AM fungus' life cycle. Figure modified from Parniske, 2008.

## 1.2 The Root Nodule Symbiosis

Although almost 80% of the earth's atmosphere consists of nitrogen gas ( $N_2$ ), it is one of the limiting factors of plant growth due to its unavailability (Vance, 2001; Galloway and Cowling, 2002). Only certain microorganisms are able to fix atmospheric nitrogen, that is to cleave the triple bond within the paired nitrogen molecules and convert them into biologically active compounds (Smil, 1997). Among these microorganisms are nitrogen-fixing bacteria that together with host plants establish the RNS. Thereby, a new plant root organ, the nodule, with intracellularly accommodated microsymbionts develops (Brewin, 1991). Host plants benefit from the fixed nitrogen supply by the bacteria, which in turn receive carbohydrates (Udvardi and Day, 1997). Two types of RNS can be distinguished; the phylogenetically more widespread actinorhiza between actinobacteria of the genus *Frankia* and estimated 200 plant species of the Fagales, Cucurbitales and Rosales (Torrey, 1978; Swensen, 1996), and the symbiosis with rhizobia, restricted to the legumes (Leguminosae or Fabaceae), with the exception of the non-legume *Parasponia* (Ulmaceae) (Becking, 1979; Young and Johnston, 1989). All nodulating plant species are members of four orders (Fabales, Fagales, Cucurbitales and Rosales) within the Eurosid I, the so-called nodulating clade, which has led to the idea that a genetic event occurred in the common ancestor that led to a predisposition to evolve nodulation in this clade (Doyle, 2011). The origin of legumes dates back to approximately 60 million years (Lavin et al., 2005; Sprent, 2007). Thus, RNS evolved much more recently than the ancient AM (Kistner and Parniske, 2002). Several important crop plants are legumes, such as soybean (*Glycine max*), common bean (*Phaseolus vulgaris*) and pea (*Pisum sativum*) (Sprent, 2007).

### Development of Root Nodule Symbiosis

The development of RNS is a highly specific process. Flavonoids exuded by legume roots are recognized by rhizobia and rhizobial *nod*(ulation) genes are induced (Peters et al., 1986; Redmond et al., 1986). These *nod* genes encode proteins that are responsible for the synthesis of Nod factors (NFs) (Fisher and Long, 1992). These NFs are 1-4 $\beta$  N-acetyl glucosamines with a long acyl chain attached to a glucosamine (Lerouge et al., 1990; Long, 1996). Different rhizobial species produce distinct NF structures and are responsible for the host-specificity (Lerouge et al., 1990; Fisher and Long, 1992; Perret et al., 2000). Putative LysM-domain containing NF receptor kinases, NFR1 and NFR5 in *Lotus* (Madsen et al., 2003; Radutoiu et al., 2003) and NFP and LYK3 in *Medicago* (Ben Amor et al., 2003; Limpens et al., 2003), are supposed to perceive the NFs and initiate downstream signaling responses. NFs induce root hair curling, where rhizobia are entrapped in a so-called infection pocket (Esseling et al., 2003; Geurts et al., 2005). From this infection pocket an infection thread containing rhizobia is growing towards the nodule primordium (Nutman, 1959; Gage et al., 1996). The infection thread is a bridge-like structure of plant cell wall and plasma membrane and the nucleus is guiding its tip (Nutman, 1959). After the infection thread has crossed the root hair cell, a pre-infection thread is formed by the adjacent cortical cell

and again the nucleus of this cell moves towards the growing tip of the infection thread (Timmers et al., 1999). Concomitantly, cortical cells close to the infection thread start to dedifferentiate and proliferate, forming a nodule primordium (Timmers et al., 1999; Crespi and Frugier, 2008).

When the infection thread has reached the nodule primordium, rhizobia are released and are endocytosed by cells of the nodule primordium. They differentiate into bacteroids enfolded by the peribacteroid membrane and these organelle-like structures are then called symbiosomes (Verma, 1992; Brewin, 2004). There are two types of nodules regarding their morphology. In spherical determinate nodules, the meristematic activity of nodule cells ceases. In contrast, elongated indeterminate nodules are characterized by a persistent apical meristem (Gibson et al., 2008). Legumes forming determinate nodules are for example *Lotus* and soybean, whereas *Medicago* and pea, for example, develop indeterminate nodules (Franssen et al., 1992; Gibson et al., 2008). Inside the bacteroids, oxygen sensitive nitrogenases catalyze the biological reduction of dinitrogen to ammonia, which is allocated to the plant in exchange for photosynthates (Dixon and Kahn, 2004). Since nitrogenases are very oxygen sensitive, leghaemoglobin with a high affinity to oxygen is present in cells containing bacteroids and reduces the concentration of free oxygen (Appleby, 1984). Leghaemoglobin is also responsible for the red color of fully developed, nitrogen-fixing nodules (Downie, 2005).

### 1.3 The Common Symbiosis (SYM) Pathway

The analysis of mutants of several legume species, such as pea (*Pisum sativum*), alfalfa (*Medicago sativa*), common bean (*Phaseolus vulgaris*), *M. truncatula* and *L. japonicus*, revealed a class of mutants that were impaired in RNS as well as AM development (Duc et al., 1989; Bradbury et al., 1991; Shirtliffe and Vessey, 1996; Wegel et al., 1998; Catoira et al., 2000). Hence, these two endosymbioses share common genetic mechanisms. Since the origin of AM (more than 400 million years ago) preceded that of the predisposition event (100 million years ago; Doyle, 2011), it is proposed that the evolutionary younger RNS recruited components of the AM signaling pathway, represented by the common SYM pathway (Kistner and Parniske, 2002). Up to date nine common SYM genes have been reported in *L. japonicus* and *M. truncatula*, whose mutant plants are characterized by defects in AM and RNS (Parniske, 2008; Charpentier and Oldroyd, 2010). These include the receptor-like kinase SYMRK/DMI2 (Endre et al., 2002; Stracke et al., 2002), three nucleoporins *NUP85*, *NUP133* and *NENA* (Kanamori et al., 2006; Saito et al., 2007; Groth et al., 2010), two cation channels *CASTOR* and *POLLUX/DMI1* (Ané et al., 2004; Imaizumi-Anraku et al., 2005; Charpentier et al., 2008), the calcium and calmodulin dependent kinase CCaMK/DMI3 (Lévy et al., 2004; Mitra et al., 2004; Tirichine et al., 2006), the nuclear localized gene *CYCLOPS/IPD3* (Messinese et al., 2007; Yano et al., 2008) and *VAPYRIN/PAM1* (Feddermann et al., 2010; Pumplin et al., 2010; Murray et al., 2011).

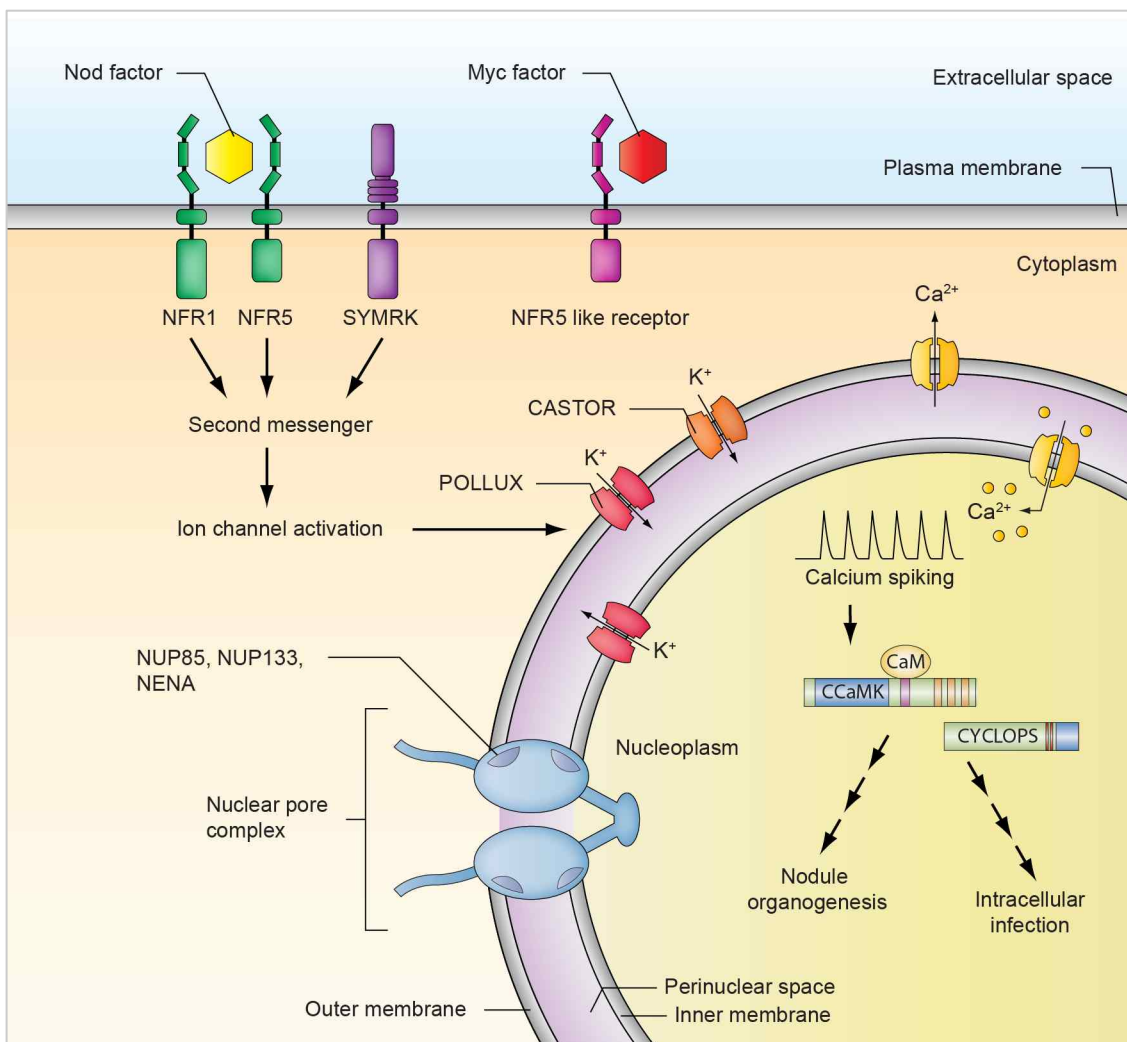


**Figure 2. Common SYM signalling pathway.**

The illustrated eight common SYM components represent the genetic overlap of AM and RNS signalling. In the case of RNS, nod factors produced by rhizobia are perceived by the receptor-like kinases NFR1 and NFR5 (Madsen et al., 2003; Radutoiu et al., 2003). AM fungi exude so-called Myc factors and it is suggested that these can be sensed by an NFR5-like receptor (Maillet et al., 2011; Op den Camp et al., 2011). The receptor-like kinase SYMRK is also localized at the plasma membrane (Stracke et al., 2002; Den Herder et al., 2012). Signal transduction from the plasma membrane to the activation of symbiosis-specific ion channels is presently unclear. The potassium-conducting ion channels CASTOR and POLLUX, which reside in the nuclear envelope, are suggested to initiate or to counterbalance the flow of calcium (Ca<sup>2+</sup>) ions through yet to be identified calcium channels in the nuclear envelope (Riely et al., 2007; Charpentier et al., 2008). The three nucleoporins NUP85, NUP133 and NENA, parts of the nucleopore complex, are also essential for the Ca<sup>2+</sup> spiking (Kanamori et al., 2006; Saito et al., 2007; Groth et al., 2010). The nuclear-localized calcium- and calmodulin-dependent kinase CCaMK is thought to perceive these rhythmic Ca<sup>2+</sup> oscillations and is able to interact with and to phosphorylate CYCLOPS. CCaMK is suggested to transduce the Ca<sup>2+</sup> spiking into activation of downstream responses that lead to nodule organogenesis and intracellular infection during AM (Tirichine et al., 2006; Yano et al., 2008). Figure modified from Parniske, 2008.

## 1.4 Calcium in Arbuscular Mycorrhiza and Root Nodule Symbiosis Signalling

Calcium ions ( $\text{Ca}^{2+}$ ) are second messengers and important for many different signal-transduction pathways involved in stomatal aperture, abiotic stress response and plant-microbe interactions, for example (Dodd et al., 2010). Due to unique spatial and temporal characteristics of these various stimulus-depending  $\text{Ca}^{2+}$  transients or oscillations, which are referred to as  $\text{Ca}^{2+}$  signatures, the cell deciphers their intrinsic information and responds according to the initial incitement (McAinsh and Hetherington, 1998; Hetherington and Brownlee, 2004). In general, these  $\text{Ca}^{2+}$  signatures are produced by  $\text{Ca}^{2+}$ -permeable channels in the plasma membrane as well as second messenger-induced  $\text{Ca}^{2+}$  release from intracellular  $\text{Ca}^{2+}$  stores, such as the vacuole, mitochondria, chloroplasts and the endoplasmic reticulum (Sanders et al., 1999).

Nod factor- and AM fungi-induced  $\text{Ca}^{2+}$  signatures are associated with the development of functional RNS and AM, respectively (Parniske, 2008). A rapid early influx of  $\text{Ca}^{2+}$  into root hair cells of legumes occurs after Nod factor treatment (Felle et al., 1998; Cardenas et al., 1999; Shaw and Long, 2003; Miwa et al., 2006), followed by a perinuclear and nuclear  $\text{Ca}^{2+}$  spiking that is characterized by periodic waves of  $\text{Ca}^{2+}$  concentrations (Ehrhardt et al., 1996; Sieberer et al., 2009). Similarly, nuclear and cytosolic  $\text{Ca}^{2+}$  spiking can be measured in epidermal root cells of legumes and non-legumes induced either by close vicinity of AM hyphae, by hyphopodium formation or by germinated spore exudates (Kosuta et al., 2008; Chabaud et al., 2011). The common *SYM* mutants *symrk/dmi2*, *castor*, *pollux/dmi1*, *nup85*, *nup133* are impaired in  $\text{Ca}^{2+}$  spiking, but the early  $\text{Ca}^{2+}$  flux still occurs (Shaw and Long, 2003; Miwa et al., 2006; Kosuta et al., 2008). Plants that carry mutations in *NFR1* or *NFR5* lack both  $\text{Ca}^{2+}$  responses (Miwa et al., 2006).

Several components important for  $\text{Ca}^{2+}$  spiking have been identified; the potassium-conducting ion channels CASTOR and POLLUX/DMI1 and the three nucleoporins NUP85, NUP133 and NENA (Figure 2; Kanamori et al., 2006; Riely et al., 2007; Saito et al., 2007; Charpentier et al., 2008; Groth et al., 2010). The SERCA-type  $\text{Ca}^{2+}$  ATPase MCA8 is believed to be involved in replenishing the  $\text{Ca}^{2+}$  store after each spike (Capoen et al., 2011). Nod factor- and AM fungi-induced  $\text{Ca}^{2+}$  spiking differs in oscillation period and shape of the individual spikes, suggesting a potential mechanism by which downstream signalling components could be specifically activated (Kosuta et al., 2008). Sieberer and associates (2012) were able to visualize  $\text{Ca}^{2+}$  spiking in nuclei of cortical root cells that are penetrated either by a hypha or an infection thread and, in contrast to the differential presymbiotic  $\text{Ca}^{2+}$  spiking, these  $\text{Ca}^{2+}$  signatures are similar regarding periodicity. Concomitant with the entry of the microsymbionts into cortical root cells, the  $\text{Ca}^{2+}$  spiking frequency is increased (Sieberer et al., 2012). These findings reveal striking similarities between the  $\text{Ca}^{2+}$  signatures during infection stages of AM and RNS formation.

A main signal integrator of the common symbiosis pathway is the potential  $\text{Ca}^{2+}$  spiking deciphering CCaMK. Deregulated versions of CCaMK are sufficient to activate spontaneous nodules and spontaneous PPA formation indicating that CCaMK is upstream of all main symbiotic

## INTRODUCTION

---

responses of the root (Madsen et al., 2010; Takeda et al., 2012). Takeda and associates (2012) provide evidence that the PPA is a result of common symbiosis signaling, underlining the similarities between PPA and preinfection thread formation (Parniske, 2008) and the essential role of the active contribution of PPA formation for successful symbiosis.

Thus,  $\text{Ca}^{2+}$  signatures play a decisive role during AM and RNS development and the identification of genes involved in the generation and decoding of these patterns could provide further insights into the endosymbiotic signalling pathways.

## 2 Results

### 2.1 A Forward Genetic Screen for Mutants Impaired in Arbuscular Mycorrhiza Development

The vast majority of AM mutants identified mostly in legumes so far are also impaired in the development of RNS (Parniske, 2008). The evolutionary younger RNS has obviously recruited parts of the ancient AM signalling pathway and therefore this common SYM pathway represents the genetic overlap between these two endosymbioses (Kistner and Parniske, 2002). Despite the fact that the two symbioses share this signalling machinery, each of them has its unique characteristics and there are strong evidences for the existence of additional AM specific signalling components (Kistner and Parniske, 2002; Gutjahr et al., 2008; Takeda et al., 2011). The most striking difference is probably the fact that during RNS a new plant organ, the nodule, is formed to host the microsymbionts, whereas in AM cortical root cells accommodate arbuscules without further rearrangement of the root structure (Harrison, 1999; Crespi and Frugier, 2008). The formation of arbuscules implies a range of different cellular processes, for example membrane biosynthesis to form the peri-arbuscular membrane, repositioning of the nucleus close to the arbuscule and the formation of a PPA-like structure (Alexander et al., 1989; Balestrini et al., 1992; Genre et al., 2008). Although these processes require an array of genes involved, only few mutants with aberrant arbuscule development have been isolated so far. The *M. truncatula* mutant *str* (*stunted arbuscule*), for example, is characterised by poorly branched small arbuscules, yet it can form nodules (Zhang et al., 2010). In addition, three mutants in *L. japonicus*, *red*, *wrd* and *dis*, identified during the AM screen described in this study, are also impaired in arbuscule development, but not in RNS (S. Hardel and M. Groth, personal communication). Phosphate is one of the limiting factors of plant growth and is therefore applied as a major fertilizer in agriculture, but nevertheless phosphorus derived from phosphate rock is a non-renewable resource and it is estimated that it will be used up within the next 125 years (Cramer, 2010). Consequently, the fact that AM enhances plant's phosphate supply is becoming more and more important (Smith et al., 2011), and a detailed understanding of the molecular and cellular processes that are responsible for the establishment of a functional AM is in demand. The aim of this study was the isolation of *L. japonicus* mutants that were impaired in their interaction with the AM fungus *Rhizophagus irregularis*. Map-based cloning of the mutated genes causing the AM mutant phenotype and further characterisation of the encoded proteins should enlighten the signalling network involved in AM.

### 2.1.1 The AM Screen

An ethyl methanesulfonate (EMS)-mutagenized population of *L. japonicus* Gifu (Perry et al., 2003) was subjected to a forward genetic screen to identify mutants that show defects in AM but not in RNS development. EMS is an alkylating mutagen that induces transitions from G/C to A/T randomly spread throughout the genome (Greene et al., 2003). Based on the *Lotus* GENPOP TILLING data, a 1:10 ratio of homozygous versus heterozygous mutations is predicted in the M2 generation (Perry et al., 2009), whereas in comparable data sets of *Arabidopsis* a 2:1 ratio is observed (Greene et al., 2003). This could be explained by differences between the *Lotus* and *Arabidopsis* germlines (Perry et al., 2009). On average, one *Lotus* M2 plant carries 940 mutations thereof 10% are homozygous. These M2 individuals of the EMS population have already been screened for mutants with defects in plant development, nodulation or starch metabolism, representing the DEVPOP, NODPOP and STARPOP stocks (Perry et al., 2009; Figure 3). The remaining M2 individuals were grown for seed and harvested in bulk per family, meaning that seed of M2 plants belonging to the same family (SL line) was combined into one M3 seed bag (Perry et al., 2009). In total, 2131 M3 families were analysed in succession by Sonja Kosuta, Martin Groth and myself in nearly equal parts during the AM screen (Figure 3).

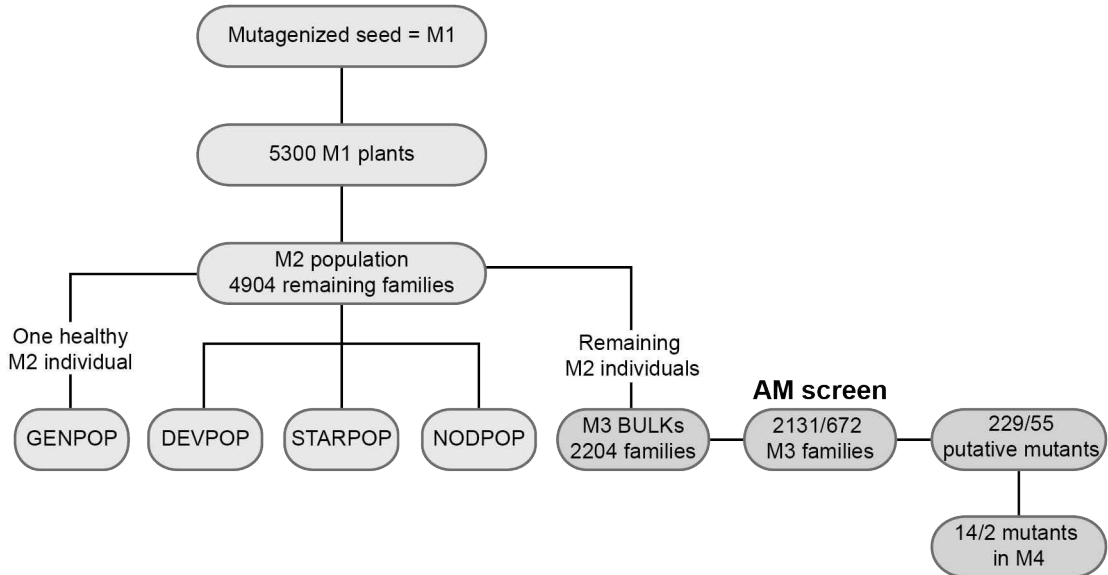


**Figure 3. Overview of *Lotus* TILLING populations and SL lines analyzed during the AM screen.**

DEVPOP, STARPOP and NODPOP consist of mutants identified during a developmental, starch and nodulation screen, respectively (Perry et al., 2009). 2131 M3 families were screened in the AM screen (672 by the author). Putative AM mutants in 229 M3 families were identified (55 by the author). AM mutant phenotypes of 14 SL lines were confirmed in the M4 generation, including two isolated by the author. Figure modified from Perry et al., 2009.

M3 seedlings were inoculated by planting them into chive nurse pots and after four weeks the root systems of eight plants per SL line were harvested, ink-stained and phenotyped. Consequently, AM structures of approximately 17,000 M3 individuals were inspected with regard

to aberrant infection sites, intraradical colonization and arbuscule formation (Figure 4). During my part of the AM screen, I have screened 672 SL lines, thereof 471 lines formed AM structures comparable to those of wild-type roots. Analysed plants of further 146 families showed an unclear or weak phenotype. Putative AM mutants were detected in 55 M3 lines (Figure 3; Figure 5). The progenies of several putative mutants were then rescreened in the M4 generation (Table 1) and the AM mutant phenotype of two families, SL1755-N and SL2042-N, could be confirmed (Figure 3; Figure 6D, E, G - I). For the sake of completeness, the final numbers of the AM screen are included in Figure 3.

### 2.1.2 Putative AM Mutants Impaired in Different Steps during AM

AM development can be outlined as a sequence of (1) penetration and (2) colonization of the root by hyphae as well as (3) arbuscule formation (Figure 4; Parniske, 2004). The 55 SL lines containing putative AM mutants were divided into three phenotypic categories, depending on the stage when AM structures appeared to be different from the wild type (Figure 5, Table 1). Many putative mutants could not be assigned clearly to only one category, most of them showed aberrant AM structures at more than one developmental step (Figure 5, Table 1).

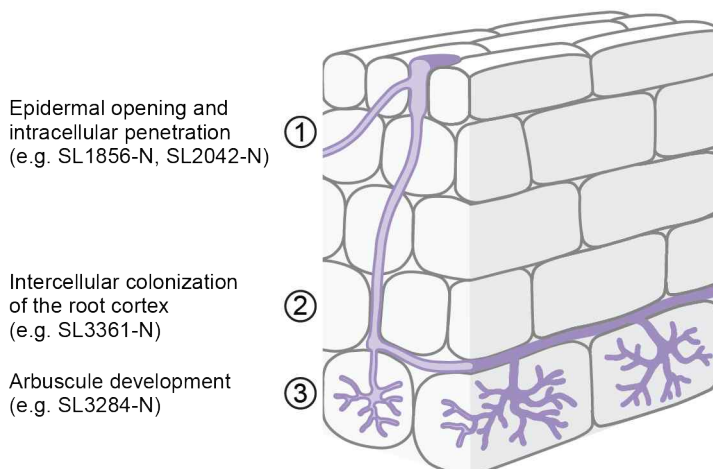


**Figure 4. Schematic overview of AM development.**

(1) The fungal hypha (purple) forms a hyphopodium on the root surface, grows between the epidermal cells below and penetrates the adjacent epi- or exodermal cells. After this intracellular passage, (2) hyphae are spreading intercellularly in the cortical tissue, (3) where they grow into cells and develop highly branched arbuscules. SL lines isolated during the AM screen with defects in AM formation are shown at the respective stages. Figure modified from Parniske, 2004.

In the beginning of AM development, when hypha and root are in contact and the hypha forms a hyphopodium on the root surface, it passes intracellularly an epi- and/or exodermal cell guided by the prepenetration apparatus (Genre et al., 2005; Genre et al., 2008). At an infection site of a wild-type root, the hypha is able to enter the roots without remarkable changes of its morphology (Figure 6C). In contrast, plants impaired in this first step exhibit straying hyphae on the root surface and so-called hyphal balloon-like swellings without any cortical colonization (Kistner et al., 2005), the typical common SYM mutant phenotype (Kistner and Parniske, 2002). Mutant roots of SL2042-N and SL1856-N (isolated by M. Groth) had these characteristics. The fungus was not

## RESULTS

---

able to colonize the mutants' roots (Figure 6D - F). Hyphae were growing only on the root surface instead (Figure 6D) and formed balloon-like swellings (Figure 6E and F, arrowheads). The aberrant infection sites presented by mutants of SL1915-N differed from those of common SYM mutants. Hyphae accumulated on the root surface without being able to enter the root (Figure 6J), but other parts of the roots showed wild-type AM structures (data not shown).

The next phase in the series of AM formation is the spreading of hyphae in the apoplastic space between cortical cells (Figure 4; Parniske, 2004). This step resulted in an equal colonization of the root system (Figure 6A). Mutants with defects in this step have been observed in SL1755-N and SL3361-N, for example. Further growth of hyphae expanding from several infection sites was hampered in SL1755-N mutants (Figure 6G - I), but they had also root stretches with wild-type AM structures (data not shown). Roots of SL3361-N mutants exhibited a patchy AM colonization pattern. Even spreading of hyphae in the mutant's root cortex appeared to be impossible at some stretches, whereas other parts of the root system were not distinguishable from the wild-type (Figure 6K).

While the root system is colonized, hyphae enter cortical cells where they form arbuscules by repeated branching (Figure 4, Figure 6A and B, arrows). Roots of mutants found in SL3284-N were devoid of wild-type-like arbuscules, instead only short branches without further ramifications developed (Figure 6L, arrow). In SL1755-N mutant roots, arbuscules were not formed next to their aberrant infection sites, whereas vesicles could be detected (Figure 6H).

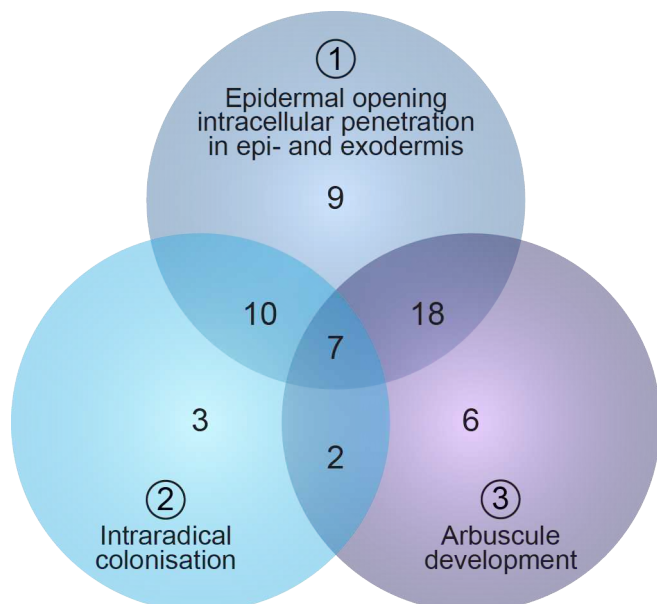


**Figure 5. Venn diagram illustrating quantities of putative AM mutant lines.**

The putative mutant lines isolated during the AM screen were subdivided into three phenotypic categories according to the impaired developmental stage of AM formation. Various mutants had defects in more than one step during AM formation. Detailed mutant phenotypes are described in Table 1.

## RESULTS

SL line	AM Phenotypes of M3 Plants	Impaired stage <sup>A</sup>	MG-20 x	M3 <sup>B</sup>	M4 wt <sup>C</sup>	M4 mut <sup>D</sup>
SL1608-N	infection sites with swollen hyphae, few, small arbuscules	1, 3		3	2	
SL1612-N	infection sites with swollen hyphae, no wt-like arbuscules	1, 3		1	1	
SL1615-N	few infection sites with swollen hyphae, only few arbuscules	1, 3		5	2	
SL1627-N	few infection sites with swollen hyphae, only few arbuscules	1, 3		4	3	
SL1660-N	very few wt-like arbuscules	3		2		
SL1674-N	some infection sites with swollen hyphae, many hyphae outside root, many degenerated arbuscules	1, 3		3	3	
SL1676-N	some aborted infection sites, some with swollen hyphae, many hyphae outside the roots, only few wt-like arbuscules	1, 3		4	3	
SL1694-N	aborted infection sites, but cortical colonization, very few wt-like arbuscules	1, 3		4	1	
SL1702-N	some aborted infection sites	1		1		
SL1705-N	some aborted infection sites, very few arbuscules	1, 3		4	3	
SL1708-N	some aborted infection sites, poorly colonized, few arbuscules	1, 2, 3		5	3	
SL1709-N	some lateral roots not colonized showing aborted infection sites, few arbuscules	1, 3	Y	4	2	
SL1710-N	abnormal infection sites with swollen hyphae, but cortical colonization	1	Y	5	3	
SL1711-N	some abnormal infection sites, hyphae grow very close to root tips	1, 2		4	1	
SL1714-N	some abnormal infection sites, only few arbuscules	1, 3		4	4	
SL1743-N	some abnormal, aborted infection sites, very few arbuscules	1, 3		4		
SL1747-N	aborted, abnormal infection sites, few arbuscules, but parts of the roots wt-like	1, 3		4		
SL1751-N	aborted infection sites with swollen hyphae	1		1	1	
<b>SL1755-N</b>	infection sites, where hyphae are growing into the cortex but further spreading and arbuscule formation is blocked there, many infection sites close to each other, lateral roots almost wt-like	2, 3	Y	4	1	2
SL1759-N	aborted and abnormal infection sites, weakly colonized, few arbuscules	1, 2, 3		2	1	
SL1769-N	hyphae and arbuscules grow close to root tips	2		3	1	
SL1770-N	many hyphae and arbuscules in lateral roots, close to root tips	2	Y	5	1	
SL1894-N	some aborted infection sites, some lateral roots not well colonized, but parts of roots wt-like	1, 2		3	2	
SL1895-N	some aborted infection sites, few, small arbuscules	1, 3	Y	5	1	
SL1909-N	some abnormal infection sites, very few arbuscules	1, 3		2	2	
<b>SL1915-N</b>	aborted infection sites, hyphae cannot grow into the cortex, many hyphae outside root, no arbuscules, other parts wt-like	1	Y	2	1	
SL1928-N	aborted infection sites, unequally and weakly colonized, very few arbuscules	1, 2, 3		4	1	
SL1940-N	some abnormal infection sites with swollen hyphae, very few arbuscules	1, 3		3		
SL1952-N	no arbuscules	3		3		
SL1973-N	few aborted infection sites	1		2	1	
SL1979-N	some aborted infection sites, few arbuscules	1, 3		3		
SL1980-N	some aborted infection sites with swollen hyphae	1		2		
SL1984-N	abnormal infection sites, parts of the root weakly colonized, but others very well colonized	1, 2		2		
SL1995-N	sections of the root without any infection site, but with many straying hyphae, unequal colonization	1, 2		3	1	
SL2015-N	lots of aborted infection sites	1		1		
SL2030-N	some aborted infection sites, septated hyphae, no arbuscule	1, 3		3	1	
<b>SL2042-N</b>	balloon-like swellings at infection sites, no colonization, straying	1		2		
SL2044-N	many hyphae on the root surface	1		3	2	
SL2068-N	some aborted infection sites, some parts not colonized	1, 2		1	1	
SL3007-N	lateral roots not colonized or colonization suddenly stops	2	Y	2	2	
SL3084-N	aborted infection sites, almost no colonization	1, 2		3	2	
SL3137-N	some wt-like arbuscules, but many degenerated ones	3		3	2	
SL3143-N	only very few arbuscules, degenerated with very few branches	3	Y	4	2	
SL3217-N	some aborted infection sites, very few arbuscules	1, 3		1	1	
SL3219-N	many hyphae outside roots, some aborted infection sites	1		4	2	
SL3229-N	some aborted infection sites, patchy colonization, very few arbuscules	1, 2, 3	Y	3	2	
SL3262-N	some aborted infection sites, very few arbuscules	1, 3		3	2	
<b>SL3284-N</b>	stumpy arbuscules with few branches	3		2	1	
SL3298-N	aborted infection sites, few arbuscules	1, 3		2	1	
SL3313-N	patchy colonization with aborted infection sites, septated hyphae	1, 2	Y	3	1	
<b>SL3361-N</b>	patchy colonization at lateral roots	2	Y	3	1	
SL3372-N	no wt-like arbuscule	3	Y	3	2	
SL3381-N	some aborted infection sites with swollen hyphae, patchy colonization at lateral roots	1, 2		4	2	
SL3488-N	lateral root with patchy colonization	2		1	1	
SL3506-N	patchy colonization at one lateral root with aborted infection sites, no wt-like arbuscule	1, 2, 3	Y	3	3	

## RESULTS

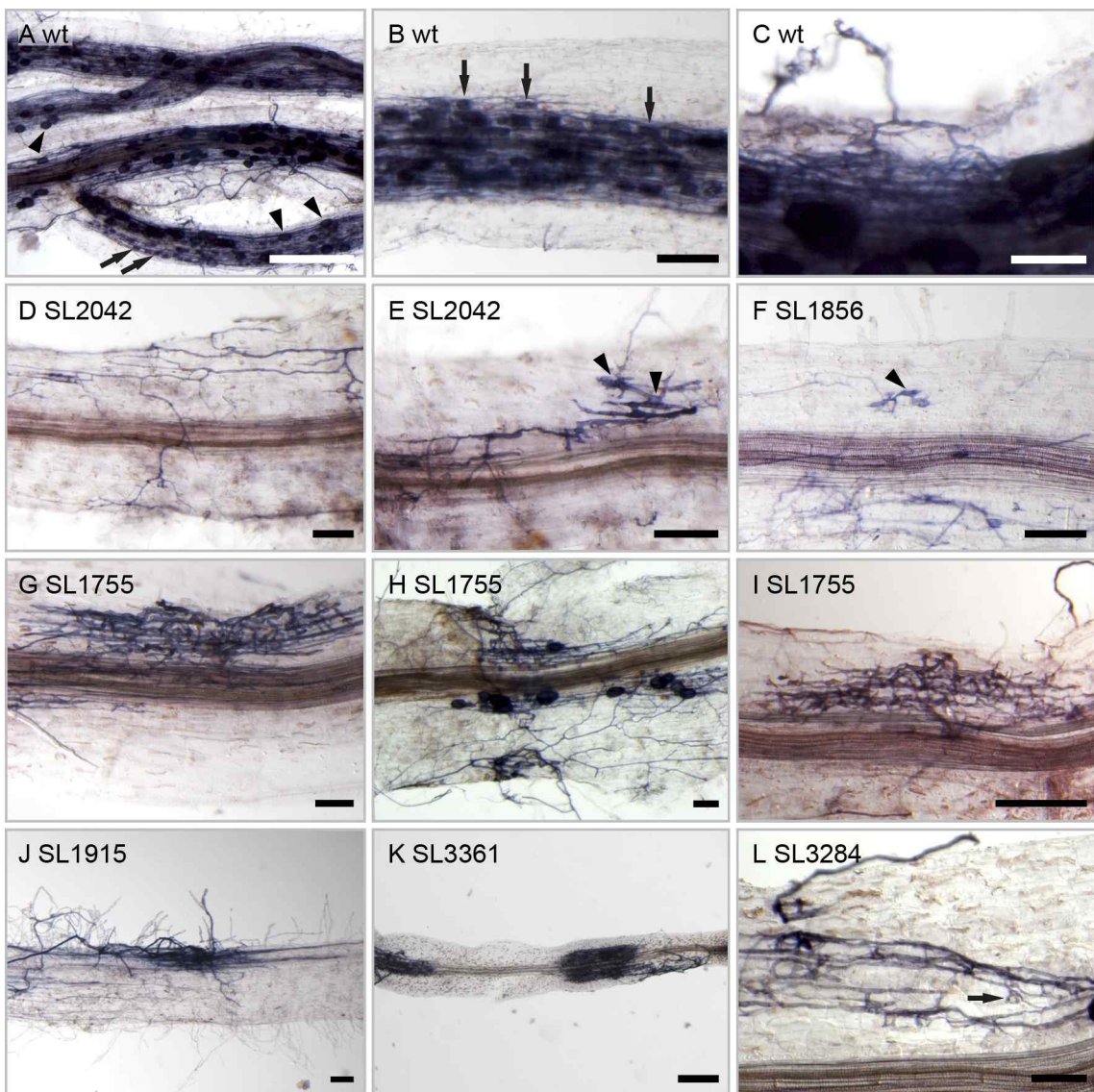


**Figure 6. AM phenotypes of putative mutants.**

Roots of *L. japonicus* Gifu (wild type) (A - C), SL2042-N (D and E), SL1856-N (F), SL1755-N (G - I), SL1915-N (J), SL3361-N (K) and SL3284-N (L) were harvested 4 wpi with *R. irregularis* BEG195, stained with acidic ink and phenotyped using a stereomicroscope.

(A and B) The whole root system of *L. japonicus* Gifu plants was colonized. Lots of arbuscules (A and B, arrows) and vesicles (A, arrowheads) could be detected.

(C) Infection site at wild-type roots did not show any swollen hyphae. The fungus was able to enter the root and colonize it.

(D - F) The passage of hyphae through the outer cell layers of the root was blocked in mutants of SL2042-N (D and E) and SL1856-N (F). Hyphae were growing only on the root surface (D - F) and formed balloon-like swellings (E and F, arrowheads).

(G - I) Hyphal growth expanding from infection sites was partially inhibited in putative mutants of SL1755-N. Moreover, no arbuscules were detected next to these infection sites. This phenotype could be detected in M3 (G and H) and M4 (I) roots.

(J) At some root stretches of SL1915-N mutants hyphae accumulated on the surface without further colonization.

(K) SL3361-N mutants had a patchy phenotype. Parts of the roots looked wild type-like, whereas others were devoid of colonization.

(L) The arbuscule formation was impaired in roots of SL3284-N mutants. Only stunted arbuscules could be detected (arrow). Scale bars = (A) 500 µm, (K) 250 µm, (B - J, L) 100 µm.

Previous page:

**Table 1. Summary of putative M3 AM mutant lines.**

Overview of the 55 SL lines with putative AM mutants identified by the author in the M3 generation and their respective AM mutant phenotypes. SL lines with grey background have been rescreened in the M4 generation and phenotypes of SL lines in bold are shown in Figure 6. <sup>a</sup>AM developmental stage at which the putative AM mutants showed aberrant phenotypes (Figure 4) 1, during penetration process; 2, in cortical colonization; 3, in arbuscule development. Y, putative M3 mutant(s) were crossed to MG-20. <sup>b</sup>Number of M3 individuals with the described phenotype isolated from the SL line.

<sup>c</sup>Number of tested M4 families with wild-type AM phenotype. <sup>d</sup>Number of tested M4 families with AM mutant phenotype.

### 2.1.3 SL2042-N

AM mutants of SL2042-N exhibited hyphal balloon-like swellings on the root surface upon inoculation with *R. irregularis* BEG195 (Figure 6D and E), which represent a characteristic feature of several common *sym* mutants (Kistner et al., 2005). Since the mutants of SL2042-N were infertile, progenies of M3 wild-type siblings were phenotyped to check whether the mutant phenotype was also present in the next generation. The wild-type siblings segregated plants with either the wild-type or the mutant AM phenotype. Hence, the mutant phenotype was heritable. To check whether SL2042-N mutants are able to form nodules, the nodulation ability of the segregating population was investigated 3 wpi with *M. loti* R7A. Subsequently, the plants were inoculated with BEG195 by repotting them into chive nurse pots. In total, 11 plants were analysed four weeks later. Three of those had only very short roots and did not produce any nodule. They died at the seedling stage, before their AM phenotype could be checked. Root systems of another three plants formed nodules and wild type-like AM structures. In contrast, five plants were impaired in both symbioses. Their roots did not show any nodule and fungal balloon-like swellings could be observed. This phenotype pointed to a mutation in one of the common SYM genes. Therefore, *CYCLOPS* (Yano et al., 2008), *SYMRK* (Stracke et al., 2002), *NUP85* (Saito et al., 2007), *NUP133* (Kanamori et al., 2006) and *POLLUX* (Imaizumi-Anraku et al., 2005) were sequenced from SL2042-N mutant DNA to find out whether any of these genes contained a mutation. A point mutation was detected in the eighth exon of *POLLUX* (Imaizumi-Anraku et al., 2005), which had already been identified in SL0729-6 and SL0729-10 (Perry et al., 2009). This mutation (G3388A) introduces a stop codon at amino acid position 651 and corresponds to the *pollux-20* allele (Perry et al., 2009). In addition, a T-to-C transition in the fourth intron of *NUP85* at position 2545 of the genomic sequence was discovered. This mutant allele is listed as *nup85-9* (Perry et al., 2009).

### 2.1.4 SL1856-N

Mutants of SL1856-N also showed balloon-like swellings after inoculation with *R. irregularis* BEG195 (Figure 6F) and have been identified by M. Groth during his part of the AM screen. After crossing the mutants to *L. japonicus* MG-20, the F2 population segregated in a 3:1 ratio (46 wild-type plants vs. 16 mutants,  $\chi^2$ -value = 0.88), pointing to a monogenic recessive mutation. Ten mutant and two wild-type F2 plants were subjected to standardized rough mapping based on the analysis of 40 SSR markers (Groth, 2010) that were evenly distributed across the five chromosomes. The resulting allelic distribution suggested a target region at the south of chromosome 2 (MG-20). Additional five markers located close to the target interval revealed that the markers TM0380 (0/18 MG-20 vs. total alleles), TM0191 (0/20), TM0324 (0/20) and TM0667 (0/18) were co-segregating with the mutation. Consequently, the common SYM gene *NUP133* (Kanamori et al., 2006), located next to the marker TM0324, was identified as a candidate gene. Sequencing *NUP133* from SL1856-N mutant DNA discovered a splice site mutation (G4496A)

changing the last base of the 5<sup>th</sup> intron, which is known as the *nup133-21* allele (Perry et al., 2009).

### 2.1.5 SL1755-N

Mutants identified in SL1755-N had AM fungal infection sites, where hyphae branched and penetrated the root, but further spreading was apparently impossible (Figure 6G - I). Although arbuscules were not detected close to these aberrant infection sites, occasionally vesicles could be observed (Figure 6H). Nevertheless, parts of the root system looked completely wild type-like regarding their AM structures (data not shown). The AM mutant phenotype of SL1755-N could be confirmed in the M4 generation (Figure 6I; Table 1). A nodulation test revealed that SL1755-N mutants formed on average 3.36 ( $\pm 1.29$  SD) nodules per root system, wild-type plants 4.10 ( $\pm 1.20$  SD). Consequently, the mutant's ability to produce nodules was not significantly different from the wild-type control, indicating that SL1755-N mutants were not impaired in nodulation. For the map-based cloning of the mutation causing this AM phenotype, a mutant was crossed to *L. japonicus* MG-20 and F1 plants were checked for heterozygosity. Phenotyping of 280 F2 individuals revealed that it was very difficult to decide whether a root belonged to a mutant or a wild-type plant, because the mutant AM phenotype of F2 roots was not as clearly visible as in the M3 or M4 generation. To exclude possible effects of the MG-20 background on the mutant phenotype, an SL1755-N mutant was crossed to *L. burttii* (Kawaguchi et al., 2005). Segregation of the mutant phenotype could not be observed analyzing 120 F2 plants resulting from this cross. A reliable distinction between mutant and wild-type F2 plants is an essential prerequisite for a successful map-based cloning approach. Since the phenotype of SL1755-N mutants after crossing to MG-20 and *L. burttii* is not detectable, crossing the mutants to wild-type Gifu plants could open another possibility. With the help of Next Generation Sequencing, EMS-induced mutations in the genomes of F2 backcross mutants could be mapped onto the Gifu genome. Homozygous mutations that are present in the F2 backcross genomes would point to potential target regions, where the mutated gene responsible for the AM mutant phenotype could be located.

## 2.2 The Calcium-Dependent Protein Kinase (CPK) 29

Calcium ions ( $\text{Ca}^{2+}$ ) are very important signalling molecules and play essential roles in various physiological and cellular processes in plants. These include, for example, abiotic stress response and stomatal aperture, circadian signalling as well as the development of tip growing structures like pollen tubes or root hairs. Furthermore,  $\text{Ca}^{2+}$  signals are indispensable key regulators for interactions of plants with pathogenic and symbiotic microorganisms (Dodd et al., 2010).  $\text{Ca}^{2+}$  transport systems, like  $\text{Ca}^{2+}$  influx channels and  $\text{Ca}^{2+}$  efflux transporters, generate and regulate  $\text{Ca}^{2+}$  signatures in plant cells according to specific environmental and developmental stimuli (McAinsh and Pittman, 2009).  $\text{Ca}^{2+}$  sensor proteins are responsible for the decoding of these  $\text{Ca}^{2+}$  signatures and their translation into changes of cellular processes (Sanders et al., 2002; Dodd et al., 2010). Calcium-dependent protein kinases (CPKs, also called CDPKs) and the  $\text{Ca}^{2+}$ - and calmodulin-dependent protein kinase (CCaMK) belong to this class of  $\text{Ca}^{2+}$  sensor proteins and consist of an N-terminal variable, a protein kinase and an autoinhibitory domain, but they differ in their C-termini. CPKs have a calmodulin-like domain consisting of mostly four  $\text{Ca}^{2+}$ -binding EF hands. In contrast, CCaMK exhibits a visinin-like domain with three EF hands (Harper and Harmon, 2005). Hence, they are classified as  $\text{Ca}^{2+}$  sensor responders, because they are able to sense  $\text{Ca}^{2+}$  due to their EF hands and they have a kinase function (Dodd et al., 2010).

Focusing on the symbiotic signalling network, CCaMK of *L. japonicus* and its orthologue DMI3 in *M. truncatula* are the best-studied  $\text{Ca}^{2+}$  sensing protein kinases (Lévy et al., 2004; Tirichine et al., 2006). Rhizobial Nod factors and AM fungi have been shown to stimulate differential  $\text{Ca}^{2+}$  spiking patterns. CCaMK could possibly represent the decoder of these distinct  $\text{Ca}^{2+}$  oscillations and activate either RNS- or AM-specific downstream pathways (Kosuta et al., 2008). In addition, CPKs also play important roles in root symbioses. So far CPKs have been identified in plants, some protozoans and green algae (McCurdy and Harmon, 1992; Zhao et al., 1994; Harmon et al., 2001) and are divided into four groups (Harmon et al., 2001; Cheng et al., 2002). Many *Arabidopsis* CPKs carry N-terminal myristylation and palmitoylation signals (Hrabak et al., 2003). Experiments analysing seven At CPKs confirmed that the presence of the N-terminal myristylation signal correlates with a membrane association of these proteins. Two CPKs without these signals were detected in the cytosol and in the nucleus (Dammann et al., 2003). The mechanism, how CPKs are activated, when  $\text{Ca}^{2+}$  levels increase, was already proposed by Harmon and associates (2000). Binding of  $\text{Ca}^{2+}$  to the EF hands present in the calmodulin-like domain leads to a conformational change that releases the inhibition of the protein kinase by the autoinhibitory/junction domain (Harmon et al., 2000). Crystal structures of apicomplexan CPKs either in the autoinhibited state (absence of  $\text{Ca}^{2+}$ ) or in the active form (with  $\text{Ca}^{2+}$ ) confirm that large conformational changes of the  $\text{Ca}^{2+}$ -binding C-terminus take place and elucidate in detail the activation mechanism (Wernimont et al., 2010).

## RESULTS

---

Two CPKs of *M. truncatula*, MtCPK3 and Mt CDPK1, and one of *O. sativa*, OsCPK18, have already been analysed in detail regarding their contribution to the establishment of RNS and AM (Ivashuta et al., 2005; Gargantini et al., 2006; Campos-Soriano et al., 2011). *MtCPK3* is induced after inoculation with *Sinorhizobium meliloti* and silencing of *MtCPK3* by RNAi revealed a twofold increase in nodule number compared to control roots (Gargantini et al., 2006). In contrast, silencing of Mt CDPK1 drastically reduces the root's ability to form nodules and AM. Furthermore, root cells and root hairs are shorter. Microarray analyses showed that silencing of Mt CDPK1 affects cell wall- and defence-related gene expression (Ivashuta et al., 2005). Recently, it was discovered that the expression of OsCPK18 is rapidly induced in root cortical cells upon inoculation with *R. irregularis* and even upon application of diffusible fungal molecules. OsCPK18 is closely related to Mt CDPK1 and therefore also part of the CPK group IV. The authors suggest that OsCPK18 is involved in the presymbiotic signalling of AM (Campos-Soriano et al., 2011).

Kistner and associates (2005) performed a cDNA-AFLP analysis to reveal transcriptional changes in roots during RNS and AM development. They compared root transcripts of inoculated and non-inoculated wild-type plants. In addition, *ccamk* and *castor* mutants were analysed for differential gene expression in the presence of *R. irregularis*. Several genes induced or repressed during AM and/or RNS have been identified (Kistner et al., 2005). In this cDNA-AFLP screen, a fragment called AM8 seemed to be upregulated in *ccamk* mutants compared to wild-type plants in the presence of *R. irregularis*. Results of a blastx search suggested that AM8 is part of a CPK gene (C. Kistner, unpublished). In this study, I analysed whether AM8 is indeed part of a CPK gene and its AM-specific induction in *ccamk* mutants can be confirmed. Furthermore, I intended to investigate potential functions of the identified CPK in plant root symbioses. The discovery of an intriguing gene structure of this CPK with two alternative first exons (AFEs) that were mutually exclusive and resulted in two partially different CPK isoforms, encouraged a search for phylogenetically related genes in further plant genomes.

### 2.2.1 CPK29 of *Lotus japonicus*

#### 2.2.1.1 Gene Structure of Lj CPK29

Initially, the genomic context of the AM8 cDNA fragment was analysed. The AM8 transcript aligned perfectly to the genomic clone LjT34O04, located at the northern end of chromosome 5 (S. Sato, Kazusa DNA Research Institute, Japan), and was found to be part of a gene, which was annotated as chr5.LjT34O04.70.r2.d. The gene prediction of this nucleotide sequence, ranging from position 58518 to 63373 of LjT34O04, with Genscan (Burge and Karlin, 1997) followed by a BLAST search and a scan for PROSITE signatures (de Castro et al., 2006) proposed a calcium-dependent protein kinase. In contrast to already described CPKs, this predicted CPK contained two protein kinase domains preceding four EF hands. However, the DNA sequence corresponding to the region spanning from the first to the second kinase domain could not be

## RESULTS

amplified by PCR from cDNA. On the other hand, DNA fragments corresponding to the region from the first or the second kinase domain to the end of the gene could be detected.

5'- and 3'-RACEs revealed the intriguing gene structure of this CPK (Figure 7A). The 3'-RACE gene specific primer was annealing to the fourth and third last exon (Figure 7B). The sequences of the 3'-RACE amplicons obtained from four clones aligned to the predicted coding sequence of the CPK and identified the 3'-UTR. The gene-specific primer used to amplify the 5'-RACE fragments was annealing to the fourth exon of the initially predicted CPK gene with two protein kinase domains (Figure 7B).

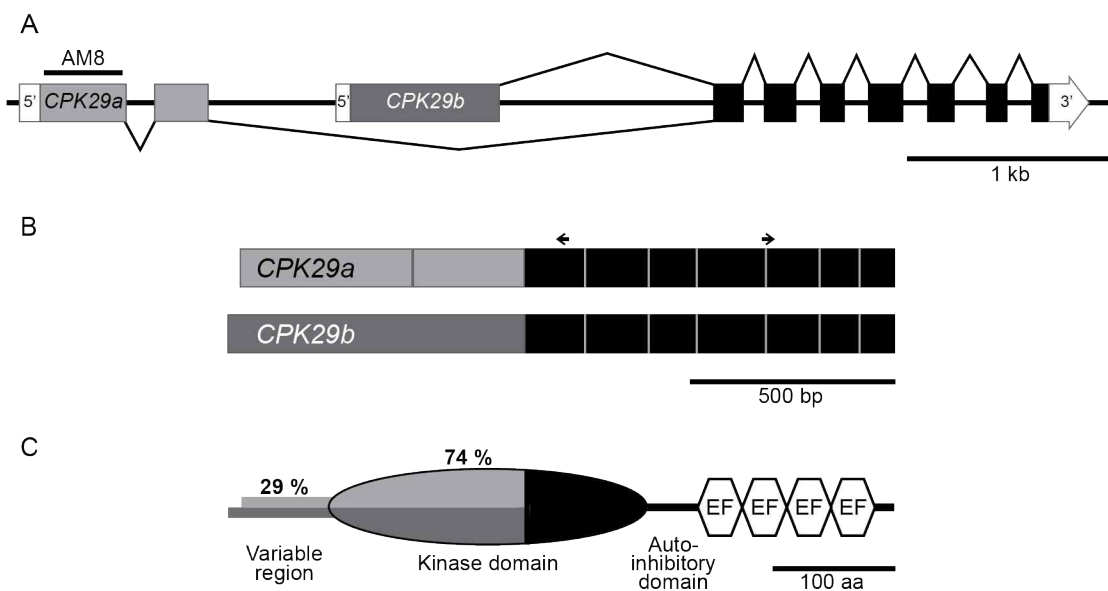


**Figure 7. Genomic, cDNA and protein domain structures of the *L. japonicus* CPK29 variants.**

(A) CPK29 gene structure. The alternative first exons of the two CPK29 variants and the second unique exon of CPK29a are represented by grey boxes; common exons are shown in black. 5'-UTRs are depicted by white boxes, the 3'-UTR by a white arrow. The length of the AM8 fragment corresponding to Exon 1 of CPK29a is indicated.

(B) Comparison of the CPK29a and CPK29b cDNA structures. Exons unique or common to both variants of CPK29 are shown in grey or black, respectively. Arrows represent the gene specific primers of the 5'- and 3'- RACEs.

(C) Comparison of the protein domain structure of CPK29a and CPK29b. The two proteins differ in their N-terminal variable region (29 % identity) and in the part of the kinase domain (74 % identity) shown in grey. The segment of the kinase domain in black, the autoinhibitory domain and the EF-Hands with the adjacent C-terminus were common to both versions. Scale bars = 1 kb (A), 500 bp (B) and 100 aa (C).

A digest with EcoRI of the 5'-RACE clones revealed two distinct restriction patterns of the 5'-RACE fragments (Figure 8). Sequencing of several clones of both patterns confirmed that the two restriction patterns correlated with the amplification of two partially different cDNA populations upstream of the 5'-RACE GSP. Hence, the analysed CPK contains two alternative first exons (AFE) with individual 5'-UTRs and one of the transcript variants additionally carries a unique second exon.

## RESULTS

---

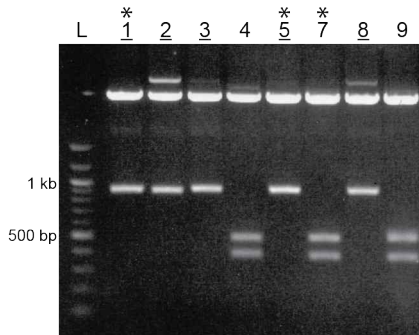


**Figure 8. Restriction analysis of cloned 5'-RACE products.**

EcoRI restriction digest of 5'-RACE clones revealed two distinct band patterns upon agarose gel electrophoresis (underlined versus non-underlined clones). Asterisks mark the clones that have been sequenced. 5'-RACE fragment of clone 7 originated from CPK29a, fragments of clones 1 and 5 derived from CPK29b. L: 100 bp-ladder.

Expression analyses using q-RT-PCRs were conducted to confirm the transcriptional differences of the CPK observed by C. Kistner. The q-RT-PCR-primers were designed according to the 5' UTRs and the very beginning of the first exon to avoid a potential misannealing. Nevertheless, a significant difference in transcript abundance comparing wild-type and *ccamk* cDNA could not be measured by q-RT-PCR.

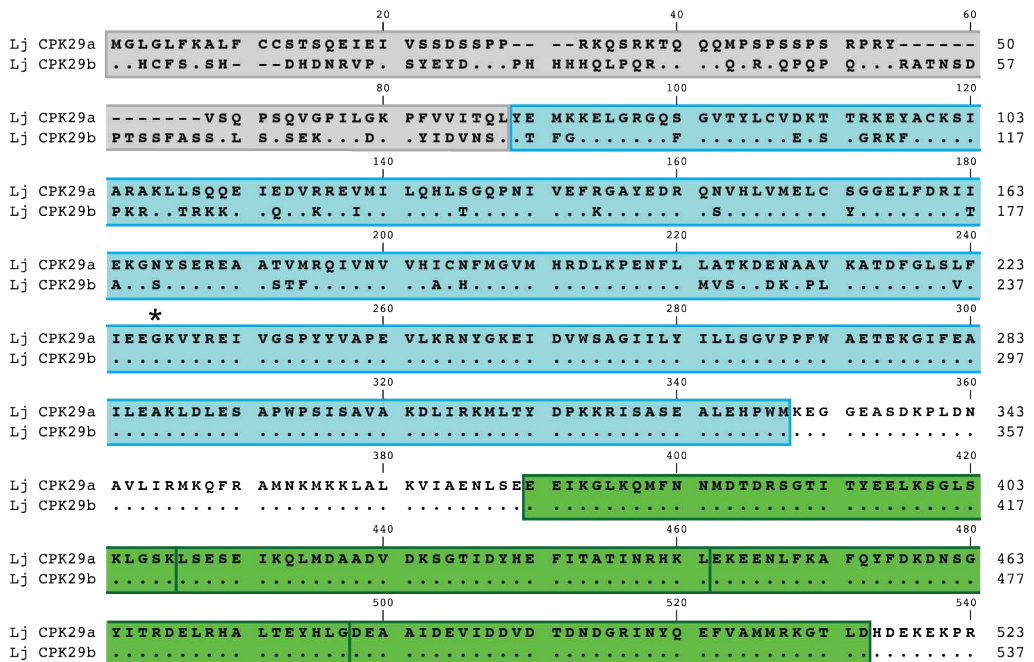


**Figure 9. Amino acid alignment of CPK29a and CPK29b of *L. japonicus*.**

The amino acid sequences of CPK29a and CPK29b were aligned. The N-terminal variable region is highlighted in grey, the protein kinase domain in blue and the four EF hands in green. Asterisk at position 244 marks the start of the sequence that is common to both versions. Equal residues are shown as dots. Sequences are attached (see appendix 9.1.1).

Phylogenetic analyses suggested that this CPK of *L. japonicus* is an ortholog of *A. thaliana* CPK29 (Figure 16). Due to the existence of the alternative first exons, the two CPK versions were called Lj CPK29a and Lj CPK29b (Figure 7A). Lj CPK29a comprised nine, Lj CPK29b eight exons. The seven last exons and the 3'-UTR were common to both versions (Figure 7A and B).

## RESULTS

According to the typical domain structure of CPKs, the two CPK29 versions contained an N-terminal variable region, a protein kinase domain and four EF hands (Figure 7C, Figure 9). The N-terminal variable region and part of the protein kinase domain consisted of unique sequences of CPK29a or CPK29b (Figure 7C; Figure 9). Comparing the N-terminal regions and the unique parts of the protein kinase domain revealed an identity of 29% and 74%, respectively.

### 2.2.1.2 Expression Patterns of *Lj CPK29a* and *Lj CPK29b* in Roots and Nodules

It has been proposed that, when two AFE are further apart than 500 bp, each of the two gene variants has its own promoter (Kimura et al., 2006). Since this was the case for *Lj CPK29*, the spatial and temporal expression patterns of *CPK29a* and *CPK29b* were analysed in *Lotus* roots. Therefore, their alternative promoters were fused to the  $\beta$ -glucuronidase gene (*ProCPK29a:GUS* and *ProCPK29b:GUS*) using the vector pKGWFS7 (Karimi et al., 2002). The promoter of *CPK29a* tested in this experiment consisted of 1139 bp, whereas the one of *CPK29b* was composed of 637 bp. The *CPK29b* promoter was shorter because of the presence of the second exon of *CPK29a*. The promoter-GUS fusion constructs were introduced into *L. japonicus* wild-type roots by hairy root transformation.

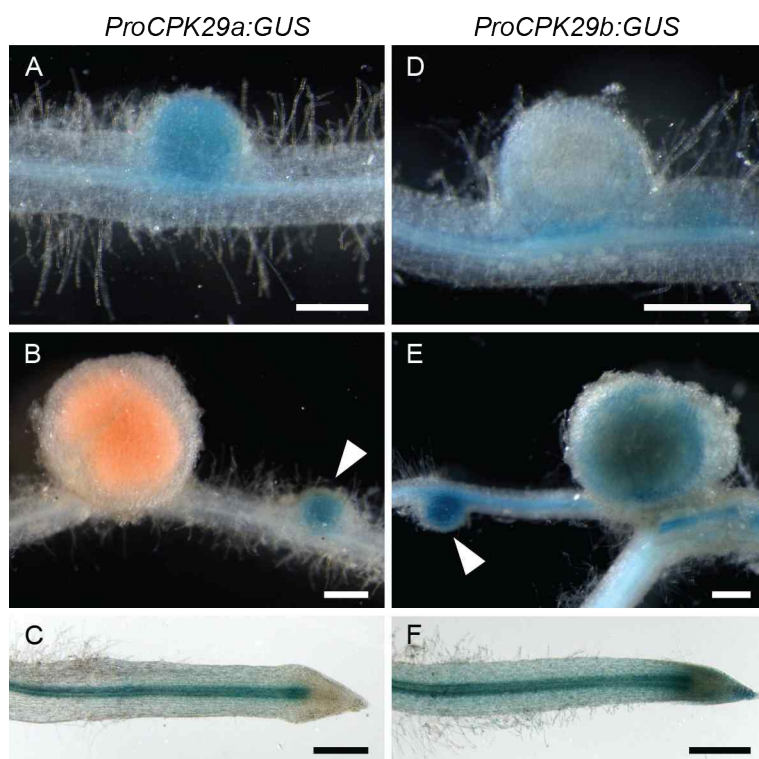


**Figure 10. Expression patterns of *Lj CPK29* versions by promoter-GUS fusions.**

Hairy roots of *L. japonicus* Gifu plants transformed with *ProCPK29a:GUS*- (A - C) or *ProCPK29b:GUS*-constructs (D - F) were inoculated with *M. loti* expressing *DsRed* and analysed 3 wpi. GUS expression induced by the promoter of *CPK29a* could be detected in young nodules (A, B), whereas older nodules were not stained (B). Staining of roots with *ProCPK29b*-driven GUS was more intense (E, F) compared to *ProCPK29a* (B, C), but young nodules were less frequently stained dark blue (D). Older nodules of roots transformed with *ProCPK29b:GUS* were always stained (E). The vascular tissue showed unspecific GUS staining in *ProCPK29a:GUS*- and *ProCPK29b:GUS*-transformed roots (C, F), but the *ProCPK29a* induced a lower general background staining (C) than *ProCPK29b* (F). Arrowheads point to young nodules (B, E). Scale bars = 500  $\mu$ m.

## RESULTS

Roots transformed with *ProCPK29a:GUS* showed a distinct staining of young nodules (Figure 10A and B, arrow), whereas older nodules were not stained (Figure 10B). In comparison, roots transformed with *ProCPK29b:GUS* exhibited a broader staining. Young nodules were stained either more (Figure 10E, arrow) or less intense (Figure 10D) and older nodules also showed a blue staining (Figure 10E). Regarding the whole root system, the *ProCPK29b:GUS*-transformed roots revealed a more intense staining than those transformed with *ProCPK29a:GUS* (Figure 10C and F). It is known that the vector pKGWFS7 induces a background staining of the vascular tissue (Takeda et al., 2011), which could also be detected in the *ProCPK29a*- and in the *ProCPK29b*-transformed roots (Figure 10C and F). Nevertheless, *ProCPK29b*-driven GUS staining was evident throughout the complete root cortex (Figure 10F). In addition, composite plants were grown for four weeks in *R. irregularis*-containing nurse pots. No differences between inoculated and non-inoculated roots comparing their GUS staining patterns could be detected (data not shown).

### 2.2.1.3 Subcellular Localization of Lj CPK29a and Lj CPK29b

Besides a tissue-specific expression of alternative splice products a different subcellular localization is possible. Several membrane-associated CPKs of *A. thaliana* carry myristoylation and palmitoylation sites (Dammann et al., 2003). The presence of myristoylation sites at the N-termini of the CPK29 versions was analysed with the web-based myristoylation prediction program, Myristoylator (Bologna et al., 2004). The Prosite pattern for myristoylation is G-{EDRKHPFYW}-x(2)-[STAGCN]-{P} (Towler et al., 1988). According to the prediction based on this motif, only Lj CPK29b carries a myristoylation site. To check, whether the two CPK29 versions had indeed different subcellular localizations, they were analysed by transient co-expression of fluorescent fusion proteins in *N. benthamiana* epidermal leaf cells. The N-terminus of CPK29a fused to the yellow fluorescent protein (YFP) and the N-terminus of CPK29b fused to the cyan fluorescent protein (CFP) clearly showed a plasma membrane association.

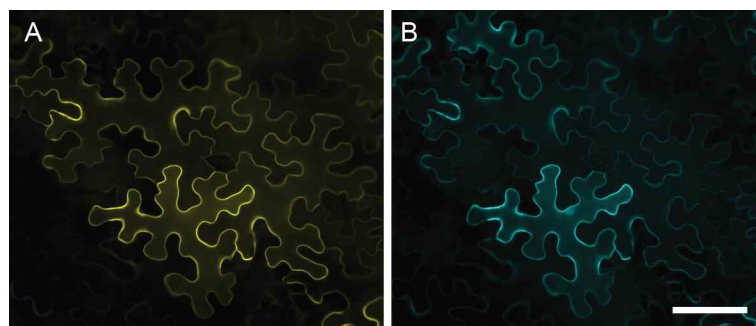


**Figure 11. Subcellular localization of Lj CPK29a and Lj CPK29b in *N. benthamiana* leaves.**

C-terminal fusions of *Lotus* CPK29a<sub>Exon1+2</sub> to YFP (A) and CPK29b<sub>Exon1</sub> to CFP (B) were co-expressed in *N. benthamiana* epidermal leaf cells under the control of the 35S promoter. Both fusion proteins were associated to the plasma membrane. Scale bar = 100 µm.

## 2.2.2 CPK29 of *Medicago truncatula*

### 2.2.2.1 *M. truncatula* CPK29 Gene Structure

Analysis of the Lj CPK29 gene structure raised the question whether the putative orthologue of CPK29 in *M. truncatula* also carried alternative first exons.

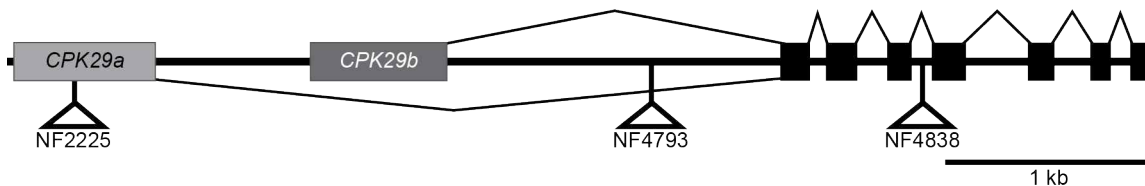


**Figure 12. *M. truncatula* CPK29 gene structure.**

Alternative first exons of Mt CPK29 are shown in grey, common exons in black boxes. Triangles mark the positions of the *Tnt1* insertions in the corresponding NF lines. Scale bar = 1 kb.

The genomic region of Lj CPK29a was used to search the *M. truncatula* IMGAG sequencing database ([http://medicago.org/genome/IMGAG\\_blast.php](http://medicago.org/genome/IMGAG_blast.php)). The best matching hit was the putative CPK Medtr1g031920.1, which was located on BAC AC202491.10. A PROSITE scan of the amino acid sequence of Medtr1g031920.1 predicted two protein kinase domains followed by four EF hands. According to the gene structure and amino acid sequence of Lj CPK29, the gene annotation of Medtr1g031920.1 was modified and a gene with two AFE could be constructed (Figure 12). Both CPKs could be amplified from *M. truncatula* cDNA (Figure 13). Since no closer homologue of At CPK29 was found in the *M. truncatula* IMGAG database and both *M. truncatula* isoforms of this CPK formed one phylogenetic cluster together with At CPK29 (Figure 15; Figure 16), they were called Mt CPK29a and Mt CPK29b.

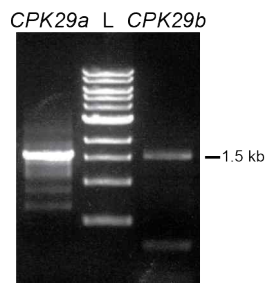


**Figure 13. Agarose gel fluorography visualizing Mt CPK29 variants amplified from cDNA.**

Mt CPK29a and Mt CPK29b were amplified from *M. truncatula* root cDNA with specific primers and PCR products were separated by agarose gel electrophoresis. L: 1 kb-ladder.

### 2.2.2.2 *Tnt1* Insertion Lines of Mt CPK29

The identification of the putative Lj CPK29 orthologue in *M. truncatula* opened the possibility to use the resources of the *Medicago truncatula* Mutant Database (Tadege et al., 2008). This database contains a *Tnt1* retrotransposon insertion mutant population with more than 19,000 lines and approximately 470,000 insertions distributed across the whole genome. On average 25 *Tnt1* insertions can be found in the genome of one mutant Noble Foundation (NF) line (<http://bioinfo4.noble.org/mutant>; Tadege et al., 2008). A blast search of the predicted genomic region of Mt CPK29a against the *Tnt1*-FST (flanking sequence tags) database resulted in 13 hits. Thereof the lines NF4838, NF4793 and NF2225 were investigated in more detail. NF4838 (E-value 0.0), the best blast hit, carried a *Tnt1*-insertion in the fourth intron, which was present in both variants of CPK29 (Figure 12). The insertion in NF4793 (E-value 0.0) was located in the first introns of both variants (Figure 12). In the case of NF2225 the first exon of CPK29a carried the insertion and therefore the expression of only this variant was supposed to be affected (Figure 12).

Seedlings of these NF lines were genotyped by PCR using a gene-specific primer that annealed in the vicinity of the insertion and one transposon-specific primer. With the exception of one plant, the tested NF4838 plants (n=35) were homozygous. The line NF2225 segregated 12 mutants, 8 heterozygous plants and 18 wild-type plants, whereas no mutant plant could be found in the line NF4793. In total, 46 NF4793 plants were analysed, thereof 33 were heterozygous and 13 wild type. Closer inspection of the pods produced by heterozygous and wild-type NF4793 plants showed that their pods were shorter and carried less seed than wild-type pods.

The AM phenotype of NF4838 and NF2225 plants was analysed four weeks after planting them into *R. irregularis*-containing nurse pots and was not obviously different from the wild type (data not shown). In addition, NF4838 and NF2225 seedlings were inoculated with *S. meliloti* expressing CFP and nodules were counted 2 wpi, because GUS staining of young nodules of *L. japonicus* hairy-roots transformed with *ProCPK29a:GUS* suggested an involvement of Lj CPK29a in early nodule development. So far, no impaired nodulation could be detected in NF4838 mutant plants. Preliminary data indicated that the number of nodules in NF2225 plants carrying the *Tnt1* insertion in CPK29 was reduced to 35% compared to the nodule number of NF2225 plants without this insertion.

### 2.2.3 Phylogeny of CPK29 Homologs

The discovery of CPK29 with two alternative first exons in *L. japonicus* and *M. truncatula* encouraged the investigation of the genomes of soybean (*Glycine max*), poplar (*Populus trichocarpa*), strawberry (*Fragaria vesca*) and rice (*Oryza sativa*) to find further putative orthologs. These could help to assess the phylogenetic distribution of CPK29a and CPK29b and to check whether this genomic structure of CPK29 in *Lotus* and *Medicago* represents a legume-specific phenomenon.

A database search of the soybean genome at the phytozome website with the genomic sequence of Lj CPK29a discovered the annotated gene Glyma14g40090.1. The Genscan prediction of the

## RESULTS

---

genomic sequence of Glyma14g40090.1 followed by a PROSITE scan proposed a CPK with two protein kinase domains. In line with Lj CPK29 and Mt CPK29, a CPK with two alternative first exons and seven common exons could be constructed. These two CPK variants would express partially different kinase domains and were therefore called Glyma14g40090a and Glyma14g40090b (Figure 14). In addition, the blast search also detected the two predicted genes Glyma17g38040.1 and Glyma17g38050.1, which were arranged in tandem. The putative amino acid sequence of Glyma17g38040.1 was predicted to contain one protein kinase domain and four EF hands, whereas Glyma17g38050.1 would consist also of a protein kinase domain, but only of three and a half EF hands. The protein sequence of Glyma17g38050.1 deposited in the phytozome database was apparently referring to a wrong gene prediction, because it did not start with a methionine. The exon-intron-structure of the N-terminal protein sequence of Glyma17g38050.1 was modified, but it was not possible to change the gene prediction in such a way that four complete EF hands were present. Glyma14g40090a, Glyma14g40090b, Glyma17g38040.1 and Glyma17g38050.1 were phylogenetically related to At CPK29 (Figure 15; Figure 16). They build together with the variants of Mt CPK29 and Lj CPK29 a subgroup of CPK class II B, the CPK29 cluster (Figure 15; Figure 16). In addition, the soybean sequences Glyma14g40090a and Glyma17g38050 were similar to Lj CPK29a and Mt CPK29a, whereas Glyma14g40090b and Glyma17g38040 form together with Lj CPK29b and Mt CPK29b a second subgroup of the CPK29 cluster (Figure 15; Figure 16).

---

Next page:

**Figure 14. Multiple Sequence Alignment of legume and *A. thaliana* CPK29 protein sequences.**

The amino acid sequences of Lj CPK29a, Lj CPK29b, Mt CPK29a, Mt CPK29b and the predicted amino acid sequences of Glyma14g40090a and Glyma14g40090b were aligned to the At CPK29 (AAF26765) protein sequence. The Glyma14g40090 sequence was downloaded from the phytozome website and modified. Equal residues are shown as dots. *G. max* Glyma14g40090 sequences, *L. japonicus* and *M. truncatula* CPK29 sequences are attached (see appendix 9.1.1).

## RESULTS

---

	20	40	60
LjCPK29a	-----	-----MGL GLFKA-LFCC	-STS--QEIE IVSS-DSSPP
MtCPK29a	-----	-----F...	-T.N--RD.P. ....SE....
Glyma14g40090a	-----	-----M.....	.KP--H..D .AD.W....
LjCPK29b	-----	-----H CFS.-SHDHD	NRVPISY.YD SPFPHHHHQL
MtCPK29b	-----	-----H CFT.-PHD--	NRVPISYDYG T---N.Q.-
Glyma14g40090b	-----	-----H CFS.-PST--	NEIPINYDY- SPFPHYQ.R
AtCPK29	MLQNQHKTTK NQRNKNIGTK	YFLRKKI..F CFS.FGKSQT	HEIPISSSSD SSPPHHYQ.L
	80	100	120
LjCPK29a	RK--QSRTQ QQM---P--	SPSSPS RPRYV-SQPS	QVG-PILGKP FVVITOLYEM
MtCPK29a	.H--S.GYGY N.PSFD.	-----KTTK S.SSS--N-	.I.A..... Y...NNI.D.
Glyma14g40090a	DH--TPKQHS KPKPKPN---	-----AAPTH. NNKQT-TTST	.I.A..... Y.N.H.M..
LjCPK29b	PQRT.QQQPR P.PQPQ.RYR	ATNSD.T.-- FA	SSS--L. SSEK...D. YIDVNS..TF
MtCPK29b	PTRN.P.QPR	YHI AAKSD.T.Y. SASSSNANA	DHHQ...R. YIDMKT..SI
Glyma14g40090b	PHSHSDSRRT	S.PQLQ.QPG YPNRT.K.DP	S.SSSSGFDQ VAAR...D. YFD.KS..NL
AtCPK29	P.PTV.QGQT	SNPTSN.QP-	-----K.KPAP P.PPST.SG. I....NR. MIDLSA..DL
	140	160	180
LjCPK29a	KKELGRGQSG VTYLCVDKTT	RKEYACKSIA RAKLLSQQE	I EDVRREVMIL QHLSGQPNIV
MtCPK29a	.....TE...	GR.....S .....	E D.....
Glyma14g40090a	....S.... E.....	KR.....S .....	T.....
LjCPK29b	G.....F.....	E.S. GRKF.....P KR...TRKK	Q..K..I....T.....
MtCPK29b	G.....F.....	....TENA GRN.....S .....	K..I....D.....
Glyma14g40090b	ER.....F.I.R..TE...	GRK.....P KR..SKKKHT	D..K...L..
AtCPK29	H.....F.I..K.T..SN	GR.....S KR..IRRKD.	.....T.....
	200	220	240
LjCPK29a	EFRGAYEDRQ NVHLVME LCS	GGELFDRIIE	---KGNYS REAAATVMRQI VNVVHICNFM
MtCPK29a	....K...Y.V.K	.....	-----T. ....I.....V.H..
Glyma14g40090a	....K.....	.....A.....	.....
LjCPK29b	..K.....S.....Y	TA -----S.....	STF.....A.H..
MtCPK29b	....K.....E.S.....L	TA RITA.S.....	SIFK.....M.....A.H..
Glyma14g40090b	..K.....W.H.....L	TA -----S.....	SIF.....A.H..
AtCPK29	.....KD.L.....	.....K.....S.....	K..NIF.....V.H..
	260	280	300
LjCPK29a	GVMHRDLKPE NFLLATKDEN	AAVKATDFGL	SLFIEEGK VY REIVGSPYYV APEVLKRNYG
MtCPK29a	.....S.....	.....	I.L.....K.L...A.....S..
Glyma14g40090a	.....NHPD	.....	I.....I.....A.....
LjCPK29b	....MVS..DK	PL.....	V.....
MtCPK29b	....S..HK	PL.....	V.....
Glyma14g40090b	....N..PK	PL.....	K.L...A.....S..
AtCPK29	....V.....VSNE.D	SPI.....	V.....I.....A.....
	320	340	360
LjCPK29a	KEIDVWSAGI ILYILLSGVP	PFWAETEKGI	FEAILEAKLD LESAPWPSIS AVAKDLIRKM
MtCPK29a	....I.....	.....	Q.....G.....VA.....
Glyma14g40090a	.....	.....G.N.R.S.	.....GG.....A.....
LjCPK29b	.....	.....	.....
MtCPK29b	....I.....	.....Q.....G.....	.....VA.....
Glyma14g40090b	.....	.....G.N.R.S.	.....GG.....A.....
AtCPK29	.....V.M.....	.....G....T.	.....G.....TS...T.. ES.....
	380	400	420
LjCPK29a	LTYDPKKRIS ASEALEHPWM	KEGGEASDKP LDNAVLIRMK	QFRAMNKM KK LALKVIAENL
MtCPK29a	..S.....T.D.....	.....	.....
Glyma14g40090a	..NN.....T.A.....	.....	.....T.....
LjCPK29b	....	.....	.....
MtCPK29b	....S..T.D.....	.....	.....
Glyma14g40090b	..NN.....T.A.....	.....	.....T.....
AtCPK29	..IR.....T.A.....	TDT-KI	INS..V.....L.....
	440	460	480
LjCPK29a	SEEEIKGLKQ MFNNMDTDRS	GTITYEELKS GLSKLGSKLS	ESEIKQLMDA ADVDKSGTID
MtCPK29a	..D.....I.....	.....	.....
Glyma14g40090a	.....	.....F.....T.....	.....
LjCPK29b	.....	.....	.....
MtCPK29b	..D.....I.....	.....	.....
Glyma14g40090b	.....	.....F.....T.....	.....
AtCPK29	.....T.K.....E.	FD..RN ..HR.....T	.....E.....
	500	520	540
LjCPK29a	YHEFITATIN RHKLEKEENL	FKAFOYFDKD NSGYITRDEL	RHALTEYH LG DEAAAIDEVID
MtCPK29a	.....R.....	.....V.E..	Q..A..QM. ....T.....
Glyma14g40090a	..Q.....	.....S.....	Q...Q..QM. ....T.....
LjCPK29b	.....	.....V.E..	Q..A..QM. ....T.....
MtCPK29b	.....R.....	.....V.E..	Q..A..QM. ....T.....
Glyma14g40090b	..Q.....	.....S.....	Q...Q..QM. ....T.....
AtCPK29	..I..V...MH ..R.....	IE..K.....R..F.....	K.SM...GM. D.T....N
	560		
LjCPK29a	DVTDNDGRI NYQEFVAMMR	KGTLHDHEKE KPR	523
MtCPK29a	.....AT...	.....N.D..	525
Glyma14g40090a	.....K.....	.....I.I....Q	526
LjCPK29b	.....	.....	537
MtCPK29b	.....AT...	.....N.D..	533
Glyma14g40090b	.....K.....	.....I.I....Q	537
AtCPK29	.....E.....	.....T.S.P.L IR-	561

## RESULTS

---

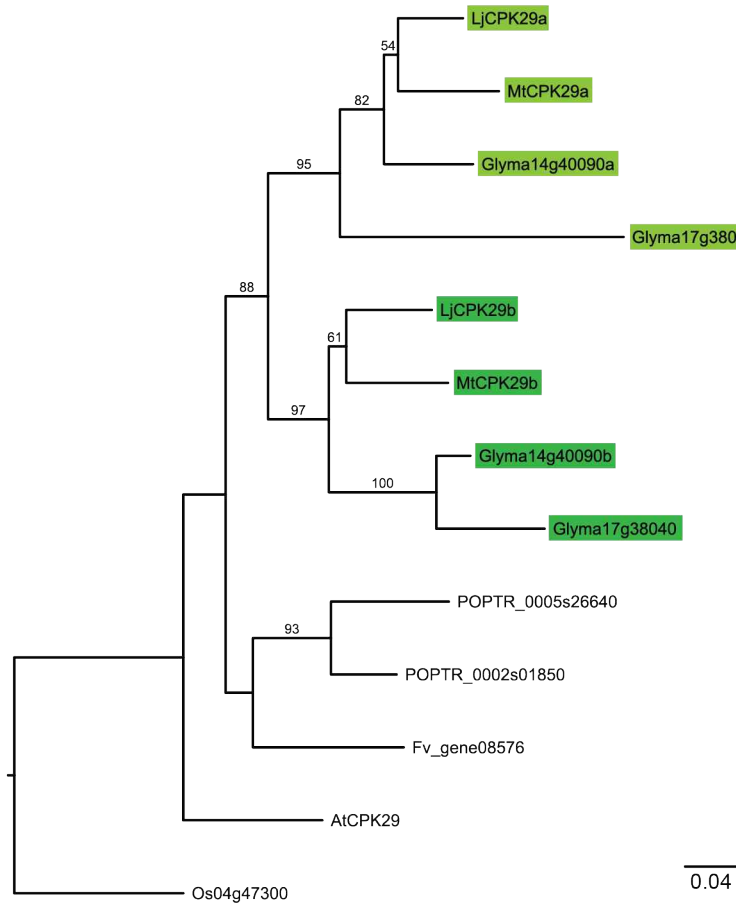


**Figure 15. Phylogenetic tree of the CPK29 cluster.**

The phylogenetic tree was calculated with RAxML-HPC2 based on a MAFFT alignment of the amino acid sequences of the protein kinase domains. Labels are bootstrap values of 100 bootstrap iterations performed. Only bootstrap values higher than 50 are indicated. Members of the CPK29a and CPK29b subgroups are highlighted in light and dark green, respectively. Notably these subgroups only contain sequences from legume species. Peptide sequences of *G. max*, *P. trichocarpa* and *O. sativa* (LOC\_Os04g47300) were downloaded from the phytozome website, the *F. vesca* sequence from the PFR strawberry server. The Genbank identifier of At CPK29 is AAF26765. The *G. max* Glyma14g40090 sequence, *L. japonicus* and *M. truncatula* CPK29 sequences are attached (see appendix 9.1.1). Scale bar represents the number of amino acid substitutions per site.

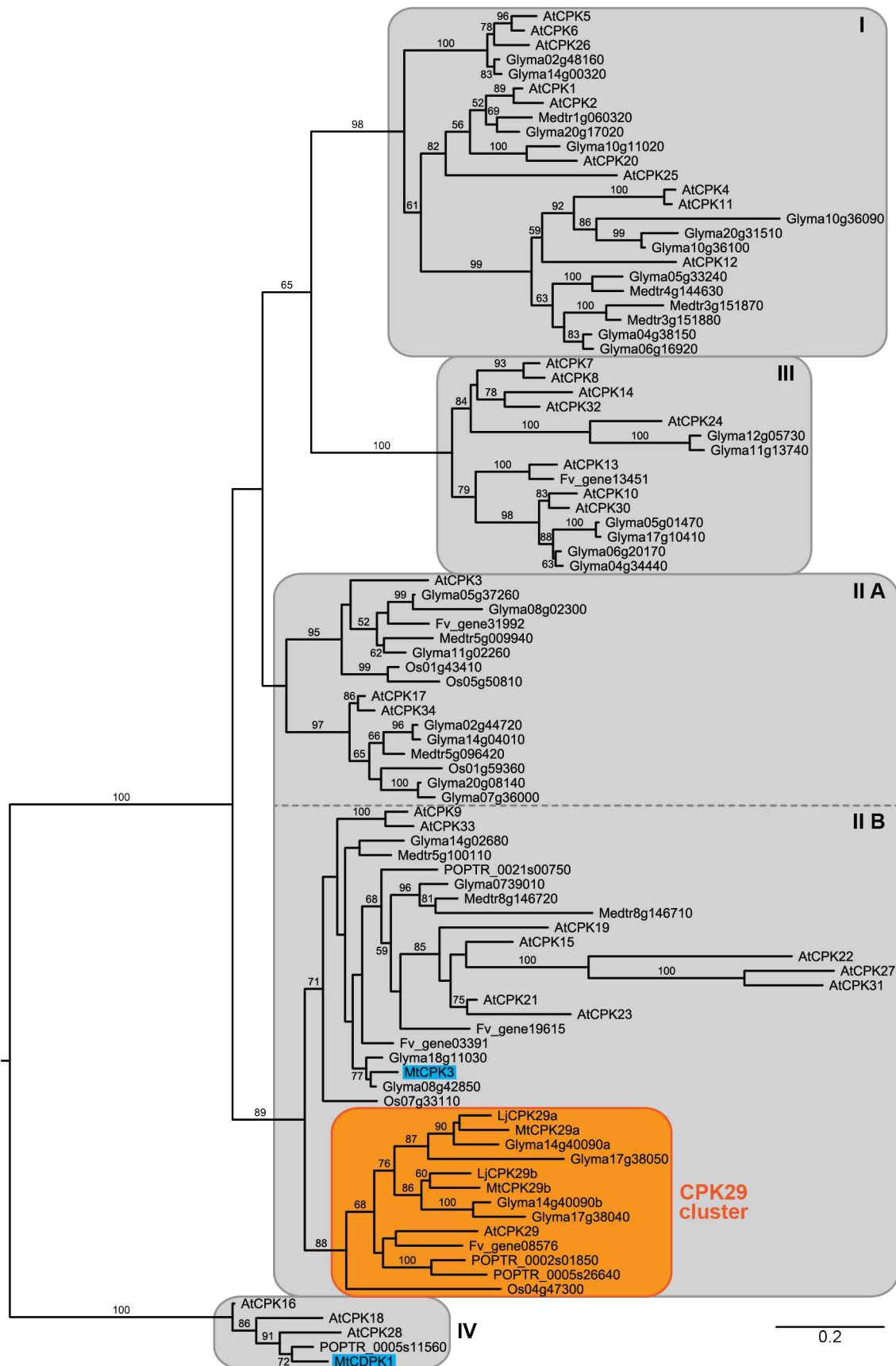
---

Next page:

**Figure 16. Phylogenetic tree of CPKs.**

The phylogenetic tree was calculated with RAxML-HPC2 based on a MAFFT alignment of the amino acid sequences of the protein kinase domains. Labels are bootstrap values of 100 bootstrap iterations performed. Only bootstrap values higher than 50 are indicated. CPK Subgroups I to IV are displayed according to Cheng et al., 2002. To reflect the results of the phylogenetic analysis in this study, subgroup II is divided into II A and II B. Orange box depicts the CPK29 cluster. MtCPK3 and MtCDPK1 are highlighted in blue. Scale bar represents the number of amino acid substitutions per site. Sequences of *G. max*, *P. trichocarpa*, *O. sativa*, and *M. truncatula* have been downloaded from the Phytozome website. *F. vesca* sequences were retrieved from the PFR strawberry server. Genbank identifiers of the *A. thaliana* CPKs are the following: CPK1 (BAB08991), CPK2 (AAF76372), CPK3 (AAK60302), CPK4 (CAB82124), CPK5 (CAB80248), CPK6 (AAB86506), CPK7 (AAK32802), CPK8 (AAA67658), CPK9 (BAB02824), CPK10 (AAF27092), CPK11 (BAA04830), CPK12 (BAA97242), CPK13 (AAC14412), CPK14 (AAB63555), CPK15 (AAK59500), CPK16 (AAD03569), CPK17 (BAB10036), CPK18 (CAB81516), CPK19 (AAC28510), CPK20 (AAC79604), CPK21 (CAB80837), CPK22 (CAB80836), CPK23 (CAB80839), CPK24 (AAD24851), CPK25 (AAD21468), CPK26 (CAB80488), CPK27 (CAB80835), CPK28 (BAB10426), CPK29 (AAF26765), CPK30 (AAF27092), CPK31 (AAF27092), CPK32 (CAB66110), CPK33 (AAG51192), CPK34 (BAB10036). *G. max* Glyma14g40090 sequences, *L. japonicus* and *M. truncatula* CPK29 sequences are attached (see appendix 9.1.1).

## RESULTS



## RESULTS

---

In the genomes of *P. trichocarpa*, *F. vesca* and *O. sativa* CPK29 orthologs with two alternative first exons could not be found. Closely related CPK sequences found by blasting the Lj CPK29a genomic sequence against the genomes of these plant species were included in the phylogenetic analysis (Figure 16). The protein sequences of POPTR\_0002s01850, POPTR\_0005s26640, Fv\_gene08576 and Os04g47300 were part of the monophyletic CPK29 cluster containing At CPK29 (Figure 15). The two CPKs of *M. truncatula*, MtCPK3 and MtCDPK1, already described to be involved in root nodule symbiosis were not part of the CPK29 cluster (Ivashuta et al., 2005; Gargantini et al., 2006). MtCPK3 is a member of the class II B, like the CPK29 cluster, but is clearly located at a different branch of the phylogenetic tree. MtCDPK1 is part of class IV and therefore not closely related to the CPK29 cluster. Two different gene models for At CPK29 are annotated in TAIR, At1g76040.1 and At1g76040.2. At1g76040.2 consists of a unique first exon followed by seven exons and its second exon is part of the first exon of At1g76040.1. Hence, the transcript of At1g76040.1 is shorter than the one of At1g76040.2. The peptide sequence of At1g76040.1 is 323 amino acids long. It has an incomplete protein kinase domain and four EF hand motifs, but has no N-terminal variable region. In contrast, the longer transcript At1g76040.2 (561 amino acids) comprises all the domains typical for CPKs and is the representative gene model of At CPK29 in TAIR.

## 2.3 The Temperature-Sensitive Nodulation and Root Development Mutant *brush*

In a forward genetic screen of an EMS mutagenized population of *L. japonicus* (Perry et al., 2003) plants of the line SL0979 exhibited abnormal root growth combined with decreased nodulation efficiency. These plants with short and thick roots and a disturbed apical root region showed an increased root hair density and were therefore denominated *brush* mutants (Maekawa-Yoshikawa et al., 2009).

The *brush* phenotype is temperature-sensitive, mutants grown at 26°C have shorter roots and less nodules compared to mutants grown at 18°C. Nevertheless, at 18°C mutant roots are still significantly different from wild-type plants. The mutant phenotype points to a mutation of a gene related to plant hormone signalling pathways, but none of the phytohormones tested, such as ethylene, auxin, abscisic acid and gibberellin, is able to restore the wild-type phenotype (Maekawa-Yoshikawa et al., 2009). The F2 progeny of a cross of a *brush* mutant with a *L. japonicus* MG-20 plant and progeny of a backcross were analysed and the root and nodulation phenotype cosegregated. Therefore, Maekawa-Yoshikawa and colleagues (2009) suggested that the pleiotropic phenotype of *brush* is induced either by a single mutation or very closely linked mutations. The SSR marker TM0312 on the short arm of chromosome 2 at 8.8 cM (<http://www.kazusa.or.jp/lotus/clonelist.html>) is closely linked to *BRUSH* (Maekawa-Yoshikawa et al., 2009). So far no gene involved in nodulation or root morphology is known in the target region, indicating that *BRUSH* is a novel gene, which interconnects root and nodule development.

During this study, a gene encoding a putative cyclic nucleotide-gated channel (CNGC) located in the *brush* target region was found to carry an EMS-induced mutation. CNGCs are conducting cations and have been identified in the genomes of various plant species, such as *A. thaliana* (Köhler et al., 1999; Leng et al., 1999), barley (Schuurink et al., 1998), tobacco (Arazi et al., 1999) and rice (Bridges et al., 2005). The 20 CNGCs of *Arabidopsis* are separated into five phylogenetic groups (Mäser et al., 2001). The protein domain structure of CNGCs consists of six transmembrane domains and a pore domain between the fifth and the sixth (Figure 17; Talke et al., 2003). In addition, overlapping calmodulin- and cyclic nucleotide-binding sites are located in the C-terminus (Arazi et al., 2000; Köhler and Neuhaus, 2000; Talke et al., 2003). A working model for the regulation of plant CNGCs suggests that upon binding of cyclic nucleotides the CNGC is activated and cations can pass the channel. If Ca<sup>2+</sup> levels increase in the cytosol, binding of Ca<sup>2+</sup>/calmodulin to the CNGC's calmodulin-binding domain interferes with cyclic nucleotide binding and leads to a closing of the channel (Kaplan et al., 2007). Most CNGCs are targeted to the plasma membrane (Gobert et al., 2006; Borsics et al., 2007; Frietsch et al., 2007), exceptions are for example AtCNGC7 and AtCNGC8, which have been shown to be present in the tonoplast (Chang et al., 2007).

## RESULTS

---

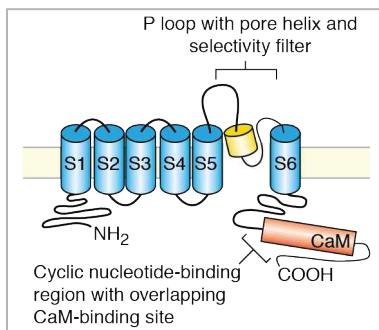


**Figure 17. Schematic domain structure of plant CNGCs.**

Plant CNGCs consist of six transmembrane domains (S1 – S6, blue), a p loop with a pore helix (yellow) and a C-terminal cyclic nucleotide-binding region with an overlapping calmodulin binding domain (red). Figure from Talke et al., 2003.

In contrast to plant CNGCs, the calmodulin-binding domain of most animal CNGCs is found at the N-terminus (Liu et al., 1994; Matulef and Zagotta, 2003). Interestingly, animal CNGCs form heterotetramers (Chen et al., 1993; Varnum and Zagotta, 1996; Matulef and Zagotta, 2003). Whether CNGCs of plants also assemble as heterotetramers is not known, but appears to be possible (Yoshioka et al., 2006; Kaplan et al., 2007; Ma et al., 2009). Notably, the pore amino acid composition of plant CNGC pores is clearly different from animal CNGC pore sequences (Talke et al., 2003; Kaplan et al., 2007).

Plant CNGCs have so far been discovered to be involved in ion homeostasis, plant immunity and plant development (Kaplan et al., 2007). AtCNGC1 and its homolog in tobacco, NtCBP4, are supposed to participate in heavy metal uptake (Sunkar et al., 2000). AtCNGC3 and AtCNGC10 have been shown to transport monovalent ions (Gobert et al., 2006; Borsics et al., 2007) and AtCNGC18 is indispensable for the polarized growth of pollen tubes (Frietsch et al., 2007). Two closely related CNGCs in *A. thaliana*, AtCNGC2 (DND1) and AtCNGC4 (DND2, HLM1), are involved in plant disease resistance (Köhler and Neuhaus, 1998; Leng et al., 1999; Clough et al., 2000; Balague et al., 2003; Jurkowski et al., 2004). The mutants *dnd1* and *dnd2* (*defense, no death*) and *hlm1* (*hypersensitive response-like lesion mimic*) with their dwarf phenotypes show an enhanced pathogen resistance. They are characterized by defects in the hypersensitive response (HR) after infection with plant pathogens and increase of salicylic acid levels (Yu et al., 1998; Jurkowski et al., 2004). Nevertheless, *dnd1* mutants still exhibit gene-for-gene-mediated resistance (Yu et al., 1998) (since Jones and Dangl (2006) referred to as effector triggered immunity). A homolog of AtCNGC4 has also been identified in barley (Rostoks et al., 2006). Mutants carrying an AtCNGC11/12 chimeric gene, generated by a 3 kb deletion that fused the two genes that are arranged in tandem, are again more resistant to the analysed plant pathogens. In contrast to *dnd* mutants, the HR is not impaired in AtCNGC11/12 mutants (Yoshioka et al., 2006). The two gene pairs AtCNGC11/AtCNGC12 and AtCNGC19/AtCNGC20 are arranged in tandem, and the expression of AtCNGC19 and AtCNGC20 is induced upon salt stress (Kugler et al., 2009). In conclusion, these examples show that plant CNGCs are connected to various physiological and developmental processes and potentially link cyclic nucleotides with calcium signalling (Talke et al., 2003; Kaplan et al., 2007).

The aim of this study was a detailed characterisation of the *brush* mutant phenotype after temperature shifts and the identification of *BRUSH* by map-based cloning. Therefore, F2 individuals were screened for informative recombination events in the target region identified by Maekawa-Yoshikawa and associates (2009). Subsequent phenotyping of their F3 progenies allowed narrowing down the interval that supposedly should contain *BRUSH* to approximately 37 kb. Within this narrow region on contig CM0435, a gene encoding a putative CNGC was found to carry an EMS-induced point mutation that introduced an amino acid exchange at the N-terminus of the protein. Four additional genes also predicted to encode CNGCs are located on the same contig.

### 2.3.1 Phenotypic Characterization of *brush* Mutants

Hitherto the phenotype of *brush* mutants was analyzed when they were constantly grown at 18°C (permissive) or 26°C (restrictive). Temperature shifts at different developmental stages of the plants were conducted to test whether the temperature sensitivity of the mutants affects their phenotype throughout the whole development or only at distinct time points.

In particular, we wanted to analyze whether the nodulation defect could be uncoupled from the root phenotype. This question was especially relevant since the observed nodulation defect might be an indirect consequence of the impaired cell identity and development in *brush* (Maekawa-Yoshikawa et al., 2009). Temperature shifts only few days after germination (dpg) were supposed to reveal a possible temperature sensitivity during early developmental stages. In contrast, temperature shifts a few weeks after germination were performed to check whether the mutant phenotype still emerges when the mutants were grown for longer time periods at lower temperatures before shifting them to restrictive temperatures.

#### 2.3.1.1 Temperature Shifts at Early Developmental Stages

To analyze the influence of temperature changes on the root and nodulation phenotype of *brush* seedlings during early development, they were shifted from 18°C to 26°C two and four dpg and their root and shoot lengths as well as their nodule number were scored. The shoot lengths were evaluated to assess a possible correlation between shoot and root lengths. Shoots of 3-week-old *brush* mutants that were grown at 26°C or shifted two or four dpg were shorter compared to those of wild-type plants (Figure 19A). In contrast, shoots of *brush* mutants cultivated at 18°C reached wild-type levels (Figure 19A). Mutant roots were significantly shorter in all four treatments than wild-type roots (Figure 18, Figure 19B).

## RESULTS

---

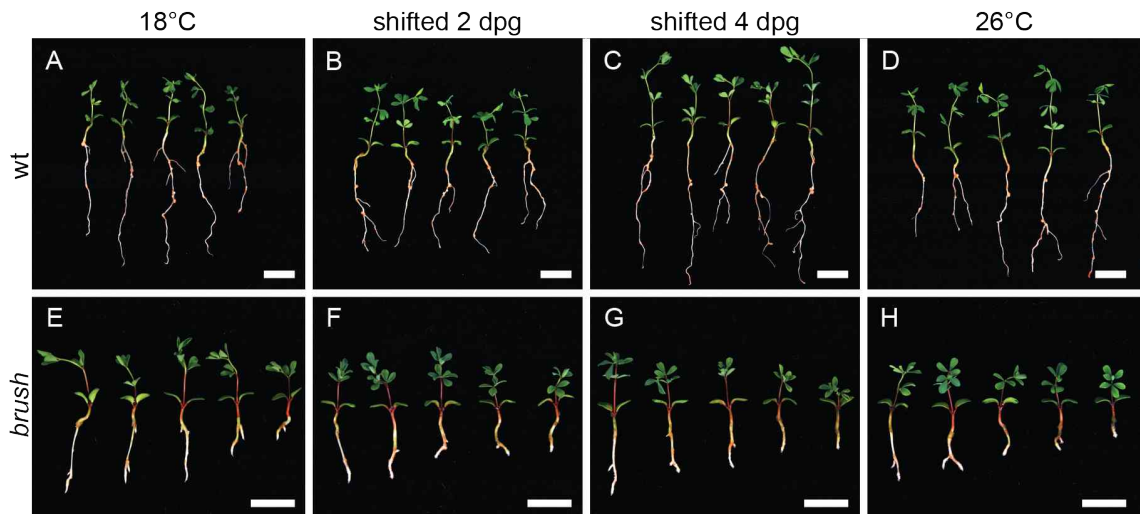


**Figure 18. Wild-type and *brush* plants after early temperature shifts.**

*L. japonicus* Gifu (A - D) and *brush* (E - H) seedlings were grown constantly at 18°C (A and E) and 26°C (D and H) or shifted 2 dpg (B and F) and 4 dpg (C and G) from 18°C to 26°C. One week after the germination, seedlings were inoculated with *M. loti* MAFF *DsRed*. Pictures were taken 2 wpi. Scale bars = 1 cm.

Furthermore, the temperature shifts few days post germination showed that the ability to form nodules was temperature-dependent in *brush* mutants. At 18°C, mutants formed significantly less nodules than wild-type plants (Figure 19C, Figure 20A and B). The rhizobium strain *Mesorhizobium loti* MAFF 303099 *DsRed* constitutively expresses a red fluorescent protein (Maekawa-Yoshikawa et al., 2009) and therefore provided an important tool for imaging the rhizobial infection process. Compared to wild-type plants, nodules of *brush* mutants were smaller and did not show the pink color that usually indicates the presence of leghemoglobin in nitrogen-fixing nodules (Downie, 2005; Figure 20A and B). Moreover, nodule primordia on mutant roots were found to develop many superficial infection threads (Figure 20C arrowhead). In contrast to those of wild-type roots (Figure 20A, arrowhead), most of the mutants' primordia were apparently not colonized by rhizobia and therefore called "white bumps". Interestingly, mutants that were grown constantly at 26°C showed neither nodules nor white bumps, whereas mutants shifted two or four dpg did not form any nodules but very few or few white bumps, respectively (Figure 19C and D). Since the temperature did not change after inoculation with rhizobia, the ability of *brush* plants to form nodule primordia seemed to be dependent on the temperature the roots encountered during the first days after germination (Figure 19C and D).

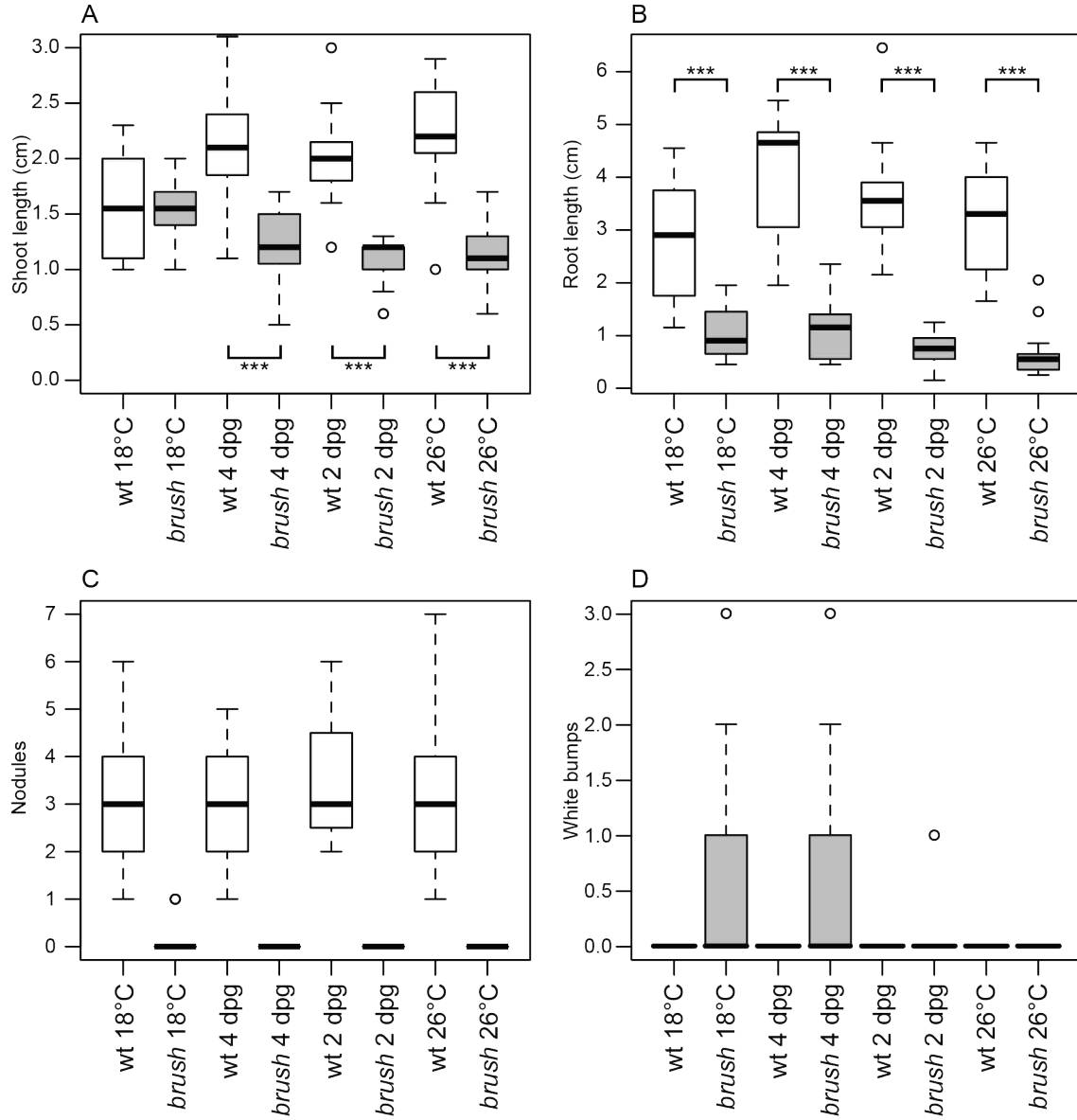


**Figure 19. Root and shoot lengths and nodulation phenotypes after early temperature shifts of wild-type and *brush* seedlings.**

*L. japonicus* Gifu wild-type (white boxplots) and *brush* mutant plants (grey boxplots) were grown at 18°C and 26°C constantly or shifted 2 or 4 dpg from 18°C to 26°C. Plants were inoculated 7 dpg with *M. loti* MAFF *DsRed*. Two wpi shoot (**A**) and root (**B**) lengths were measured (cm) and the number of nodules (**C**) and white bumps (**D**) per root system was assessed. The thick line within the boxplots represents the median (n = 11–18).

(**A**) Shoots of wild-type seedlings were longer after the temperature shifts 2 and 4 dpg and when the plants were grown at 26°C. At 18°C the shoot lengths did not differ.

(**B**) *brush* mutants exhibited shorter roots compared to wild-type plants in all the four treatments.

(**A and B**) The significance of differences between the different treatments was tested by ANOVA followed by Tukey's honestly significant difference (HSD) test. \*\*\* p-value < 0.001.

(**C**) Only three *brush* mutants out of 18 showed one fluorescent nodule at 18°C; no nodules were formed after temperature shifts 2 and 4 dpg and at 26°C.

(**D**) Instead of nodules, *brush* mutants produced few white bumps at 18°C and after the temperature shift 4 dpg. Only one seedling out of 14 had one white bump after the temperature shift 2 dpg.

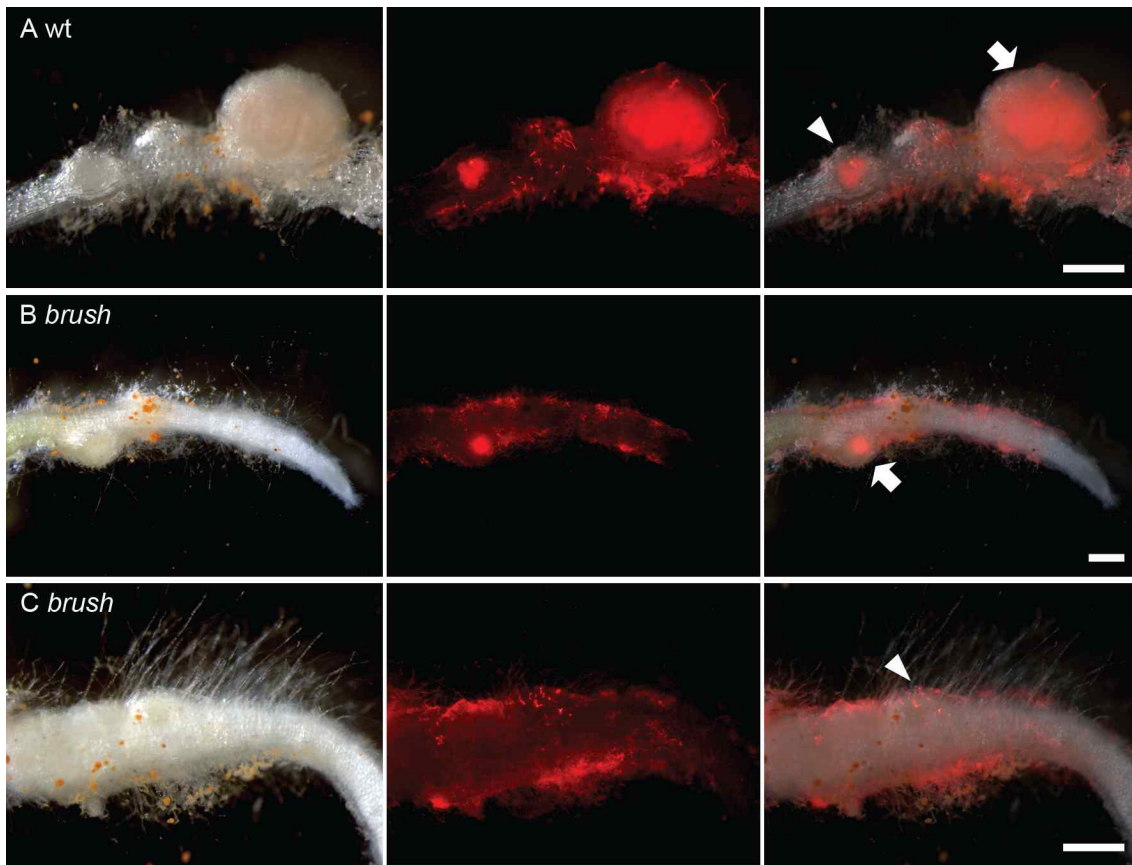


**Figure 20. Nodulation phenotypes of wild-type and *brush* roots.**

*L. japonicus* Gifu (A) and *brush* (B and C) plants were grown at 18°C and inoculated with *M. loti* expressing *DsRed* 1 wpg. Pictures were taken 2 wpi. Wild-type roots showed pink and red fluorescing nodules (A, arrow) and nodule primordia infected with rhizobia (A, arrowhead). *brush* mutant roots formed few nodules (B, arrow), instead predominantly white bumps emerged (C, arrowhead). Left panels: bright field images; middle panels: red fluorescence of *M. loti* *DsRed*; right panels: overlay of middle and left panels. Scale bars = 500 µm.

### 2.3.1.2 Temperature Shift Two Weeks after Germination

Since roots of *brush* seedlings grown at 26°C were very short (Figure 18H, Figure 19B), the number of infection threads on these roots was difficult to determine and a concealing effect of the short roots on infection thread development could not be excluded. Therefore, seedlings were grown for two weeks at 18°C before half of them was shifted to 26°C to allow the plants to grow longer at the permissive temperature so they could produce longer roots. Although mutant plants were cultivated at the permissive temperature for two weeks, their root lengths and infection thread numbers did not reach wild-type levels. Mutant roots were significantly shorter and the number of infection threads per cm of root system was significantly lower compared to the wild-type, irrespective of the temperature shift (Figure 21).

## RESULTS

---

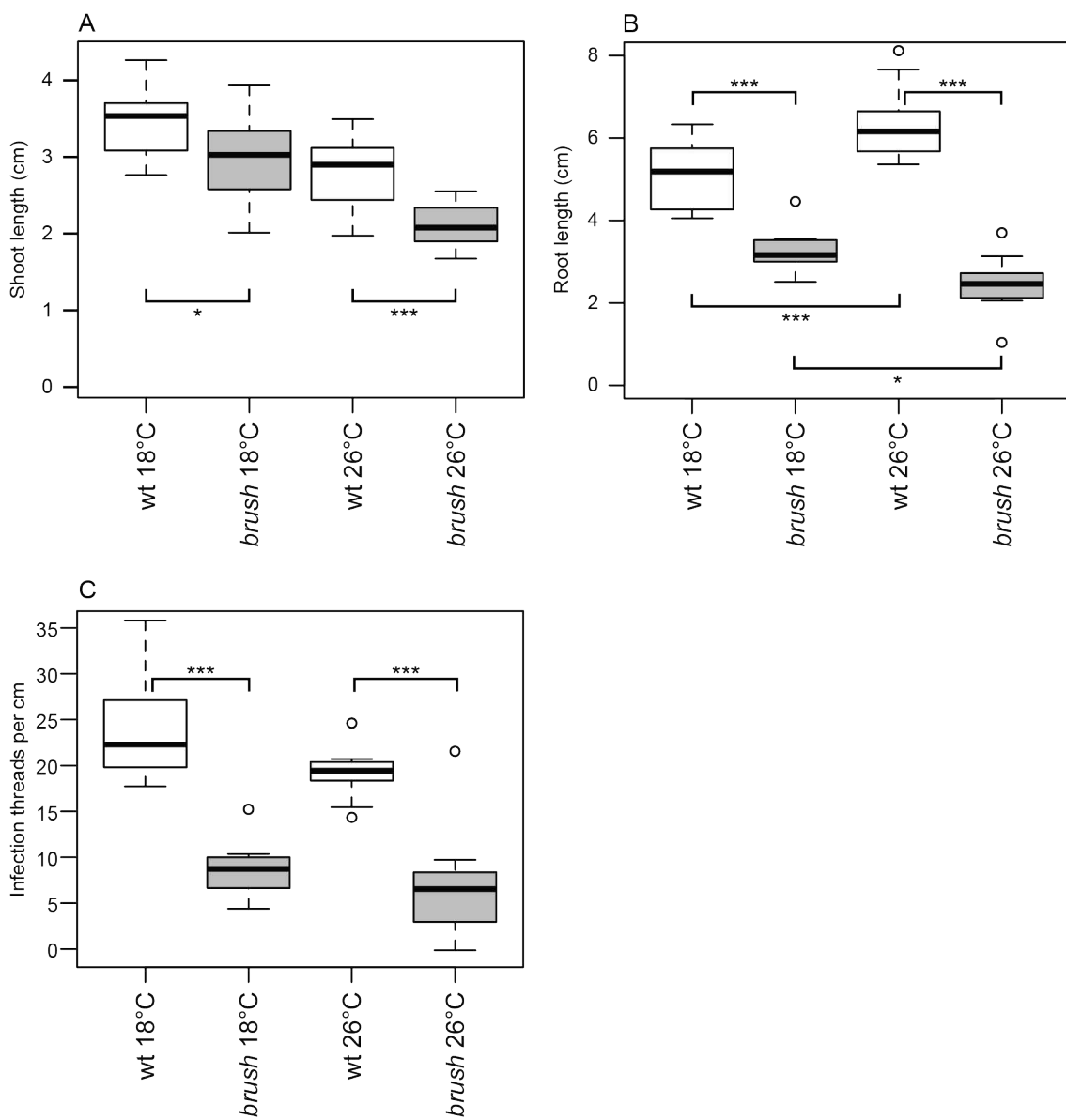


**Figure 21. Plant growth and infection threads of wild-type and *brush* plants after temperature shift two weeks post germination.**

*L. japonicus* Gifu wild-type (white boxplots) and *brush* mutant plants (grey boxplots) were grown at 18°C constantly or shifted 2 wpg to 26°C. The seedlings were inoculated with *M. loti* MAFF DsRed 1 week after the temperature shift.

Two weeks after the inoculation, shoot (**A**) and root (**B**) lengths were measured (cm) and infection threads (**C**) were counted. The thick line within the boxplots represents the median ( $n = 12$ ).

(**A**) At 18°C and at 26°C, shoots of *brush* plants were shorter than those of wild-type plants (Student's t-test, \* p-value < 0.05, \*\*\* p-value < 0.001).

(**B**) Whereas wild-type roots were longer at 26°C than at 18°C, the root length of *brush* mutants decreased at the higher temperature. At both conditions mutant roots were shorter than wild-type roots. (ANOVA followed by Tukey's HSD test, \* p-value < 0.05, \*\*\* p-value < 0.001).

(**C**) Less infection threads per cm root formed on *brush* mutant roots compared to wild-type roots at 18°C and at 26°C (Student's t-test, \*\*\* p-value < 0.001).

### 2.3.1.3 Temperature Shift Six Weeks after Germination

The nodulation phenotype of *brush* mutants grown for six weeks at 18°C before the temperature shift and inoculation with rhizobia was analyzed to check whether these plants were still impaired in nodulation although wild-type and *brush* plants were similar regarding root architecture and morphology of the root tips (Figure 22) and whether shifting to the restrictive temperature later during plant development still has an impact on the nodulation phenotype.

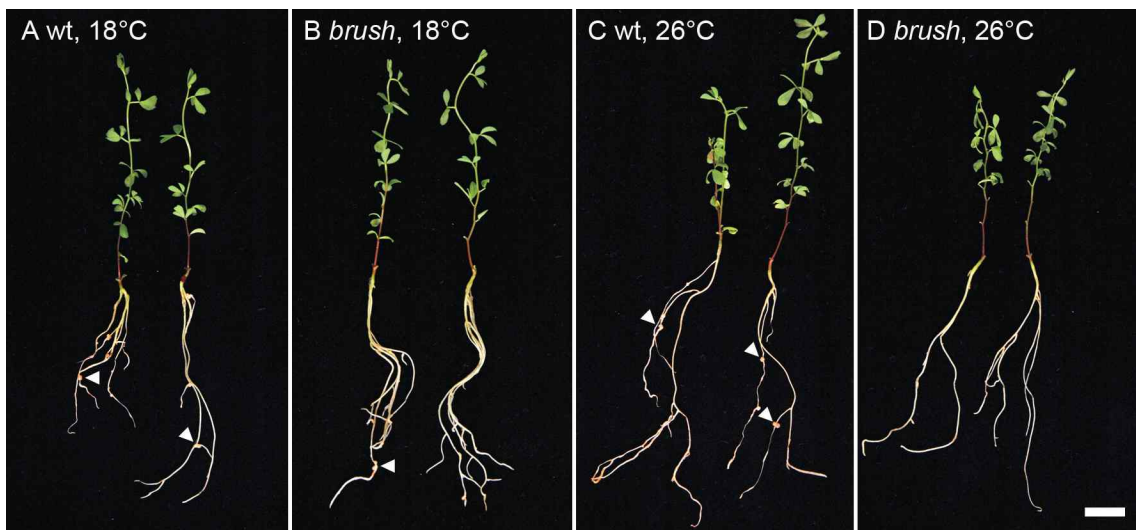


**Figure 22. Wild type-like roots of *brush* mutants.**

*L. japonicus* Gifu (**A, C**) and *brush* mutant (**B, D**) plants were grown for 6 weeks at 18°C. Half of the plants was then shifted to 26°C (**C, D**). One day after the temperature shift the plants were inoculated with *M. loti* MAFF expressing *DsRed* and pictures were taken 3 wpi. Arrowheads point to nodules. Scale bar = 1 cm.

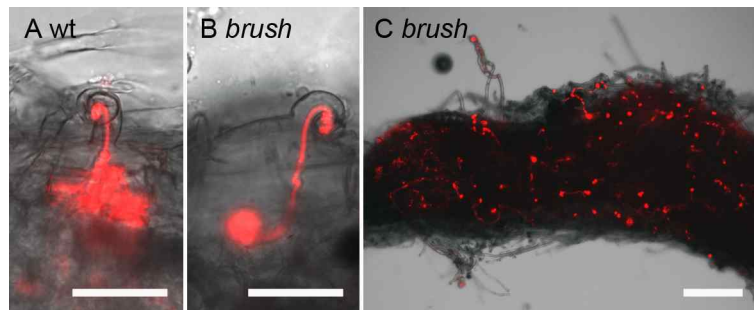


**Figure 23. Infection threads of wild type-like *brush* roots.**

*L. japonicus* Gifu (**A**) and wild type-like *brush* mutant roots (**B, C**) cultivated at 18°C for 6 weeks, inoculated with *M. loti* MAFF *DsRed* and analysed 3 wpi. (**A**) Rhizobia (red fluorescence) were released from the infection thread into the root cortex of wild-type plants. (**B**) *brush* infection thread formed a dot-like structure. (**C**) Infection threads with dot-like ends covered *brush* nodule primordia. Scale bars = (A, B) 50 µm, (C) 250 µm.

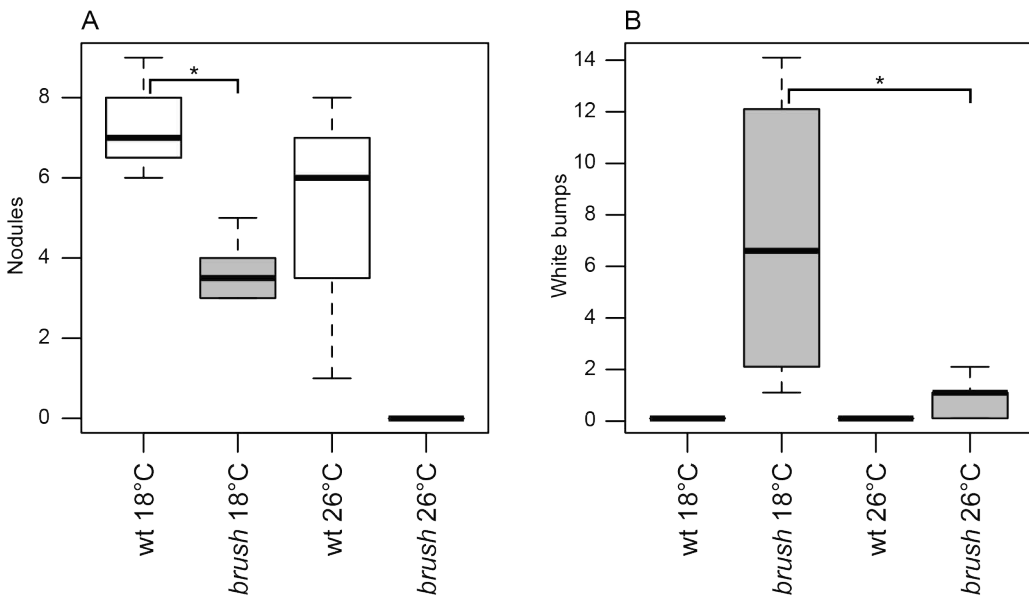


**Figure 24. Nodulation phenotype of wild type-like *brush* roots.**

*L. japonicus* Gifu wild-type plants and *brush* mutants were grown for six weeks at 18°C before shifting half of them to 26°C. One day after the temperature shift the plants were inoculated with *M. loti* MAFF DsRed. Nodules (**A**) and white bumps (**B**) per root system were counted 3 wpi (n = 3-6). (**A**) At 18°C, *brush* mutants had less nodules compared to the wild type (Welsh's t-test, \* p-value < 0.05). When shifted to 26°C, *brush* roots did not form any nodules. (**B**) The number of white bumps on *brush* roots was reduced when mutants were shifted to 26°C (Welsh's t-test, \* p-value < 0.05).

Analysis of the nodulation three weeks after inoculation with rhizobia revealed significant differences between wild-type and *brush* plants in this experiment. At 18°C *brush* mutants formed significantly less nodules compared to wild type plants and at 26°C no nodule was apparent (Figure 24A). Instead, white bumps emerged at mutant roots in both conditions (Figure 23C), which never formed on wild-type roots (Figure 24B). The number of white bumps on *brush* roots was significantly higher at the permissive temperature (Figure 24B).

Infection threads of *brush* mutant roots differed from those of wild-type roots (Figure 23). At the infection thread tip of wild-type roots rhizobia were released into the cortex cells (Figure 23A), whereas infection threads of *brush* mutants very often ended in a dot-like structure (Figure 23B). Apparently rhizobia were stuck and their release into the root cortex was hampered. These abnormal infection threads were found preferentially on the surface of mutant nodule primordia and white bumps. Nodule organogenesis was already initiated, but rhizobia seemed to be unable to colonize the developing nodule (Figure 23C). Consequently, the wild type-like root phenotype of *brush* mutants did not rescue their impaired infection and nodulation. These observations demonstrated that the symbiotic defect of *brush* was not a consequence of the lack of a proper root system, thus implying a direct role of *BRUSH* in the infection and nodulation process.

### 2.3.2 Map-Based Cloning of *brush*

Maekawa-Yoshikawa and associates (2009) positioned the mutation responsible for the phenotype of *brush* mutants on the short arm of chromosome 2 at 8.8 cM, linked to the marker TM0312 (G177; Maekawa-Yoshikawa et al., 2009). Since the target interval was still too large for the identification of candidate genes, a large-scale recombinant screen of F2 plants (MG-20 x *brush*) was initiated to narrow down the target region.

#### 2.3.2.1 Screening for Recombinants

During the recombinant screen more than 1700 F2 plants (MG-20 x *brush*) were genotyped to identify plants with recombinant chromosomes in the target interval. This was done by PCRs with fluorescently labelled simple sequence repeat (SSR) ‘power mapping’ markers (Groth, 2010; Figure 25; Supplementary Table 1), a subsequent fragment analysis run on a capillary sequencer and data analysis using the GeneMapper® software.

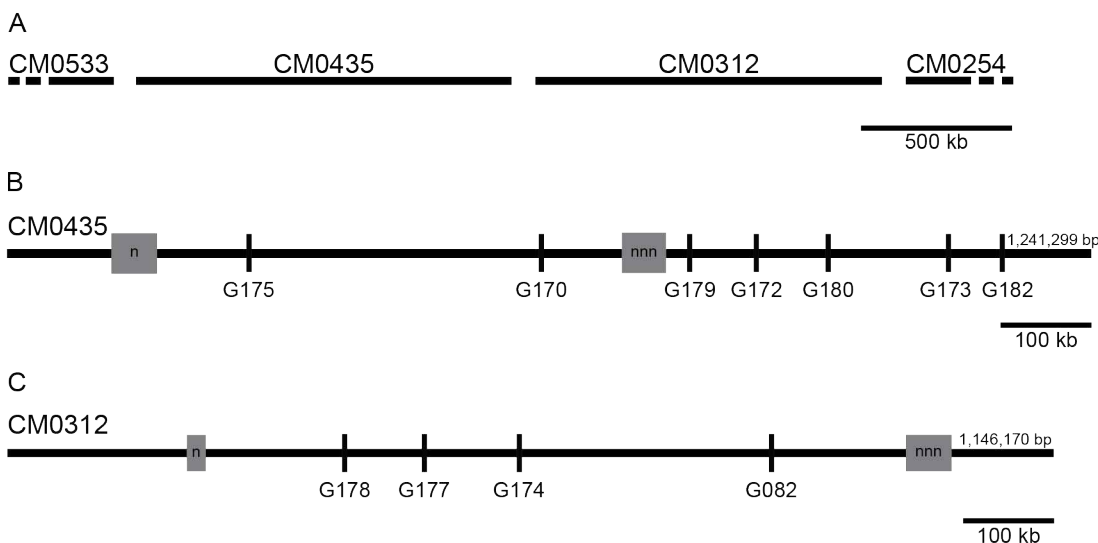


**Figure 25. SSR mapping marker positions on contigs of *L. japonicus* chromosome 2.**

(A) Order of contigs on the short arm of chromosome 2 around the *brush* target interval. CM0533 and CM0254 are only shown partially. (B and C) Schemes of the contigs CM0435 (B) and CM0312 (C) with the analyzed SSR power mapping markers indicated. Boxes with ‘nnn’ represent gaps of approximately 50 kb in the genome sequence assembly. Boxes with ‘n’ represent regions with 13 (CM0435) or 6 (CM0312) gaps of approximately 100 bp distributed in the genome sequence. Scale bars = 500 kb (A), 100 kb (B and C).

In total, 20 of 1148 tested F2 individuals showed recombination events between the flanking markers G172 and G174. This roughly results in a genetic distance of 0.87 cM. The calculated physical distance from G172 to G174, without the gap between CM0435 and CM0312 taken into account, was 939 kb. Since in the *L. japonicus* genome 1 cM corresponds to approximately 1 Mb (Ito et al., 2000; Hayashi et al., 2001), the genetic and the physical distances are similar in this region.

## RESULTS

---

F2 plant	F3 seedbag	F3 phenotypes						F2 genotypes						
		wt root wt nodules	wt root white bumps	wt root no nodules	mutant root wt nodules	mutant root white bumps	mutant root no nodules	G175	G170	G179	G180	G173	G182	
L2704	76421	0	0	0	0	4	6	H	H	H	G	G	G	G
L2707	76961	0	0	0	3/1w	2	8	G	G	G	G	G	H	H
L2709	76963	0	0	0	2/2w	3	7	H	G	G	G	G	G	G
L2717	76426	6	1	1	0	1	3	G	G	H	H	H	H	H
L2717	77247	19/2w	1	0	0	0	9							
L5932	81548	0	0	0	0	0	9	G	G	G	G	G	H	H
L5935	81414	10	0	0	0	0	0	M	M	M	M	M	M	
L5936	82570	10	0	0	0	2	7	H	H	H	G	G	G	G
L5936	84608	22/9w	0	1	0	0	8							
L5938	81549	2	0	4	0	0	2	H	H	H	H	H	G	G
L5938	82329	29/2w	2	1	0	10	8	G	G	G	G	H	H	
L5939	81524	2	0	1	0	0	17				G		G	H
L5939	82330	0	8	0	3/3w	18	0	G	G	G	G	G	G	H
L5940	81550	0	0	0	0	0	9	G	G	G	G	G	H	H
L5940	82331	0	0	0	1	9	15				G		G	
L5941	82332	0	0	0	0	4	27	G	G	G	G	G	H	H
L5943	81527	0	0	0	0	0	7	G	G	G	G	G		G
L5944	81528	0	0	0	0	4	18	G	G	G	G	G	H	H
L5944	82335	0	0	0	2/1w	17	6				H	H	H	H
L5945	81421	5	0	2	0	0	3	H	H	H	H	H	H	G
L5945	82336	16	0	0	0	1	9				H	H	H	
L5949	81551	9	0	2	0	0	3	H	H	H	H	H	H	G
L5949	82340	19/5w	0	0	0	1	5				G			
L5952	82343	0	0	0	0	17	9	G	G	G	G			G
L5953	83139	17	1	1	0	2	5	H		H				H
L5953	83277	15	0	0	1	5	4			H				
L5954	81552	11	1	2	0	0	3	H	H	H	H	H	H	
L5954	82344	13/2w	3	0	2/2w	4	0				G			
L5955	81429	2	0	2	0	0	3	H	H	H	H	H	H	
L5955	82345	17/4w	0	1	0	0	6			M	M	M	H	H
L6489	81803	19	0	0	0	0	0			M	M	M	M	H
L6489	83287	55	0	0	0	0	0			M	M	M	M	H
L6490	83288	35	0	0	0	0	0			H	H	H	H	
L6492	82569	13	0	0	0	0	3			H	H	H	G	G
L6492	84139	12/2w	1	1	0	0	13			H	H	H	H	
L6495	81542	14	0	0	0	0	4			H	H	H	H	H
L6497	83290	0	0	0	0	1	17			G	G	G		
L6498	81543	10	0	0	0	0	0			M	M	M	H	H
L6499	81804	12	0	2	0	0	1			H	H	H	G	G
L6499	83292	16/2w	1	0	0	3	2			H	H	H	G	G
L6499	84136	9/2w	2	2	0	0	6			H	H	H	H	
L6500	81809	14	0	0	3	0	1			H	H	H	G	G
L6500	83293	35/2w	2	1	0	2	14			H	H	H	H	
L6501	81544	14	2	2	0	1	3			H	H	H	H	G
L6501	83294	21/4w	3	0	0	0	2			G	G	G		
L6919	82572	0	0	0	0	2	6			G				
L6920	83325	32/11w	0	0	0	1	8			G				H

**Figure 26. F2 genotypes and corresponding F3 progeny phenotypes.**

F3 phenotypes: plants with indicated phenotype were counted. X/Yw, Y of X plants showed nodules and white bumps. F2 genotypes: M, MG-20; G, Gifu; H, Heterozygous; empty fields, marker not analyzed or allele call not clear. G-numbers refer to SSR markers (Supplementary Table 1). F2 plants in red represent closest recombinants; the F4 progeny of F2 plants with grey background was analyzed. F3 plants were grown at 26°C and their phenotypes were scored 3 wpi with *M. loti* *DsRed*.

Individual plants with recombination events between the tested markers or with missing allele calls were subjected to a second round of DNA extraction and refined mapping procedures. To ascertain the genotypes of recombinant plants, the phenotypes of their progeny, the F3

## RESULTS

generation, were analysed. In the F3 screen the root morphology and nodulation development at 26°C was determined. In addition to the already described mutant phenotypes, some F3 progenies also included plants with either wild type-like roots and white bumps or short mutant roots with small nodules. Therefore, these different phenotypes were recorded separately (Figure 26). The F2 genotyping and the following F3 phenotyping led to a further refinement of the target region. The genotype of the F2 plants L2717, L5936, L6492, L6499 and L6500 was heterozygous at G179 and Gifu at G173; their progeny was segregating wild-type and mutant plants. F2 plant L2704, a mutant plant with only mutant progeny, was also heterozygous at G179 and carried Gifu alleles at G173. Therefore, the mutation should be located between the markers G170 and G173. To further refine the target interval, SNPs between the genomes of MG-20 and Gifu were sequenced (Figure 27; Figure 28B and C). Finally, a region consisting of 37,473 bp between SNP24-1 and SNP43 could be determined that should include *BRUSH* (Figure 27).

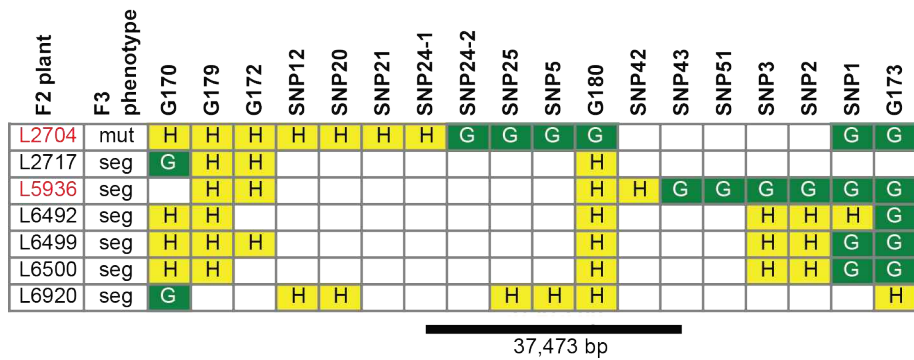


**Figure 27. Fine mapping of *brush*.**

In addition to the SSR power mapping markers, recombinant plants were analyzed with SNP markers by sequencing. The target region on chromosome 2 between the flanking markers consisted of 37,473 bp. Genotypes at marker positions are represented either by yellow with H (heterozygous) or by green with G (Gifu alleles). White cells indicate that this marker/DNA combination was not analyzed. The two most important recombinants are shown in red. The phenotypes of the corresponding F3 progenies were analyzed: mut, all F3 plants were mutants; seg, mutant and wild-type F3 plants were scored. (For detailed phenotypes, see Figure 26.)

Parallel to the fine mapping, the interval between G172 and SNP3 (Figure 28), which consisted of approximately 103 kb, was sequenced. First, DNA of a *brush* plant was analysed and its sequence was compared to the MG-20 sequence. Then, regions with SNPs between the *brush* and MG-20 genomes were also sequenced in Gifu DNA. Several SNPs between the Gifu and MG-20 genomes (Figure 27; Figure 28) were found that could be used to investigate the target region in more detail. Furthermore, sequencing of this interval of the *brush* mutant should have identified EMS-induced mutations, one of which could be responsible for the phenotype of *brush* plants. Since many transposable elements were present between G172 and SNP3, sequencing of the complete interval was not feasible. In total, approximately 50% of the 103 kb could be analysed, because parts of the sequence could not be amplified by PCR and some sequencing reads were difficult to analyse. Either no clear base calls could be assigned or sequence stretches could align to several locations in the sequence. One EMS-induced mutation was detected (Figure 28, asterisk), which was located in the coding sequence of a predicted candidate gene, *CNGC1*.

## RESULTS

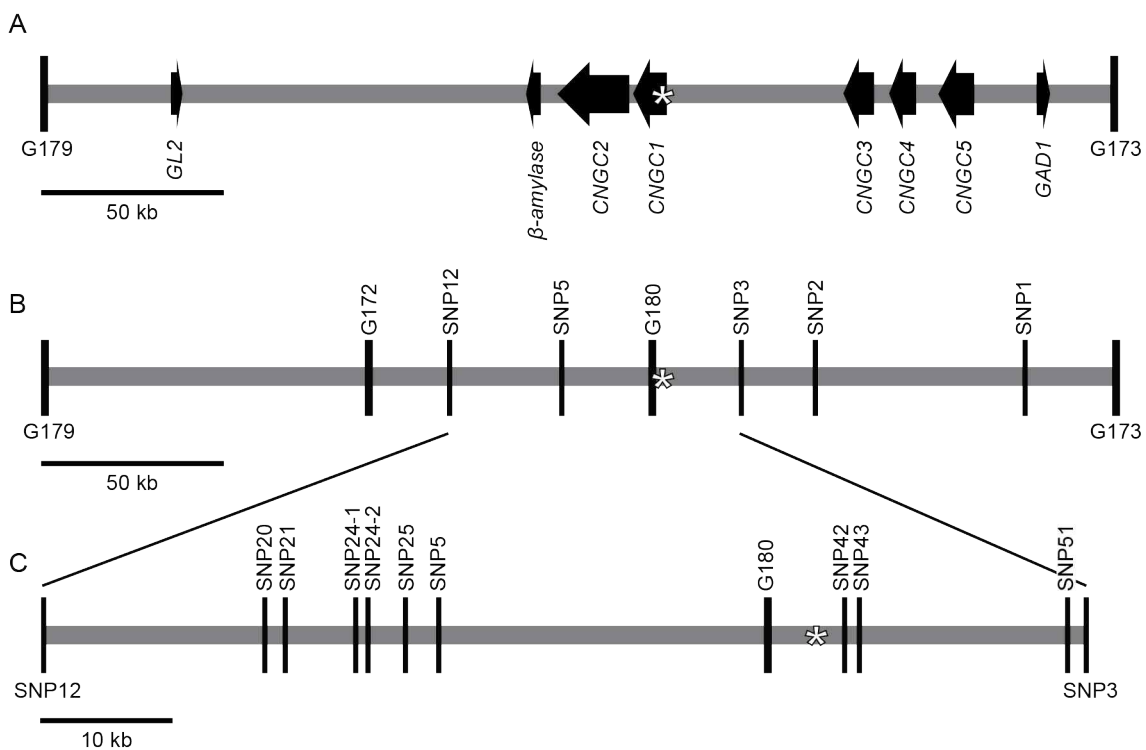


**Figure 28. Annotations of candidate genes and positions of SSR and SNP markers between G179 and G173 on CM0435.**

(A) Annotated candidate genes in and around the target region and genes of the CNGC cluster are shown by arrows. *GL2* – *GLABRA2*, *GAD1* – glutamate decarboxylase.  
 (B and C) SSR and SNP markers used for fine mapping. The asterisk indicates the EMS-induced mutation found in *brush* mutants. SSR markers were analysed by fluorescent PCRs and SNPs were genotyped by sequencing.  
 Scale bars = 50 kb (A, B), 10 kb (C).

In addition to the sequencing of the 103 kb region, whole genome Next Generation Sequencing of *brush* DNA was performed. After assembling the *brush* sequence reads *de novo* and comparing the resulting contigs to those of the Gifu and MG-20 genomes, no chromosomal rearrangements, as well as deletions or insertions, could be detected. The *brush* sequence reads were also mapped onto the MG-20 genome sequence and, after confirming that the SNPs were not present in the Gifu genome, *brush*-specific EMS-induced SNPs have been identified. Within the 37 kb target interval, the already discovered mutation in *CNGC1* was confirmed and no additional EMS-induced SNP could be found.

### 2.3.2.2 Phenotypes and Genotypes of F4 and F5 Progenies

During the F3 screen, plants with long, wild type-like roots and white bumps or even wild type-like roots without nodules were observed. Since these plants exhibited neither the original *brush* mutant nor the wild-type phenotype, progenies of selected plants with these phenotypes were analysed (Figure 26; Figure 29). Progeny of the F3 plants L9731, L9733 and L9737, which had wild type-like roots with white bumps, consisted only of seedlings with short and thick roots without any nodules (Table 2). Offspring of L9739 and L9736 showed mostly mutant roots without nodules, but additionally one or two plants with long roots (Table 2). Moreover, progenies of four

## RESULTS

other F3 plants were cultivated and inoculated at 18°C and 26°C to assess also temperature-dependent phenotypes of F4 plants. Analysing the progeny of three of them (L9739, L9744, L9758) revealed that plants with wild-type roots and those with mutant roots segregated in a 3:1 ratio. At 26°C some plants with wild-type roots formed white bumps or showed no nodules, whereas at 18°C plants with wild-type roots also showed wild-type nodules (Table 2; Figure 30).

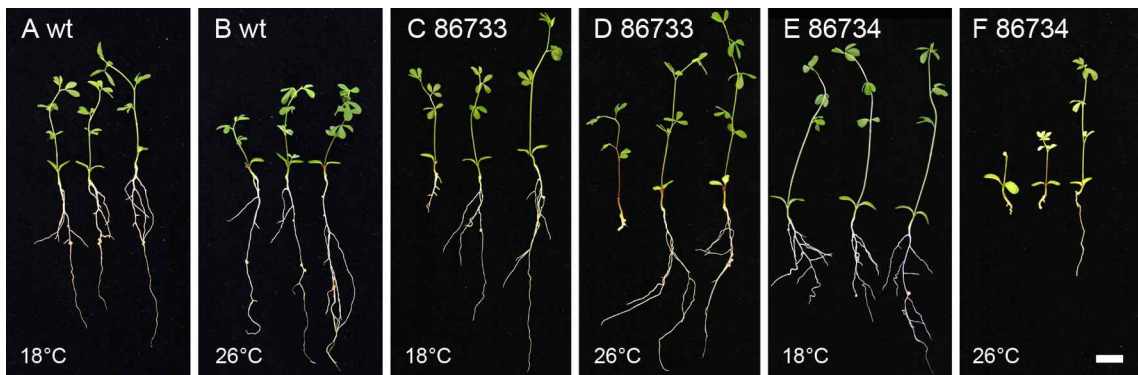


**Figure 29. F4 plants grown at 18°C and 26°C.**

(**A and B**) *L. japonicus* Gifu, (**C and D**) progeny of L9758 (seed bag 86733) and (**E and F**) progeny of L9759 (seed bag 86734) were grown at 18°C (**A, C, E**) or 26°C (**B, D, F**) and inoculated with *M. loti* MAFF DsRed 1 wpg. (**C and D**) Left plant: mutant root phenotype, middle and right plant: wt roots. (**E and F**) Progeny of L9759 differed extremely depending on the temperature. Pictures were taken 4 wpg. Scale bar = 1 cm.

F3 plant	F4 seedbag	F2 plant	F3 phenotype			F4 phenotypes						
			wt nodules	white bumps	root phenotype	wt root wt nodules	wt root white bumps	wt root no nodules	mutant root wt nodules	mutant root white bumps	mutant root no nodules	
L9730	86707	L5939	0	9	wt	26°C 1	0	1	0	1	12	
L9731	86708	L5954	0	3	wt	26°C 0	0	0	0	0	15	
L9733	86709	L5954	0	3	wt	26°C 0	0	0	0	0	5	
L9736	86711	L6501	0	4	wt	26°C 0	0	1	0	0	10	
L9737	86712	L6501	0	2	wt	26°C 0	0	0	0	0	20	
L9739	86714	L6920	1	3	wt	18°C 10	0	0	1/1w	2	1	
						26°C 3/1w	3	25	0	1	11	
L9744	86719	L5955	0	0	wt	18°C 7/1w	0	0	0	0	4	
L9758	86733	L5955	1	2	wt	26°C 11/2w	10	5	0	0	7	
L9759	86734	L5939	0	6	wt	18°C 9	0	0	1	0	2	
						26°C 4	2	8	0	0	11	
						18°C 10/5w	1	0	0	0	0	
						26°C 0	0	0	0	6	26	

**Table 2. Overview of phenotypes of F3 plants and their F4 progeny.**

F3 phenotype: numbers indicate amount of nodules or bumps per F3 root system. F3 plants were grown at 26°C.  
F4 phenotypes: number of F4 plants with indicated phenotype. X/Yw, Y of X plants showed wild-type nodules and white bumps. Plants were grown at 18°C or 26°C and inoculated with *M. loti* MAFF DsRed. Phenotypes were scored 3 wpi.

## RESULTS

---

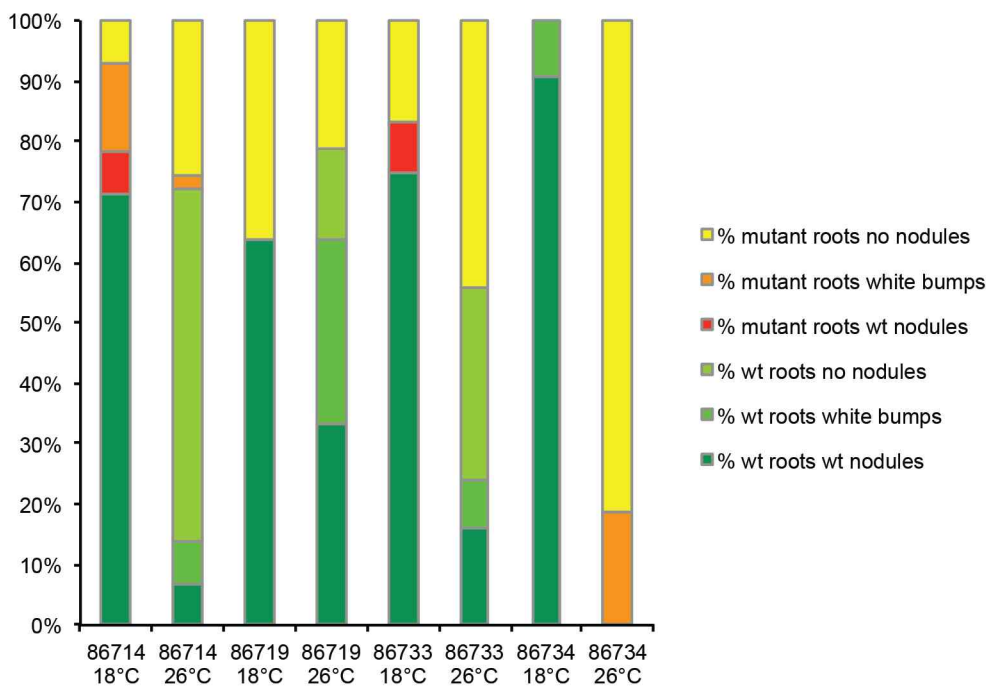


**Figure 30. Diagram showing percentages of F4 phenotypic categories at 18°C and 26°C.**

Numbers of plants in each category are shown in Table 2. Plants with wild-type nodules and white bumps were scored as plants with wild-type nodules only.

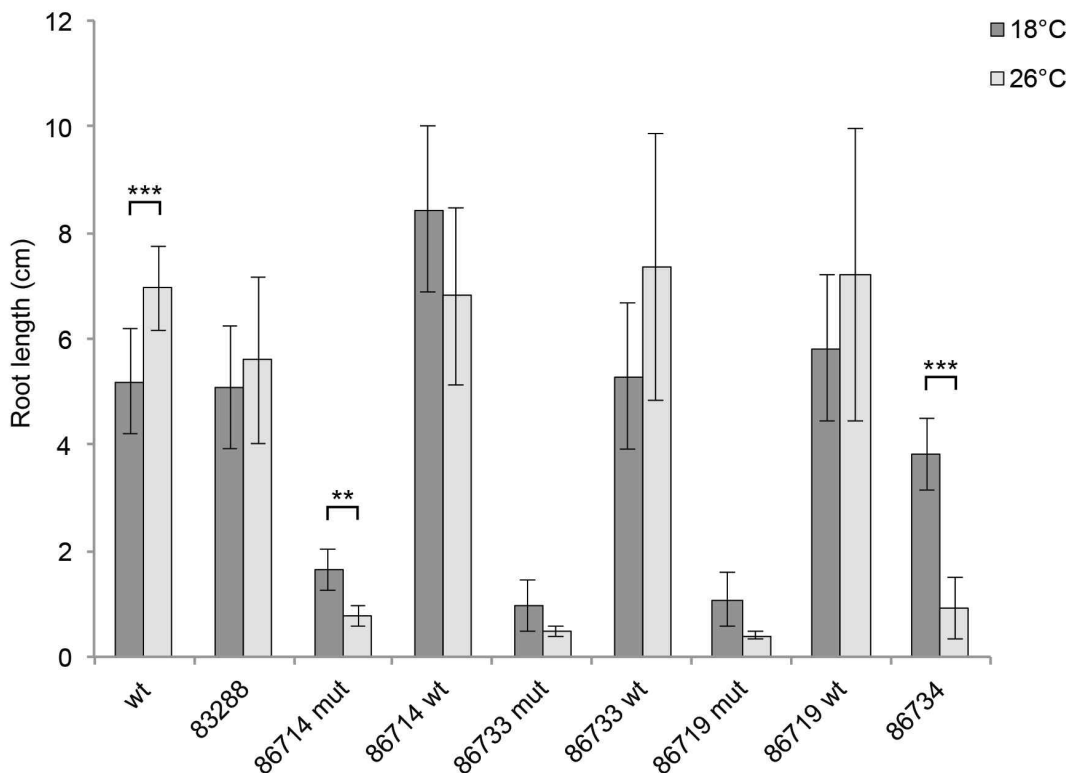


**Figure 31. Chart of root lengths of F4 plants grown at 18°C and 26°C.**

*L. japonicus* Gifu wild-type and SL0979 F4 seedlings cultivated at 18°C or 26°C for 4 weeks were measured (cm). In case of segregating populations root lengths of mutant (mut) and wild type-like (wt) plants are shown in separate columns. Roots of wild-type plants were longer at 26°C than at 18°C. Mutant roots of progeny of L9739 (seed bag 86714) and progeny of L9759 (seed bag 86734) were significantly shorter at 26°C (Student's t-test, \*\* p-value < 0.01, \*\*\* p-value < 0.001). Error bars represent standard deviation.

Obviously, the nodulation phenotype of F4 plants was temperature dependent. An exception was the progeny of L9759. At 26°C only mutants with short and thick roots were observed and at 18°C all the plants had wild-type roots (Table 2; Figure 30; Figure 29). At both conditions white bumps were detected (Table 2). In addition, the root lengths of these F4 plants were measured. When segregating F4 populations of L9758 and L9744 were divided into plants with wild-type and with mutant roots, no significant difference of their root lengths regarding the different temperatures could be determined in this experiment (Figure 31). Progeny of L9759, which did not segregate, and the mutants of the L9739 progeny (seed bag 86714) showed a temperature-dependent difference in root length (Figure 31).

Different F4 progeny populations – seed bags 86714 (L9739-F3/L6920-F2), 86733 (L9758-F3/L5955-F2), 86719 (L9744-F3/L5955-F2) and 86734 (L9759-F3/L5939-F2) – were also genotyped in the *brush* target region to check the correlation between their phenotypes and genotypes. Only F4 plants with a mutant root phenotype always possessed two Gifu alleles between the markers G170 and G174 (data not shown). Consequently, the mutation responsible for the short and thick root phenotype of *brush* mutants should have been located between these markers. Furthermore, the nodulation phenotype also correlated with the genotypes in the analysed region (Figure 32). F4 plant M0443 was cultivated at 26°C and showed long roots with wild-type nodules but also white bumps. Its progeny had either mutant roots, wild type-like roots with white bumps or wild type-like roots with wild-type nodules in a ratio of 1:2:1 ( $\chi^2 = 0.93$ ). F5 plants with short and thick roots carried only the EMS-induced SNPs, those with white bumps were heterozygous and wild type-like plants had wild-type SNPs in the analysed region on contig CM0435 (Figure 32).

## RESULTS

---

Plant	Root phenotype	Nodulation phenotype	G077	G83	G175	8844892	G170	9069492	G179	9302361	9363400	G182	9566814	9632266	G174
1	mut	no nodules				mut		mut		mut	mut		mut	mut	
2	wt	white bumps				Het		Het		Het	Het		Het	Het	
3	wt	wt nodules				wt		wt		wt	wt		wt	wt	
4	mut	no nodules				mut		mut		mut	mut		mut	mut	
5	wt	white bumps				Het		Het		Het	Het		Het	Het	
6	wt	wt nodules				wt		wt		wt	wt		wt	wt	
7	mut	no nodules				mut		mut		mut	mut		mut	mut	
8	wt	white bumps				Het		Het		Het	Het		Het	Het	
9	wt	white bumps				Het		Het		Het	Het		Het	Het	
10	mut	no nodules				mut		mut		mut	mut		mut	mut	
11	wt	wt nodules				wt		wt		wt	wt		wt	wt	
12	mut	no nodules				mut		mut		mut	mut		mut	mut	
13	mut	no nodules				mut		mut		mut	mut		mut	mut	
14	wt	white bumps				Het		Het		Het	Het		Het	Het	
15	wt	wt nodules				wt		wt		wt	wt		wt	wt	
16	wt	wt nodules				wt		wt		wt	wt		wt	wt	
17	wt	white bumps				Het		Het		Het	Het		Het	Het	
18	wt	white bumps				Het		Het		Het	Het		Het	Het	
19	wt	white bumps				Het		Het		Het	Het		Het	Het	
20	wt	white bumps				Het		Het		Het	Het		Het	Het	
21	wt	white bumps				Het		Het		Het	Het		Het	Het	
M0443	wt	2 wt nodules + 2 white bumps	M	Het	Het		Het		Het		Het		Het		G

**Figure 32. Phenotypes of F5 plants and their corresponding genotypes.**

F5 progeny (plants 1 – 21) of the F4 plant M0443 was genotyped at positions, at which EMS-induced mutations had been identified by Next Generation Sequencing. Plants 1 to 21 were grown at 22°C, inoculated with *M. loti* MAFF DsRed one wpg and phenotyped 3 wpi. M0443 was grown at 26°C, inoculated with *M. loti* MAFF DsRed 1 wpg and phenotyped 3 wpi. Root phenotype: mut – short and thick roots, wt – long, wt-like roots. Genotypes: mut – EMS mutation at specific position, Het – heterozygous at specific position, wt – wild-type (Gifu and MG-20) sequence at specific position, M – MG-20-specific SSR pattern. G – Gifu-specific SSR-pattern. M0443 has been genotyped with SSR-markers, F5 plants with KASP SNP assays. The position of the EMS-SNP refers to the MG-20 genome annotation.

### 2.3.3 *brush* Backcross Mutants Resemble *brush* Mutants

The EMS mutagenized SL-lines carry a mutation load of one mutation per 502 kb in the M2 generation (Perry et al., 2009). Backcrossing of an identified mutant plant to its wild-type ecotype background decreases this mutation load by 50% and produces plants that still carry the mutation of interest, but less background mutations that probably could interfere with the original mutant phenotype. Therefore, *brush* mutants were crossed to *L. japonicus* Gifu wild-type plants and progenies of these crosses were already determined to segregate the mutant phenotype in a 3:1 ratio and to show the same phenotypes as the original *brush* mutants (Maekawa-Yoshikawa et al., 2009). Since the phenotyping of the F3 (MG-20 x *brush*) progenies revealed new phenotypic classes, progenies of the *brush* backcross populations were analysed in detail. The cosegregation of the root and nodulation phenotype as well as the cosegregation of the mutant phenotypes and the EMS-induced mutation located in CNGC1 was determined. In total, three backcross progenies were checked and segregating populations were phenotyped and genotyped (Figure 33). All the analysed progenies segregated mutant roots and some of these showed white bumps or nodules and also some without nodules could be observed, whereas all plants with wild-type roots also had wild-type nodules (Figure 33).

parent plant	seedbag	analysed	phenotypes of progeny					
			wt root wt nodules	wt root white bumps	wt root no nodules	mutant root wt nodules	mutant root white bumps	mutant root no nodules
K6216/F1	70420	31	20	0	0	0	2	9
K6222/F1	75769	17	14	0	0	1	0	2
K6227/F1	75773	28	21	0	0	0	2	5
L2571/F2	75804	15	12	0	0	1	1	1
L8566/F3	84220	17	11	0	0	1/1w	5*	0

**Figure 33. Phenotypes of *brush* backcross progenies.**

Backcross progenies were grown at 26°C, inoculated with *M. loti* expressing *DsRed* and phenotyped 3 wpi. All three F1 plants had the same parent plants (K3790/SL0979 x K6215/Gifu). K6216 and K6222 originated from one F1 pod. \*One plant (M0027) was heterozygous at the EMS-induced mutation in *CNGC1*, but showed a mutant phenotype.

A dCAPS marker was used to genotype the EMS-mutation in *CNGC1* in *brush* backcross progenies. One individual (M0027, F4) showed a mutant phenotype, but was heterozygous for the mutation in *CNGC1* (Figure 33), as confirmed by sequencing. All the other mutant backcross plants were homozygous for the mutant allele at the site of the mutation. To confirm this result, more backcross plants were investigated to find further mutant plants that are heterozygous at the mutation in *CNGC1*. Their number could determine the distance from the mutation in *CNGC1* to the putative *brush* locus. In total, 215 F4 plants were phenotyped and genotyped with the dCAPS marker. Thereof three plants were again heterozygous at the mutation in *CNGC1*, but showed a mutant root phenotype. This results in a calculated distance of 0,9 cM from the mutation in *CNGC1* to the putative mutation causing the root phenotype, under the assumption that the dCAPS scoring was correct.

Progeny of M0027 (*brush* x Gifu wt, F4) was phenotyped at 18°C and at 26°C to check whether the temperature-sensitive nodulation and root growth phenotype could still be observed and whether they were cosegregating. Therefore, seedlings were grown for six weeks at 18°C on plates before transferring them to pots to prevent a masking effect of the short and thick roots on the nodulation phenotype, because these very short roots almost never exhibited infection structures. Previous temperature-shift experiments already demonstrated that after transferring the plants to 26°C, long, wild type-like roots of *brush* mutants were still impaired in nodulation (Figure 24).

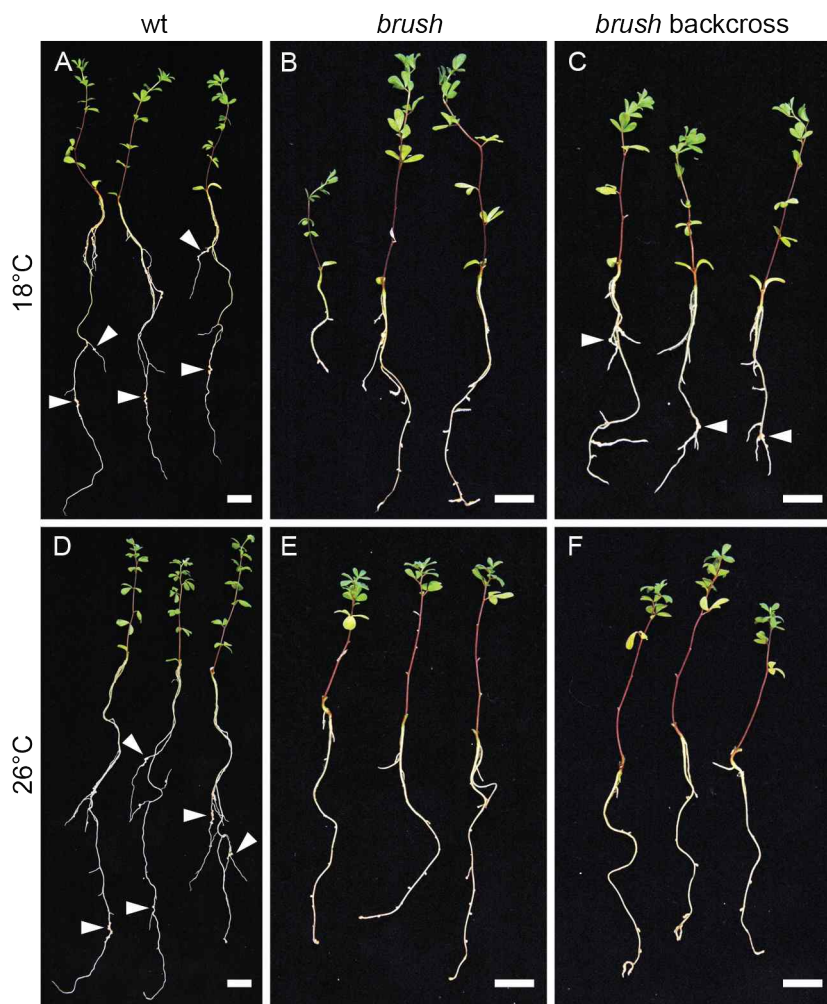


**Figure 34. Root systems of *brush* backcross mutants resembled the *brush* root phenotype.**

*L. japonicus* Gifu (A, D), *brush* mutants (B, E) and *brush* backcross mutants (BC F5, progeny of M0027; C, F) were grown for six weeks at 18°C on plates before transferring them to pots, where they were cultivated at 18°C (A - C) or 26°C (D - F). After one week plants were inoculated with *M. loti* MAFF *DsRed*. Pictures were taken 12 dpi. Arrowheads point to nodules. At 18°C *brush* backcross mutants (C) exhibited more nodules compared to *brush* mutants (B). The root systems of *brush* backcross mutants (C, F) resembled *brush* mutant roots (B, E) at 18°C and at 26°C. Scale bars = 1 cm. Wild-type plants are shown at lower magnification than the mutants.

M0027 showed a mutant root and nodulation phenotype and therefore should have carried two mutant alleles in case of a recessive mutation, but, as already mentioned, is was heterozygous at the mutation in *CNGC1*. Measuring the root lengths of wild-type plants, *brush* mutants and self-progeny of M0027 revealed that at 18°C and at 26°C roots of M0027 self-progeny plants were significantly longer than those of *brush* mutants, but still shorter than wild-type roots (Figure 35C). Importantly, self-progeny did not segregate wild-type plants thus excluding a phenotypic miss-scoring of the M0027 recombinant individual. Furthermore, the two different temperatures did not influence the root lengths (Figure 35C). At 18°C the backcross plants produced more nodules compared to *brush* mutants by trend, but significantly less than wild-type plants (Figure 34A – C, Figure 35A). At 26°C, neither backcross nor *brush* mutants showed any infected nodule, instead at both conditions white bumps could be detected (Figure 35A and B). There was a tendency of backcross plants compared to *brush* mutants to have more white bumps (Figure 35B). Additionally, the backcross mutant plants showed the distorted root tips of the *brush* mutants

## RESULTS

(Figure 34B, C, E and F), although a more severe phenotype could be detected in the mutants. It seemed that also the lateral root growth was less impaired in the backcross mutants at 18°C compared to *brush* mutants (Figure 34B and C). Apparently the reduced mutation load of the backcross mutants led to a reduced phenotypic strength of the characteristic *brush* root and nodulation phenotype, but still both phenotypes were evident and significantly different from the wild type. This result, together with the F4 data from the *brush* x MG-20 cross, strongly suggests the presence of multiple (EMS-generated) modifier loci that influence the strength of the temperature response as well as the root length of *brush* mutants.

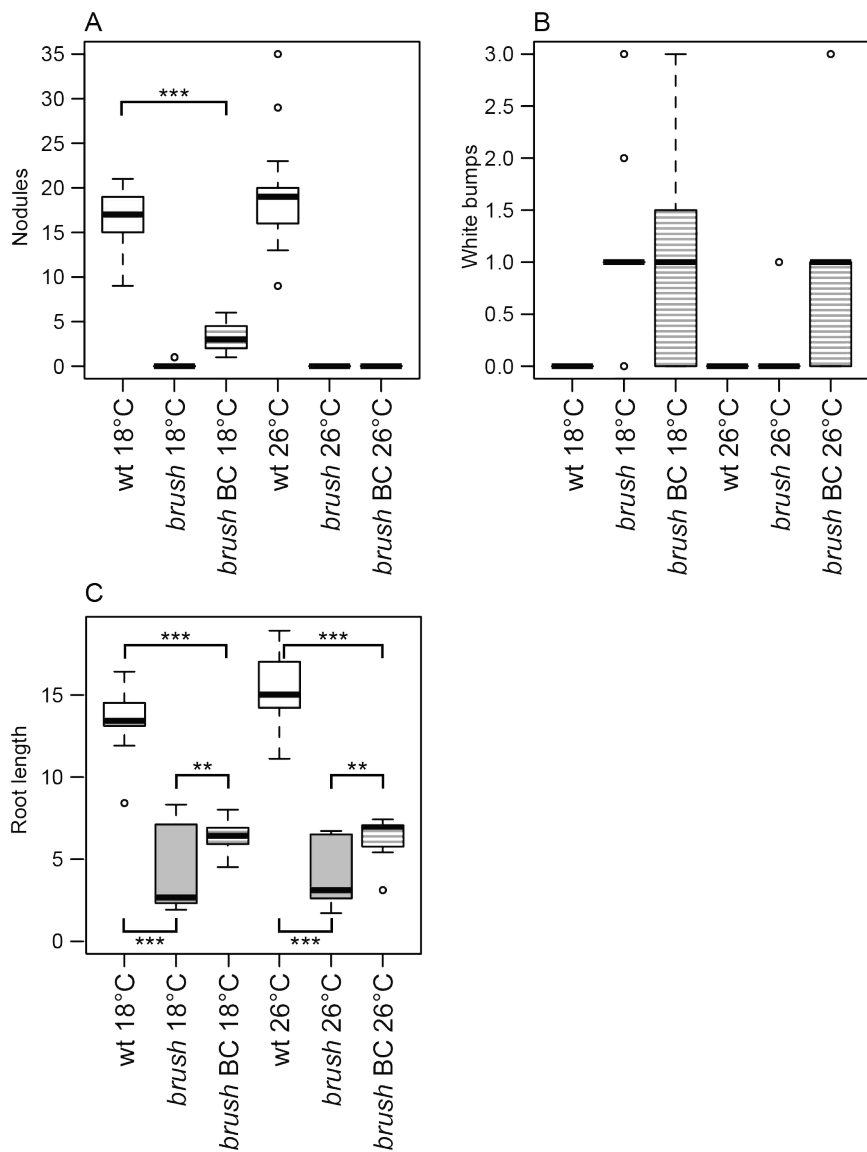


**Figure 35. Analysis of nodulation and root lengths of *brush* and *brush* backcross mutants.**

*L. japonicus* Gifu wild-type plants (white boxplots), *brush* mutants (grey boxplots) and *brush* backcross plants (BC F5, progeny of M0027; striped boxplots) had been grown for 6 weeks at 18°C. Subsequently they had been cultivated at 18°C or 26°C for one week, before they were inoculated with *M. loti* MAFF expressing *DsRed*. Twelve dpi nodules (**A**) and white bumps (**B**) per root system were counted and the length of their root systems was measured in cm (**C**) (n = 10-13). **(A)** Compared to wild-type plants *brush* backcross mutants formed less nodules at 18°C (Welsh's t-test, \*\*\* p-value < 0.001). Only two *brush* mutants out of 10 showed 1 nodule. At 26°C neither *brush* mutants nor *brush* backcross mutants formed any nodule. **(B)** At 18°C white bumps could be detected at *brush* mutants and *brush* backcross plants. At 26°C only one *brush* mutant plant out of 11 formed one white bump, whereas 8 out of 12 *brush* backcross plants exhibited white bumps. **(C)** Regarding the root lengths, *brush* mutants and *brush* backcross mutants had significantly shorter roots compared to the wild-type at 18°C and at 26°C, but *brush* backcross mutants produced longer roots than *brush* mutants at both conditions (ANOVA followed by Tukey's HSD test, \*\* p-value < 0.01, \*\*\* p-value < 0.001).

### 2.3.4 Cyclic Nucleotide-Gated Channel 1 of *Lotus japonicus*

#### 2.3.4.1 EMS-Induced Mutation in *CNGC1*

Sequencing of two candidate genes, a  $\beta$ -amylase and a glutamate decarboxylase (*GAD*) gene, did not reveal any mutations in a *brush* mutant plant (Figure 28). In contrast, the predicted genomic sequence of *CNGC1* carried a guanine to adenine transition at position 401 that corresponded to an amino acid exchange from glycine to glutamic acid (Figure 39). *CNGC1* consists of 12 exons and has an intron in the 5' UTR (Figure 36).

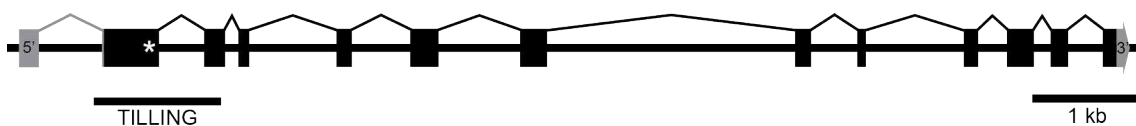


**Figure 36. Illustration of the gene structure of *CNGC1*.**

*CNGC1* consists of 12 exons (black boxes), The 5'- and 3'-UTRs are shown by grey boxes. The 5'-UTR contains an intron. The region of the TILLING is indicated. The white asterisk in exon 1 shows the location of the EMS-induced mutation. Scale bar = 1 kb.

#### 2.3.4.2 Complementation of *brush* with *CNGC1*

To investigate whether the EMS-induced mutation found in *CNGC1* is the mutation causing the *brush* mutant phenotype, the genomic full-length sequence of *CNGC1* was expressed in *brush* mutant seedlings via hairy-root transformations. Therefore, constructs including 2 kb *CNGC1* promoter plus the genomic sequence of *CNGC1* (pK7WG2D<sub>no Pro35S</sub>-*ProCNGC1-CNGC1*<sub>genomic</sub>, pK7RWG2<sub>no Pro35S, GFP</sub>-*ProCNGC1-CNGC1*<sub>genomic</sub>-RFP) or including a 35S promoter (pK7WG2D-*CNGC1*<sub>genomic</sub>) were tested. Two versions of pK7RWG2<sub>no Pro35S, GFP</sub>-*ProCNGC1-CNGC1*<sub>genomic</sub>-RFP were transformed, one with the stop codon TAG of *CNGC1* and one without to circumvent possible negative effects of the C-terminal RFP-fusion.

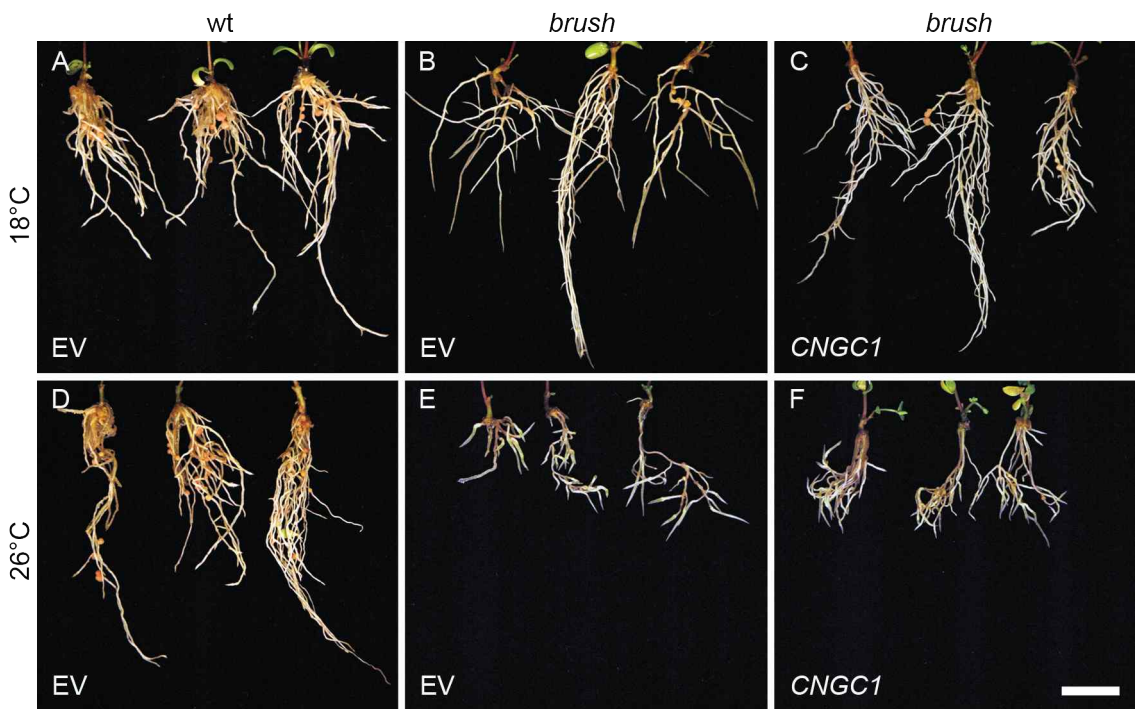


**Figure 37. Hairy-roots of *brush* mutants transformed with *CNGC1*.**

*L. japonicus* Gifu plants were transformed with the empty vector pK7RWG2<sub>no Pro35S, GFP</sub> (EV) (A, D), *brush* mutants with the EV (B, E) or with pK7RWG2<sub>no Pro35S, GFP-ProCNGC1-CNGC1<sub>genomic</sub>-RFP</sub> (C, F). Composite plants were grown at 18°C (A to C) or 26°C (D to F), inoculated with *M. loti* expressing *DsRed* and analyzed 4 wpi. Scale bar = 1 cm.

Wild-type roots transformed with the empty vector showed numerous pink nodules (Figure 37A and D, Figure 38A, D, G). None of the transformed mutant roots showed wild-type growth and nodulation. Moreover, no difference between the mutant roots transformed with the empty vector and the complementation constructs could be determined (Figure 37B, C, E, F; Figure 38B, C, E, F, H, I). The root length was still temperature-dependent with much shorter roots when grown at 26°C instead of 18°C and the short thick root phenotype of *brush* mutants was very obvious at 26°C (Figure 37E and F). After inoculation with rhizobia, nodule primordia and nodules emerged on the transformed mutant roots, but most of them were not infected (Figure 38B, C, E, F, H and I) and showed the characteristic superficial rhizobial colonization on the white bumps (Figure 20). A PCR fragment ranging from *CNGC1* to the *RFP* gene could be amplified from the cDNAs of four root systems transformed with pK7RWG2<sub>no Pro35S, GFP-ProCNGC1-CNGC1<sub>genomic+TAG</sub>-RFP</sub> (data not shown). Therefore, the construct was expressed in the roots. Thus, neither the short thick root nor the white bump phenotype of *brush* mutants could be rescued by the expression of *CNGC1* in transgenic roots.

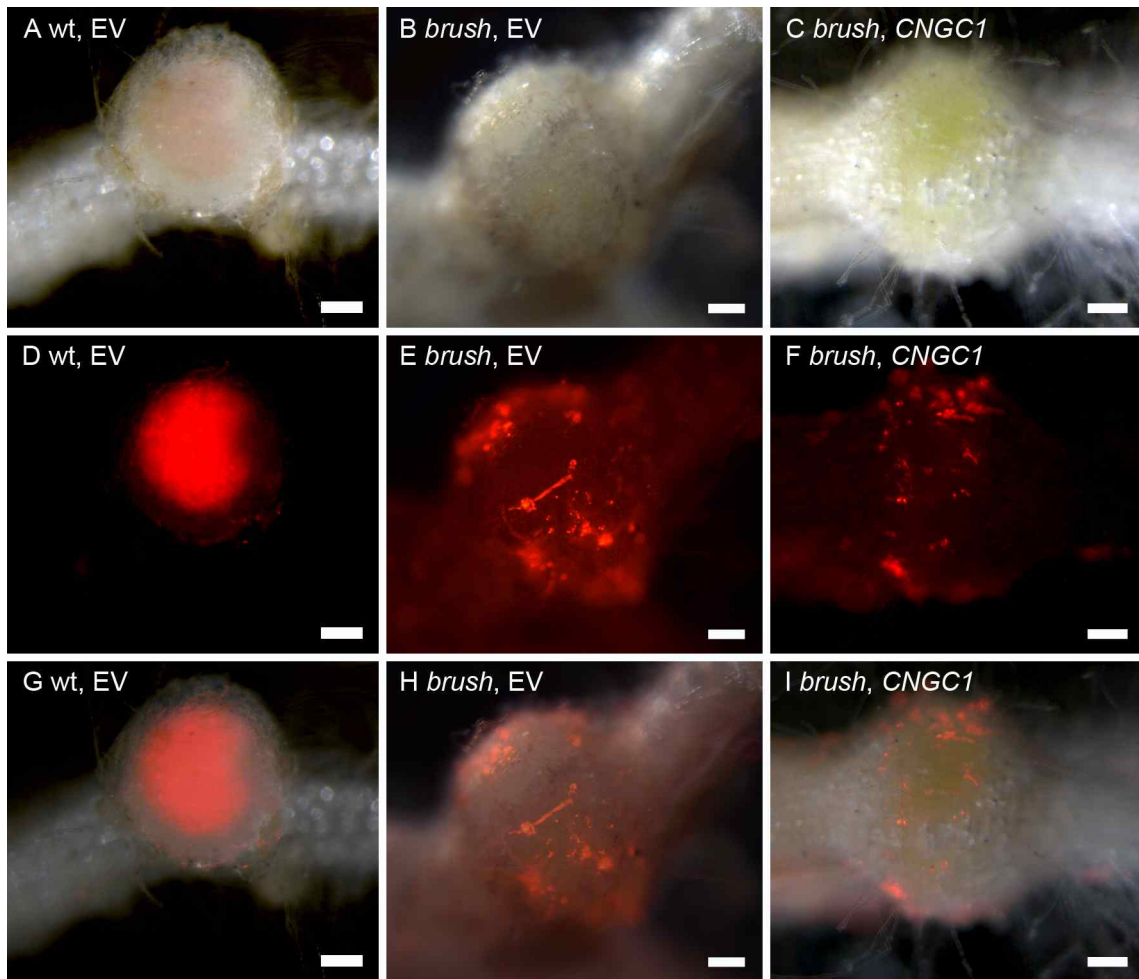


**Figure 38. White bumps of brush hairy roots after attempted complementation with CNGC1.**

Nodules of hairy roots of *L. japonicus* Gifu (wt) transformed with the empty vector (EV) pK7RWG2<sub>no Pro35S GFP</sub> (**A, D, G**) were infected with rhizobia (**D**) and showed a pink colour (**A**). Hairy roots of *brush* mutants transformed with the empty vector (EV) (**B, E, H**) or with pK7RWG2<sub>no Pro35S GFP</sub>-*ProCNGC1-CNGC1*<sub>genomic+TAG-RFP</sub> (**C, F, I**) showed non-infected white bumps. Composite plants were cultivated at 26°C, inoculated with *M. loti* MAFF expressing *DsRed* and analyzed 4 wpi. (**A - C**) Bright-field images, (**D - F**) red fluorescence of rhizobia, (**G - I**) overlay of bright-field and fluorescence images. Scale bars = 200 µm.

### 2.3.4.3 TILLING Mutants of CNGC1

The severe root phenotype of *brush* already obvious at early developmental stages of the mutants could not be complemented by hairy root transformation. Another possibility to confirm that the mutation found in the *CNGC1* gene is responsible for the phenotype of *brush* mutants is the identification of further mutant alleles of the same gene. In collaboration with the *Lotus* TILLING facility (John Innes Centre, Norwich, UK) we obtained four *CNGC1* TILLING lines (Perry et al., 2003; Figure 39, Table 3).

**Table 3. EMS-induced mutations of CNGC1 TILLING lines and their nodulation ability.**

	Nucleotide <sup>#</sup>	Amino acid <sup>#</sup>	Nodules*
wt	-	-	5.90 ( $\pm 0.99$ )
SL0791-1 <sup>a</sup>	C128A	P43Q	3.89 ( $\pm 2.85$ )
SL0822-1 <sup>b</sup>	G280A	A94T	5.89 ( $\pm 2.37$ )
SL0957-1 <sup>a</sup>	C161T	T54I	4.90 ( $\pm 2.23$ )
SL1484-1 <sup>a</sup>	G357A	W119Stop	5.63 ( $\pm 2.72$ )

<sup>#</sup>, Numbers indicate the position of the mutations relative to the A of the ATG (nucleotide) or to the Methionine (amino acid). \*, Arithmetic mean with standard deviation of the nodule number counted 2 wpi after inoculation with *M. loti* MAFF *DsRed* at 26°C (n = 8-10). The SL lines consisted either of a population of seed carrying the mutation in both *CNGC1* alleles (b) or the mutation segregated in the population (a).

Regarding the number of nodules, there was no significant difference between the wild-type and the analysed TILLING lines. None of the TILLING individuals showed the *brush* root or nodulation phenotype. White bumps with the characteristic aborted infection threads could not be observed. Since only seed of SL0822-1 was homozygous for the indicated mutation, seedlings of the other lines were additionally genotyped after phenotyping.

**Table 4. Nodule number and genotype of SL1484-1 individuals.**

#	Nodules	Genotype
1	8	Het
2	9	Het
3	7	mut
4	3	wt
5	6	mut
6	7	mut
7	4	wt
8	1	Het

#: individual plant; Nodules: number of nodules counted on the individual root system; Genotype: heterozygous (Het), mutant (mut), wild-type (wt) regarding the mutation in *CNGC1* present in this line (see Table 3). Plants were cultivated at 26°C, inoculated with *M. loti* MAFF *DsRed* 12 dpg and analyzed 2 wpi. Plants were genotyped by sequencing.

## RESULTS

---

		20		40		60	
Gifu wt	<b>M P Q F D K D G V P</b>	V L L E T H A Q Q S	DEF M D S N C R R	L S Y R T R S A S I	S I P M V P I E P Y	E G G T H L V G H T	60
SL0791	.....	.....	.....	.....	.....	.....	60
SL0822	.....	.....	.....	.....	.....	.....	60
SL0957	.....	.....	.....	.....	.....	.....	60
SL0979	.....	.....	.....	.....	.....	.....	60
SL1484	.....	.....	.....	.....	.....	.....	60
AtCNGC19	. A -----	----- HT . T	F T S . N .. V . L	. N . S F S . D G F	D N S . V T L . Y .	36	
AtCNGC20	. A S H N E N D D I	P M . P I -----.	. P S S R T R A . A	F T S . S .. V . L	. N . T S S .. G F	D T S . V V L . Y .	56
		80		100		120	
Gifu wt	<b>G P L R S V R - K P</b>	P S G Q M S G P L Y	A T T A G A G N H F	Q H S I A V P G K K	A V E G K T Q ---	Q L S T F D G T D E	116
SL0791	.....	.....	.....	.....	.....	.....	116
SL0822	.....	.....	.....	.....	.....	.....	116
SL0957	.....	.....	.....	.....	.....	.....	116
SL0979	.....	.....	.....	.....	.....	.....	116
SL1484	.....	.....	.....	.....	.....	.....	116
AtCNGC19	.... T Q . I R .	. L V ..... I H	S . R R T E P L F S	P S ----- Q - E	S P D S S S T V D V	P P -----	83
AtCNGC20	.... T Q . - R .	. L V ..... T	S . R K H E P L F L	P . ----- S S D	S . G V S S . P E R	Y P . F A A L E H K	111
		140					
Gifu wt	<b>N L W N N N Y D R K</b>	N E H L L R S G Q L	G M C N D P Y C T T	146			
SL0791	.....	.....	.....	.....	146		
SL0822	.....	.....	.....	.....	146		
SL0957	.....	.....	.....	.....	146		
SL0979	.....	.....	.....	.....	146		
SL1484	.. *	.....	.....	.....	146		
AtCNGC19	--- E D D F V F .	. A N ..	.....	.....	110		
AtCNGC20	. S S E D E F V L .	H A N ..	.....	.....	141		

**Figure 39. The *L. japonicus* CNGC1 amino acid sequence in comparison to CNGC1 sequences in the analyzed SL lines and the *Arabidopsis* CNGC19 and CNGC20.**

The first 146 amino acids of Lj CNGC1 were aligned to *Arabidopsis* CNGC19 (AT3g17690) and CNGC20 (AT3g17700). The amino acid exchanges and the stop codon (\*) of the individual SL lines are highlighted by grey boxes.

No correlation between the nodule number of the CNGC1 TILLING plants and their respective genotype was observed (Table 4). These results showed that the mutations in CNGC1, which were present in these TILLING lines, did not affect the phenotypes of the seedlings regarding root growth and nodulation ability.

#### 2.3.4.4 ProCNGC1-GUS Analysis

A reporter gene assay was performed to reveal the expression pattern of CNGC1 in roots. 2 kb DNA sequence (-1 to -2000) upstream of the CNGC1 start codon (+1 to +3) were fused to the  $\beta$ -glucuronidase (GUS) gene using the vector pKGWFS7 (Karimi et al., 2002). This construct was introduced into wild-type roots by hairy root transformation. Blue GUS staining was mainly visible at the root tips (Figure 40A) and in the vascular tissue, often occurring as background staining in transformed hairy-roots. However, a very intensive staining was observed at the tips of emerging lateral roots (Figure 40B). In addition, young nodule primordia and the outer layers of young nodules showed a blue staining (Figure 40C and D), whereas older nodules were not stained at all.

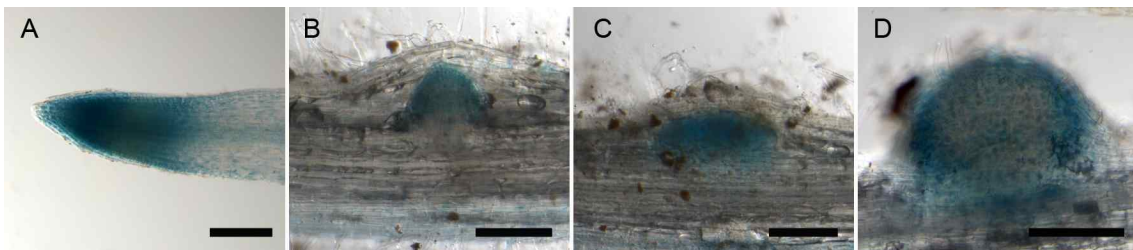


**Figure 40. Expression patterns of CNGC1 in roots and nodules visualized by ProCNGC1-GUS staining.**

Hairy roots transformed with 2 kb CNGC1-promoter sequence fused to the  $\beta$ -glucuronidase gene were inoculated with *M. loti* MAFF *DsRed* and analyzed 3 wpi. (A) Root tips were intensively stained, (B) even at very young emerging roots. (C) GUS staining was visible in nodule primordia and (D) in the epidermis of nodules. Scale bars = 200  $\mu$ m.

#### 2.3.4.5 The CNGC Gene Cluster

Detailed analysis and gene annotation of the contig CM0435 revealed four additional genes with high homologies to CNGCs of *A. thaliana* (Figure 28A). The gene CNGC2 was located next to CNGC1 and contained a large predicted transposon in the sixth intron. So far, CNGC2 could not be amplified from cDNA. The genes CNGC3, CNGC4 and CNGC5 were annotated upstream of CNGC1 with help of the Kazusa *Lotus* genome browser (<http://gsv.kazusa.or.jp/cgi-bin/gbrowse/lotus>). Their exon-intron boundaries were slightly modified according to the alignment of the five putative CNGCs. These were highly conserved in the C-terminal region, especially in parts of the sequence that form the pore helix, the selectivity filter and the inner helix (Figure 41).

## RESULTS

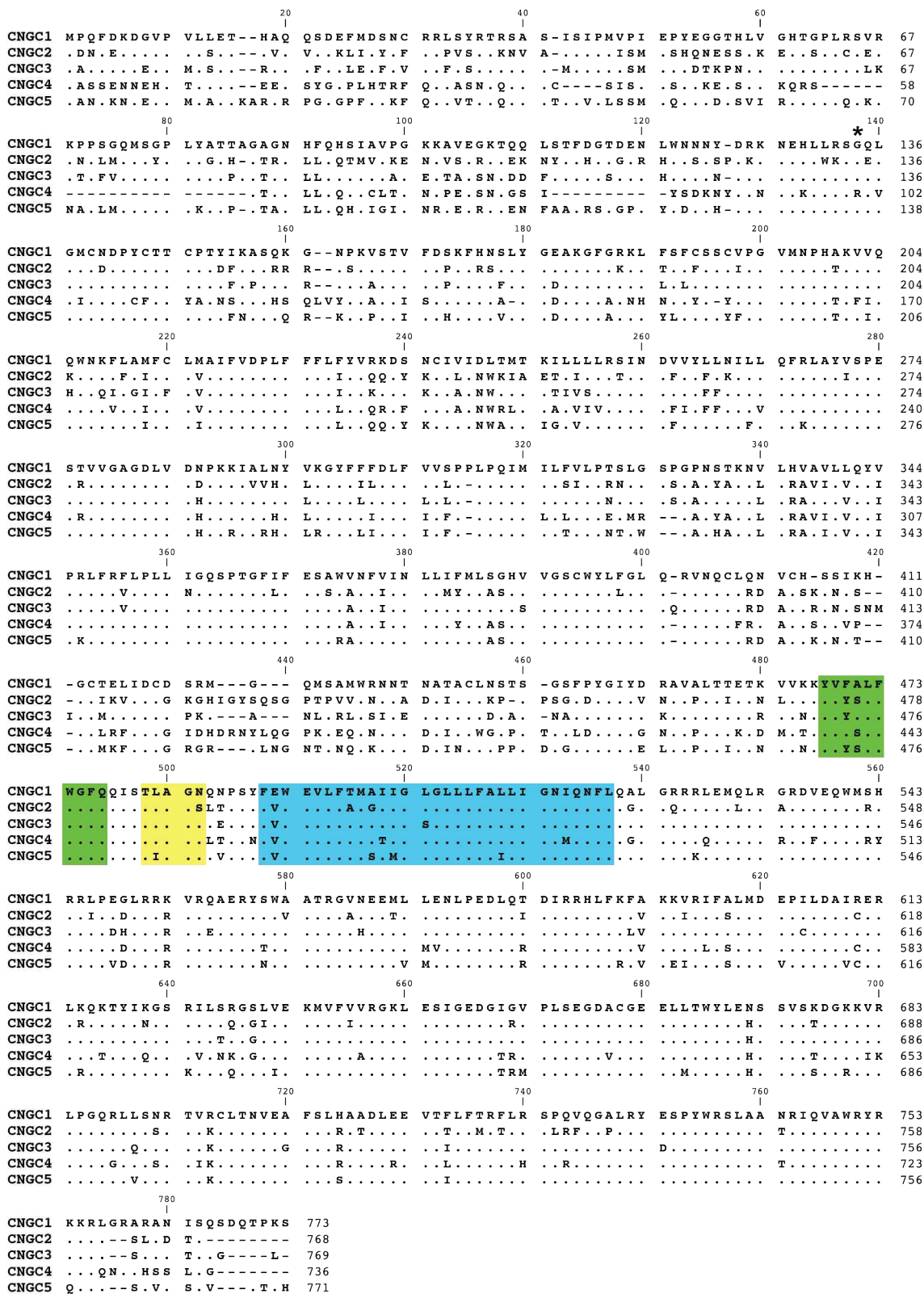


**Figure 41. Alignment of amino acid sequences of the five CNGCs.**

The predicted amino acid sequences of CNGC2, CNGC3, CNGC4 and CNGC5 were aligned to the amino acid sequence of CNGC1. According to Talke et al., 2003, following structures are highlighted: green - the pore helix, yellow - selectivity filter, blue - inner helix/S6. The asterisk at position 138 marks the identified mutation of the glycine to glutamic acid. Equal residues are shown as dots. CNGC sequences are attached (see appendix 9.1.2).

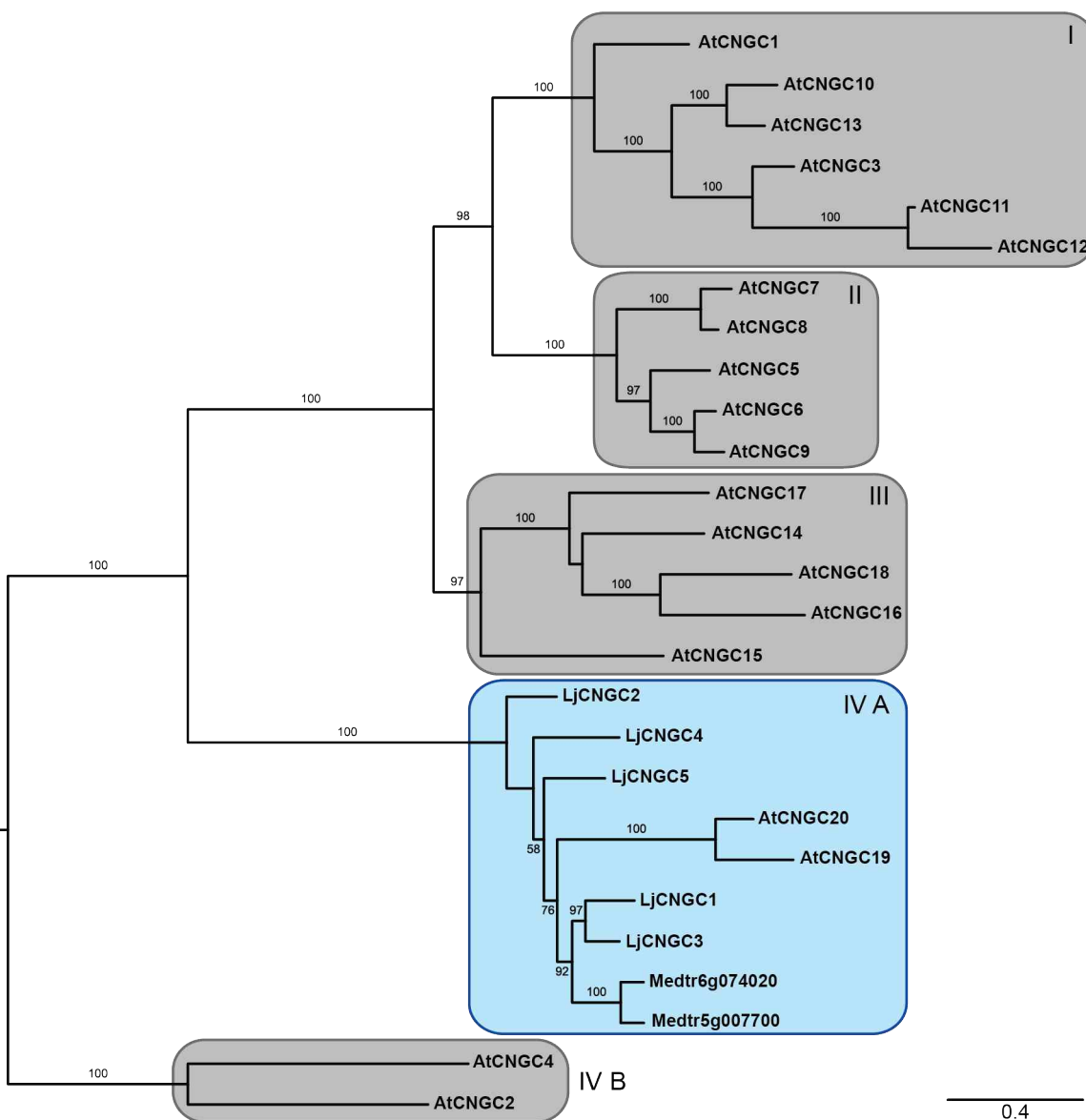
## RESULTS

---

### 2.3.4.6 Phylogenetic Relationships of CNGCs of *L. japonicus*, *M. truncatula* and *A. thaliana*

CNGCs of *A. thaliana* form five phylogenetic clusters, which are called I, II, III, IVa, IVb (Mäser et al., 2001). Two putative CNGCs of *M. truncatula*, Medtr5g007700 and Medtr6g074020, were found in the *Medicago* genome by a BLAST search on the Phytozome website using the *Lotus* CNGC1 genomic sequence. In contrast to the *Lotus* CNGCs or the *Arabidopsis* AtCNGC19 and AtCNGC20, they are not located on the same chromosome. Additional Phytozome database searches of the *Medicago* genome were performed using the *Lotus* CNGC2 to CNGC5 genomic sequences, but only the already identified putative *Medicago* CNGCs were retrieved again.

A phylogenetic tree was calculated from an alignment containing amino acid sequences of the 20 known CNGCs of *A. thaliana*, the five of *L. japonicus* and the two of *M. truncatula* (Figure 42). The *Lotus* and *Medicago* CNGCs cluster together with AtCNGC19 and AtCNGC20 in group IV A.



## RESULTS

---

---

Previous page:

**Figure 42. Phylogenetic tree showing the five CNGC clusters of *A. thaliana* with the identified *L. japonicus* and *M. truncatula* CNGCs.**

Amino acid sequences of 20 CNGCs of *A. thaliana*, of the five CNGCs of *L. japonicus* located on CM0435 and of two CNGCs of *M. truncatula* were aligned using MAFFT. The phylogenetic tree was calculated based on this alignment using RAxML. 100 bootstrap iterations were performed and only bootstrap values >50 are depicted. Scale bar shows the number of amino acid substitutions per site. The five phylogenetic classes of CNGCs are indicated according to Talke et al., 2003. The five *Lotus* CNGCs cluster together with AtCNGC19, AtCNGC20 and the two *Medicago* CNGCs in group IV A. *M. truncatula* and *A. thaliana* CNGC peptide sequences were downloaded from the Phytozome website. *A. thaliana* locus names: CNGC1 (AT5g53130), CNGC2 (AT5g54250), CNGC3 (AT2g46430), CNGC4 (AT5g54250), CNGC5 (AT5g57940), CNGC6 (AT2g23980), CNGC7 (AT1g15990), CNGC8 (AT1g19780), CNGC9 (AT4g30560), CNGC10 (AT1g01340), CNGC11 (AT2g46440), CNGC12 (AT2g46450), CNGC13 (AT4g01010), CNGC14 (AT2g24610), CNGC15 (AT2g28260), CNGC16 (AT3g48010), CNGC17 (AT4g30360), CNGC18 (AT5g14870), CNGC19 (AT3g17690), CNGC20 (AT3g17700). *L. japonicus* CNGC sequences are attached (see appendix 9.1.2).

### 3 Discussion

#### 3.1.1 A Forward Genetic Screen for Mutants Impaired in Arbuscular Mycorrhiza Development

##### Phenotypes of Putative AM Mutants

The putative AM mutants have been classified according to their phenotypes (Figure 4; Table 1). The vast majority of the putative AM mutants showed aberrant fungal structures at more than one developmental step and 25 of the 55 putative AM mutant lines exhibited defects during epidermal penetration and arbuscule development (Figure 5). The mutant *pam1* (*penetration and arbuscule morphogenesis1*), which was discovered in a screen of a transposon-mutagenized population of *Petunia hybrida* for AM defective plants, is also impaired at these two phases of AM formation, characterized by many aborted infection sites and the absence of arbuscules (Reddy et al., 2007). Nevertheless, the fungus occasionally colonizes the root cortex, where it repeatedly enters cortical cells with short branches incapable of forming arbuscules (Reddy et al., 2007). The *PAM1* gene and its homologue in *M. truncatula*, *VAPYRIN*, encode a protein with a N-terminal MSP domain and an ankyrin domain (Feddermann et al., 2010; Pumplin et al., 2010). Since intracellular penetration of the fungal hyphae is important for the epidermal infection process and arbuscule formation, it is possible that *VAPYRIN* is required for the intracellular accommodation that occurs in both of these developmental steps (Reddy et al., 2007). It can be suggested that also the 25 AM mutant lines, whose phenotypes resemble the one of *pam1* mutants, are impaired in this intracellular accommodation process.

Mutants that are impaired in intercellular spreading of the hyphae in the root cortex have already been reported. Hyphae are able to enter roots of the AM maize mutant *taci1* (*taciturn1*), although the number of infection sites is lower in mutants than in wild-type roots, but proliferation in the apoplastic space and colonization of the root cortex seem to be affected (Paszkowski et al., 2006). This phenotype is comparable to that of the mutants of the lines SL1755-N and SL1915-N (Figure 6G - J), where also infection sites seem to be normal and hyphae can grow towards the root cortex, but then further spreading seemed to be inhibited.

The mutant *str* (*stunted arbuscule*) was isolated in a forward genetic screen of an EMS-mutagenized population of *M. truncatula* and exhibits small arbuscules (Zhang et al., 2010). Compared to *str*, arbuscules of SL3284-N seemed to have even less branches. Putative orthologues of *STR* and *STR2* have been identified in *L. japonicus* (Zhang et al., 2010), opening the possibility to check whether SL3284-N mutants carry mutations in these genes. Furthermore, it will be interesting to cross these mutants with *dis* and *red* mutants (S. Hardel and M. Groth, personal communication) to test whether the mutant phenotypes can be complemented.

### The AM Screen – Potential and Drawback

A forward genetic screen of a mutagenized population for mutants showing defects in a biological process of interest is a powerful tool to discover novel genes (Page and Grossniklaus, 2002). Thereby, no anticipation of the genes' identities and functions is necessary, what opens the possibility to isolate mutants without any bias (Alonso and Ecker, 2006). Forward genetic screens for plants impaired in AM have already been conducted in petunia (Reddy et al., 2007), maize (Paszkowski et al., 2006), *Medicago* (Zhang et al., 2010), and tomato (Barker et al., 1998; David-Schwartz et al., 2001; David-Schwartz et al., 2003), which resulted in the identification of eight AM mutants, whose phenotypes have been described in detail. The goal of the AM screen presented in this study was the isolation of AM mutants in *L. japonicus* that were not impaired in the root nodule symbiosis. Two mutants impaired in arbuscule formation, *red* (*reduced and degenerate arbuscules*) and *dis* (*disturbed arbuscules*), were found by S. Kosuta during this AM screen. Both mutant lines were able to form nodules and preliminary mapping data suggest that they carry mutations in novel genes that have so far not been reported to be involved in arbuscule development (S. Hardel and M. Groth, personal communication).

The vast majority of the mutants detected during my part of the AM screen could not be confirmed in the M4 generation (Figure 3; Table 1). Success of a forward genetic screen is highly dependent on the sensitivity, specificity and reproducibility of the mutant phenotype (Alonso and Ecker, 2006). Hence, parameters that could influence the phenotype during the screen should be kept as constant as possible. The level of AM colonization is substantially determined by the vigour of the AM fungus. Since the inoculation strength of the individual chive nurse pot could not be monitored, phenotypic differences in AM structures and intensities of colonization could have resulted from variability in inoculation pressure.

Whether we would have been able to identify mutants whose phenotypes were weak when inoculated with the high infection strength using chive nurse pots is questionable. For example, the AM mutant called *pmi* (*premycorrhizal infection*) isolated from a fast-neutron-mutagenized tomato population exhibits severe phenotypic differences depending on the inoculum type (David-Schwartz et al., 2001). When mutants were grown in one pot together with wild-type plants and spores of AM fungi or with inoculated root pieces, their roots were colonized and AM structures were visible as in the wild-type control. In contrast, inoculation with only spores leads to mutant roots that are almost not infected (David-Schwartz et al., 2001; David-Schwartz et al., 2003). We would not have been able to identify this class of mutants during our AM screen, because of the high inoculum pressure and the fact that wild-type plants would have been growing together with mutants in the same compartment.

Hence, AM phenotypes can be affected by various factors, what entails a drawback of the AM screen. Nevertheless, the forward genetic AM screen holds a huge potential regarding the already identified interesting AM mutant phenotypes.

### 3.1.2 The Calcium-Dependent Protein Kinase 29 of *Lotus japonicus*

The AFLP fragment AM8 was found to originate from an alternative first exon of a *CPK*, indicating a possible involvement of an alternatively spliced  $\text{Ca}^{2+}$  sensor protein in the molecular signalling network of root symbioses.

#### ***CPK29* of *L. japonicus* and its Two Alternative, Mutually Exclusive First Exons**

Alternative splicing has already been reported for several *CPK* genes. The rice *CPKs* Os $CPK13$  and Os $CPK4$  show two different types of alternative splicing. In the case of Os $CPK13$ , one alternative transcript holds an additional splice site leading to a 35 amino acid deletion in the N-terminal variable region (Asano et al., 2005). Two alternatively spliced Os $CPK4$  cDNA variants differ in the eleventh splice site with a 6-bp insertion/deletion between the third and the fourth EF hand (Asano et al., 2005). Alternative splicing events in the 5'-UTR result in different transcripts of Os $CDPK2$ , Os $CPK7$ , Os $CPK19$  and Os $CPK23$ . It is not known whether these different transcripts have any distinct biological function (Asano et al., 2005; Morello et al., 2006). Another example of alternative splicing of a *CPK* was found in the liverwort *Marchantia polymorpha*. Two exons are mutually exclusively spliced out and two proteins are produced that differ in the amino acid composition in the EF-hand region (Nishiyama et al., 1999). Since one of the transcripts is more abundant in male sexual organs compared to other tissues, the authors propose that alternative splicing regulates the expression of the analysed *CPK* in sexual organs (Nishiyama et al., 1999). According to the TAIR database ([www.arabidopsis.org](http://www.arabidopsis.org)), nine *Arabidopsis* *CPKs* (CPK7, CPK8, CPK14, CPK15, CPK23, CPK26, CPK28, CPK29) are reported to produce alternatively spliced transcripts. Since none of these exhibits a gene structure with two AFEs affecting part of the functional region, Lj *CPK29* is the first analysed *CPK* with two alternative and mutually exclusive first exons (Figure 7A).

A bioinformatic screen for genes with alternative first exons discovered this feature in approximately 5.9% of expressed rice genes and in circa 5% of expressed *Arabidopsis* genes (Chen et al., 2007). Two different kinds of alternative first exon scenarios were analysed. In Type I AFEs only one of the alternative first exons is present after the splicing, whereas in Type II AFEs one of the first exons is an internal exon of the alternative transcript (Chen et al., 2007). According to this classification, Lj *CPK29* belongs to the Type I AFEs. Regarding all AFE events, Chen and associates (2007) discovered that 90% in rice and 83% in *Arabidopsis* are Type II AFEs. In addition, most of the Type I AFEs are located in the 5'-UTRs, meaning that the resulting ORFs are not affected and identical proteins are produced. Only 5 of 137 and 1 of 99 genes of Type I AFEs in rice and *Arabidopsis* show a N-terminal diversification overlapping with a functional protein domain. In contrast, 62 of 137 genes in rice and 22 of 99 genes in *Arabidopsis* carry putative alternative promoters (Chen et al., 2007). These numbers clearly show that the intriguing gene structure of Lj *CPK29* producing two *CPKs* with unique N-terminal variable regions and partially different protein kinase domains is a rare genetic feature (Figure 7C).

**Are the Alternatively Spliced Transcripts of *Lj CPK29* Regulated in a Tissue- and/or Development-Specific Manner?**

Many genes with AFEs are supposedly regulated in a tissue- and/or development-specific manner (Kitagawa et al., 2005; Chen et al., 2007). The results of q-RT-PCRs performed to confirm the differential expression of the two transcripts of *Lj CPK29* in wild-type and *ccamk* roots were not conclusive. The primers used to amplify the two variants were designed based on the sequence information of the UTRs and adjacent exons to minimize potential mis-annealing to other *CPKs* in the genome. The low expression levels of both variants detected by the q-RT-PCRs could point to an expression of the gene variants in only a very limited number of cells in the root cortex. A cell-type specific expression has recently been shown for *OsCPK18*. Cortical and epidermal cells from inoculated rice root were collected by laser capture microdissection and transcripts of *OsCPK18* are only present in the sample containing cortical cells (Campos-Soriano et al., 2011). Therefore, the *CPK29* transcripts could be too diluted when the complete root tissue is analysed, what could hamper the exact evaluation of expression differences.

Promoter-GUS analyses revealed two distinct expression patterns of the two *CPK29* versions in *Lotus* hairy roots. Since the distance between the transcription start sites of the alternative first exons comprised 1534 bp, each of the variants has probably its own promoter sequence (Kimura et al., 2006). This could be confirmed, because each of the promoter sequences tested induced transcription of the  $\beta$ -glucuronidase resulting in a clearly visible GUS staining of hairy roots (Figure 10). The differences of the promoter-driven GUS staining patterns between the two constructs pointed to an expression of *CPK29a* during early nodule development. Young nodules emerging from *ProCPK29a-GUS*-transformed hairy roots were intensively stained blue, indicating that *CPK29a* is expressed during early nodule development (Figure 10).

Differential expression patterns induced by the *ProCPK29a-GUS*- or *ProCPK29b-GUS*-construct could not be observed comparing hairy roots that were inoculated with AM fungi to non-inoculated ones. However, since the original AM8 AFLP fragment was induced in *ccamk* mutant roots, a visible effect of the promoter-GUS experiment using wild-type roots is not mandatory. It would be interesting to compare GUS expression patterns induced by the two *CPK29* promoters in the *ccamk* mutant background after inoculation with AM fungi.

**Do *CPK29* Isoforms Have Different Subcellular Localizations and Functions?**

In addition to a tissue-specific expression driven by alternative promoters, the alternative splice products could also differ in their subcellular localization. The alternatively spliced isoforms of the tomato protein phosphatase 5 (LePP5) are found in different subcellular compartments, for example (de la Fuente van Bentem et al., 2003). One of the transcripts carries an additional exon that converts it to an integral membrane protein and is localized in the ER and the nuclear envelope. The transcript without this additional exon produces a soluble protein, present in the cytoplasm and inside the nucleus (de la Fuente van Bentem et al., 2003). Alternative splicing affecting the N-terminus of OsBWMK1, a member of the MAPK-family, produces three transcripts

with different subcellular localizations (Koo et al., 2007). Therefore, the two alternative isoforms of CPK29 could also be present at different sites in the cells. In total, 27 CPKs of *Arabidopsis* are predicted to carry a myristoylation motif (Hrabak et al., 2003; Podell and Gribskov, 2004). AtCPK2, OsCPK2 and OsCPK18 are examples of CPKs that have been shown to be myristoylated and membrane-targeted (Martin and Busconi, 2000; Lu and Hrabak, 2002; Campos-Soriano et al., 2011). In addition, the subcellular localization of nine At CPKs has been determined. Seven CPKs carried a myristoylation and palmitoylation signal (At CPK1, 7, 8, 9, 16, 21, 28) and all beside At CPK1 were shown to be associated with the plasma membrane. At CPK1 was targeted to peroxisomes. Furthermore, At CPK3 and CPK4, which do not contain a myristoylation signal, are located in the cytosol and in the nucleus (Dammann et al., 2003).

The alternative CPK29 proteins carry different N-terminal sequences (Figure 14). Only Lj CPK29b, Mt CPK29b and Glyma14g40090b were predicted to be myristoylated. Transient co-expression of the N-termini of Lj CPK29a and Lj CPK29b fused to fluorescent proteins in *N. benthamiana* leaves revealed that both fusion proteins were associated with the plasma membrane (Figure 11). Analysis of the subcellular localization and tissue-specific expression of the two CPK29 versions in transgenic *Lotus* hairy roots are important to confirm the involvement of Lj CPK29a in nodule development.

To investigate whether the two isoforms are indeed involved in different signalling pathways and have differential functions, *Medicago Tnt1* lines with insertions in the *CPK29* gene were analysed. The *Tnt1* line NF4838 carries an insertion in the common part of both transcripts. Potential mutant phenotypes of this line could help to elucidate developmental processes where both CPK29 isoforms are involved. I could not obtain any mutant plant of line NF4793. This could indicate that the presence of the insertion in both alleles of *CPK29* in the genome results in lethality. Detailed analysis is necessary to check at which developmental stage the embryos die and whether it is really a specific effect of the insertion into *CPK29* in this line. In contrast to NF4838 and NF4793, line NF2225 carries the transposon insertion in the AFE specific for Mt CPK29a. Hence, mutant phenotypes that occur in NF2225 plants carrying two *CPK29* copies with insertion and that are absent in NF2225 plants without this insertion could reveal specific functions of Mt CPK29a. Preliminary data suggested a reduced nodule number in NF2225 homozygous plants. Further experiments have to be performed to confirm the potential involvement of Mt CPK29a in root symbioses. Q-RT-PCR analyses, for example, could determine expression levels of the two transcripts in wild-type and *dmi3* mutant roots that are inoculated either with AM fungi or with rhizobia compared to non-inoculated ones. Furthermore, hairy root transformations of NF2225 homozygous plants have to show that the mutant phenotype can be complemented with the wild-type Mt *CPK29a* isoform.

Regarding the data about genes with AFEs in the literature and the promoter-GUS-expression data, it could be hypothesized that the two CPK29 isoforms are components of different molecular signalling pathways and/or are involved in specific biological processes. CPK29a is probably part of the signalling cascade active in root symbioses.

### Are the Alternative First Exons of CPK29 Legume-Specific?

The predicted genes of non-leguminous species in the CPK29 cluster did not carry alternative first exons (Figure 15). Therefore, the question arises whether AFEs of *CPK29* are a legume-specific phenomenon. Wang and associates (2008) already discovered legume-specific alternative splicing (AS) events by comparing EST data from *L. japonicus*, *M. truncatula*, *G. max*, *A. thaliana* and *O. sativa*. For example, they report that a 3'-UTR intron of a carbonic anhydrase gene is alternatively spliced only in the analysed legume species, but not in *Arabidopsis* and rice (Wang et al., 2008). Hence, the AFEs of *CPK29* could be one of these legume-specific AS events. Evaluations of the synteny between the genomes of *Arabidopsis* and *Medicago* revealed that after divergence of the two lineages many homologous genes have been duplicated and genes are selectively lost after duplication (Zhu et al., 2003). These events could also have happened in case of *CPK29* (Figure 43). Originally, only one copy of *CPK29* would have been present in plants (Figure 43A), as it is still the case in *Arabidopsis*, strawberry and rice. In an ancient legume this *CPK29* could have undergone duplication (Figure 43B) and subsequently partial gene loss could have occurred (Figure 43C). Since the promoter and the first exon could have still existed, a new splicing event could have generated a functional *CPK29* with two AFEs (Figure 43D).

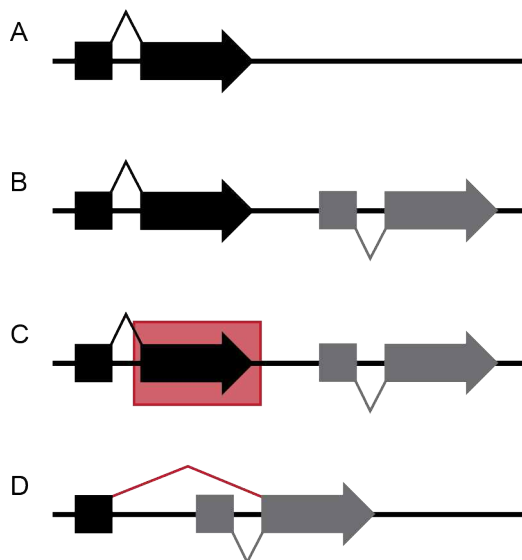


**Figure 43. Model for the evolution of CPK29 with two alternative first exons.**

(A) Originally, one *CPK29* gene is present in plants, as it is still present in *Arabidopsis*, rice or strawberry, for example. (B) A segmental duplication event that could have occurred in the genome of an ancient legume led to the existence of a second *CPK29* gene shown in grey. (C) Partial gene loss (red box) deleted genomic sequence between the duplicated genes. (D) A new splice event (red) combined the remaining first exon (black) with the previously duplicated gene and generates the gene structure with two alternative first exons of *CPK29* as seen in *Medicago*, *Lotus* and most probably soybean. Black and grey boxes represent the putative first exons, black or grey arrows the remaining gene including exons and introns.

It is known from analysing traces of whole genome duplications that genes of specific functional categories were often retained, especially when the duplicated genes diverge in their functions (Blanc and Wolfe, 2004; Adams and Wendel, 2005). Duplicated genes encoding for example kinases, phosphatases, transcription factors and calcium-binding proteins are found to be preferentially retained in the *Arabidopsis* genome (Blanc and Wolfe, 2004). According to the slogan ‘Use it or lose it’ (Blanc and Wolfe, 2004), each of the CPK29 isoforms could be involved in specific cellular processes, where CPK29a probably plays a role in the molecular signalling network of root symbioses.

In the case of *G. max*, four predicted CPKs belonged to the CPK29 cluster (Figure 15). There were Glyma14g40090a and Glyma14g40090b, supposed to be encoded by Glyma14g40090 with two AFEs, as well as Glyma17g38040 and Glyma17g38050, which were encoded by two adjacent but independent genes. For the later gene pair, AFEs could not be constructed by bioinformatics and both genes were predicted to contain EF hands. Therefore, the tandem repeat on chromosome 17 resembles the hypothetical ancestral intermediate depicted in Figure 43B. The phylogenetic analysis (Figure 15) indicated that Glyma17g38050 is part of the CPK29a subgroup, whereas Glyma17g38040 belongs to the CPK29b subgroup. Interestingly, such a duplicated CPK29 could not be found in the genomes of *Medicago* or *Lotus*. A final statement explaining the existence of CPK29 with two AFEs in *Lotus*, *Medicago* and soybean and, in addition, the two related soybean CPKs is so far impossible, because the timing of the individual evolutionary events cannot be determined. Further analyses are necessary to resolve the phylogenetic relationships of the soybean genes in the CPK29 cluster in detail. First of all, it is important to check by RACE experiments whether Glyma14g40090 indeed carries two AFEs. Furthermore, it has to be analysed, whether all the soybean genes related to CPK29 encode functional CPKs, regarding the missing EF hand of Glyma17g38050 and the absent myristoylation signals in Glyma17g38040 and Glyma17g38050.

A database search with the Lj CPK29a genomic sequence in the *P. trichocarpa* genome sequence revealed two unlinked genes, POPTR\_0005s26640 and POPTR\_0002s01850 that were predicted to encode CPKs. The phylogenetic analysis placed them into the CPK29 cluster, but not within the CPK29a and CPK29b subgroups. The existence of two poplar genes within the CPK29 cluster could be explained by a WGD of the poplar genome (Tuskan et al., 2006). It should be noted that this is not a tandem duplication; the two genes are located on two different scaffolds.

In summary, the phylogenetic data suggest that CPK29 with AFEs is legume-specific. It will be interesting to further analyse their specific gene expression patterns and to investigate the functions of the partially different CPK29 proteins. The fact that CPK29 with AFEs is only found in legumes so far strongly points to an involvement in the root nodule symbiosis signalling network.

### 3.1.3 The *Lotus japonicus* Mutant *brush*

#### The Complex Phenotype of *brush* Mutants

Short and thick roots as well as deficient nodulation are the characteristic features of *brush* mutants (Figure 18, Figure 20; Maekawa-Yoshikawa et al., 2009). With regard to the temperature-sensitive phenotype of *brush*, two hypotheses could be put forward. First, the altered root morphology of *brush* mutants could be the reason for their nodulation deficiency. Hence, the nodulation phenotype would be a side effect of the distorted *brush* roots. Second, the nodulation could be impaired regardless of the root morphology. To figure out which of the hypotheses holds true for *brush* mutants, their root and nodulation phenotype was analysed in detail by performing several temperature shift experiments.

It was shown that *brush* roots are longer and exhibited more infection structures after inoculation with rhizobia when they were grown at 18°C compared to 26°C (Maekawa-Yoshikawa et al., 2009). To find out whether root growth and nodulation defects could be separated, temperature shifts from 18°C to 26°C were performed at several different time points during plant development and the plants were inoculated with rhizobia after shifting the plants to the restrictive temperature. The shifts some days and two weeks post germination revealed that mutant plants still had the mutant phenotype without significant differences regarding the time point of the shift. They only showed a tendency to form more infection threads and white bumps, as well as longer roots, when they were grown longer at 18°C (Figure 19, Figure 21). A high variability in root lengths could be observed (Figure 18), probably counteracting a meaningful result.

Interestingly, the temperature-shift experiment six weeks post germination demonstrated that the root and nodulation phenotype of *brush* mutants could be uncoupled; significantly less nodules were formed on wild type-like *brush* roots and at 26°C no nodule could be observed (Figure 22, Figure 24). According to this experiment the nodulation phenotype of *brush* would not be a side effect of its short-thick roots and would also be temperature-sensitive on its own (Figure 24). This result favours the second hypothesis.

In early rhizobia recognition responses like root hair deformation or calcium spiking *brush* mutants do not differ from the wild type (Maekawa-Yoshikawa et al., 2009). Nevertheless, instead of wild-type nodules only nodule primordia with many superficial infection threads emerged predominantly from *brush* roots (Figure 20C; Maekawa-Yoshikawa et al., 2009). These infection threads usually ended in the epidermal or cortical cell layers with a dot-like structure (Figure 23B). The release of rhizobia from the infection thread and their endocytosis into cells of the already produced nodule primordium was apparently affected, what led to the formation of so-called white bumps without colonizing rhizobia. Very few small nodules could be detected with rhizobia inside (Figure 20B; Maekawa-Yoshikawa et al., 2009), showing that in rare cases rhizobia were able to enter the developing nodule. However, even though the white bumps were covered with many infection threads, in total less infection threads were observed on mutant compared to wild-type roots (Figure 21C). Therefore, *brush* mutants seemed to be impaired in infection thread initiation as well as in cortical infection of nodule primordia.

***Lotus* and *Medicago* Mutants Resembling *brush***

Several mutants with phenotypes similar to that of *brush* have been reported recently. The developmental program for lateral root formation probably has been recruited by the evolution of nodulation and genes that are involved in root and nodule development at the same time have been already described (Szczyglowski and Amyot, 2003). The *LATD/NIP* gene of *M. truncatula* encoding a member of the *NRT(PTR)* transporter family, is one of those (Yendrek et al., 2010). The mutant phenotype resembles *brush*, because *latd* (*lateral root organ defective*)/*nip* (*numerous infections and polyphenolics*) mutants have disorganized root tips, very short lateral roots and shorter primary roots than wild-type plants. In addition, immature, non-fixing nodules are formed (Bright et al., 2005; Yendrek et al., 2010). Nevertheless, it is unlikely that *brush* is the orthologue of *LATD/NIP* in *Lotus*. First, the primary roots of *latd* mutants are wild type-like during early development (Bright et al., 2005). Second, *latd* mutants produce wild-type roots after application of abscisic acid (Liang et al., 2007), whereas *brush* mutants do not (Maekawa-Yoshikawa et al., 2009).

The *Medicago* mutant *api* shows similar defects like *brush* regarding its nodulation phenotype (Teillet et al., 2008). Many nodule primordia of *api* (*altered nodule primordium invasion*) mutants are not colonized by rhizobia, because the infection thread growth stops in the root cortex before it reaches the developing nodule. Infection thread defects and the prevention of rhizobia being released into nodule primordia can be overcome in rare cases resulting in nitrogen-fixing nodules. Since even these nodules are not completely wild type-like, they fix nitrogen only suboptimal and abnormal infection threads are observed. Therefore, Teillet and associates (2008) suggest that API is required throughout the nodulation process. Despite these obvious analogies between *brush* and *api* mutants, one striking difference is that on *api* roots often large infection pockets are formed next to nodule primordia. These have not been found in *brush* mutants, which only show a dot-like structure at the end of infection threads (Figure 23B).

Lots of white bumps and only very few pink nodules emerge from *Lotus nap1* and *pir1* roots upon rhizobia inoculation, again resembling *brush*. Comparing *nap1* and *pir1* to the wild type, less infection threads are formed and these have growth defects. In addition to the nodulation phenotype, these mutants are characterized by distorted trichomes (Yokota et al., 2009). The authors conclude that the genes *Nap1* and *Pir1* are important for reorganisation of the actin cytoskeleton during rhizobial infection and for trichome development (Yokota et al., 2009). Despite the parallels in the nodulation process between *brush*, *nap1* and *pir1* mutants, *Nap1* and *Pir1* have been cloned and mapped to chromosome 4 and chromosome 1, respectively, and are probably single genes (Yokota et al., 2009). In contrast, the *brush* target interval was located on chromosome 2 (Figure 25). Furthermore, trichomes of *brush* mutants appear to be wild type-like (Maekawa-Yoshikawa et al., 2009). Therefore, it is unlikely that *BRUSH* represents a gene related to *Nap1* or *Pir1*. In summary, the gene mutated in *brush* causing its complex mutant phenotype is probably a novel gene, which has not been reported yet.

### Segregation of the *brush* Root and Nodulation Phenotype

To identify the mutation responsible for the root and nodulation phenotype of *brush* mutants by map-based cloning, F2 progenies of MG-20 x *brush* crossings were analysed. Since the root and the nodulation phenotype of *brush* mutants could be uncoupled (Figure 22, Figure 24), the question is whether these two phenotypes are caused by a mutation in a single gene or by mutations in two closely linked genes. A stringent cosegregation of the two phenotypes would support the first possibility, the occurrence of plants with either root or nodulation phenotype would point to the second. Maekawa-Yoshikawa and associates (2009) only observed cosegregation of the two phenotypes among analysed F2 (MG-20 x *brush*) individuals and F2 (*brush* x Gifu) backcross lines.

Accordingly, phenotypic analyses of backcross plants in this study detected only plants with short and thick roots that showed defects in nodulation (Figure 33). In contrast, during phenotyping of F3 plants (MG-20 x *brush*) individuals with wild-type root systems plus white bumps and occasionally very few nodules or without any nodules appeared (Figure 26). These plants were grown at 26°C, the temperature at which mutant roots usually did not form nodules. Interestingly, all F3 progenies segregating these wild-type roots with the mutant nodulation phenotype also segregated mutants with short and thick roots. Hence, these progenies were called ‘segregating’. Moreover, their F2 parent plants carried a Gifu/Het recombination event between G175 and G082 (Figure 26). In contrast, F3 progenies of F2 plants with MG-20/Het recombination events between these markers segregated either only wild-type plants with wild-type nodules or mutants with short and thick roots (Figure 26). Ratios between the detailed phenotypic classes as scored in Figure 26 for example varied in some cases considerably, when the progeny of the same F2 plant was phenotyped a second time. Also the fact that the temperature plants are cultivated at had a strong impact on only some of the F3 progenies (Figure 29; Figure 30), suggests a phenotypic variability that could interfere with a proper assigning of the phenotypes.

The most extreme temperature-sensitive phenotypic variance was discovered in the progeny of L9759; at 26°C all plants had short and thick roots and at 18°C only plants with wild-type roots were detected (Table 2, Figure 30). Their roots were significantly longer at 18°C than at 26°C, which represented the only progeny that showed these clear temperature-dependent root lengths (Figure 31). The occurrence of these variable, temperature-dependent phenotypes cannot be rationalized so far and the high degree of variability observed during phenotyping of F3 and F4 progenies makes it very difficult to draw definite conclusions.

Phenotyping and genotyping of F4 and F5 (MG-20 x *brush*) populations revealed that plants with wild-type roots and white bumps are heterozygous at EMS-induced SNP or at SSR-marker positions in the target interval (Figure 32). These results and the fact that progeny of F3 and F4 plants with wild-type roots and white bumps again segregated plants with mutant roots suggest that the putative mutation in *BRUSH* is responsible for both phenotypes. A plant carrying two mutant alleles would exhibit the short and thick root phenotype and, if only one mutant allele is present, nodulation would be impaired. This hypothesis implies that nodulation is more sensitive to the mutation than root development.

**Is the EMS-Induced Mutation in CNGC1 Responsible for the *brush* Phenotype?**

The mapping data and sequencing of candidate genes in the 37 kb target interval discovered an EMS-induced guanine to adenine transition (Figure 28). This mutation was located in an open reading frame encoding a gene with high similarity to cyclic nucleotide-gated channels, which was called *CNGC1* (Figure 36). Within this gene, the mutation led to a substitution of the amino acid glycine with glutamic acid at the N-terminus of the predicted protein sequence (Figure 41). Unbiased *de novo* assembly of *brush* and Gifu wild-type genomes sequenced by ILLUMINA hiSeq technology and subsequent comparison to the MG-20 genome did not reveal any evidence for inconsistencies between MG-20, Gifu and *brush* in this region. Moreover, additional EMS-induced mutations within the target interval were not detected.

AtCNGC19 or AtCNGC20 are phylogenetically closely related to CNGC1 as well as the additional CNGCs located next to CNGC1 and cluster together in CNGC group IVa (Figure 28, Figure 42). T-DNA insertion lines of these two *Arabidopsis* CNGCs, which are arranged in tandem, resemble wild-type plants, but the expression of both genes is induced in response to salt stress (Kugler et al., 2009). With respect to their close relationship, the *Lotus* CNGCs, AtCNGC19 and AtCNGC20 are supposedly associated with similar physiological processes. Talke and associates (2003) already suggested that CNGCs present in the same phylogenetic subgroup could have similar functions.

The promoter-GUS experiment performed to analyse expression patterns of CNGC1 in roots after inoculation with rhizobia (Figure 40) pointed to a function of CNGC1 during early nodule development.  $\text{Ca}^{2+}$  influx and  $\text{Ca}^{2+}$  spiking triggered by either rhizobial Nod factors or mycorrhizal Myc factors are characteristic key steps during the establishment of RNS and AM (Shaw and Long, 2003; Kosuta et al., 2008). Several CNGCs have been shown to conduct  $\text{Ca}^{2+}$  (Leng et al., 1999; Ali et al., 2006; Frietsch et al., 2007), thus it could be rationalized that they play a role in symbiotic signalling. Since *brush* mutants are able to form AM (Maekawa-Yoshikawa et al., 2009), a specific involvement of CNGC1 in the establishment of RNS, especially in the generation of the early  $\text{Ca}^{2+}$  influx could be proposed. According to Miwa and associates (2006) the  $\text{Ca}^{2+}$  flux is important for the activation of infection thread growth and requires relatively high concentrations of Nod factor that could be caused by rhizobia entrapped inside in the curling root hair. The fact that infection threads on the surface of the white bumps were ending in a dot-like structure (Figure 23) and in total less infection threads were formed on *brush* roots (Figure 21C) corroborates the hypothesis that CNGC1 could be involved in the generation of this  $\text{Ca}^{2+}$  influx.

Despite these possible roles of CNGC1 in the establishment of RNS and root growth, complementation tests of *brush* mutants with the genomic sequence of CNGC1 failed to restore the wild-type phenotype (Figure 37). Since it was shown that also plants that are heterozygous in the target interval are impaired in nodulation, it is possible that the disturbed gene dosage effects in mutant plants can not be restored by transient expression of CNGC1. Nonetheless, CNGC1 TILLING mutants, one of which carries a premature stop codon, were wild type-like (Table 3). In addition, four *brush* backcross mutants were heterozygous at the mutation in CNGC1 (Figure 33).

## DISCUSSION

---

Several authors propose that plant CNGCs form heterotetramers, as they do in animals (Yoshioka et al., 2006; Kaplan et al., 2007; Ma and Berkowitz, 2011). This possibility and the existence of additional four predicted CNGCs next to *CNGC1* offer an interesting hypothesis. *CNGC1* forms a heterotetramer with one of the CNGCs of the CNGC cluster in wild types. In *brush* mutants *CNGC1* carries the identified EMS-induced mutation. Hence, the mutated *CNGC1* is still present in the complex, but interferes with the function of the heterotetramer in a temperature-sensitive manner. In case of the TILLING *CNGC1* stop codon mutant another CNGC is able to replace *CNGC1* resulting in a functional channel complex.

Further experiments, such as the expression of the mutated *CNGC1* version in the TILLING stop codon mutant background, are necessary to finally unravel the complex genetics and phenotype of *brush*.

## 4 Summary

Legumes, such as *Lotus japonicus* and *Medicago truncatula*, are able to engage in two different root endosymbioses, the Arbuscular Mycorrhiza (AM) with AM fungi and the Root Nodule Symbiosis (RNS) with rhizobia. Both microbial symbiotic partners induce nuclear and perinuclear calcium ( $\text{Ca}^{2+}$ ) spiking in root cells. In addition, an early  $\text{Ca}^{2+}$  influx occurs in root hair cells treated with high rhizobial Nod factor concentrations. How these cytosolic changes in  $\text{Ca}^{2+}$  concentrations are generated and deciphered is still not understood.

To analyze genes involved specifically in the AM or RNS signaling pathway, I conducted a forward genetic screen of an EMS-mutagenized *L. japonicus* population and investigated the already described *Lotus* root development and nodulation mutant *brush*. I screened more than 5300 plants inoculated with the AM fungus *Rhizophagus irregularis* and identified putative mutants with defects at different developmental stages.

The temperature-sensitive mutant *brush* develops short and thick roots as well as small and white nodules that are not colonized by rhizobia, while the wild type forms thin and long roots with large pink nodules. Two plants carrying recombinant chromosomes identified in a screen of approximately 1700 F2 (MG-20 x *brush*) individuals, were critical in narrowing down the target interval to 37 kb on the upper arm of chromosome 2. Within this region a mutation was found in the first exon of a gene encoding a putative cyclic nucleotide-gated channel (CNGC1) introducing an amino acid exchange (G134E). Next generation sequencing of the mutant DNA confirmed this mutation and revealed no further mutations in the target region. However, the mutant phenotype could not be complemented by transient expression of CNGC1 in transgenic *brush* roots. F4 and F5 plants from segregating populations (MG-20 x *brush*) with wild-type roots but white bumps were heterozygous in the target interval. These results suggested that *brush* is semi-dominant under the assumption that nodulation is more sensitive to the mutation than root development. CNGCs are  $\text{Ca}^{2+}$ -permeable channels in the plasma membrane, and could hypothetically be involved in the generation of the early Nod factor-induced  $\text{Ca}^{2+}$  influx.

Calcium-dependent protein kinases (CPKs) perceiving changes in cytosolic  $\text{Ca}^{2+}$  concentrations are prime candidates for coupling extracellular stimuli to cellular signaling processes. CPK29 of *L. japonicus*, previously identified in a cDNA-AFLP screen, has two alternative promoters with alternative first exons. Consequently, the two protein versions of this CPK, CPK29a and CPK29b, differ in their N-terminus but share the C-terminus. Analysis of promoter-GUS fusions indicated that CPK29a could be induced in young nodules and CPK29b could be expressed also in mature nodules. CPK29 homologs with two alternative first exons were identified *in silico* also in the genomes of *M. truncatula* and *G. max*. Based on phylogenetic analysis, CPK29 with two alternative first exons is legume-specific, pointing to a role of CPK29 in legume- or nodulation-specific developmental processes.

## 5 Materials and Methods

### 5.1 Materials

#### 5.1.1 Plant Material, Fungal and Rhizobial Strains

*L. japonicus* ecotype Gifu (accession number B-129) (Handberg and Stougaard, 1992), ecotype Miyakojima MG-20 (Kawaguchi et al., 2001) wild-type and EMS mutant (Perry et al., 2003) plants were used. The *Lotus* CNGC1 TILLING lines (SL1484-1, SL0957-1, S0791-1, SL0822-1) were received from the *Lotus* TILLING facility (John Innes Centre, Norwich, UK). *M. truncatula* R108 wild type (Barker et al., 1990) and *Tnt1* insertion lines (NF2225, NF4793, NF4838) (Tadege et al., 2008) were obtained from the Samuel Roberts Noble Foundation (Ardmore, USA). During AM experiments plants were inoculated with the AM fungus *Rhizophagus irregularis* (formerly known as *Glomus intraradices*) BEG195 (Stockinger et al., 2009; Krüger et al., 2012). Nodulation experiments were carried out by inoculating *Lotus* plants with *Mesorhizobium loti* MAFF303099 expressing *DsRed* (Markmann et al., 2008) or *Medicago* plants with *Sinorhizobium meliloti* 2011 expressing CFP (Fournier et al., 2008), respectively.

#### 5.1.2 Oligonucleotides

Oligonucleotides were designed using the web-based program primer3plus (Untergasser et al., 2007) and ordered from Metabion (Martinsried, Germany). KASP SNP Assays were purchased from kbioscience (Hoddesdon, UK).

#### 5.1.3 Media and Solutions

##### 5.1.3.1 Plant Cultivation Media

###### 5.1.3.1.1 FP-Medium

FP-Medium	ml/l
<u>Macronutrients</u>	
CaCl <sub>2</sub> (40 g/l)	2.5
MgSO <sub>4</sub> •7H <sub>2</sub> O (40 g/l)	3
KH <sub>2</sub> PO <sub>4</sub> (30 g/l)	3.33
Na <sub>2</sub> HPO <sub>4</sub> (45 g/l)	3.33
KNO <sub>3</sub> (1 M)	0.1
<u>Micronutrients</u>	
Ferric citrate (2.5 g/l)	2
Gibson's Trace	1

**Gibson's Trace**

H <sub>3</sub> BO <sub>3</sub> (2.86 g/l)
MnSO <sub>4</sub> (2.03 g/l)
ZnSO <sub>4</sub> (0.22 g/l)
CuSO <sub>4</sub> (0.08 g/l)
H <sub>2</sub> MoO <sub>4</sub> (0.08 g/l)

The pH was adjusted to 6.3 – 6.7 using KOH before autoclaving. For FP-plates, 3.2 g Bactoagar per 400 ml FP-Medium were added.

**5.1.3.1.2 B5-Medium**

B5-Medium	g/l
Gamborg B5 salt mix	3,3
Sucrose	20

Gamborg B5 basal salt mixture and Gamborg B5 vitamin mixture were ordered from Duchefa, Belgium. The pH was adjusted to 5.5 with 1 M NaOH, 1% Bactoagar was added and the medium was autoclaved. Before pouring the plates 1x B5 Vitamin Mix (stock solution 1000x) was added. For plates with Cefotaxim, 1 g Cefotaxim (Hexal, Germany) was resuspended in 3.33 ml sterile H<sub>2</sub>O and the antibiotic was added just before pouring to a final concentration of 300 µg/ml.

**5.1.3.2 Media for Bacteria Cultivation****5.1.3.2.1 LB-Medium**

LB-Medium	g/l
Bacto Tryptone	10
Yeast Extract	5
NaCl	10

The pH was adjusted to 7.0 with 1 M NaOH and the medium was autoclaved. For the preparation of LB-plates, 1% Bactoagar was added before autoclaving.

**5.1.3.2.2 TY-Medium**

TY-Medium	g/l
Bacto Tryptone	5
Yeast Extract	3

The pH was adjusted to 7.0 and the solution was autoclaved. For the preparation of TY-plates, 1% Bactoagar was added before autoclaving.

### 5.1.3.3 GUS Staining Buffer

GUS buffer	Final concentration
0.5 M NaPO <sub>4</sub> (pH 7.0)	100 mM
0.5 M EDTA (pH 7.0)	10 mM
100 mM Potassium Ferricyanide	1 mM
100 mM Potassium Ferrocyanide	1 mM
10% Triton X	0.1%

The X-Gluc stock solution (100 mg/ml) was prepared by dissolving X-Gluc powder (Roth, Germany) in DMSO (Roth, Germany) and stored at -20°C. For the GUS staining solution, 40 µl X-Gluc stock solution were mixed with 4 ml GUS buffer just before use.

### 5.1.3.4 RNA Extraction Buffer

RNA extraction buffer	Final concentration
10% CTAB	2%
10% PVP	2%
1 M Tris (pH 8.0)	100 mM
500 mM EDTA (pH 8.0)	25 mM
5 M NaCl	2 M
β-Mercaptoethanol	2%

### 5.1.3.5 Buffers for DNA Extraction

#### 5.1.3.5.1 DNA Extraction Buffer

DNA extraction buffer	Final concentration
Tris (pH 7.5)	200 mM
NaCl	250 mM
EDTA	25 mM
SDS	0.5%

**5.1.3.5.2 HB Buffer**

10x HB buffer	Final concentration
Trizma base	100 mM
KCl	800 mM
EDTA	100 mM
Spermine	10 mM
Spermidine	10 mM

The pH was adjusted to 9.4 with NaOH. For preparing the 1x HB buffer, the 10x HB buffer was diluted 1:10 and supplemented with 0.5 M sucrose and 0.5% Triton X-100. Just before use 0.15%  $\beta$ -mercaptoethanol were added.

**5.1.3.5.3 Wash Buffer**

The wash buffer was prepared by diluting the 10x HB buffer 1:10 and adding 0.5 M sucrose and 0.5% Triton X-100.

**5.1.3.5.4 CTAB Buffer**

CTAB buffer	Final concentration
CTAB	55 mM
NaCl	1.4 M
EDTA (pH 8.0)	20 mM
Tris-HCl (pH 8.0)	100 mM

**5.1.3.6 DNA Storage Buffer**

The buffer T0.1E was used for DNA storage.

DNA storage buffer	Final concentration
Tris (pH 8.0)	10 mM
EDTA (pH 8.0)	0.1 mM

## 5.2 Methods

### 5.2.1 Plant Cultivation and Crossings

*L. japonicus* and *M. truncatula* seeds were scarified with sandpaper and sterilized for 7 min immersed in 10% Danklorix (Colgate Palmolive GmbH, Germany) with 0.1% SDS. After three washing steps with sterile H<sub>2</sub>O seeds were incubated in H<sub>2</sub>O at 4°C overnight. Seeds were placed either onto 0.8% Bactoagar-plates for sterile cultivation, in pots filled with a 1:1 mixture of sand and vermiculite for inoculation with rhizobia or onto AM nurse pots for inoculation with *R. irregularis* BEG195 (Krüger et al., 2012). Seedlings were cultivated in growth cabinets at 18°C, 24°C or 26°C (16 h light/8 h dark). Plants chosen for seed production were repotted to soil and grown under glasshouse conditions (22°C). Crossings of putative AM mutants with MG-20 wild-type plants were performed as described by Jiang and Gresshoff (1997).

### 5.2.2 AM Inoculation and Staining

*Lotus* or *Medicago* seedlings were grown together with chive (*Allium schoenoprasum*) or *Plantago lanceolata* plants, which were inoculated with *R. irregularis* BEG195, in so-called nurse pots. After four weeks of co-cultivation, the lower three quarters of the root systems were harvested and the plants were retained in water. High throughput staining of the root samples was achieved by simultaneously staining of 96 independent roots using a 96-well storage plate with holes at the bottom as a support. The roots were cleared with 10% KOH (w/v) at 90°C for 75 min and, after rinsing with tap water, stained for 45 min at 90°C with 5% black ink (Pelikan, Germany) in 5% acetic acid (Vierheilig et al., 1998). In case of the AM screen, plants that showed an AM mutant phenotype were grown to seed to check the AM formation in the next generation.

### 5.2.3 Inoculation with Rhizobia

25 ml TY medium (5 g/l Bacto triptone, 5 g/l Yeast extract) with 15 mg/l Gentamycin were inoculated with *M. loti* MAFF *DsRed* (Markmann et al., 2008) and were incubated for three days in a 28°C shaker at 180 rpm. For inoculation of *M. truncatula* *S. meliloti* CFP (Fournier et al., 2008) was used, cultivated like *M. loti* but with Tetracyclin instead of Gentamycin. Rhizobia were pelleted by centrifugation for 10 min at 3000 rpm and washed twice with sterile H<sub>2</sub>O. The rhizobia were diluted to an OD<sub>600</sub> of 0.01 in liquid Fahraeus plant (FP) medium (Fahraeus, 1957) and applied to the plants. Two to three weeks post infection (wpi) the infected roots were analysed.

### 5.2.4 GUS-Staining

Root tissue was incubated with GUS-staining solution at 37°C overnight. Then, the GUS solution was removed, roots were washed with water and analysed with the binocular or microscope.

### 5.2.5 Temperature-Shift Experiments

#### 5.2.5.1 Temperature-Shift Two and Four Days post Germination

*L. japonicus* Gifu and *brush* (SL0979) mutant seed were sterilized, transferred to 1 l tulip-shaped weck jars (ca. 10 seed/jar) filled with 250 ml Seramis (Mars, Germany) and watered with 100 ml FP-Medium. 8 jars per line were prepared. 2 jars per line were placed in the 26°C growth chamber and the remaining jars into the 18°C growth chamber. Lights were switched off in both chambers. After 2 days (2 dpg), 2 jars with wt and *brush* seed were shifted from 18°C to 26°C and the lights in the growth chambers were switched on (16 h light, 8 h dark). After additional 2 days (4 dpg), another 2 jars with wt and *brush* seed were moved from 18°C to 26°C. 2 jars per line were grown at 18°C as control. The seedlings were inoculated 7 dpg by applying 500 µl *M. loti* MAFF *DsRed* solution ( $OD_{600} = 0.005$ ) to every seedling. 2 wpi the nodulation was analysed and root and shoot length was measured.

#### 5.2.5.2 Temperature-shift Two Weeks post Germination

*L. japonicus* Gifu wt and *brush* mutant seed were sterilized, transferred to FP-plates and cultivated at 18°C (16 h light, 8 h dark) for two weeks. Then, seedlings were transferred to 1 l tulip-shaped weck jars (12 seedlings/jar) containing 250 ml Seramis (Mars, Germany) and 100 ml FP-medium. The weck jars were placed in 18°C or 26°C growth chambers and one week later the plants were inoculated by applying 1 ml *M. loti* MAFF *DsRed* solution ( $OD_{600} = 0.005$ ) to each plant. Two wpi root and shoot lengths of 12 mutants and 12 wild-type plants per condition were measured and the infection threads visible at one side of the roots systems were counted.

#### 5.2.5.3 Temperature-Shift Six Weeks post Germination

*L. japonicus* Gifu wt and *brush* mutant seed were sterilized, transferred to FP-plates and cultivated at 18°C (16 h light, 8 h dark) for 6 weeks. Then, the plants were planted in 1 l tulip-shaped weck jars containing 250 ml Seramis (Mars, Germany) watered with 100 ml FP-medium and placed in 18°C or 26°C growth chambers. The plants were inoculated the next day by applying 500 µl *M. loti* MAFF *DsRed* solution ( $OD_{600} = 0.007$ ) to each plant and their nodulation was analysed 3 wpi. Root systems of 3 mutant and 3 wt plants per condition were cut into 1 cm pieces and the infection threads of 10 randomly chosen root fragments were counted.

### 5.2.6 *Lotus japonicus* Hairy-Root Transformation

The *Agrobacterium rhizogenes* strain AR1193 (Stougaard et al., 1987) induces transgenic hairy roots on *L. japonicus* seedlings. Seeds were sterilized as described above and germinated on 0,8% Bactoagar-plates for five days in a growth chamber (3 days dark, 2 days 16 h light/8 h dark, 24°C). The roots were cut with a scalpel and the remaining hypocotyls were dipped into the *Agrobacterium* suspension carrying the plasmid of interest. Seedlings were transferred to B5

plates. After 2 days dark and 3 days 16 h light/ 8 h dark (24°C) they were transferred to B5 plates containing Cefotaxim and transferred to fresh plates 2 and 4 days later. Plants with hairy roots were potted two to three weeks after the transformation.

### 5.2.7 Transient Transformation of *N. benthamiana* Leaves

The subcellular localization of the two different Lj CPK29 versions, in *N. benthamiana* leaves by *A. tumefaciens*-mediated transient transformation was performed as described by Yano and associates (2008). The genomic sequence of *CPK29a* comprising the first and the second exon and the first exon of *CPK29b* were cloned into the expression vectors pXCSG-YFP and pXCSG-CFP, respectively (Feys et al., 2005). Then, the constructs were transformed into the *A. tumefaciens* strain GV3101 (Koncz and Schell, 1986) and coinfiltrated into tobacco leaves. Fluorescence of the fusion proteins was checked with an inverted microscope two days after the infiltration.

### 5.2.8 DNA Extraction from Plant Leaves

DNA from plant leaves was extracted in single reaction tubes or in 96-well-plate-format.

#### 5.2.8.1 Small-Scale DNA Extraction

Leaves from *Lotus* or *Medicago* plants were collected in reaction tubes. After addition of 100 µl DNA extraction buffer and one wolfram bead, the tissue was ground using the bead mill (Retsch, Germany) at 30/sec for 1 min. Then, the ground tissue was incubated at 65°C for 10 min and centrifuged for 5 min at 6000 rpm. 50 µl of the supernatant were transferred to a new reaction tube and 1 volume of isopropanol was added. Tubes were inverted and incubated at RT for 10 min. DNA was precipitated by centrifugation at 12,000 rpm for 10 min. Supernatant was decanted and pellet was air-dried. The DNA pellets were dissolved in 80 µl T0.1E and tubes were incubated at 65°C for 10 min. After a final centrifugation step (5 min, 6000 rpm), 60 µl of the supernatant were transferred to new reaction tubes.

#### 5.2.8.2 Large-Scale DNA Extraction

Leaves from *Lotus* or *Medicago* plants were collected into 96-well-collection tubes (Qiagen, Germany) and one wolfram bead per well was added. 300 µl of preheated (65°C) DNA extraction buffer per sample were distributed and the tissue was homogenized with the bead mill (Retsch, Germany) for 2 min at 30/sec. After 1 min the plate was turned. Afterwards, the plate was incubated at 65°C for 30 min. 135 µl 5 M potassium acetate (pH 5.2) were added. The plate was centrifuged at maximum speed for 10 min at 4°C. 200 µl of the supernatant were transferred to a 96-well DNA storage plate (ABgene) with already prepared 160 µl isopropanol per well. Plate was inverted and stored at -20°C overnight. DNAs were pelleted by centrifugation at 4°C for 30 min at

maximum speed. The supernatants were discarded and DNA pellets were air-dried. DNAs were dissolved in 50 µl T0.1E.

#### 5.2.8.3 Isolation of Nuclear DNA from Plant Leaves

Four-week-old seedlings were grown in the dark for two days before their leaf material was harvested. The leaf tissue was pulverized in a mortar using a pestle and by adding liquid nitrogen. Approximately 2 g of the powder was transferred to a 50 ml Falcon tube and redissolved in 20 ml ice-cold 1x HB buffer by gentle shaking on ice. The solution was filtered through two layers of Miracloth (Calbiochem, Merck, Germany). The flow-through was transferred to a 15 ml Falcon tube and the nuclei were pelleted by centrifugation at 1800 g and 4°C for 15 min. The pellet was washed two times by resuspending it in the wash buffer and centrifugation at 1800 g and 4°C for 5 min. Then, the pellet was resuspended in 500 µl CTAB buffer preheated to 60°C and the solution was incubated at 60°C for 30 min. 500 µl chloroform:isoamylalcohol (24:1) were added and mixed by inverting the tube several times. After a centrifugation step at 8000 rpm and 4°C for 10 min, the upper phase was transferred to a new tube. 5 µl RNase (10 mg/ml stock concentration) were added and the RNA digest was carried out at 37°C for 30 min. Afterwards, 0.6 volumes ice-cold isopropanol were added and mixed by inverting the tube several times. The nuclear DNA was then precipitated at -20°C overnight and spun down for 10 min at 16,000 rpm and 4°C. The supernatant was discarded and the pellet was washed with 70% ethanol and a centrifugation step for 10 min at 16,000 rpm and 4°C. The ethanol was decanted and the pellet air-dried. Finally, the pellet was resuspended in 55 µl TE. The concentration of the DNA was measured using the Nanodrop (ThermoFisher, Germany) and the DNA quality was checked by agarose electrophoresis.

#### 5.2.9 RNA Extraction

The RNA extraction protocol was based on the extraction method described by Kistner and associates (2005). Solutions for RNA extraction were prepared using DEPC-treated H<sub>2</sub>O. RNA extraction buffer was preheated (65°C) and the β-mercaptoethanol was added just before use. Plant roots were collected in reaction tubes and frozen in liquid nitrogen. One bead was added per tube and tissue was homogenized in the bead mill (Retsch, Germany) for 1 min at 30/sec. 500 µl RNA extraction buffer were added per sample that was vortexed and incubated at 55°C for 10 min. 500 µl Phenol:Chloroform:Isoamylalcohol (PCI, 25:24:1, pH 7.0, Roth, Germany) were added and sample was vortexed for 1 min. After centrifugation (10 min, 12,000 rpm) the aqueous phase was transferred to a new reaction tube. One volume of PCI was added and sample was again vortexed and centrifuged as before. The upper phase was transferred to a new reaction tube and one volume of 6 M LiCl was added. RNA was precipitated on ice overnight at 4°C. RNA samples were centrifuged for 20 min at 4°C at 14,000 rpm. Supernatant was removed and the RNA pellet was washed with 1 ml 70% ethanol. Samples were centrifuged at 4°C, 10,000 rpm, 10 min and supernatant was removed. The RNA pellet was air-dried carefully, redissolved in

RNAsecure<sup>TM</sup> Resuspension Solution (Ambion, Germany) according to manufacturer's instructions and stored at -80°C. Contaminating DNA in the RNA samples was removed by using the TURBO DNA-free<sup>TM</sup> kit (Ambion, Germany).

### **5.2.10 Nucleic Acid Quantification**

DNA and RNA concentrations were measured using the Nanodrop (ThermoFisher, Germany) according to manufacturer's instructions. In addition, RNA concentration and integrity was analysed using the Bioanalyzer (Agilent, Germany).

### **5.2.11 cDNA Synthesis**

cDNA was synthesized using the SuperScript<sup>®</sup> VILO<sup>TM</sup> cDNA Synthesis Kit (Invitrogen, Germany) according to manufacturer's instruction.

### **5.2.12 Polymerase Chain Reactions**

#### **5.2.12.1 Standard and High-Fidelity PCRs**

Routine PCRs were set up with 0.5 units *Taq* DNA polymerase (NEB, Germany), 1x standard *Taq* buffer (NEB, Germany), ca. 5 to 50 ng DNA, 0.5 µM forward and 0.5 µM reverse primer and 200 µM each dNTP. For high fidelity PCRs the Phusion<sup>TM</sup> DNA Polymerase (Finnzymes, Finland) was used according to the instruction manual.

#### **5.2.12.2 5'- and 3'-RACEs**

The 5'- and 3'-RACEs (rapid amplification of cDNA ends) were performed using the SMART<sup>®</sup> RACE cDNA Amplification Kit (Clontech, France) according to the user manual.

### **5.2.13 Standardized Gene Mapping and SSR Marker Analysis**

A high-throughput *Lotus* genotyping setup, called power mapping (Groth, 2010), was used to perform the standardized gene mapping, with the help of SSR markers discriminating the *L. japonicus* genetic backgrounds Gifu and MG-20 ([www.kazusa.or.jp/lotus/markerdb\\_index.html](http://www.kazusa.or.jp/lotus/markerdb_index.html)). These SSR regions were amplified by PCRs in which the PCR fragments were fluorescently labelled based on the method developed by Schuelke (2000). The forward primer consisted of a universal 5'-adapter sequence and the genome-specific primer sequence (Supplementary Table 1). By adding a fluorescently labelled adapter primer to the PCR reaction, the sizes of the resulting PCR amplicons could be discriminated by a fragment analysis run on the ABI 3730 capillary sequencer of the in-house sequencing service (Dye Set G5 with 6-FAM, PET, NED, VIC). The size standard GeneScan<sup>TM</sup>-500 LIZ<sup>®</sup> (Applied Biosystems) was added. The data were then analysed using the GeneMapper<sup>®</sup> software (Applied Biosystems, Germany).

### 5.2.14 dCAPS Marker Analysis

Genotyping of DNAs to discriminate between the *CNGC1* wild-type and mutant allele was performed using a dCAPS primer. According to the web-based dCAPS Finder 2.0 (Neff et al., 2002) the primer KH180 was designed, which introduced a base-pair exchange (A to C) three bases downstream of the mutation and therefore generated a *Hae*III restriction site in the wild-type sequence. After PCRs with the primer pair KH160 and KH180 that amplified a 182 bp region and a subsequent *Hae*III restriction digest (37°C, 1h), wild-type DNAs produced fragments 24 bp shorter than *cngc1* mutant DNAs. The size difference was visualized by gel electrophoresis using a 3% agarose gel. For large-scale dCAPS analysis, the PCRs were set up with a modified version of KH160, KH219, where a 5'-PET-anchor-sequence has been added, the fluorescent PET-primer and KH180. After the *Hae*III digestion, 1 µl of each PCR was subjected to a fragment analysis run on the 3730 DNA Analyzer (Applied Biosystems, Germany). The lengths of the PCR fragments were evaluated with the GeneMapper® software (Applied Biosystems, Germany).

### 5.2.15 SNP Analysis by KASP Assays

SNP KASPar by Design assays were purchased from kbioscience (UK) to check individual EMS-induced SNPs identified by Next Generation Sequencing of *brush* DNA. The assays were performed according to the KASP manual by adding 4 µl DNA (10 ng/µl) and with a total reaction volume of 8 µl. The reactions were subjected to the KASP thermal cycling program in the CFX96™ Real-Time PCR Detection System (Bio-Rad, Germany). After a final 10 min incubation step at 15°C, the FAM and HEX fluorescence was measured in a plate read step. Finally, the data were analyzed and visualized with the Allelic Discrimination option of the CFX96™ software (Bio-Rad, Germany).

### 5.2.16 DNA Extraction from Agarose Gels

DNA was extracted from agarose gels by cutting the DNA band of interest from the agarose gel and using either the JETSORB gel extraction kit (Genomed, Germany) or the NucleoSpin® Extract II kit (Macherey-Nagel, Germany) according to manufacturer's instructions.

### 5.2.17 Clean-Up of PCR Reactions

PCR-products were cleaned-up prior to sequencing either by using the NucleoSpin® Extract II kit (Macherey-Nagel, Germany) according to manufacturer's instructions or by adding ExoSAP-IT® (USB, USA). For the treatment with ExoSAP-IT®, 9.5 µl PCR reaction were mixed with 0.5 µl ExoSAP-IT® and incubated at 37°C for 30 min and at 80°C for 15 min.

### 5.2.18 Sequencing

Sequencing was performed by the Sequencing Service (Genomics Service Unit, LMU München, Department Biologie; <http://www.genetik.biologie.uni-muenchen.de/sequencing>) on the ABI 3730 48-capillary DNA Analyzer (Applied Biosystems, Germany). Sequencing reactions were set up according to the sample submission requirements for the “Cycle, Clean and Run” protocol.

Nuclear DNA of *brush* seedlings was subjected to Next Generation Sequencing, which was performed at Eurofins MWG, Germany, by using an Illumina HiSeq 2000 (Illumina, USA) with a read length of 2x 100 bp.

### 5.2.19 Cloning

For standard cloning procedures the pENTR<sup>TM</sup>/D-TOPO<sup>®</sup> cloning kit (Invitrogen, Germany) was used according to the manufacturer's guidelines. The destination vectors were produced with the Gateway<sup>®</sup> LR Clonase<sup>™</sup> II Enzyme Mix (Invitrogen, Germany) according to manufacturer's instructions. The Golden-Gate-Cloning strategy (Engler et al., 2008) was used to clone the *Lotus* CPK promoters and *Medicago* CPK versions into the BSA-compatible pENTR. The 3'- and 5'-RACE products were cloned into and sequenced from the pGEM<sup>®</sup>-T Easy Vector (Promega, USA).

### 5.2.20 Plasmid DNA Purification

Plasmids were isolated from *E. coli* liquid cultures using the NucleoSpin<sup>®</sup> Plasmid kit (Macherey-Nagel, Germany) according to the user manual.

### 5.2.21 Bioinformatics

BLASTN, BLASTP and BLASTX searches were performed on the NCBI BLAST website (<http://blast.ncbi.nlm.nih.gov/Blast.cgi>; Altschul et al., 1990). Genes were annotated based on the gene predictions of Genscan (<http://genes.mit.edu/GENSCAN.html>; Burge and Karlin, 1997) with the help of the program Artemis (Rutherford et al., 2000). The ScanProsite tool was used to identify protein domains (<http://prosite.expasy.org/scanprosite>; de Castro et al., 2006). The CLC Main Workbench (CLC bio, Denmark) was used to analyse sequencing data and with the CLC Genomics Workbench (CLC bio, Denmark) the Next Generation Sequencing data was evaluated. Multiple sequence alignments for the phylogenetic and sequence identity analyses were generated using the program MAFFT (Katoh et al., 2005) and edited using the program Jalview 2.6.1 (Waterhouse et al., 2009). Sequence identities were calculated using the Sequences Identities And Similarities website (SIAS, <http://imed.med.ucm.es/Tools/sias.html>) with gaps in the alignment taken into account ( $PID_3$ ).

### 5.2.21.1 Databases

Plants and seed bags were introduced into the ZopRA Plant and Seed Database ([www.zopra.de](http://www.zopra.de)). Thereby, plant numbers, consisting of one letter and four digits, and seed bag numbers, consisting of five digits, were assigned. Genomic sequences and gene information were retrieved from Phytozome v7.0 ([www.phytozome.net](http://www.phytozome.net)), the PFR strawberry server ([www.strawberrygenome.org](http://www.strawberrygenome.org)), TAIR ([www.arabidopsis.org](http://www.arabidopsis.org); Swarbreck et al., 2008) or miyakogusa ([www.kazusa.or.jp/lotus](http://www.kazusa.or.jp/lotus); Sato et al., 2008).

### 5.2.21.2 Phylogenetic Analyses

Maximum Likelihood phylogenetic trees were calculated using the program RAxML-HPC2 7.2.8 (Stamatakis, 2006; Stamatakis et al., 2008) at the CIPRES Science Gateway (Miller et al., 2010). For phylogenetic trees based on protein sequences the RAxML parameters CAT for protein substitution matrix and the JTT amino acid substitution model were chosen. 100 bootstrapping iterations were conducted. The phylogenetic trees were visualized with the program FigTree v.1.3.1 (<http://tree.bio.ed.ac.uk/software/figtree/>).

### 5.2.22 Microscopy

The stereomicroscope MZ16 FA (Leica, Germany) and the inverted microscope DMI6000 B (Leica, Germany) were used in this study. The fluorescence of *M. loti* expressing the *DsRed* fluorophore was visualized either with a high-intensity mercury lamp and the *DsRed* filter (excitation filter 545/12) of the stereomicroscope or an external light source for fluorescence excitation with a mercury metal halide bulb (Leica EL6000) and the N3 filter cube (excitation filter 546/12) of the inverted microscope. The YFP and CFP fluorescence of the CPK29 fusion proteins were analysed with the YFP filter cube (excitation filter 500/20) and CFP filter cube (excitation filter 436/20), respectively. Photographs were taken with Leica digital cameras attached to the microscopes.

### 5.2.23 Statistics

The arithmetic mean was calculated with the function AVERAGE of Microsoft® Excel for Mac 2011. Standard deviations were analysed by the function STDEVA of Microsoft® Excel. Student's T-Test was performed using the function T.Test of Microsoft® Excel for Mac 2011, with two-tailed distribution and homoscedastic test.  $\chi^2$ -values were obtained from the QUISQ.TEST function of Microsoft® Excel for Mac 2011.

For the statistical analysis of *brush* mutants versus wild-type plants, statistical tests were performed to proof whether wild-type plants and mutants differed in number of nodules, number of white bumps, root and shoot lengths. Moreover, it was analyzed whether any of the tested correlations was temperature dependent. Given that measurable data existed for all combinations of wild-type/mutant (= type) and each temperature level, a two-way ANOVA with the measure of

interest as dependent variable and type, temperature, and the type/temperature interaction as independent variables in the full model was applied. Non-significant terms were deleted from the model until the minimum AIC (Akaike's Information Criterion) was achieved (Burnham and Anderson, 2002). To gain significance values for comparisons of specific type/temperature combinations within a model, the Tukey's HSD (Honestly Significant Difference) test was performed. If for specific type/temperature combinations only zero values were measured, the remaining combinations were analyzed by t-test or the non-parametric U-test (also known as Wilcoxon test) depending on (non-)normality of the data. Box plots and diagnostic plots were used to evaluate normality of the data and patterns in the residuals to proof that assumptions of ANOVA were fulfilled. These statistical tests were performed in R 2.14.1 (R Development Core Team, 2011).

## 6 Supplementary Tables

**Supplementary Table 1. Power mapping markers**

Name	cM <sup>a</sup>	Marker <sup>b</sup>	SSR	MG-20 <sup>c</sup>	Gifu <sup>c</sup>	Forward primer	Reverse primer	Label <sup>d</sup>	Dilute
G018	48,5	TM0541	AAT	141	149	AAATGTGTAATTATATTTCGATG	GTAAATTGACATCAAAGTTGAA	PET	1/30
G077	4,0	TM1456	AT	146	170	CATCACCGCCATGTTATAGC	GCTAGATATGTGGTGCCTG	NED	1/70
G078	0,8	TM1637	CT	149	179	AATTGTCATAGTCAGCGTGC	TGACAGGGAAAATAACAGTG	FAM	1/30
G082	8,8	TM0490	AAG	85	79	GCCATTGATTTCCACTTTG	TTGTCCTCTCTCTCTTTCCC	NED	1/80
G083	6,2	TM0074	11 bp deletion	164	153	TGACCGTTCTATTACAACAG	AATAAATTAGTTCTTTAAGCCAT	VIC	1/60
G170	8,8	TM2387	CT	157	144	GCAACTCAAGTAACGAATATGTC	GTGTGCATGGAAAGCTTGAC	VIC	1/70
G172	8,8	TM2432	AT	203	185	GGCTATCGAATTGTATTGG	TGGTTTGCTTGTACACGC	PET	1/70
G173	8,8	TM2433	AT	196	200	ACAATCTCATCCAAAAGGG	AAATAAAAGCGGCATGTTC	FAM	1/70
G174	8,8	TM0348	6 bp deletion	110	116	ACCGTCGACCCTCTAACAC	AACAAACATTCCATTGGTAG	PET	1/70
G175	8,8	TM0435	AT	120	124	CATGTATGCTTACCCGTGG	CGATCTTCAACTATAAAAGACTGC	FAM	1/70
G178	8,8	TM2301	AT	177	185	TCATCTCTATGGTAAAACATC	AGTGTTCATTCAACCCTTG	NED	1/60
G179	8,8	TM2498	AT	182	176	CCCTTGCATTGAATAAGAG	CGAGTGTAGTGTACATATTGGTG	PET	1/70
G180	8,8	TM2499	AT	145	159	GTTCATGATCATAGTTGCC	CAAATGGGCTTAATAAAACG	NED	1/70
G182	8,8	BM2500	AT	160	170	CCAGACAGATTAATTAAATGCTC	CATCAGCAAGCAACTCAAAC	VIC	1/70

All markers are located on chromosome 2. Primer sequences are shown in the 5' to 3' direction.

<sup>a</sup> Refers to the MG-20 genome.

<sup>b</sup> Marker informations are listed at the miyakogusa website.

<sup>c</sup> PCR product size in bp.

<sup>d</sup> 3'-Fluorescent label of the corresponding adaptor primer.

Following sequences were added at the 5'-end of the respective forward primer.

PET-M13 adaptor sequence: 5' –GTAAAACGACGCCAGT–3';

VIC-BKRSV adaptor sequence: 5' –CGCCATTGACCATTCA–3';

NED-KS adaptor sequence: 5' –TCGAGGTGACCGTATC–3';

FAM-LUF adaptor sequence: 5' –CTCGTAGACTGCGTACCA–3'.

**Supplementary Table 2. Primers used for the sequencing of SNPs.**

SNP	Forward primer	Reverse primer	Sequencing primer
SNP12	CATTGAATATAAAACAACACC	GGAAGGTTGGATGCCATA	CGATGCATATAGTAGTGGATGTAC
SNP20	TGAGGACTGGTGGTTTTG	ATGGGGCCAAGTTCTCTT	TGGTTGACATGGATAGGGAGATGC
SNP21	ATGTCGCTTGGAGAGAGA	AGGGGAGGATCACAAGGTCT	GTTGGAGGCCACGATCTAGCTGCC
SNP24-1	CCCGAGAAAAATGCAGCTA	CGGCCAGTACCAAGCTAAAG	GCTAACATGTTGACTTAAGCTGAC
SNP24-2	CCCGAGAAAAATGCAGCTA	CGGCCAGTACCAAGCTAAAG	GCTCCGGAGAGACAAACAGCGTCGG
SNP25	ACAAAGAGTATATGCCAAGAGG	AATTGTGCCAGGTTGGAGAG	TAGTATTCAAAGGTGCTGTGCTG
SNP5	TGTTGTTGCGTTATTGGTG	GGATGTGAAAGAGTGGTAGC	Forward primer
SNP42	GAATGAAAGGCCAACGAAA	TTCGTCCTCATTGGATTAA	GATAGCTGGGCTTCCGGTGCAGC
SNP43	TCCGTATGAAACATTGAGATG	CTCCTAAAGATAGCGTTGAGC	Forward primer
SNP51	CGTATGCCAGCTACAAGCAA	CAATTGCAAGCAGGAACTGA	ATCTGGGCTTCCCTCTGACTCTG
SNP3	AGATTGTCTGCGCGTATGT	ACAATGCCGATTCTGAGGTC	Forward primer
SNP2	CCAACTCATATCAACCTCTCG	CTCGGGATTCTCCATTCT	Forward primer
SNP1	TTACGAGGGATGACTCACCT	TTGAACCAAACGTGACAACCT	Forward primer

The genomic regions surrounding the SNP of interest were amplified by PCR using the indicated forward and reverse primers. The sequencing reaction was set up with the corresponding sequencing primer or the forward primer.

**Supplementary Table 3. List of primers used in this study.**

Primer name	Primer sequence (5' to 3')	
KH108-MtCDPK-m1-F	CCACAGAGAAATCAACCTC	Amplification of Mt CPK29b
KH109-MtCDPK-m2-F	TCCCCAAACACAAATCTC	Amplification of Mt CPK29a
KH110-MtCDPK-EF-R	TGGAGCCACATAGTATGCAC	Amplification of Mt CPK29
KH119-LjGAD1-seq1-F	GAAAATTCCCATCTCCTCAGT	Sequencing of Lj GAD
KH120-LjGAD1-seq2-F	TGAAATTGAAGACTGAGTGATGTT	Sequencing of Lj GAD
KH121-LjGAD1-seq3-F	TGTAGTGATTGATGTGCCAGA	Sequencing of Lj GAD
KH122-LjGAD1-seq4-F	TGGGTTGCTGGAGGAGTAA	Sequencing of Lj GAD
KH123-LjGAD1-seq5-F	TGGTGCATGATAACAAGCAAG	Sequencing of Lj GAD
KH124-LjGAD1-seq6-R	TCCTTACATACATTAGGTGAATGC	Sequencing of Lj GAD
KH125-LjGAD1-seq7-F	TTCTTGCTGAGATAGCAGTGA	Sequencing of Lj GAD
KH138-b-amylase-F	TGATTGTGAAGCGAGGGTTA	Sequencing of Lj $\beta$ -amylase
KH139-b-amylase-R	CTCGTGGCTACTTTCTAACG	Sequencing of Lj $\beta$ -amylase
KH140-b-amylase-R	CTGGAGCATGAGACCTTGT	Sequencing of Lj $\beta$ -amylase
KH141-b-amylase-R	TGCACCTTGTACAGCATTG	Sequencing of Lj $\beta$ -amylase
KH142-CNGC1-F	TCGTTTGGCTTTCATTCTG	Sequencing of CNGC1
KH143-CNGC1-R	AATGTAAGGGAGGCCAGAG	Sequencing of CNGC1
KH144-CNGC1-F	CCAAGTGGTATCCCCATCA	Sequencing of CNGC1
KH145-CNGC1-R	TGTGCAAATTACTTAAGGAAC	Sequencing of CNGC1
KH146-CNGC1-F	AAGGTACTCATCAAATACTTGTCA	Sequencing of CNGC1
KH147-CNGC1-F	TCACTAAAATTCCCACAAATGGT	Sequencing of CNGC1
KH148-CNGC1-R	GGGATAGGGAATTCATCAGGA	Sequencing of CNGC1
KH149-CNGC1-F	TCACTTTATTAGGTTATGCTACA	Sequencing of CNGC1
KH150-CNGC1-R	CACTTTACAATCTAGTTCTATGG	Sequencing of CNGC1
KH151-CNGC-ATG-F	ATGCCCTAATTGACAAAG	Amplification of CNGC1
KH152-CNGC-TAG-R	CTACGACTTCGGTGTGAT	Amplification of CNGC1
KH153-CNGC-CDS-F	ACAAGTTCTGGCCATGTT	Amplification of CNGC1 CDS
KH154-CNGC-CDS-F	CGGAATTGATTGATTGTGAT	Amplification of CNGC1 CDS
KH155-CNGC-5'RACE-R	CAGCTGCCAGACCTCAAGTGT	5'-RACE of CNGC1
KH156-CNGC-5'RACEnes-R	AAAGTTGTTGTGCTTGCCTCCAC	5'-RACE of CNGC1
KH157-CNGC-3'RACE-F	GTGGAGGGCAAGACACAACACTT	3'-RACE of CNGC1
KH158-CNGC-3'RACEnes-F	GGGAGGCAAAAGGTTTGGAGAAA	3'-RACE of CNGC1
KH159-CNGC-CDS-Ex1-R	TTGGATTTCTTCTGAGAACG	Amplification of CNGC1 CDS
KH160-CNGC-CDS-Ex1-F	CTGCAGGAGCTGGAAATCAT	dCAPS analysis of mutation in CNGC1
KH161-CNGC-CDS-Ex7-R	CCGGCCAGAGTACTGATTG	Amplification of CNGC1 CDS
KH162-CNGC-CDS-Ex2-R	AAATCGCCATCAAGCAAAC	Amplification of CNGC1 CDS, reverse TILLING primer
KH163-CNGC-CDS-Ex11-R	CACGCACACAAAGACCATC	Amplification of CNGC1 CDS
KH164-CNGC-CDS-Ex10-F	TGAAGGAGATGCTTGTGGTG	Amplification of CNGC1 CDS
KH165-CNGC-prom1-F	CACCTCCGTATGAACATTGAGATG	Cloning of 3kb ProCNGC1 into pENTR
KH166-CNGC-prom2-F	CACCTCGTTGACTCCATTCAA	Cloning of 2kb ProCNGC1 into pENTR
KH167-CNGC-prom-R	GTTTCCCTGACGTTCTGTAGTT	Cloning of ProCNGC1
KH169-CNGC-w/oTAG-R	CGACTTCGGTGTGATCTG	Cloning of CNGC1 without stop codon
KH172-CNGC-ATG+CACC	CACCATGCCCTAACGCAAAC	Cloning of CNGC1 into pENTR
KH174-CNGC-prom3-F	CAATTGGCTCACCTAAAACA	Amplification of CNGC1 promoter
KH175-CNGC-prom4-F	GCTCAACGCTATCTTAGGAG	Amplification of CNGC1 promoter
KH176-CNGC-prom5-F	TGCGTGTGAGAAGGATTG	Amplification of CNGC1 promoter
KH177-CNGC-prom6-F	TTCCCTTCAGTTAACG	Amplification of CNGC1 promoter, forward TILLING primer
KH178-CNGC-prom7-F	GATTGTATTGCTAGCTACT	Amplification of CNGC1 promoter
KH179-CNGC-3'UTR-R	GTTCTCTATGGCATACAAATCA	Amplification of CNGC1 promoter
KH180-CNGC-dCAPS-R	AGGATCATTACACATCCCAGCGGC	dCAPS analysis of mutation in CNGC1
KH188-NF4838-Ins5-F	TCATCGATAAGGTCAAGAC	Amplification of the <i>Tnt1</i> insertion in NF4838
KH189-NF4838-Ins5-R	GCATCCATTAGCTGCTTAT	Amplification of the <i>Tnt1</i> insertion in NF4838

Table continues on next page.

SUPPLEMENTARY TABLES

Supplementary Table 3 continued.

Primer name	Primer sequence (5' to 3')	
KH190-NF2225-Ins21-F	CATTGTCTCCTTCCGGAGT	Amplification of the <i>Tnt1</i> insertion in NF2225
KH191-NF2225-Ins21-R	CTTCGCGTTCCGTAGTTT	Amplification of the <i>Tnt1</i> insertion in NF2225
KH192-NF4793-Ins15-F	AGGGTTTGACCTAACAAAGG	Amplification of the <i>Tnt1</i> insertion in NF4793
KH193-NF4793-Ins15-R	CCTTGCTTTCTTCTGTTGC	Amplification of the <i>Tnt1</i> insertion in NF4793
KH196-Tnt1-R	TCAGTGAACGAGCAGAACCT	Amplification of the <i>Tnt1</i> insertion in NF lines
KH201-CNGC-2-F	GTTTGGTTTCATCCCTCCG	Amplification of CNGC2
KH202-CNGC-2-R	CACCTGGCCTCATTAATCCC	Amplification of CNGC2
KH203-CNGC-2-F2	AAACGTAGACTCGCAAGG	Amplification of CNGC2
KH204-CNGC-2-R2	GGTTGCTTAGTAGCAGAACAGT	Amplification of CNGC2
KH205-CNGC-2-F	ATCAAGGACAAAGAACATGAGC	Amplification of CNGC2
KH206-CNGC-2-F	AGGAACACACTAGCCCCATT	Amplification of CNGC2
KH207-CNGC-2-R	AGAGGTCTTGAAAACGTAG	Amplification of CNGC2
KH208-CNGC-2-R	GACCATCTTCTCCACTATACCA	Amplification of CNGC2
KH209-CDPK1-CACCATG-F	<b>CACCATGGGACACTGCTTCAGCAA</b>	Cloning of Lj CPK29b into pENTR
KH210-CDPK2-CACCATG-F	<b>CACCATGGGATTGGGGTTCTCAA</b>	Cloning of Lj CPK29a into pENTR
KH211-CDPKs-TAA-R	TTATCGTGGTTCTTTCTCA	Cloning of Lj CPK29 into pENTR
KH212-CDPK1-BSA-prom-F	<b>TAGGTCTC</b> TACACCTTGTCTCTATCTCTTCC	Cloning of Lj ProCPK29b into pENTR-BSA
KH213-CDPK1-BSA-prom-R	<b>TAGGTCTC</b> ACCTTATCGAAGAAAGGAATTAAATGTTA	Cloning of Lj ProCPK29b into pENTR-BSA
KH214-CDPK2-BSA-prom-F	<b>TAGGTCTC</b> TCACCTGTGTCGTGCAAGAATT	Cloning of Lj ProCPK29a into pENTR-BSA
KH215-CDPK2-BSA-prom-R	<b>TAGGTCTC</b> ACCTTGTTGATTGGTTAACCTTCAG	Cloning of Lj ProCPK29a into pENTR-BSA
KH216-CDPKs-nostop-R	TCGTGGTTCTTTCTCATC	Cloning of Lj CPK29 into pENTR
KH217-CDPK1-GSP-F	ATCCCCACCCACCTCACCCAC	5'-RACE Lj CPK29b
KH218-CDPK1-NGSP-F	ACCTCAACCTAACCTAACCTCGT	5'-RACE Lj CPK29b
KH219-PET-dCAPS-F	<b>GTAAAACGACGCCAGT</b> CTGCAGGAGCTGGAAATCAT	dCAPS analysis of mutation in CNGC1 using capillary sequencer
KH220-CDPK1-cDNA-BSA-F	<b>TAGGTCTC</b> TACCATGGGACACTGCTTCAGCAA	Cloning of Lj CPK29b CDS into pENTR-BSA
KH221-CDPK1-cDNA-BSA-Ex1-R	<b>TAGGTCTC</b> TTTACCTTCTCAATGAAGACG	Cloning of Lj CPK29b CDS into pENTR-BSA
KH222-CDPK1-cDNA-BSA-Ex2-F	<b>TAGGTCTC</b> GGTAAAGTGTAGAGAAATTGTG	Cloning of Lj CPK29a CDS into pENTR-BSA
KH223-CDPK1-cDNA-BSA-nostop-R	<b>TAGGTCTC</b> ACCTTCTCGTGGTTCTCTTCAT	Cloning of Lj CPK29a CDS into pENTR-BSA

Primer names ending with F indicate forward primers and names ending with R reverse primers. *Bsal* recognition sites added to the primers used for cloning PCR products into the pENTR-D-TOPO-BSA vector are marked blue. The PET adaptor sequence of primer KH219 is indicated in red. The sequence CACC shown in bold was added at the 5' end of forward primers, if the PCR product was cloned into pENTR-D-TOPO.

**Supplementary Table 4. KASPar by Design Assays**

KASP by Design Assay	Sequence around SNP (5' to 3')
Chr2_4376117	CCTCCTTGTGATGAGGGACATAATTCAATTAGGAGGTCTACTATTGT[G/A]TTGTGCTGATGTGTTGCTGGGTCATCTAGCGTTGATGAGAAGCTCTGAAC
Chr2_6257640	ATCGGCCTAGTATTTAGTCGACCATTGAATCATCCTAGCAACCTCATCTGAAT[G/C/T]CGCCTCAAGTATCTTGCACTCCCTCTGTG
Chr2_6609880	ACTAGTTGAGAACATAGTGGCATTGACTGAGCTCAAATCACAAATTAGAGGGAAAC[G/A]TTGAATATAGATTAAC
Chr2_8844892	AATTGCTAAATAAACTACTAATTCTGTGTTAGAAAAAT
Chr2_9069492	ATTCAGAAATTAGTATTCACACCCCCCTCTCAATTCAATTAAACATTTTTTGTC[C/T]TATCTCTCAT
Chr2_912796	TTTCATCACATCATCTACATTCTCACATTCTACTTCTTCTTAAAC
Chr2_9302361	CTCATGGCGCTCTGCAGCCATAGACCTCTCAGGCCGCTGCCACTGCCATCGCCGCTCCCGTT[C/T]CGAAT
Chr2_9363400	GACATCCTCTAGTCTCGCTCCACCTCTGAATTCTCATCGAAGAAGGACATTTCGCC
Chr2_9566814	CTTCAACAAATCACTGATGATTGTTGAGATATGAAGATTCCCTTTAGAATGG[G/A]CCACTCAATTCCAAA
Chr2_9632266	AATACTCAATTCCCAGGTCTTAATTCAAAATTCTGG
Chr2_10591450	TTGAGATGAAATACTGCATTCCTGAGTGGATTACTGTTTTATTGAGATAATGGATTG[C/T]TCGCGTTCTATT
Chr2_11197409	TCGTGTAGTCCCTCGATTGATTCTGAATGGATTGAGGAAGGTT
Chr2_11754284	AAGCCTTAATATAAGTAGGGCAACTAGTGCATAAGGATCATTACACATCCCAGCCTGC[C/T]CAGACCTCAGTAAGTGT
Chr2_12795460	TCATTTCATCATAGTGTGTTCCAAGGATTCTCATCTG
Chr2_13459617	CCGGTGACTIONTGTGCTCGCATGACTAAACAAGAGTCAGAGCCATTCCCTCTCATGTCG[C/T]TCCTCAAGGGT
	GAAGTCTAGAAAAGGACTAAAGGTGCTATTGGACGAGCAAGGGTTGGTT
	AAGATTCCCATCTCTGTCTCCGACTATACTAGCGTCAAGACAAGCCTTGACCTGCGCC[C/T]CTACCGTTGTA
	GGGTTCCCTTTATGCAAAGTTGGTACATCAGCGTACTGGCTCGACTGTCCC
	CTAATAACATGTGGTATTGGAGAACTATTATGATAGGAAGGTTACTGAGAAAACCC[C/T]TAATGTGAATAATTATG
	ACAGCTACCCCTAACATGTGAATAATTATGACAGCTAACGGTT
	TTGACTTTGGTGTACTGACTGATCATAACAGTTCTATTGGGGATCTGATTGGCCATACAAACAT[C/T]TATTTTTA
	TGTGTTACTTATTGAATTACATCTAACTTCTACAAACACTAAACTCCAATTAG[G/A]CGTGTACAAACACGCAC
	TGACACAGAGTTAAGAAAATGTGTGTTAGGCAATTGTT
	ATTGTGAAGCATTAAAGTACCCATGAAGTACCAAGAGTACAAGTACCGGGTACGG[G/A]TACGTTGGCCAAACTG
	GGGTACCCGTGCATCATAGGATTCCGTTTCAGTTGGTAATTGCTATCATCAATTCA
	GTTCAAGTAGTCCCCCTGGTAAAGCATATTGCAAGTGTGTTACATGTTACATTATAAA[C/T]CCAACAAATGTTGGG
	GTAGCACTGAGGAGAACATTCACTGCTACTTTAGTATC

Position of the SNPs refers to the MG-20 genome. The individual SNPs are indicated by square brackets in the sequences.

## 7 References

- Adams, K.L., and Wendel, J.F.** (2005). Polyploidy and genome evolution in plants. *Curr Opin Plant Biol* **8**, 135-141.
- Akiyama, K., Matsuzaki, K., and Hayashi, H.** (2005). Plant sesquiterpenes induce hyphal branching in arbuscular mycorrhizal fungi. *Nature* **435**, 824-827.
- Alexander, T., Toth, R., Meier, R., and Weber, H.C.** (1989). Dynamics of arbuscule development and degeneration in onion, bean, and tomato with reference to vesicular–arbuscular mycorrhizae in grasses. *Canadian Journal of Botany* **67**, 2505-2513.
- Ali, R., Zielinski, R.E., and Berkowitz, G.A.** (2006). Expression of plant cyclic nucleotide-gated cation channels in yeast. *J Exp Bot* **57**, 125-138.
- Alonso, J.M., and Ecker, J.R.** (2006). Moving forward in reverse: genetic technologies to enable genome-wide phenomic screens in *Arabidopsis*. *Nat Rev Genet* **7**, 524-536.
- Altschul, S.F., Gish, W., Miller, W., Myers, E.W., and Lipman, D.J.** (1990). Basic local alignment search tool. *J Mol Biol* **215**, 403-410.
- Ané, J.M., Kiss, G.B., Riely, B.K., Penmetsa, R.V., Oldroyd, G.E., Ayax, C., Levy, J., Debelle, F., Baek, J.M., Kalo, P., Rosenberg, C., Roe, B.A., Long, S.R., Denarie, J., and Cook, D.R.** (2004). *Medicago truncatula* DMI1 required for bacterial and fungal symbioses in legumes. *Science* **303**, 1364-1367.
- Appleby, C.A.** (1984). Leghemoglobin and rhizobium respiration. *Annual Review of Plant Physiology* **35**, 443-478.
- Arazi, T., Kaplan, B., and Fromm, H.** (2000). A high-affinity calmodulin-binding site in a tobacco plasma-membrane channel protein coincides with a characteristic element of cyclic nucleotide-binding domains. *Plant Mol Biol* **42**, 591-601.
- Arazi, T., Sunkar, R., Kaplan, B., and Fromm, H.** (1999). A tobacco plasma membrane calmodulin-binding transporter confers Ni<sup>2+</sup> tolerance and Pb<sup>2+</sup> hypersensitivity in transgenic plants. *Plant Journal* **20**, 171-182.
- Asano, T., Tanaka, N., Yang, G., Hayashi, N., and Komatsu, S.** (2005). Genome-wide identification of the rice calcium-dependent protein kinase and its closely related kinase gene families: comprehensive analysis of the CDPKs gene family in rice. *Plant Cell Physiol* **46**, 356-366.
- Bago, B., Pfeffer, P.E., and Shachar-Hill, Y.** (2000). Carbon metabolism and transport in arbuscular mycorrhizas. *Plant Physiology* **124**, 949-958.
- Bago, B., Pfeffer, P.E., Abubaker, J., Jun, J., Allen, J.W., Brouillette, J., Douds, D.D., Lammers, P.J., and Shachar-Hill, Y.** (2003). Carbon export from arbuscular mycorrhizal roots involves the translocation of carbohydrate as well as lipid. *Plant Physiology* **131**, 1496-1507.
- Balague, C., Lin, B., Alcon, C., Flottes, G., Malmstrom, S., Kohler, C., Neuhaus, G., Pelletier, G., Gaymard, F., and Roby, D.** (2003). HLM1, an essential signaling component in the hypersensitive response, is a member of the cyclic nucleotide-gated channel ion channel family. *Plant Cell* **15**, 365-379.
- Balestrini, R., Berta, G., and Bonfante, P.** (1992). The plant nucleus in mycorrhizal roots: positional and structural modifications. *Biology of the Cell* **75**, 235-243.

- Barker, D., Bianchi, S., Blondon, F., Dattée, Y., Duc, G., Essad, S., Flament, P., Gallusci, P., Génier, G., Guy, P., Muel, X., Tourneur, J., Dénaire, J., and Huguet, T.** (1990). *Medicago truncatula*, a model plant for studying the molecular genetics of the Rhizobium-legume symbiosis. *Plant Molecular Biology Reporter* **8**, 40-49.
- Barker, S.J., Stummer, B., Gao, L., Dispain, I., O'Connor, P.J., and Smith, S.E.** (1998). A mutant in *Lycopersicon esculentum* Mill. with highly reduced VA mycorrhizal colonization: isolation and preliminary characterisation. *Plant Journal* **15**, 791-797.
- Bécard, G., and Piché, Y.** (1989). New aspects on the acquisition of biotrophic status by a vesicular-arbuscular mycorrhizal fungus, *Gigaspora margarita*. *New Phytologist* **112**, 77-83.
- Becking, J.** (1979). Root-nodule symbiosis between *Rhizobium* and *Parasponia* (Ulmaceae). *Plant and Soil* **51**, 289-296.
- Ben Amor, B., Shaw, S.L., Oldroyd, G.E., Maillet, F., Penmetsa, R.V., Cook, D., Long, S.R., Denarie, J., and Gough, C.** (2003). The NFP locus of *Medicago truncatula* controls an early step of Nod factor signal transduction upstream of a rapid calcium flux and root hair deformation. *Plant Journal* **34**, 495-506.
- Besserer, A., Puech-Pages, V., Kiefer, P., Gomez-Roldan, V., Jauneau, A., Roy, S., Portais, J.C., Roux, C., Becard, G., and Sejalon-Delmas, N.** (2006). Strigolactones stimulate arbuscular mycorrhizal fungi by activating mitochondria. *PLoS biology* **4**, e226.
- Blanc, G., and Wolfe, K.H.** (2004). Functional divergence of duplicated genes formed by polyploidy during *Arabidopsis* evolution. *Plant Cell* **16**, 1679-1691.
- Bologna, G., Yvon, C., Duvaud, S., and Veuthey, A.L.** (2004). N-Terminal myristoylation predictions by ensembles of neural networks. *Proteomics* **4**, 1626-1632.
- Borsics, T., Webb, D., Andeme-Ondzighi, C., Staehelin, L.A., and Christopher, D.A.** (2007). The cyclic nucleotide-gated calmodulin-binding channel AtCNGC10 localizes to the plasma membrane and influences numerous growth responses and starch accumulation in *Arabidopsis thaliana*. *Planta* **225**, 563-573.
- Bouwmeester, H.J., Matusova, R., Zhongkui, S., and Beale, M.H.** (2003). Secondary metabolite signalling in host-parasitic plant interactions. *Current Opinion in Plant Biology* **6**, 358-364.
- Bouwmeester, H.J., Roux, C., Lopez-Raez, J.A., and Becard, G.** (2007). Rhizosphere communication of plants, parasitic plants and AM fungi. *Trends in Plant Science* **12**, 224-230.
- Bradbury, S.M., Peterson, R.L., and Bowley, S.R.** (1991). Interactions between three alfalfa nodulation genotypes and two *Glomus* species. *New Phytologist* **119**, 115-120.
- Brewin, N.J.** (1991). Development of the legume root nodule. *Annu Rev Cell Biol* **7**, 191-226.
- Brewin, N.J.** (2004). Plant cell wall remodelling in the rhizobium-legume symbiosis. *Critical Reviews in Plant Sciences* **23**, 293-316.
- Bridges, D., Fraser, M.E., and Moorhead, G.B.** (2005). Cyclic nucleotide binding proteins in the *Arabidopsis thaliana* and *Oryza sativa* genomes. *BMC Bioinformatics* **6**, 6.
- Bright, L.J., Liang, Y., Mitchell, D.M., and Harris, J.M.** (2005). The LATD gene of *Medicago truncatula* is required for both nodule and root development. *Molecular Plant-Microbe Interactions* **18**, 521-532.

- Buee, M., Rossignol, M., Jauneau, A., Ranjeva, R., and Becard, G.** (2000). The pre-symbiotic growth of arbuscular mycorrhizal fungi is induced by a branching factor partially purified from plant root exudates. *Molecular Plant-Microbe Interactions* **13**, 693-698.
- Burge, C., and Karlin, S.** (1997). Prediction of complete gene structures in human genomic DNA. *J Mol Biol* **268**, 78-94.
- Burnham, K.P., and Anderson, D.R.** (2002). Model selection and multi-model inference. (New York: Springer-Verlag).
- Campos-Soriano, L., Gomez-Ariza, J., Bonfante, P., and San Segundo, B.** (2011). A rice calcium-dependent protein kinase is expressed in cortical root cells during the presymbiotic phase of the arbuscular mycorrhizal symbiosis. *BMC Plant Biol* **11**, 90.
- Capoen, W., Sun, J., Wysham, D., Otegui, M.S., Venkateshwaran, M., Hirsch, S., Miwa, H., Downie, J.A., Morris, R.J., Ané, J.M., and Oldroyd, G.E.** (2011). Nuclear membranes control symbiotic calcium signaling of legumes. *Proc Natl Acad Sci USA* **108**, 14348-14353.
- Cardenas, L., Feijo, J.A., Kunkel, J.G., Sanchez, F., Holdaway-Clarke, T., Hepler, P.K., and Quinto, C.** (1999). Rhizobium nod factors induce increases in intracellular free calcium and extracellular calcium influxes in bean root hairs. *Plant Journal* **19**, 347-352.
- Catoira, R., Galera, C., de Billy, F., Penmetsa, R.V., Journet, E.P., Maillet, F., Rosenberg, C., Cook, D., Gough, C., and Denarie, J.** (2000). Four genes of *Medicago truncatula* controlling components of a nod factor transduction pathway. *Plant Cell* **12**, 1647-1666.
- Chabaud, M., Venard, C., Defaux-Petras, A., Bécard, G., and Barker, D.G.** (2002). Targeted inoculation of *Medicago truncatula* in vitro root cultures reveals *MtENOD11* expression during early stages of infection by arbuscular mycorrhizal fungi. *New Phytologist* **156**, 265-273.
- Chabaud, M., Genre, A., Sieberer, B.J., Faccio, A., Fournier, J., Novero, M., Barker, D.G., and Bonfante, P.** (2011). Arbuscular mycorrhizal hyphopodia and germinated spore exudates trigger Ca<sup>2+</sup> spiking in the legume and nonlegume root epidermis. *New Phytologist* **189**, 347-355.
- Chang, F., Yan, A., Zhao, L.-N., Wu, W.-H., and Yang, Z.** (2007). A putative calcium-permeable cyclic nucleotide-gated channel, CNGC18, regulates polarized pollen tube growth. *Journal of Integrative Plant Biology* **49**, 1261-1270.
- Charpentier, M., and Oldroyd, G.** (2010). How close are we to nitrogen-fixing cereals? *Curr Opin Plant Biol* **13**, 556-564.
- Charpentier, M., Bredemeier, R., Wanner, G., Takeda, N., Schleiff, E., and Parniske, M.** (2008). *Lotus japonicus* CASTOR and POLLUX are ion channels essential for perinuclear calcium spiking in legume root endosymbiosis. *Plant Cell* **20**, 3467-3479.
- Chen, T.Y., Peng, Y.W., Dhallan, R.S., Ahamed, B., Reed, R.R., and Yau, K.W.** (1993). A new subunit of the cyclic nucleotide-gated cation channel in retinal rods. *Nature* **362**, 764-767.
- Chen, W.H., Lv, G., Lv, C., Zeng, C., and Hu, S.** (2007). Systematic analysis of alternative first exons in plant genomes. *BMC Plant Biol* **7**, 55.
- Cheng, S.H., Willmann, M.R., Chen, H.C., and Sheen, J.** (2002). Calcium signaling through protein kinases. The *Arabidopsis* calcium-dependent protein kinase gene family. *Plant Physiology* **129**, 469-485.
- Clough, S.J., Fengler, K.A., Yu, I.C., Lippok, B., Smith, R.K., Jr., and Bent, A.F.** (2000). The *Arabidopsis dnd1* "defense, no death" gene encodes a mutated cyclic nucleotide-gated ion channel. *Proc Natl Acad Sci USA* **97**, 9323-9328.

## REFERENCES

---

- Cook, C.E., Whichard, L.P., Turner, B., Wall, M.E., and Egley, G.H.** (1966). Germination of witchweed (*Striga lutea* Lour.): Isolation and properties of a potent stimulant. *Science* **154**, 1189-1190.
- Cook, C.E., Whichard, L.P., Wall, M., Egley, G.H., Coggon, P., Luhan, P.A., and McPhail, A.T.** (1972). Germination stimulants. II. Structure of strigol, a potent seed germination stimulant for witchweed (*Striga lutea*). *J Am Chem Soc* **94**, 6198-6199.
- Cramer, M.** (2010). Phosphate as a limiting resource: introduction. *Plant and Soil* **334**, 1-10.
- Crespi, M., and Frugier, F.** (2008). De novo organ formation from differentiated cells: root nodule organogenesis. *Sci Signal* **1**, re11.
- Dammann, C., Ichida, A., Hong, B., Romanowsky, S.M., Hrabak, E.M., Harmon, A.C., Pickard, B.G., and Harper, J.F.** (2003). Subcellular targeting of nine calcium-dependent protein kinase isoforms from *Arabidopsis*. *Plant Physiology* **132**, 1840-1848.
- David-Schwartz, R., Badani, H., Smadar, W., Levy, A.A., Galili, G., and Kapulnik, Y.** (2001). Identification of a novel genetically controlled step in mycorrhizal colonization: plant resistance to infection by fungal spores but not extra-radical hyphae. *Plant Journal* **27**, 561-569.
- David-Schwartz, R., Gadkar, V., Wininger, S., Bendov, R., Galili, G., Levy, A.A., and Kapulnik, Y.** (2003). Isolation of a premycorrhizal infection (*pmi2*) mutant of tomato, resistant to arbuscular mycorrhizal fungal colonization. *Molecular Plant-Microbe Interactions* **16**, 382-388.
- de Castro, E., Sigrist, C.J., Gattiker, A., Bulliard, V., Langendijk-Genevaux, P.S., Gasteiger, E., Bairoch, A., and Hulo, N.** (2006). ScanProsite: detection of PROSITE signature matches and ProRule-associated functional and structural residues in proteins. *Nucleic Acids Res* **34**, W362-365.
- de la Fuente van Bentem, S., Vossen, J.H., Vermeer, J.E., de Vroomen, M.J., Gadella, T.W., Jr., Haring, M.A., and Cornelissen, B.J.** (2003). The subcellular localization of plant protein phosphatase 5 isoforms is determined by alternative splicing. *Plant Physiology* **133**, 702-712.
- Den Herder, G., Yoshida, S., Antolin-Llovera, M., Ried, M.K., and Parniske, M.** (2012). *Lotus japonicus* E3 ligase SEVEN IN ABSENTIA4 destabilizes the symbiosis receptor-like kinase SYMRK and negatively regulates rhizobial infection. *Plant Cell* **24**, 1691-1707.
- Dixon, R., and Kahn, D.** (2004). Genetic regulation of biological nitrogen fixation. *Nat Rev Microbiol* **2**, 621-631.
- Dodd, A.N., Kudla, J., and Sanders, D.** (2010). The language of calcium signaling. *Annu Rev Plant Biol* **61**, 593-620.
- Downie, J.A.** (2005). Legume haemoglobins: symbiotic nitrogen fixation needs bloody nodules. *Curr Biol* **15**, R196-198.
- Doyle, J.J.** (2011). Phylogenetic perspectives on the origins of nodulation. *Molecular Plant-Microbe Interactions* **24**, 1289-1295.
- Drissner, D., Kunze, G., Callewaert, N., Gehrig, P., Tamasloukht, M., Boller, T., Felix, G., Amrhein, N., and Bucher, M.** (2007). Lyso-phosphatidylcholine is a signal in the arbuscular mycorrhizal symbiosis. *Science* **318**, 265-268.
- Duc, G., Trouvelot, A., Gianinazzi-Pearson, V., and Gianinazzi, S.** (1989). First report of non-mycorrhizal plant mutants (Myc-) obtained in pea (*Pisum sativum* L.) and fababean (*Vicia faba* L.). *Plant Science* **60**, 215-222.

## REFERENCES

---

- Ehrhardt, D.W., Wais, R., and Long, S.R.** (1996). Calcium spiking in plant root hairs responding to Rhizobium nodulation signals. *Cell* **85**, 673-681.
- Endre, G., Kereszt, A., Kevei, Z., Mihacea, S., Kalo, P., and Kiss, G.B.** (2002). A receptor kinase gene regulating symbiotic nodule development. *Nature* **417**, 962-966.
- Engler, C., Kandzia, R., and Marillonnet, S.** (2008). A one pot, one step, precision cloning method with high throughput capability. *PLoS One* **3**, e3647.
- Esseling, J.J., Lhuissier, F.G., and Emons, A.M.** (2003). Nod factor-induced root hair curling: continuous polar growth towards the point of nod factor application. *Plant Physiology* **132**, 1982-1988.
- Fahraeus, G.** (1957). The infection of clover root hairs by nodule bacteria studied by a simple glass slide technique. *J Gen Microbiol* **16**, 374-381.
- Feddermann, N., Muni, R.R., Zeier, T., Stuurman, J., Ercolin, F., Schorderet, M., and Reinhardt, D.** (2010). The *PAM1* gene of petunia, required for intracellular accommodation and morphogenesis of arbuscular mycorrhizal fungi, encodes a homologue of VAPYRIN. *Plant Journal* **64**, 470-481.
- Felle, H.H., Kondorosi, É., Kondorosi, Á., and Schultze, M.** (1998). The role of ion fluxes in Nod factor signalling in *Medicago sativa*. *Plant Journal* **13**, 455-463.
- Feys, B.J., Wiermer, M., Bhat, R.A., Moisan, L.J., Medina-Escobar, N., Neu, C., Cabral, A., and Parker, J.E.** (2005). *Arabidopsis* SENESCENCE-ASSOCIATED GENE101 stabilizes and signals within an ENHANCED DISEASE SUSCEPTIBILITY1 complex in plant innate immunity. *Plant Cell* **17**, 2601-2613.
- Fisher, R.F., and Long, S.R.** (1992). Rhizobium-plant signal exchange. *Nature* **357**, 655-660.
- Fournier, J., Timmers, A.C., Sieberer, B.J., Jauneau, A., Chabaud, M., and Barker, D.G.** (2008). Mechanism of infection thread elongation in root hairs of *Medicago truncatula* and dynamic interplay with associated rhizobial colonization. *Plant Physiology* **148**, 1985-1995.
- Frank, A.B.** (1885). Über die auf Wurzelsymbiose beruhende Ernährung gewisser Bäume durch unterirdische Pilze. *Berichte der Deutschen Botanischen Gesellschaft* **3**, 128-145.
- Frank, A.B., and Trappe, J.M.** (2005). On the nutritional dependence of certain trees on root symbiosis with belowground fungi (an English translation of A.B. Frank's classic paper of 1885). *Mycorrhiza* **15**, 267-275.
- Franssen, H.J., Vijn, I., Yang, W.C., and Bisseling, T.** (1992). Developmental aspects of the Rhizobium-legume symbiosis. *Plant Mol Biol* **19**, 89-107.
- Frietsch, S., Wang, Y.F., Sladek, C., Poulsen, L.R., Romanowsky, S.M., Schroeder, J.I., and Harper, J.F.** (2007). A cyclic nucleotide-gated channel is essential for polarized tip growth of pollen. *Proc Natl Acad Sci USA* **104**, 14531-14536.
- Gage, D.J., Bobo, T., and Long, S.R.** (1996). Use of green fluorescent protein to visualize the early events of symbiosis between *Rhizobium meliloti* and alfalfa (*Medicago sativa*). *J Bacteriol* **178**, 7159-7166.
- Galloway, J.N., and Cowling, E.B.** (2002). Reactive nitrogen and the world: 200 years of change. *AMBIO: A Journal of the Human Environment* **31**, 64-71.
- Gargantini, P.R., Gonzalez-Rizzo, S., Chinchilla, D., Raices, M., Giannmaria, V., Ulloa, R.M., Frugier, F., and Crespi, M.D.** (2006). A CDPK isoform participates in the regulation of nodule number in *Medicago truncatula*. *Plant Journal* **48**, 843-856.

- Genre, A., Chabaud, M., Timmers, T., Bonfante, P., and Barker, D.G.** (2005). Arbuscular mycorrhizal fungi elicit a novel intracellular apparatus in *Medicago truncatula* root epidermal cells before infection. *Plant Cell* **17**, 3489-3499.
- Genre, A., Chabaud, M., Faccio, A., Barker, D.G., and Bonfante, P.** (2008). Prepenetration apparatus assembly precedes and predicts the colonization patterns of arbuscular mycorrhizal fungi within the root cortex of both *Medicago truncatula* and *Daucus carota*. *Plant Cell* **20**, 1407-1420.
- Geurts, R., Fedorova, E., and Bisseling, T.** (2005). Nod factor signaling genes and their function in the early stages of Rhizobium infection. *Current Opinion in Plant Biology* **8**, 346-352.
- Gibson, K.E., Kobayashi, H., and Walker, G.C.** (2008). Molecular determinants of a symbiotic chronic infection. *Annu Rev Genet* **42**, 413-441.
- Giovannetti, M., Sbrana, C., Avio, L., Citernesi, A.S., and Logi, C.** (1993). Differential hyphal morphogenesis in arbuscular mycorrhizal fungi during pre-infection stages. *New Phytologist* **125**, 587-593.
- Gobert, A., Park, G., Amtmann, A., Sanders, D., and Maathuis, F.J.** (2006). *Arabidopsis thaliana* cyclic nucleotide gated channel 3 forms a non-selective ion transporter involved in germination and cation transport. *J Exp Bot* **57**, 791-800.
- Gomez-Roldan, V., Fermas, S., Brewer, P.B., Puech-Pages, V., Dun, E.A., Pillot, J.-P., Lettisse, F., Matusova, R., Danoun, S., Portais, J.-C., Bouwmeester, H., Becard, G., Beveridge, C.A., Rameau, C., and Rochange, S.F.** (2008). Strigolactone inhibition of shoot branching. *Nature* **455**, 189-194.
- Gough, C., and Cullimore, J.** (2011). Lipo-chitooligosaccharide signaling in endosymbiotic plant-microbe interactions. *Molecular Plant-Microbe Interactions* **24**, 867-878.
- Govindarajulu, M., Pfeffer, P.E., Jin, H., Abubaker, J., Douds, D.D., Allen, J.W., Bucking, H., Lammers, P.J., and Shachar-Hill, Y.** (2005). Nitrogen transfer in the arbuscular mycorrhizal symbiosis. *Nature* **435**, 819-823.
- Greene, E.A., Codomo, C.A., Taylor, N.E., Henikoff, J.G., Till, B.J., Reynolds, S.H., Enns, L.C., Burtner, C., Johnson, J.E., Odden, A.R., Comai, L., and Henikoff, S.** (2003). Spectrum of chemically induced mutations from a large-scale reverse-genetic screen in *Arabidopsis*. *Genetics* **164**, 731-740.
- Groth, M.** (2010). Genetic Analysis of Arbuscular Mycorrhiza Development in *Lotus japonicus*, PhD-Thesis (Munich: Ludwig-Maximilians-Universität).
- Groth, M., Takeda, N., Perry, J., Uchida, H., Dräxl, S., Brachmann, A., Sato, S., Tabata, S., Kawaguchi, M., Wang, T.L., and Parniske, M.** (2010). NENA, a *Lotus japonicus* homolog of Sec13, is required for rhizodermal infection by arbuscular mycorrhiza fungi and rhizobia but dispensable for cortical endosymbiotic development. *Plant Cell* **22**, 2509-2526.
- Gutjahr, C., Banba, M., Croset, V., An, K., Miyao, A., An, G., Hirochika, H., Imaizumi-Anraku, H., and Paszkowski, U.** (2008). Arbuscular mycorrhiza-specific signaling in rice transcends the common symbiosis signaling pathway. *Plant Cell* **20**, 2989-3005.
- Handberg, K., and Stougaard, J.** (1992). *Lotus japonicus*, an autogamous, diploid legume species for classical and molecular genetics. *Plant Journal* **2**, 487-496.
- Harmon, A.C., Grbiskov, M., and Harper, J.F.** (2000). CDPKs - a kinase for every Ca<sup>2+</sup> signal? *Trends in Plant Science* **5**, 154-159.

## REFERENCES

---

- Harmon, A.C., Grubkov, M., Gubrium, E., and Harper, J.F.** (2001). The CDPK superfamily of protein kinases. *New Phytologist* **151**, 175-183.
- Harper, J.F., and Harmon, A.** (2005). Plants, symbiosis and parasites: A calcium signalling connection. *Nature Reviews Molecular Cell Biology* **6**, 555-566.
- Harrison, M.J.** (1999). Molecular and cellular aspects of the arbuscular mycorrhizal symbiosis. *Annu Rev Plant Physiol Plant Mol Biol* **50**, 361-389.
- Harrison, M.J., and van Buuren, M.L.** (1995). A phosphate transporter from the mycorrhizal fungus *Glomus versiforme*. *Nature* **378**, 626-629.
- Harrison, M.J., Dewbre, G.R., and Liu, J.** (2002). A phosphate transporter from *Medicago truncatula* involved in the acquisition of phosphate released by arbuscular mycorrhizal fungi. *Plant Cell* **14**, 2413-2429.
- Hayashi, M., Miyahara, A., Sato, S., Kato, T., Yoshikawa, M., Taketa, M., Pedrosa, A., Onda, R., Imaizumi-Anraku, H., Bachmair, A., Sandal, N., Stougaard, J., Murooka, Y., Tabata, S., Kawasaki, S., Kawaguchi, M., and Harada, K.** (2001). Construction of a genetic linkage map of the model legume *Lotus japonicus* using an intraspecific F2 population. *DNA Res* **8**, 301-310.
- Helber, N., Wippel, K., Sauer, N., Schaarschmidt, S., Hause, B., and Requena, N.** (2011). A versatile monosaccharide transporter that operates in the arbuscular mycorrhizal fungus *Glomus* sp is crucial for the symbiotic relationship with plants. *Plant Cell* **23**, 3812-3823.
- Hetherington, A.M., and Brownlee, C.** (2004). The generation of Ca<sup>2+</sup> signals in plants. *Annu Rev Plant Biol* **55**, 401-427.
- Hodge, A., Campbell, C.D., and Fitter, A.H.** (2001). An arbuscular mycorrhizal fungus accelerates decomposition and acquires nitrogen directly from organic material. *Nature* **413**, 297-299.
- Hrabak, E.M., Chan, C.W., Grubkov, M., Harper, J.F., Choi, J.H., Halford, N., Kudla, J., Luan, S., Nimmo, H.G., Sussman, M.R., Thomas, M., Walker-Simmons, K., Zhu, J.K., and Harmon, A.C.** (2003). The *Arabidopsis* CDPK-SnRK superfamily of protein kinases. *Plant Physiology* **132**, 666-680.
- Imaizumi-Anraku, H., Takeda, N., Charpentier, M., Perry, J., Miwa, H., Umehara, Y., Kouchi, H., Murakami, Y., Mulder, L., Vickers, K., Pike, J., Downie, J.A., Wang, T., Sato, S., Asamizu, E., Tabata, S., Yoshikawa, M., Murooka, Y., Wu, G.J., et al.** (2005). Plastid proteins crucial for symbiotic fungal and bacterial entry into plant roots. *Nature* **433**, 527-531.
- Ito, M., Miyamoto, J., Mori, Y., Fujimoto, S., Uchiumi, T., Abe, M., Suzuki, A., Tabata, S., and Fukui, K.** (2000). Genome and chromosome dimensions of *Lotus japonicus*. *Journal of Plant Research* **113**, 435-442.
- Ivashuta, S., Liu, J., Lohar, D.P., Haridas, S., Bucciarelli, B., VandenBosch, K.A., Vance, C.P., Harrison, M.J., and Gantt, J.S.** (2005). RNA interference identifies a calcium-dependent protein kinase involved in *Medicago truncatula* root development. *Plant Cell* **17**, 2911-2921.
- Javot, H., Penmetsa, R.V., Terzaghi, N., Cook, D.R., and Harrison, M.J.** (2007). A *Medicago truncatula* phosphate transporter indispensable for the arbuscular mycorrhizal symbiosis. *Proc Natl Acad Sci USA* **104**, 1720-1725.
- Jiang, Q., and Gresshoff, P.M.** (1997). Classical and molecular genetics of the model legume *Lotus japonicus*. *Molecular Plant-Microbe Interactions* **10**, 59-68.
- Jones, J.D., and Dangl, J.L.** (2006). The plant immune system. *Nature* **444**, 323-329.

- Jurkowski, G.I., Smith, R.K., Jr., Yu, I.C., Ham, J.H., Sharma, S.B., Klessig, D.F., Fengler, K.A., and Bent, A.F.** (2004). *Arabidopsis DND2*, a second cyclic nucleotide-gated ion channel gene for which mutation causes the "defense, no death" phenotype. *Molecular Plant-Microbe Interactions* **17**, 511-520.
- Kanamori, N., Madsen, L.H., Radutoiu, S., Frantescu, M., Quistgaard, E.M., Miwa, H., Downie, J.A., James, E.K., Felle, H.H., Haaning, L.L., Jensen, T.H., Sato, S., Nakamura, Y., Tabata, S., Sandal, N., and Stougaard, J.** (2006). A nucleoporin is required for induction of Ca<sup>2+</sup> spiking in legume nodule development and essential for rhizobial and fungal symbiosis. *Proc Natl Acad Sci USA* **103**, 359-364.
- Kaplan, B., Sherman, T., and Fromm, H.** (2007). Cyclic nucleotide-gated channels in plants. *FEBS Lett* **581**, 2237-2246.
- Karimi, M., Inze, D., and Depicker, A.** (2002). GATEWAY vectors for *Agrobacterium*-mediated plant transformation. *Trends Plant Sci* **7**, 193-195.
- Katoh, K., Kuma, K., Toh, H., and Miyata, T.** (2005). MAFFT version 5: improvement in accuracy of multiple sequence alignment. *Nucleic Acids Res* **33**, 511-518.
- Kawaguchi, M., Motomura, T., Imaizumi-Anraku, H., Akao, S., and Kawasaki, S.** (2001). Providing the basis for genomics in *Lotus japonicus*: the accessions Miyakojima and Gifu are appropriate crossing partners for genetic analyses. *Mol Genet Genomics* **266**, 157-166.
- Kawaguchi, M., Pedrosa-Harand, A., Yano, K., Hayashi, M., Murooka, Y., Saito, K., Nagata, T., Namai, K., Nishida, H., Shibata, D., Sato, S., Tabata, S., Harada, K., Sandal, N., Stougaard, J., Bachmair, A., and Grant, W.F.** (2005). *Lotus burtii* takes a position of the third corner in the *Lotus* molecular genetics triangle. *DNA Res* **12**, 69-77.
- Kimura, K., Wakamatsu, A., Suzuki, Y., Ota, T., Nishikawa, T., Yamashita, R., Yamamoto, J., Sekine, M., Tsuritani, K., Wakaguri, H., Ishii, S., Sugiyama, T., Saito, K., Isono, Y., Irie, R., Kushida, N., Yoneyama, T., Otsuka, R., Kanda, K., et al.** (2006). Diversification of transcriptional modulation: large-scale identification and characterization of putative alternative promoters of human genes. *Genome Res* **16**, 55-65.
- Kistner, C., and Parniske, M.** (2002). Evolution of signal transduction in intracellular symbiosis. *Trends Plant Sci* **7**, 511-518.
- Kistner, C., Winzer, T., Pitzschke, A., Mulder, L., Sato, S., Kaneko, T., Tabata, S., Sandal, N., Stougaard, J., Webb, K.J., Szczyglowski, K., and Parniske, M.** (2005). Seven *Lotus japonicus* genes required for transcriptional reprogramming of the root during fungal and bacterial symbiosis. *Plant Cell* **17**, 2217-2229.
- Kitagawa, N., Washio, T., Kosugi, S., Yamashita, T., Higashi, K., Yanagawa, H., Higo, K., Satoh, K., Ohtomo, Y., Sunako, T., Murakami, K., Matsubara, K., Kawai, J., Carninci, P., Hayashizaki, Y., Kikuchi, S., and Tomita, M.** (2005). Computational analysis suggests that alternative first exons are involved in tissue-specific transcription in rice (*Oryza sativa*). *Bioinformatics* **21**, 1758-1763.
- Kloppholz, S., Kuhn, H., and Requena, N.** (2011). A secreted fungal effector of *Glomus intraradices* promotes symbiotic biotrophy. *Current Biology* **21**, 1204-1209.
- Köhler, C., and Neuhaus, G.** (1998). Cloning and partial characterization of two putative cyclic nucleotide-regulated ion channels from *Arabidopsis thaliana*, designated CNGC1 (Accession No. Y16327) and CNGC2 (Accession No. Y16328). *Plant Physiology* **116**, 1604.
- Köhler, C., and Neuhaus, G.** (2000). Characterisation of calmodulin binding to cyclic nucleotide-gated ion channels from *Arabidopsis thaliana*. *FEBS Lett* **471**, 133-136.

- Köhler, C., Merkle, T., and Neuhaus, G.** (1999). Characterisation of a novel gene family of putative cyclic nucleotide- and calmodulin-regulated ion channels in *Arabidopsis thaliana*. *Plant Journal* **18**, 97-104.
- Koncz, C., and Schell, J.** (1986). The promoter of TL-DNA gene 5 controls the tissue-specific expression of chimaeric genes carried by a novel type of *Agrobacterium* binary vector. *Molecular and General Genetics MGG* **204**, 383-396.
- Koo, S.C., Yoon, H.W., Kim, C.Y., Moon, B.C., Cheong, Y.H., Han, H.J., Lee, S.M., Kang, K.Y., Kim, M.C., Lee, S.Y., Chung, W.S., and Cho, M.J.** (2007). Alternative splicing of the *OsBWMK1* gene generates three transcript variants showing differential subcellular localizations. *Biochem Biophys Res Commun* **360**, 188-193.
- Koske, R.E.** (1981). *Gigaspora gigantea*: Observations on spore germination of a VA-mycorrhizal fungus. *Mycologia* **73**, 288-300.
- Kosuta, S., Chabaud, M., Lougnon, G., Gough, C., Denarie, J., Barker, D.G., and Becard, G.** (2003). A diffusible factor from arbuscular mycorrhizal fungi induces symbiosis-specific *MtENOD11* expression in roots of *Medicago truncatula*. *Plant Physiology* **131**, 952-962.
- Kosuta, S., Hazledine, S., Sun, J., Miwa, H., Morris, R.J., Downie, J.A., and Oldroyd, G.E.** (2008). Differential and chaotic calcium signatures in the symbiosis signaling pathway of legumes. *Proc Natl Acad Sci USA* **105**, 9823-9828.
- Krüger, M., Krüger, C., Walker, C., Stockinger, H., and Schüßler, A.** (2012). Phylogenetic reference data for systematics and phylotaxonomy of arbuscular mycorrhizal fungi from phylum to species level. *New Phytologist* **193**, 970-984.
- Kugler, A., Kohler, B., Palme, K., Wolff, P., and Dietrich, P.** (2009). Salt-dependent regulation of a CNG channel subfamily in *Arabidopsis*. *BMC Plant Biol* **9**, 140.
- Kuhn, H., Küster, H., and Requena, N.** (2010). Membrane steroid-binding protein 1 induced by a diffusible fungal signal is critical for mycorrhization in *Medicago truncatula*. *New Phytologist* **185**, 716-733.
- Lavin, M., Herendeen, P.S., and Wojciechowski, M.F.** (2005). Evolutionary rates analysis of Leguminosae implicates a rapid diversification of lineages during the tertiary. *Syst Biol* **54**, 575-594.
- Leng, Q., Mercier, R.W., Yao, W., and Berkowitz, G.A.** (1999). Cloning and first functional characterization of a plant cyclic nucleotide-gated cation channel. *Plant Physiology* **121**, 753-761.
- Lerouge, P., Roche, P., Faucher, C., Maillet, F., Truchet, G., Prome, J.C., and Denarie, J.** (1990). Symbiotic host-specificity of *Rhizobium meliloti* is determined by a sulphated and acylated glucosamine oligosaccharide signal. *Nature* **344**, 781-784.
- Lévy, J., Bres, C., Geurts, R., Chalhoub, B., Kulikova, O., Duc, G., Journet, E.P., Ané, J.M., Lauber, E., Bisseling, T., Dénaire, J., Rosenberg, C., and Debellé, F.** (2004). A putative Ca<sup>2+</sup> and calmodulin-dependent protein kinase required for bacterial and fungal symbioses. *Science* **303**, 1361-1364.
- Liang, Y., Mitchell, D.M., and Harris, J.M.** (2007). Abscisic acid rescues the root meristem defects of the *Medicago truncatula latd* mutant. *Dev Biol* **304**, 297-307.
- Limpens, E., Franken, C., Smit, P., Willemse, J., Bisseling, T., and Geurts, R.** (2003). LysM domain receptor kinases regulating rhizobial Nod factor-induced infection. *Science* **302**, 630-633.
- Liu, J., Maldonado-Mendoza, I., Lopez-Meyer, M., Cheung, F., Town, C.D., and Harrison, M.J.** (2007). Arbuscular mycorrhizal symbiosis is accompanied by local and systemic

REFERENCES

---

- alterations in gene expression and an increase in disease resistance in the shoots. *Plant Journal* **50**, 529-544.
- Liu, M., Chen, T.Y., Ahamed, B., Li, J., and Yau, K.W.** (1994). Calcium-calmodulin modulation of the olfactory cyclic nucleotide-gated cation channel. *Science* **266**, 1348-1354.
- Long, S.R.** (1996). Rhizobium symbiosis: nod factors in perspective. *Plant Cell* **8**, 1885-1898.
- Lopez-Pedrosa, A., Gonzalez-Guerrero, M., Valderas, A., Azcon-Aguilar, C., and Ferrol, N.** (2006). *GintAMT1* encodes a functional high-affinity ammonium transporter that is expressed in the extraradical mycelium of *Glomus intraradices*. *Fungal Genet Biol* **43**, 102-110.
- Lu, S.X., and Hrabak, E.M.** (2002). An *Arabidopsis* calcium-dependent protein kinase is associated with the endoplasmic reticulum. *Plant Physiology* **128**, 1008-1021.
- Ma, W., and Berkowitz, G.A.** (2011). Ca<sup>2+</sup> conduction by plant cyclic nucleotide gated channels and associated signaling components in pathogen defense signal transduction cascades. *New Phytologist* **190**, 566-572.
- Ma, W., Qi, Z., Smigel, A., Walker, R.K., Verma, R., and Berkowitz, G.A.** (2009). Ca<sup>2+</sup>, cAMP, and transduction of non-self perception during plant immune responses. *Proc Natl Acad Sci USA* **106**, 20995-21000.
- Madsen, E.B., Madsen, L.H., Radutoiu, S., Olbryt, M., Rakwalska, M., Szczyglowski, K., Sato, S., Kaneko, T., Tabata, S., Sandal, N., and Stougaard, J.** (2003). A receptor kinase gene of the LysM type is involved in legume perception of rhizobial signals. *Nature* **425**, 637-640.
- Madsen, L.H., Tirichine, L., Jurkiewicz, A., Sullivan, J.T., Heckmann, A.B., Bek, A.S., Ronson, C.W., James, E.K., and Stougaard, J.** (2010). The molecular network governing nodule organogenesis and infection in the model legume *Lotus japonicus*. *Nat Commun* **1**, 10.
- Maekawa-Yoshikawa, M., Müller, J., Takeda, N., Maekawa, T., Sato, S., Tabata, S., Perry, J., Wang, T.L., Groth, M., Brachmann, A., and Parniske, M.** (2009). The temperature-sensitive *brush* mutant of the legume *Lotus japonicus* reveals a link between root development and nodule infection by rhizobia. *Plant Physiology* **149**, 1785-1796.
- Maillet, F., Poinsot, V., Andre, O., Puech-Pages, V., Haouy, A., Gueunier, M., Cromer, L., Giraudet, D., Formey, D., Niebel, A., Martinez, E.A., Driguez, H., Becard, G., and Denarie, J.** (2011). Fungal lipochitooligosaccharide symbiotic signals in arbuscular mycorrhiza. *Nature* **469**, 58-63.
- Maldonado-Mendoza, I.E., Dewbre, G.R., and Harrison, M.J.** (2001). A phosphate transporter gene from the extra-radical mycelium of an arbuscular mycorrhizal fungus *Glomus intraradices* is regulated in response to phosphate in the environment. *Molecular Plant-Microbe Interactions* **14**, 1140-1148.
- Markmann, K., Giczey, G., and Parniske, M.** (2008). Functional adaptation of a plant receptor-kinase paved the way for the evolution of intracellular root symbioses with bacteria. *PLoS Biol* **6**, e68.
- Martin, M.L., and Busconi, L.** (2000). Membrane localization of a rice calcium-dependent protein kinase (CDPK) is mediated by myristoylation and palmitoylation. *Plant Journal* **24**, 429-435.
- Mäser, P., Thomine, S., Schroeder, J.I., Ward, J.M., Hirschi, K., Sze, H., Talke, I.N., Amtmann, A., Maathuis, F.J., Sanders, D., Harper, J.F., Tchieu, J., Gribskov, M., Persans, M.W., Salt, D.E., Kim, S.A., and Guerinot, M.L.** (2001). Phylogenetic

## REFERENCES

---

- relationships within cation transporter families of *Arabidopsis*. *Plant Physiology* **126**, 1646-1667.
- Matulef, K., and Zagotta, W.N.** (2003). Cyclic nucleotide-gated ion channels. *Annu Rev Cell Dev Biol* **19**, 23-44.
- McAinsh, M.R., and Hetherington, A.M.** (1998). Encoding specificity in Ca<sup>2+</sup> signalling systems. *Trends in Plant Science* **3**, 32-36.
- McAinsh, M.R., and Pittman, J.K.** (2009). Shaping the calcium signature. *New Phytologist* **181**, 275-294.
- McCurdy, D.W., and Harmon, A.C.** (1992). Calcium-dependent protein kinase in the green alga *Chara*. *Planta* **188**, 54-61.
- Messinese, E., Mun, J.H., Yeun, L.H., Jayaraman, D., Rouge, P., Barre, A., Lougnon, G., Schornack, S., Bono, J.J., Cook, D.R., and Ané, J.M.** (2007). A novel nuclear protein interacts with the symbiotic DMI3 calcium- and calmodulin-dependent protein kinase of *Medicago truncatula*. *Molecular Plant-Microbe Interactions* **20**, 912-921.
- Miller, M.A., Peiffer, W., and Schwartz, T.** (2010). Creating the CIPRES Science Gateway for inference of large phylogenetic trees. *Proceedings of the Gateway Computing Environments Workshop (GCE)*, 1-8.
- Mitra, R.M., Gleason, C.A., Edwards, A., Hadfield, J., Downie, J.A., Oldroyd, G.E., and Long, S.R.** (2004). A Ca<sup>2+</sup>/calmodulin-dependent protein kinase required for symbiotic nodule development: Gene identification by transcript-based cloning. *Proc Natl Acad Sci USA* **101**, 4701-4705.
- Miwa, H., Sun, J., Oldroyd, G.E., and Downie, J.A.** (2006). Analysis of Nod-factor-induced calcium signaling in root hairs of symbiotically defective mutants of *Lotus japonicus*. *Molecular Plant-Microbe Interactions* **19**, 914-923.
- Morello, L., Bardini, M., Cricri, M., Sala, F., and Breviario, D.** (2006). Functional analysis of DNA sequences controlling the expression of the rice OsCDPK2 gene. *Planta* **223**, 479-491.
- Mosse, B., and Hepper, C.** (1975). Vesicular-arbuscular mycorrhizal infections in root organ cultures. *Physiological Plant Pathology* **5**, 215-223.
- Murray, J.D., Muni, R.R., Torres-Jerez, I., Tang, Y., Allen, S., Andriankaja, M., Li, G., Laxmi, A., Cheng, X., Wen, J., Vaughan, D., Schultze, M., Sun, J., Charpentier, M., Oldroyd, G., Tadege, M., Ratet, P., Mysore, K.S., Chen, R., et al.** (2011). VAPYRIN, a gene essential for intracellular progression of arbuscular mycorrhizal symbiosis, is also essential for infection by rhizobia in the nodule symbiosis of *Medicago truncatula*. *Plant Journal* **65**, 244-252.
- Neff, M.M., Turk, E., and Kalishman, M.** (2002). Web-based primer design for single nucleotide polymorphism analysis. *Trends Genet* **18**, 613-615.
- Newsham, K.K., Fitter, A.H., and Watkinson, A.R.** (1995). Arbuscular mycorrhiza protect an annual grass from root pathogenic fungi in the field. *Journal of Ecology* **83**, 991-1000.
- Nishiyama, R., Mizuno, H., Okada, S., Yamaguchi, T., Takenaka, M., Fukuzawa, H., and Ohyama, K.** (1999). Two mRNA species encoding calcium-dependent protein kinases are differentially expressed in sexual organs of *Marchantia polymorpha* through alternative splicing. *Plant Cell Physiol* **40**, 205-212.
- Nutman, P.S.** (1959). Some observations on root-hair infection by nodule bacteria. *J Exp Bot* **10**, 250-263.

- Op den Camp, R., Streng, A., De Mita, S., Cao, Q., Polone, E., Liu, W., Ammiraju, J.S., Kudrna, D., Wing, R., Untergasser, A., Bisseling, T., and Geurts, R.** (2011). LysM-type mycorrhizal receptor recruited for rhizobium symbiosis in nonlegume *Parasponia*. *Science* **331**, 909-912.
- Page, D.R., and Grossniklaus, U.** (2002). The art and design of genetic screens: *Arabidopsis thaliana*. *Nat Rev Genet* **3**, 124-136.
- Parniske, M.** (2004). Molecular genetics of the arbuscular mycorrhizal symbiosis. *Curr Opin Plant Biol* **7**, 414-421.
- Parniske, M.** (2008). Arbuscular mycorrhiza: the mother of plant root endosymbioses. *Nat Rev Microbiol* **6**, 763-775.
- Paszkowski, U., Jakovleva, L., and Boller, T.** (2006). Maize mutants affected at distinct stages of the arbuscular mycorrhizal symbiosis. *Plant Journal* **47**, 165-173.
- Perret, X., Staehelin, C., and Broughton, W.J.** (2000). Molecular basis of symbiotic promiscuity. *Microbiol Mol Biol Rev* **64**, 180-201.
- Perry, J., Brachmann, A., Welham, T., Binder, A., Charpentier, M., Groth, M., Haage, K., Markmann, K., Wang, T.L., and Parniske, M.** (2009). TILLING in *Lotus japonicus* identified large allelic series for symbiosis genes and revealed a bias in functionally defective ethyl methanesulfonate alleles toward glycine replacements. *Plant Physiology* **151**, 1281-1291.
- Perry, J.A., Wang, T.L., Welham, T.J., Gardner, S., Pike, J.M., Yoshida, S., and Parniske, M.** (2003). A TILLING reverse genetics tool and a web-accessible collection of mutants of the legume *Lotus japonicus*. *Plant Physiology* **131**, 866-871.
- Peters, N.K., Frost, J.W., and Long, S.R.** (1986). A plant flavone, luteolin, induces expression of *Rhizobium meliloti* nodulation genes. *Science* **233**, 977-980.
- Podell, S., and Gribskov, M.** (2004). Predicting N-terminal myristoylation sites in plant proteins. *BMC Genomics* **5**, 37.
- Pumplin, N., Mondo, S.J., Topp, S., Starker, C.G., Gantt, J.S., and Harrison, M.J.** (2010). *Medicago truncatula* VAPYRIN is a novel protein required for arbuscular mycorrhizal symbiosis. *Plant Journal* **61**, 482-494.
- R Development Core Team.** (2011). R: A language and environment for statistical computing. (Vienna, Austria: R Foundation for Statistical Computing).
- Radutoiu, S., Madsen, L.H., Madsen, E.B., Felle, H.H., Umehara, Y., Gronlund, M., Sato, S., Nakamura, Y., Tabata, S., Sandal, N., and Stougaard, J.** (2003). Plant recognition of symbiotic bacteria requires two LysM receptor-like kinases. *Nature* **425**, 585-592.
- Reddy, D.M.R.S., Schorderet, M., Feller, U., and Reinhardt, D.** (2007). A petunia mutant affected in intracellular accommodation and morphogenesis of arbuscular mycorrhizal fungi. *Plant Journal* **51**, 739-750.
- Redecker, D., Kodner, R., and Graham, L.E.** (2000). Glomalean fungi from the Ordovician. *Science* **289**, 1920-1921.
- Redmond, J.W., Batley, M., Djordjevic, M.A., Innes, R.W., Kuempel, P.L., and Rolfe, B.G.** (1986). Flavones induce expression of nodulation genes in *Rhizobium*. *Nature* **323**, 632-635.
- Remy, W., Taylor, T.N., Hass, H., and Kerp, H.** (1994). Four hundred-million-year-old vesicular arbuscular mycorrhizae. *Proc Natl Acad Sci USA* **91**, 11841-11843.

- Riely, B.K., Lougnon, G., Ané, J.-M., and Cook, D.R.** (2007). The symbiotic ion channel homolog DMI1 is localized in the nuclear membrane of *Medicago truncatula* roots. *Plant Journal* **49**, 208-216.
- Rostoks, N., Schmierer, D., Mudie, S., Drader, T., Brueggeman, R., Caldwell, D.G., Waugh, R., and Kleinhofs, A.** (2006). Barley necrotic locus *nec1* encodes the cyclic nucleotide-gated ion channel 4 homologous to the *Arabidopsis* HLM1. *Mol Genet Genomics* **275**, 159-168.
- Rutherford, K., Parkhill, J., Crook, J., Horsnell, T., Rice, P., Rajandream, M.A., and Barrell, B.** (2000). Artemis: sequence visualization and annotation. *Bioinformatics* **16**, 944-945.
- Saito, K., Yoshikawa, M., Yano, K., Miwa, H., Uchida, H., Asamizu, E., Sato, S., Tabata, S., Imaizumi-Anraku, H., Umehara, Y., Kouchi, H., Murooka, Y., Szczyglowski, K., Downie, J.A., Parniske, M., Hayashi, M., and Kawaguchi, M.** (2007). NUCLEOPORIN85 is required for calcium spiking, fungal and bacterial symbioses, and seed production in *Lotus japonicus*. *Plant Cell* **19**, 610-624.
- Sanders, D., Brownlee, C., and Harper, J.F.** (1999). Communicating with calcium. *Plant Cell* **11**, 691-706.
- Sanders, D., Pelloux, J., Brownlee, C., and Harper, J.F.** (2002). Calcium at the crossroads of signaling. *Plant Cell* **14 Suppl**, S401-417.
- Sato, S., Nakamura, Y., Kaneko, T., Asamizu, E., Kato, T., Nakao, M., Sasamoto, S., Watanabe, A., Ono, A., Kawashima, K., Fujishiro, T., Katoh, M., Kohara, M., Kishida, Y., Minami, C., Nakayama, S., Nakazaki, N., Shimizu, Y., Shinpo, S., et al.** (2008). Genome structure of the legume, *Lotus japonicus*. *DNA Res* **15**, 227-239.
- Schuelke, M.** (2000). An economic method for the fluorescent labeling of PCR fragments. *Nat Biotechnol* **18**, 233-234.
- Schüßler, A., and Walker, C.** (2010). The *Glomeromycota*: a species list with new families and new genera. . Schüßler A, Walker C, Gloucester, Published in libraries at The Royal Botanic Garden Edinburgh, The Royal Botanic Garden Kew, Botanische Staatssammlung München, and Oregon State University; electronic version freely available online at <http://www.amf-phylogeny.com>.
- Schüßler, A., Schwarzott, D., and Walker, C.** (2001). A new fungal phylum, the *Glomeromycota*: phylogeny and evolution. *Mycol Res* **105**, 1413-1421.
- Schuurink, R.C., Shartzer, S.F., Fath, A., and Jones, R.L.** (1998). Characterization of a calmodulin-binding transporter from the plasma membrane of barley aleurone. *Proc Natl Acad Sci USA* **95**, 1944-1949.
- Shaw, S.L., and Long, S.R.** (2003). Nod factor elicits two separable calcium responses in *Medicago truncatula* root hair cells. *Plant Physiology* **131**, 976-984.
- Shirtliffe, S.J., and Vessey, J.K.** (1996). A nodulation (Nod+Fix-) mutant of *Phaseolus vulgaris* L. has nodule-like structures lacking peripheral vascular bundles (Pvb-) and is resistant to mycorrhizal infection (Myc-). *Plant Science* **118**, 209-220.
- Sieberer, B.J., Chabaud, M., Fournier, J., Timmers, A.C.J., and Barker, D.G.** (2012). A switch in Ca<sup>2+</sup> spiking signature is concomitant with endosymbiotic microbe entry into cortical root cells of *Medicago truncatula*. *Plant Journal* **69**, 822-830.
- Sieberer, B.J., Chabaud, M., Timmers, A.C., Monin, A., Fournier, J., and Barker, D.G.** (2009). A nuclear-targeted cameleon demonstrates intranuclear Ca<sup>2+</sup> spiking in *Medicago truncatula* root hairs in response to rhizobial nodulation factors. *Plant Physiology* **151**, 1197-1206.

## REFERENCES

---

- Smil, V.** (1997). Global population and the nitrogen cycle. *Anglais* **277**, 6.
- Smith, S.E., and Gianinazzi-Pearson, V.** (1988). Physiological interactions between symbionts in vesicular-arbuscular mycorrhizal plants. *Annu Rev Plant Physiol Plant Mol Biol* **39**, 221-244.
- Smith, S.E., and Read, D.J.** (2008). Mycorrhizal Symbiosis. (London: Academic Press).
- Smith, S.E., Smith, F.A., and Jakobsen, I.** (2003). Mycorrhizal fungi can dominate phosphate supply to plants irrespective of growth responses. *Plant Physiology* **133**, 16-20.
- Smith, S.E., Jakobsen, I., Gronlund, M., and Smith, F.A.** (2011). Roles of arbuscular mycorrhizas in plant phosphorus nutrition: interactions between pathways of phosphorus uptake in arbuscular mycorrhizal roots have important implications for understanding and manipulating plant phosphorus acquisition. *Plant Physiology* **156**, 1050-1057.
- Sokolski, S., Dalpé, Y., Séguin, S., Khasa, D., Lévesque, C.A., and Piché, Y.** (2010). Conspecificity of DAOM 197198, the model arbuscular mycorrhizal fungus, with *Glomus irregularis*: molecular evidence with three protein-encoding genes. *Botany* **88**, 829-838.
- Sprent, J.I.** (2007). Evolving ideas of legume evolution and diversity: a taxonomic perspective on the occurrence of nodulation. *New Phytologist* **174**, 11-25.
- Stamatakis, A.** (2006). RAxML-VI-HPC: maximum likelihood-based phylogenetic analyses with thousands of taxa and mixed models. *Bioinformatics* **22**, 2688-2690.
- Stamatakis, A., Hoover, P., and Rougemont, J.** (2008). A rapid bootstrap algorithm for the RAxML Web servers. *Syst Biol* **57**, 758-771.
- Stockinger, H., Walker, C., and Schüßler, A.** (2009). '*Glomus intraradices* DAOM197198', a model fungus in arbuscular mycorrhiza research, is not *Glomus intraradices*. *New Phytologist* **183**, 1176-1187.
- Stougaard, J., Abildsten, D., and Marcker, K.A.** (1987). The *Agrobacterium rhizogenes* pRi TL-DNA segment as a gene vector system for transformation of plants. *Molecular and General Genetics MGG* **207**, 251-255.
- Stracke, S., Kistner, C., Yoshida, S., Mulder, L., Sato, S., Kaneko, T., Tabata, S., Sandal, N., Stougaard, J., Szczęglowski, K., and Parniske, M.** (2002). A plant receptor-like kinase required for both bacterial and fungal symbiosis. *Nature* **417**, 959-962.
- Sunkar, R., Kaplan, B., Bouche, N., Arazi, T., Dolev, D., Talke, I.N., Maathuis, F.J., Sanders, D., Bouchez, D., and Fromm, H.** (2000). Expression of a truncated tobacco *NtCBP4* channel in transgenic plants and disruption of the homologous *Arabidopsis CNGC1* gene confer Pb<sup>2+</sup> tolerance. *Plant Journal* **24**, 533-542.
- Swarbreck, D., Wilks, C., Lamesch, P., Berardini, T.Z., Garcia-Hernandez, M., Foerster, H., Li, D., Meyer, T., Muller, R., Ploetz, L., Radenbaugh, A., Singh, S., Swing, V., Tissier, C., Zhang, P., and Huala, E.** (2008). The Arabidopsis Information Resource (TAIR): gene structure and function annotation. *Nucleic Acids Res* **36**, D1009-1014.
- Swensen, S.M.** (1996). The evolution of actinorhizal symbioses: Evidence for multiple origins of the symbiotic association. *American Journal of Botany* **83**, 1503-1512.
- Szczęglowski, K., and Amyot, L.** (2003). Symbiosis, inventiveness by recruitment? *Plant Physiology* **131**, 935-940.
- Tadege, M., Wen, J., He, J., Tu, H., Kwak, Y., Eschstruth, A., Cayrel, A., Endre, G., Zhao, P.X., Chabaud, M., Ratet, P., and Mysore, K.S.** (2008). Large-scale insertional mutagenesis using the *Tnt1* retrotransposon in the model legume *Medicago truncatula*. *Plant Journal* **54**, 335-347.

- Takeda, N., Maekawa, T., and Hayashi, M.** (2012). Nuclear-localized and deregulated calcium- and calmodulin-dependent protein kinase activates rhizobial and mycorrhizal responses in *Lotus japonicus*. *Plant Cell* **24**, 810-822.
- Takeda, N., Sato, S., Asamizu, E., Tabata, S., and Parniske, M.** (2009). Apoplastic plant subtilases support arbuscular mycorrhiza development in *Lotus japonicus*. *Plant Journal* **58**, 766-777.
- Takeda, N., Haage, K., Sato, S., Tabata, S., and Parniske, M.** (2011). Activation of a *Lotus japonicus* subtilase gene during arbuscular mycorrhiza is dependent on the common symbiosis genes and two cis-active promoter regions. *Molecular Plant-Microbe Interactions* **24**, 662-670.
- Talke, I.N., Blaudez, D., Maathuis, F.J., and Sanders, D.** (2003). CNGCs: prime targets of plant cyclic nucleotide signalling? *Trends Plant Sci* **8**, 286-293.
- Tamasloukht, M., Sejalon-Delmas, N., Kluever, A., Jauneau, A., Roux, C., Becard, G., and Franken, P.** (2003). Root factors induce mitochondrial-related gene expression and fungal respiration during the developmental switch from symbiosis to presymbiosis in the arbuscular mycorrhizal fungus *Gigaspora rosea*. *Plant Physiology* **131**, 1468-1478.
- Teillet, A., Garcia, J., de Billy, F., Gherardi, M., Huguet, T., Barker, D.G., de Carvalho-Niebel, F., and Journet, E.P.** (2008). *api*, A novel *Medicago truncatula* symbiotic mutant impaired in nodule primordium invasion. *Molecular Plant-Microbe Interactions* **21**, 535-546.
- Timmers, A.C., Auriac, M.C., and Truchet, G.** (1999). Refined analysis of early symbiotic steps of the *Rhizobium-Medicago* interaction in relationship with microtubular cytoskeleton rearrangements. *Development* **126**, 3617-3628.
- Tirichine, L., Imaizumi-Anraku, H., Yoshida, S., Murakami, Y., Madsen, L.H., Miwa, H., Nakagawa, T., Sandal, N., Albrektsen, A.S., Kawaguchi, M., Downie, A., Sato, S., Tabata, S., Kouchi, H., Parniske, M., Kawasaki, S., and Stougaard, J.** (2006). Deregulation of a Ca<sup>2+</sup>/calmodulin-dependent kinase leads to spontaneous nodule development. *Nature* **441**, 1153-1156.
- Torrey, J.G.** (1978). Nitrogen fixation by Actinomycete-nodulated angiosperms. *BioScience* **28**, 586-592.
- Towler, D.A., Gordon, J.I., Adams, S.P., and Glaser, L.** (1988). The biology and enzymology of eukaryotic protein acylation. *Annu Rev Biochem* **57**, 69-99.
- Trappe, J.M.** (2005). A.B. Frank and mycorrhizae: the challenge to evolutionary and ecologic theory. *Mycorrhiza* **15**, 277-281.
- Tuskan, G.A., Difazio, S., Jansson, S., Bohlmann, J., Grigoriev, I., Hellsten, U., Putnam, N., Ralph, S., Rombauts, S., Salamov, A., Schein, J., Sterck, L., Aerts, A., Bhalerao, R.R., Bhalerao, R.P., Blaudez, D., Boerjan, W., Brun, A., Brunner, A., et al.** (2006). The genome of black cottonwood, *Populus trichocarpa* (Torr. & Gray). *Science* **313**, 1596-1604.
- Udvardi, M.K., and Day, D.A.** (1997). Metabolite transport across symbiotic membranes of legume nodules. *Annu Rev Plant Physiol Plant Mol Biol* **48**, 493-523.
- Umehara, M., Hanada, A., Yoshida, S., Akiyama, K., Arite, T., Takeda-Kamiya, N., Magome, H., Kamiya, Y., Shirasu, K., Yoneyama, K., Kyozuka, J., and Yamaguchi, S.** (2008). Inhibition of shoot branching by new terpenoid plant hormones. *Nature* **455**, 195-200.
- Untergasser, A., Nijveen, H., Rao, X., Bisseling, T., Geurts, R., and Leunissen, J.A.** (2007). Primer3Plus, an enhanced web interface to Primer3. *Nucleic Acids Res* **35**, W71-74.

REFERENCES

---

- van der Heijden, M.G.A., Klironomos, J.N., Ursic, M., Moutoglis, P., Streitwolf-Engel, R., Boller, T., Wiemken, A., and Sanders, I.R.** (1998). Mycorrhizal fungal diversity determines plant biodiversity, ecosystem variability and productivity. *Nature* **396**, 69-72.
- Vance, C.P.** (2001). Symbiotic nitrogen fixation and phosphorus acquisition. Plant nutrition in a world of declining renewable resources. *Plant Physiology* **127**, 390-397.
- Varnum, M.D., and Zagotta, W.N.** (1996). Subunit interactions in the activation of cyclic nucleotide-gated ion channels. *Biophys J* **70**, 2667-2679.
- Verma, D.** (1992). Signals in root nodule organogenesis and endocytosis of *Rhizobium*. *Plant Cell* **4**, 373-382.
- Vierheilig, H., Coughlan, A.P., Wyss, U., and Piche, Y.** (1998). Ink and vinegar, a simple staining technique for arbuscular-mycorrhizal fungi. *Appl Environ Microbiol* **64**, 5004-5007.
- Wang, B.B., O'Toole, M., Brendel, V., and Young, N.D.** (2008). Cross-species EST alignments reveal novel and conserved alternative splicing events in legumes. *BMC Plant Biol* **8**, 17.
- Waterhouse, A.M., Procter, J.B., Martin, D.M., Clamp, M., and Barton, G.J.** (2009). Jalview Version 2-a multiple sequence alignment editor and analysis workbench. *Bioinformatics* **25**, 1189-1191.
- Wegel, E., Schäuser, L., Sandal, N., Stougaard, J., and Parniske, M.** (1998). Mycorrhiza mutants of *Lotus japonicus* define genetically independent steps during symbiotic infection. *Molecular Plant-Microbe Interactions* **11**, 933-936.
- Wernimont, A.K., Artz, J.D., Finerty, P., Jr., Lin, Y.H., Amani, M., Allali-Hassani, A., Senisterra, G., Vedadi, M., Tempel, W., Mackenzie, F., Chau, I., Lourido, S., Sibley, L.D., and Hui, R.** (2010). Structures of apicomplexan calcium-dependent protein kinases reveal mechanism of activation by calcium. *Nat Struct Mol Biol* **17**, 596-601.
- Wilkinson, D.M.** (2001). At cross purposes. *Nature* **412**, 485.
- Xie, X., and Yoneyama, K.** (2010). The strigolactone story. *Annu Rev Phytopathol* **48**, 93-117.
- Yano, K., Yoshida, S., Müller, J., Singh, S., Banba, M., Vickers, K., Markmann, K., White, C., Schuller, B., Sato, S., Asamizu, E., Tabata, S., Murooka, Y., Perry, J., Wang, T.L., Kawaguchi, M., Imaizumi-Anraku, H., Hayashi, M., and Parniske, M.** (2008). CYCLOPS, a mediator of symbiotic intracellular accommodation. *Proc Natl Acad Sci USA* **105**, 20540-20545.
- Yendrek, C.R., Lee, Y.C., Morris, V., Liang, Y., Pislaru, C.I., Burkart, G., Meckfessel, M.H., Salehin, M., Kessler, H., Wessler, H., Lloyd, M., Lutton, H., Teillet, A., Sherrier, D.J., Journet, E.P., Harris, J.M., and Dickstein, R.** (2010). A putative transporter is essential for integrating nutrient and hormone signaling with lateral root growth and nodule development in *Medicago truncatula*. *Plant Journal* **62**, 100-112.
- Yokota, K., Fukai, E., Madsen, L.H., Jurkiewicz, A., Rueda, P., Radutoiu, S., Held, M., Hossain, M.S., Szczyglowski, K., Morieri, G., Oldroyd, G.E., Downie, J.A., Nielsen, M.W., Rusek, A.M., Sato, S., Tabata, S., James, E.K., Oyaizu, H., Sandal, N., et al.** (2009). Rearrangement of actin cytoskeleton mediates invasion of *Lotus japonicus* roots by *Mesorhizobium loti*. *Plant Cell* **21**, 267-284.
- Yoshioka, K., Moeder, W., Kang, H.G., Kachroo, P., Masmoudi, K., Berkowitz, G., and Klessig, D.F.** (2006). The chimeric *Arabidopsis* CYCLIC NUCLEOTIDE-GATED ION CHANNEL11/12 activates multiple pathogen resistance responses. *Plant Cell* **18**, 747-763.
- Young, J.P., and Johnston, A.W.** (1989). The evolution of specificity in the legume-rhizobium symbiosis. *Trends Ecol Evol* **4**, 341-349.

## REFERENCES

---

- Yu, I.C., Parker, J., and Bent, A.F.** (1998). Gene-for-gene disease resistance without the hypersensitive response in *Arabidopsis dnd1* mutant. *Proc Natl Acad Sci USA* **95**, 7819-7824.
- Zhang, Q., Blaylock, L.A., and Harrison, M.J.** (2010). Two *Medicago truncatula* half-ABC transporters are essential for arbuscule development in arbuscular mycorrhizal symbiosis. *Plant Cell* **22**, 1483-1497.
- Zhao, Y., Pokutta, S., Maurer, P., Lindt, M., Franklin, R.M., and Kappes, B.** (1994). Calcium-binding properties of a calcium-dependent protein kinase from *Plasmodium falciparum* and the significance of individual calcium-binding sites for kinase activation. *Biochemistry* **33**, 3714-3721.
- Zhu, H., Kim, D.J., Baek, J.M., Choi, H.K., Ellis, L.C., Küster, H., McCombie, W.R., Peng, H.M., and Cook, D.R.** (2003). Syntenic relationships between *Medicago truncatula* and *Arabidopsis* reveal extensive divergence of genome organization. *Plant Physiology* **131**, 1018-1026.

## 8 Abbreviations

°C	Degree(s) Celsius
A	Adenine
AFLP	Amplified Fragment Length Polymorphism
AM	Arbuscular Mycorrhiza
BC	Backcross
BLAST	Basic Local Alignment Search Tool
bp	nucleic acid base pair(s)
C	Cytosine
ca.	circa
Ca <sup>2+</sup>	Calcium
CCamK	Calcium/Calmodulin-dependent Protein Kinase
cDNA	complementary DNA
CFP	Cyan Fluorescent Protein
cm	centimetre
CNGC	Cyclic Nucleotide-Gated Channel
CPK	Calcium-dependent Protein Kinase
CTAB	Cetyltrimethylammonium bromide
dCAPS	derived Cleaved Amplified Polymorphic Sequence
DNA	Desoxyribonucleic acid
dNTPs	desoxynucleotides
dpi	days post infection
<i>DsRed</i>	<i>Discosoma striata</i> sp. Red Fluorescent Protein
EDTA	Ethylenediaminetetraacetic acid
EMS	Ethyl-Methanesulfonate
G	Guanine
g/l	gram per litre
GUS	β-glucuronidase
h	hour(s)
IT	Infection Thread
kb	kilobase(s)
LRR	Leucine-Rich Repeat
min	minute(s)
ml	millilitre(s)
mm	millimetre(s)
mRNA	messenger RNA
MYA	Million Years Ago
n	number of tested individuals or specimens
NF	Nod Factor

---

## ABBREVIATIONS

---

NFR	Nod Factor Receptor
ng	nanogram
nm	nanometre(s)
NUP	Nucleoporin
OD <sub>600</sub>	Optical Density at a wavelength of 600 nm
PCR	Polymerase Chain Reaction
PK	Protein Kinase
PPA	Prepenetration Apparatus
PVP	Polyvinylpyrrolidone
q-RT-PCR	quanitative RT-PCR
RACE	Rapid Amplification of cDNA Ends
RFP	Red Fluorescing Protein
RNA	Ribonucleic Acid
RNAi	RNA interference
RNS	Root Nodule Symbiosis
rpm	rounds per minute
RT-PCR	Reverse Transcription of RNA
SD	Standard Deviation
SDS	Sodium Dodecyl Sulfate
sec	seconds
SNP	Single Nucleotide Polymorphism
SSR	Simple Sequence Repeat
SYMRK	Symbiosis Receptor-like Kinase
T	Thymine
TILLING	Targeted Induced Local Lesions in Genomes
TM	Transmembrane Domain
UTR	Untranslated Region
UV	Ultra-Violet
w/v	weight per volume
wpi	weeks post infection
wt	wild type
YFP	Yellow Fluorescent Protein
μl	microliter(s)
μm	micrometre
μM	micromolar

## 9 Appendix

### 9.1 Sequence Information of Genes Annotated in This Study

#### 9.1.1 CPK Sequences

##### *L. japonicus* CPK29 Genomic Sequence

ACAATGTATATATGATATATAGGTCTTCAAATGTTGAAGGCAGAGCATATAGAGAAAATTCAAGTTGGTAGCTGAAATTAAAC  
 CAAATCAAACAAATGGGATTGGGGTTGTCAGGCCATTTCAGTGTACAGCTCTCAAGAAATTGAAATTGTCCTCAGATTGCTCTC  
 CTCCCTCGGAAACAACTAGGAAAACCCAACAACAAATGCCAACGTCATCATCTCCTCTCGTCCCAGATATGTGTCACCAAC  
 TTGGACCAATTCTAGGGAAACCGTCTGGTGTATAACTCAGTTGATGAAATGAAGAAAGAACCTGGGAGGGTCAATCTGGTGTCA  
 ATATCTATGTGTCATAAGGACACGAGGAAAGAGTATGCATGCAAGTCATTGCAAGGGCAAACAAACATAGTGAATTCAAGGAGATG  
 TTAGAAGAGAGGTATGATTCTCAGCACCTTCAGGCAACCAAAACATAGTGAATTCAAGGAGATGGACACTAGGAACTAAGTACTA  
 AAATAGGGCGTCCGCCACCGCGCTAATAAAATAGTATTCAAATGTTGATTAAATGTTGATTACTTCAAATTTCTGGTCCGTC  
 TCTTAATGATGCAAGGGAGCTTATGAGGACAGGCAACGTGCACTTGTGATGGAGTTGTCAGCGGGGTGAACTGTTGATCGATC  
 ATTGAGAAGGAAACTCTGGAGCTGAAGCAGAACAGTGTAGGAGCATAGTGAATTGTCATGCAATTGCAATTGCAATTGGGTG  
 ATGCATAGAGACCTGAAGGCCAGAGAATTCTTGTGTCAGGCCACCAAGGACGAGAATGCTGAGCTGACTGATTGGACTATCTT  
 TTCATTGAAGAGTCATTACTTAATTCTCTGCTTCTATTGCTACATCTTGTGCTTCTATATCTCTTCCATTCTATAACTGCTTT  
 TTCTATTATTCTCCCTGAAATTCAATTAACTTGCAATGCACTGTATCATCTCTTCAATTCTATAACTGCTTTATCATG  
 AATTAGATTACAGAAGTCATATTAAACCTTAACATATAAAATTAAATTAAAGCGCAGCTCTTAAACATTACACATATTAAAGAA  
 AACATGTATCTCATTCTCATATTAAAGGTGGACAATTACGCATATTAAAGTTATTGCTATTCTACAGAATTATGTTGGACAAAGG  
 GTAATAAGAATTGGTTTAAATTACGATTTCATATTCTCTCCCTCAAATAATAACGAGAACTCTTCTTGCAGTAGAA  
 GCACAAACCTTCTCACTGTCTAGCAAAGCGTACTGATGCAAAAGGGTGAATTGCTTCTTGCCTGAGGACCATCAACC  
 CAAAAGAAAGCATAAAATTAAAGTGAATTGCAATATAAATAATAGAACCTCTTCTTACACTCTCTAAAGCTGAATT  
 TCATATAGATAAAATTACATCAATTCTCAGAACACACTAACATTAATTCTTCTCGATATGGACACTGCTTCAAGCAA  
 TCCCACGACCACGACAACAGAGTACCTATCTCCTATGAATATGATTCCCCACACCTCACACCACCAACTGCCACAAAGAAC  
 CAACAACAACCTCGACCTCAACCTCAACCTCAACCTCGTACCGTGTACAAACTCAGACCCAACCTCATCTGCTCATCAT  
 TCATCTAGTAAAAACCAAACTAGACAAACCATACATTGACGTGAACTCTCTACACTTTGGCAAGGAATTGGAAAGGGGACA  
 GGTGTCATTCTCTGGCTGAGAAACCAACTGGACGCAATTGCTGTAATCCATTCCAAGGAAAGCTAACTAGAAAGGAG  
 ATTCAAGGATGTTAAGGGAAATTCAATTGATCTCGCAGCATACAGGAAACCAACACATTGAGTTCAAGGGTCTTATGAGG  
 CAGAGCGTCAATTGGTGTGAGCTTGTGTTATGGTGTGAGCTTTTGATAGGATACCCCAAGGGTAGTACTCTGAGCGTAA  
 GCTTCCACATTCAAGGAAATTGTGAATTGTTGATCTGCTGCTTGTGATTTATGGGGTAGTGCATAGGGACCTCAAGCCAG  
 AGAATTCTGAGGTTAAGGGACTTAAAGGACCTTGAAAGCCACGATTGTTGATCTCTTGTGATGAGGTTAGAGTATATT  
 ATGATTAAACCTTAAAGGATGATAAGGCACTTGTGTTCTTTTCAATTGTTAGTAAAGTATTCTAAACATTGCTTCA  
 CCAACTTGAAGGAAAGAAAATTGAGCTAAGGGCTCAGCATGGGAAACTTAATTGCTGACCAAAACTATTGAGTTAAA  
 GTTATTAAAGCTGAGTTATTGAGAAGAATACATCTATGTTGATCTTGTGACCATGCAAAAGTGGATGTTAGC  
 AAAAGTGGTTAATTAGCTGACCTTAAACTTAATTAGTTAGTAAAGCTGAGTTGATGAAACTAAATTATGTT  
 GATACTTGTGGCACTCATATAATGAATGTTAGCACTTGTGAGATAAGAAGTGAACGAAACTCATGTATGA  
 ATTGATGAAATTCTTACACTTAACGGTATTCAAAACATAGGAGTCTACATTGTGGATCACATTGACCAAGTC  
 AAACATGGAGTCAGCAAGAACGATCTTATGTGATAATGACAAGTCACCGAGTCCTCATTATAAAAGAGCA  
 AGGAGCATAGGCTAATTAGTGTCTGGAGCGCAGGAATCATTGAAACCTACAAATTAGTGGACCCACATAAAGTA  
 ACACGAAACACTCTGCTTCTCTCTTGTGATAGTGTGAACTTGTGTTGAAATTGCTGTAATTGCAACCTT  
 AACCGAAAAGGATATTGAGCTTGTGAAAGCTAAGCTGTTGATCTGGAGAGCGCACCATGGCCTCTATT  
 TGTGCTTGTGAAAGGAGGAGGAGGAGGAGGAGGAGGAGGAGGAGGAGGAGGAGGAGGAGGAGGAGGAG  
 TTTGATCAGAAAAATTGAGCTTGTGACTTGTGATGTTGTTGTTGTTGTTGTTGTTGTTGTTGTTGTTGTT  
 CCATGCTTACCATGAAGCTGTGCCCTACAGAACAACTTGTGTTGTTGTTGTTGTTGTTGTTGTTGTTGTTGTT  
 ATGGATGAAGGAAGGTGGTGAAGCATCTGACAAAGCTCTAGACAATGCTGTTAATTAGGATGAAACAG  
 GAAGAAACTTGCCTTAAAGGTAACCTCAAGACTTTCAAGTGTGTTCAATGATGAAGAGAGCAC  
 ATCTTTCTAGTGTGACTTGTGATGTTTGTGTTGTTGTTGTTGTTGTTGTTGTTGTTGTTGTTGTTGTT  
 ATGTTCAACACACATGGCAACTGATGCCAGTGGCACAATGACATGAAAGAATTCAAGGAAACCTG  
 GAATCTGAAATAAAACAGCTAATGGCAGCTGTAAGCTCAGTTGCTCAAAGATTAGTGTGAAATT  
 CAAGAATAAAATGAACTTAATGCTTTGTTGATTACTCATATGTTGTTGTTGAGCTGATGTTG  
 GAATTTATTACTGCCACTATAAATGGCATAAAACTGAAAAGGAAGAGAAATTGTTCAAGGCTT  
 GACAAGGATAACAGC  
 GGGTAAGTAAAAGTGTCAATAGCATTAATCAGAACACTTATTGACAGTATTGAGCTGACTG  
 ATCTCTTTAAATTGAGTTCTTGTGTTCTGCTTACCTGAGTGTCTGTTGGCCTACATTCTCAG  
 TTGAGACATGCTTGTGACTGAAATATCACCTGGGAGAGTGAAGCGGCTATAGATGAGCTG  
 TAGTTTACGGATGTTGCTTCTTATCAATATGTTGTTGTTGTTGTTGTTGTTGTTGTTGTTG  
 CGCTTCACTGCAAGGAGGAGGAGGAGGAGGAGGAGGAGGAGGAGGAGGAGGAGGAGGAG  
 ACCACGATAATGGTGTGAGTATTGAGAAAAGGAAACAGAGCGTTCTGGATTGTTCTGCTGTT  
 TGACTTGTGAGTACTCTGTAATTCAAGGGCACTGGAAATGCAAAACTTGTATACCTGTTG  
 GATAAATTAAAGTAAATTCCAGAT

*L. japonicus CPK29a Coding Sequence*

ATGGGATTGGGTTGTTCAAGCGTTATTTGCTGTAGCACGCTCAAGAAATTGAAATTGTCCTCAGATTGTCCTCCCTCGAAA  
 CAATCTAGGAAACCAACAACAAATGCCAAGTCATCATCTCCTCTGTCAGATATGTCCTCAACCTCACAAGTTGGACCAATT  
 CTAGGGAAACCGTTGTTGATAACTCAGTTGATGAAATGAAGAAAAGTCACTGGGAGAGGTCAATCTGGTGTACATATCTATGTGC  
 GATAAGACACAGAGGAAGAGTATGCATGCAAGTCCATTGCGAGGGCAAACACTCTGAGCCAGCAAGAGATTGAGGATTTAGAAGAG  
 GTCATGATTCTTCAGCAGCTTCAAGGCAACCAAACATAGTGGAAATTCAAGGGAGCTTATGAGGACAGGCAGAACGTGACCTTGATG  
 GAGTTGTGAGCGGGGGTGAACCTGTTGATCGGATCATGGGAGAAAGGGAAACTACTCGGAGCGTAAGCAGCAACAGTGATGAGGAG  
 GTGAATGTGTTACATATGCAATTGTCATGGGAGTGCATAGACAGCTGAAGCCAGAGAATTCTGGTGGCCACCAAGGAG  
 GCTGAGTCAGCTAACAGTACTGATTGGACTATCTCTTTCATTGAAGAAGGTAAGTGATAGAGAATTGTTGGAAAGTCCACTATG  
 GCTCCAGAGGTGTTAAACCGGAACTATGAAAGGAGATAGATGTCAGGCGAGGAATCATTTATACATCCTCTCAGTGGGGTGCCT  
 CCATTGTTGGCTGAAACCGAAAAGGCATATTGAAAGCTATTGGAAGCTAAGCTTGTGATCGGAGAGCGCACCAGGCCCTTATTC  
 GCTGTTGCAAAAGATTGATCAGAAAATGTCAGCTTATGACCCAAGACGCTTCAAGGAGCTTCAAGCCCTTGAAACATCCATGGATG  
 AAGGAAGGGTGTGAAGCATTGACAAGCCTCTAGAACATGCTGTTAATTAGGATGAAAGCAGTGCAGAGCAATGAACAGATGAAGAAA  
 CTTGCTTAAAGGTAATGAGCAGAAAACCTGTCAGAGGAGGAATCAAGGGTTGAAACAAATTGTCACAAACATGGACACTGATCGAGT  
 GGCACAATCATGAAAGAACTAAATCTGGATTGCAAACTGGATCAAAGCTTAGTGAAATCTGAAACAAACAGCTAATGGACGCT  
 GCTGATGTTGACAAGAGTGGAACTATTGACTATCAGAATTATTACTGCCACTATAAACCGCATAAACTGAAAAGGAAGAGAATTG  
 TTCAAGGCTTTCAATACTTGTGACAAGGATAACAGCGTTATATAACAAGAGATGAACATTAGACATGTTGACTGAATATCACCTGGG  
 GATGAAGCGGTATAGATGAAGTCATGATGATGAGCAGTACAATGATGAGGATTAATTACCAAGGAGTTGTAGCTATGAG  
 AAGGGGACACTGTGATGAGAAGAGAAACACGATAA

*L. japonicus CPK29b Coding Sequence*

ATGGGACACTGCTTCAGCAAATCCCACGACCACGACAACAGAGTACCTATCCTCTATGAAATTGATTCCCCACCCACCTCACCACAC  
 CAACTGCCAACAAAAGAACCAAACAAACAAACACCTCGACCTCAACCTCAACCTCGTTACCGTCTACAAACTCGACACCAACTTC  
 TCATTGCTCATCATCATTATCATCTAGTGGAAAACCAACTAGACAAACCATACATTGAGTCAGCTAACACTCTCTACACTTTG  
 GAACTTGGAAAGGGACAATTGCTGCACTTATCTCGTCAGGAAATCCACTGGACGCAATTGCTGTAATCCATTCCAAAGCG  
 AAGCTAAGTAAAGAAGGAGATTCAAGGATGTTAAGAGGAAATCATGATCTGAGCATCTAACAGGACAACCCACATCGTGA  
 AAGGGTCTTATGAGGACCCGGCAGAGCGTGCATTGGTGTGATGGAGTTGTTATGGTGGTGAAGCTTTGATAGGATCACCGCAAAGGGT  
 AGTTACTCTGAGCGTGAAGCTGCTTCACATTGAGGAAATTGTAATGTTGATGGTGTGATGTTGCTATTGATGGGGTGTGATGC  
 AGTGGCAGGAAATTCTTCTGAGGATGAAAGGACCTTGGGACCTTGGGAAAGCCACCTGGGATTTGGATTGTCGCTTCATTG  
 GGTAAGGTATAGAGAATTGTTGAGTCATATGTCAGGAGGTTAAACCGGAACTATGGAAGGAGATAGATGTG  
 AGCAGGAAATCATTTTACATCCTCTCAGTGGGTGCTCATTGGCTGCTGAAACCGAAAAGGCAATTGAGCTATTGAA  
 GCTAAGCTGATCTGGAGAGCGCACCAGGCTTCTATTGAGCTGTTGCAAAAGATTGATCAGAAAAATTGTTGACTATTGAC  
 AAACGCATTTCAGCTCTGAAAGCCCTGAAACATCCATGGATGAGGAAGGTTGGAAGCATCTGACAAGCCTCTAGACAATG  
 ATTAGGATGAAACAGTTCAGAGCAATGAAAGAACTTGCCTTAAAGGTAATGAGGAAACCTGTCAGAGGAGGAAATCAAG  
 GGGTGAACAAATGTTCAACACATGGACACTGTCAGTGGCAGGAACTACATGAGGAAACTAAAATCTGGATTGTC  
 TCAAAGCTTAGTGAATCTGAAATAAACAGCTAATGGACGCTGATGTTGACAAGAGTGGAACTATTGACTATCAGAATT  
 GCCACTATAAACCGCATAAACTGAAAGGAAGAGAATTGTTCAAGGCTTTCAACTTGACAAGGATAACAGCGGTATATAACA  
 AGAGATGAACCTAGACATGTTGACTGAATATCACCTGGGAGATGAAGCGGTATAGATGAAGTCATGATGATG  
 ATGAGGATTAATTACCAAGGAGTTGTAGCTATGAGAAGAGGACACTTGTGATGAGAAGAGAAACACGATAA

*L. japonicus CPK29a Protein Sequence*

MGLGLFKALFCSTSQEIEIVSSDSSPPRKQRKTQQQMPSPSSPSRPRYVSPSQPSQVGPILGKPFVVITOLYEMKKELGRGQSGVTYLCV  
 DKTTRKEYACKSIARAKLLSQEIEDVRREVMILQHLSQPNIVEFRGAYEDRQNVLHVMELCSGGELFDRRIEKGNYSEREATVMRQI  
 VNVVHICNFMGVMHRDLKPENLLATKDENAALKATDFGLSLFIEKGKVYREIVGSPYYVAPEVLKRNYKEIDVWSAGIILYILLSGVP  
 PFWAETEKIGFEIALEAKLDLESAPWPSISAVAKDLIRKMLTYDPKKRISASEALEHPWMKEGGEASDKPLDNAVLIRMKQFRAMNKMK  
 LALKVIAENLSEEIKGKQMFNNMDTDRGSTITYEELKSGLSKLGSKLSESEIKQLMDAADVDKSGTIDYHEFITATINRHKEE  
 ENLFKAQYFDKDNSGYITRDELHALTEYHLGDEAAIDEVIDDVDTNDGRINYQEFVAMMRKGTLHDKEKPR

*L. japonicus CPK29b Protein Sequence*

MGHFSKSHDHNRVPISYEYDSPPPHHHQLPQRTQQQPRPQPQPRYRATNSDPTSSFASSLSSSEKPILDKPYIDVNSLYTFG  
 ELGRGQFGVYTLCKVEKSTGRKFAKSIPKRKLTRKEIQDVKREIMILQHLTGQPNIVEFKGAYEDRQSVHLMELCYGGELFDRITAKG  
 SYSEREAASTFRQIVNVVHACHFMGVHMRLDKPENFLMVKDDKAPLKATDFGLSVFIEKGKVYREIVGSPYYVAPEVLKRNYKEIDV  
 W SAGIILYILLSGVPPFWAETEKIGFEIALEAKLDLESAPWPSISAVAKDLIRKMLTYDPKKRISASEALEHPWMKEGGEASDKPLDNA  
 LIRMKQFRAMNKMKLALKVIAENLSEEIKGKQMFNNMDTDRGSTITYEELKSGLSKLGSKLSESEIKQLMDAADVDKSGTIDYHEF  
 ITATINRHKEEENLFKAQYFDKDNSGYITRDELHALTEYHLGDEAAIDEVIDDVDTNDGRINYQEFVAMMRKGTLHDKEKPR

*M. truncatula CPK29 Genomic Sequence*

ATGGGATTAGGATTGTTAAGCGTTTTCTGTTGACTACAAACCGAGACATTCCATTGTCCTCTCGGAGTCCCTCCAGGCAT  
 AGCTCTGGCTATGGCTACAATCAACCAAGTTTGATCCATCTCCAAAACCAAAATCTCATCTCTAGTAATCCACAAATAGGT  
 GCAATTAGGAAACCAACTACGTTGATGAAATACGATATGAGGAAAGAAGTCACTGGAGAGGTCATCAGGGTGTGACATATCTA  
 TGCAAGAGAAAACAACGAGAAGAATATGCTGCAAAATCGATATCAAGAGCAGAAACTATTAGCGAGGAAGAGATAGATGATG  
 AGAGAGGTTATGATTGCAACATCTTGGGGCAACCGAATATAGTGAATTGAGGAGCTTATGAGGATAAACAGAAATGTGATT  
 GTGATGGAGGTTGTAAGGTTGACTTTTGATAGGATTATTGAAAGGAAACTACCGAACGCGAAGCTGACTATTATGAGA  
 CAGATTGTAATGTTGTCATGTCATTGAGGTTATGCACTGTCATTGAGGTTATGCAAGCTGAGAATTCTGCTGCTCAAAGAT  
 GAGAATGCTGCTGTTAAAGCTACTGATTGGACTCTCATTTCCTGAGAAGAAGGTCATTTAGTATTACTTACTTTCTTAAAT  
 TTAATTACTACTTACTCCCATTCTCATATTGCAACTGTTTGTGTTAGTATCTGTTACTCGATTAGTGTGTTAATTCTCC  
 CTCTAGCTGATGTTGGTTAAAGTGAAGTAAAGGAAATATGAGCTATTGTCGCTTATGAGTGAAGTCATTCAAGGGTTGTCATT  
 TAAAGATGCTCATTAGGTTGAGAAGCGTGAATGTTACATATAAACTGTCATTGACCTCAATTCTGAGAACATGCGATGTT  
 ATTTGAGCAGGGCGTCTATGAAAGTAATTCTCATAGATTAGTGAAGTGAAGCTAAAGTCCACTCACAAAATTCTGACTTTGG  
 TGGGCTAAAGGGCTGTAACATGAAACAACTCTGATAATCTCATGGAATAGAAAAGTCAAGAACAGTTCCTGACTGAGCAA

AGCGTACTAATGCAAAAGAAAGGAATTGCTTTATGCTATGTGACTATGTGAGGACCATCCAAACCAAGAAAAAGACAAAGCAT  
 AAATTGAAACTTAATACCATACCAAAATACATAGTTAATTATATACATAAATAATACCCCTCAAGTTATATAACACCCTCAAGT  
 CACAAATCAATCTCCATCAACAAACATCATTCAACATGGGACACTGCTTCACCAAACCCACGACAACAGAGTACCTATCTCTTATGA  
 CTATGGTACTAATTCCCAACCCCCCAGAGAAAATCACCTCGCAACCGCATATGCCACACCATATTGCTGCTAAATCAGACCCGACTTC  
 ATATTCTCCGCTTCATCATCGAATGCGAATGCACTGATCATCATCAACCAATTAGGAAGGCCATACATTGACATGAAGACACTCA  
 TAGTATTGAAAGGAACTAGGGAGGGTCAATTGGTCACTTATCTTGACCGAAAATGCCACTGGAAGAAACTATGCTTGAAGTC  
 CATTTCGAGACGAAAGCTAACAGAAAGAAAGATTGAGGATGTTAAAGGGAAATCATGATCCTCAGGACTTAAGTGGACAACCAAA  
 CATAGTTGAGTCAAGGGTCTTATGAGGATAGAGAGAGTGTGCATTGGTGTAGGGAGTTAGTGGAGCTTCTGATCGGAT  
 CACTGCACGGTCACTGCAAGGGTAGTTACTCTGACGCGTAAGCTGCTTATATTAAACCGAGATTAGTGAATGCTGCTCATGCTTGTCA  
 TTTATGGGGTCTCATGATGGACCTTAAGCCTGAGAATTCTGCTGCTAGTAAAGATCATAAGGCTCCTTGAAGGCCACTGATT  
 TGGATTGCTGTTTATTGAAGAAGTTAGTAGTTAGGGTCACTTATTGATGCTTCTCTTCTAGTTAGTCAAGTCTCAGTCTTGT  
 ATTTCAATTACACATGATTGATTGGATCAATTCTAGTTGTTCTCTTCTAGTTAGTAAAGGATTAAACACA  
 TTACCATTTGTTCAATTGTTGATTCCAATTAGATAAGAAATTAGTGAATAGTATTGAGAAAAACAAACACATTGAGTTAGAC  
 TAAATAAAATTACCAACCAATCAATGTTGCTGCTTGTATATTGGTTTGATATTAGTAAAGACTCAAATCTGAGATGGTGT  
 TCTGTAACCTAATATCAGGTACGCCGCTAGTTAGTGCCTCGCCCTTCTGGCTGACGTTCTGGGCTGTGTTGGTATCTAGTATT  
 GACTTTAGGGAAACAATCATGGACAAAGTGTGACGGTGCCTCATAAATGTCAGGCTACTGTGAATGACCCGTCAGGGTCTAGAGCT  
 AGGATTGACAGTTGATGACTGAGTGTGAGACATAGGGAGGGTAACTGAGCATGATCTAATTAAAGCTTAGACCT  
 ATGGCTAGCATGCTCGGGTGTAGATAAGACTCCTAAGTGTAAAGACCTTACAGGCTAAATTAGGTTGACTAAACAAAGGGATAAGTCAAACCTG  
 TAATTATTGTTAATCATGGGAGAATATATGTTGGGATCATAAGGCTAAATTAGGTTGACTAAACAAAGGGATAAGTCAAACCTG  
 GAAATGTAACGTTTAAAGACATAAGGGTAGAGAGATAACGGTACACTTCACACGATTCTCAAAGACTAATGCCACATCTGAAA  
 TGTTGCTGAGGCAATCACGATAGGAAAATACTAGATTATCCTAACAGGATAACAGCGAACCTTGTGTTAACCTAGGCTTAA  
 TGTTCTAGACTAAACATATGTCACAAGATGTCATTATACAAGGAACTTAAAGGTTAGTGGTCTCCACCATAACAATTAGG  
 ATTAAATCCCCTAAGTTAAAGCTTGTGAAATGAAAAACAGCTTGGTGTGATATGGACCAAGTCAACTGCAATTAGGAAACATT  
 GAGTCAACCAAGTAAACGATCATCATCTGATGATAAGGACAGGTCAACTGAAACGTTTACATTAAAGGTTACATTAAAGGAGGTT  
 AAAAGCAAGGACAAGAACCAAGCACTTAAACGTGAAACCTATAATTCACTGAGGACATCTGTTATATGATTCAAAATTGCA  
 TAGAACTTAAAGAGACATACATATTAAATTGGGATGTTGCTCCACCATAACAATTAGG  
 GTTTTGTGCTTCTGCTTGCATGCAAATGCACATGTCGCTGAAACCATGTTATATCATGCACTGCTTGTGACATATACTC  
 ATATCATGATGCATGGTCACTGTTATGCTTGTGAAACAACTCTACGTAATGTTGATAACATATTGTTGTCATCTGT  
 ATCTCATTTTATATTACAGGTTAAAGTAAAGAGCTTGTGAGGAGTCAACTATGTTGCTCCAGAGGTTAAAACGGAGGTT  
 TGAAAGGAGATTGATATGGAGTGCAGGAATCATTTTATATTCTCTAAGTGGGCTCCTCATTGGGCTGTTAGTAAAGGTT  
 AACACAATGTTAATTCTGTTCTGGTTACACAGATAGTGACATTATTGTTGAAACATTAGGTTAGAAACAAAGGCATATTCAAGC  
 AATTAGGTTAGGTAAGCTGATCTGGAGAGTGCACCTGGCTCTATTGCTGTCGAAAGATTGATCAGGAAATGTTGAGTTA  
 TGACCCCTAAGAACGCTTACAGTCTGATGCCCTGGTAAGTACTTATAGAAACCAATTAAAGGTTGATTAACCTGTTGTTGATGCT  
 AGCATGATCAGCTGTTATTTATGTTGTTGACCAATTTCATCGATAAGGCTCAAGACTCACATTAAAGTGGAGGTT  
 ACATCCATGGATGAGGAAGGGTGTGAGGATCAGACAAGCCTTAGATAATGCTGTTTAATTAGGATGAAACAATTGAGCAATGAA  
 CAAGATGAAAGAACCTCTTTAAAGGTCTTAATAGTAAACATCTGTTAATCAACAAACAGACTAGTGTCTGATCTTCTCATGAA  
 TAATATTATTTCTTATTTTATGGAGGAAATAGCAGAAAACCTTCTAGATGAGGAAATCAAGGGCTGAAACAATGTTCAA  
 CAATATAGATCGATGAGGAAACATCACATGAGAAACTAAACATCTGACTGTCAAATTGGGATCCAAGCTAGTGAATCTGA  
 AATAAAGCAGTAATGGATGCTGAAAGTCAGTCTCCGGCAGTTAGAAATTAGGAAACAGTTGAGGAGAACATTTCGCT  
 ATTTCATGTTGTTTTTATTGACACATTGTTTCACTTTAACAAACTTTGACAATTAAAGGAAATGAAATAACAT  
 GATTTCATGTTGAAATAGAATAAACAAAAAAATTCTCACATCAAACAGACACTAGTGTCTGATCTTCTCATGAA  
 AAAGTATAAAATAAAAGAACTTACATAGTTCTCTAATTGACATGTTGGCTGAGGCTGATGTTGAGAAGAATGGAACATTGACTATCATG  
 AATTCTTAATTGCTCCAAACGGCATAAAACTTGTGAGGGAGAGAATTGTTCAAGGCTTCAATTACTTTGACAAGGATAACAGCG  
 GGTCAGTATTGGCTCTTGTCTTACCTTAACTATGACACACATTGCTGATTAACAAGTAATTGAGTATAAAAGACAGATT  
 TGGCCATAAAATTCACTGATTATGACATTGGCTCTATTCTCAGATTGCTTACCTTAAGTTGTTGGGTGACTGTTAGTT  
 TGTAACAAGAGAGGAACCTAGACAAGCTTGGCTGAATATCAAATGGAGATGAGCAACTATAGATGAGCTATTGATGTTGACAC  
 CGACAATGTATGTCACATATACTATATTGAGTATTGACCTTATAAGTGTCTCTATGTAATTGCTACTTATGGTGAAGCTTC  
 TTATTGCAAGGATGGCAGAATTAAATTACAGGAGTTGCAACTATGATGAGAAAGGGACCTTGGATAATTGACAAAGAGAAACCGCG  
 ATA

### *M. truncatula CPK29a Coding Sequence*

ATGGGATTAGGATTGTTAAGCGTTTCTGTTGACTACAAACCGAGACATTCCATTGTCCTCTCGGAGTCCTCTCCCAGGCAT  
 AGCTCTGGTATGGCTACAATACCAAGTTTGATCCATCTCCAAACCCACAAATCTCATCTTCTCTAGTAATCCACAAATAGGT  
 GCAATTAGTAAACCATACGCTAGTGAATTAAACATATACGATATGAAGAAAGAAGTCCGAAGGGTCACTCAGGTGTGACATATCTA  
 TGCACAGAGAAAACAACGGAAGAGAATATGCTGCAATCGATATCAAGAGCGAAACTATTAGCGAGCAAGAGATAGATGATGTAAGA  
 AGAGAGGTTATGTTGCAACATCTTGGGGCAACCGAATATAGTTGAAATTGAGGTTATGAGGAAAGGAAACTATACGGCAACGCGACT  
 GTGAGTGGAGGTTGTTAAAGGAGACTTGTGAGGTTATGAGGAAAGGAAACTATGAGGTTATGAGGATAAAACAGAATGTTGAGGTT  
 CAGATTGTAATGTTGCTGATGTCATTAGGTTGTTAGGTTGATCTGATCTTCTGCTGAGGTTGAGGTTGAGGTTGAGGTT  
 GAGAATGCTGTTAAAGGTTAAAGGACTGTTGAGGTTATGAGGAAAGGAGATTGAGTATGAGGAGGTTGAGGTTGAGGTTGAGGTT  
 TATGTTGCTCCAGAGGTTGTTAAAGGACTGTTGAGGTTATGAGGAAAGGAGATTGAGTATGAGGAGGTTGAGGTTGAGGTTGAGGTT  
 GTGCTCTTCTGCTGAGGTTGAGGTTGAGGTTGAGGTTGAGGTTGAGGTTGAGGTTGAGGTTGAGGTTGAGGTTGAGGTTGAGGTT  
 ATTTCAGTTGCTGCAAAGATTGATCAGGAAAATGTTGAGTTATGACCTAAGAAACGCAATTACAGCTCTGATGCCCTTGAAACATCCA  
 TGGATGAAGGAAGGTGGTGAAGGATCAGACAAGCCTTAGATAATGCTGTTTAATTAGGATGAAACAATTGAGCAATGAAACAAGATG  
 AAGAAAATCTGTTAAAGGTTAAAGGAGACTGAGGAAACCTTCTAGATGAGGAAATCAAGGGCTTGAAGAAACAAATGTTCAACAAATAGATACCGAT  
 CGAAGTGGCACAATCACATGAGAAACTAAACCTGGACTGTCCTAAATTGGGATCCAAGGTTAGTGAATCTGAATAAAGCAGCTAATG  
 GATGCTGCTGATGTTGACAAGAATGGAACATTGACTATCATGAAATTCTACTGCCACAATAAACCGGCATAAAACTTGAGAGGGAAAGAG  
 AATTGTTCAAGGTTTCAATTGACAAGGATAACAGCGTTATGTAACAAGAGAGGAACCTAGACAAGCTTGGCTGAATATCAA  
 ATGGGAGATGAGCAACTATAGATGAGTCATTGATGATGTTGACACCAGACAATGATGGCAGAATTAAATTACAGGAGTTGCAACTATG  
 ATGAGAAAGGGACCTTGGATAATTGACAAAGAGAAACCGCGATAA

*M. truncatula* CPK29b Coding Sequence

ATGGGACACTCTCACCAACCACACGACAACAGACTACCTATCTTATGACTATGGACTAATTCCCAACCCCCAACGAGAAATCAA  
 CCTCGTCACCGCGATATCCACACCATATTGCTGCTAAATCAGACCGCCTTCATATTCTCCGCTTCATCATCGAATGCGAATGCAAGT  
 GATCATCATCAACCAATATTAGGAAGGCCATACATGAGACATGAAGACACTCTATAGTATTGGAAAGGAACTAGGGAGGGTCAATTGGT  
 GTCACTTATCTTGACCGAAATGCCACTGGAAGAAACTATGCTGTAAGTCCATTGAGACGAAAGCTAACAGAAAGAAATT  
 GAGGATGTTAAAGGGAAATCATGATCCTCAGGACTTAAGTGGACAACCAAACATAGTTGAGTCAGGGTCTTATGAGGATAGAGAG  
 AGTGTGCATTGGTGATGGAGTTAGGTGGTGAGCTTCGATCGGATCACTGCACGGATCACTGCAAAAGGGTAGTTACTCTGAG  
 CGTGAAGCTGCTTCTATATTAAAGCAGATTATGAAATGTTGCTCATGCTTGTCTATTGAGGGTCTGATGAGGGACCTTAAGGCTGAG  
 AATTCTGCTGCTGAGTAAAGCATAAAGGCTCCCTTGAAGGACACTGATTGGGATTCGTTTATTGAAGAAGGTAAGTAT  
 AAAGAGCTTGGAGGAAAGCTGATCATGTTGCTCAGAGGTTAAAAGGAGATTGAGATATGGAGTCAGGAACT  
 ATTTATATATTCTCTAAGTGGGTGCTCCATTGGGCTGAAACCGAAAAGGCATAATTCAAGCAATTAGGTAAGCTGAT  
 CTGGAGAGTGCACCTGGCCTCTATTCAGTTGTCGCAAAAGATTGATCAGGAAATGTTGAGTTATGACCTAAGGAAACGCATTACA  
 GCTTCTGATGCCCTGAACATCATGGATGAAGGAAGGTTGAGGATCAGACAAGCCTTATGAGATAATGCTGTTAATTAGGATGAAA  
 CAATTCAAGGAACTGAACAAGTGAAGAAACTTGCCTTAAAGGTAATAGCAGAAAACCTTCAGATGAGGAAATCAAGGGCTTGAACAA  
 ATGTCACAAATATAGATACCGATCGAACATCATGAGAAACTAAATCTGACTGTCCTAAGGATCCAAGCTTAGT  
 GAATCTGAATAAGCAGCTAATGGATGCTGCTGAGCAGGAAATGGAACATTGACTATCATGAATTACTGCCCACAA  
 CGGCATAAAACTTGAGAGGAAAGGAAATTGTCAGGCTTTCAATCTTGAGGATAACAGCGGTATGTAACAGAGAGGAACT  
 AGACAAGCTTGGCTGAATATCAAATGGGAGATGAAGCAACTATAGATGAAGTCATTGATGATGTTGACACCACAATGATGGCAGAATT  
 ATTACCAAGGAGTTGCAACTATGATGAGAAAGGGACCTGGATAATGATGACAAAGAGAAACCGCGATAA

*M. truncatula* CPK29a Protein Sequence

MGLGLFKAFFCCTNRDIPIVSSSESSPRHSSGYNQPSFDPSPKTTKSPSSSNPQIGAILGPYVVINNIYDMKELGRGQGVTL  
 CTEKTGREYACKSISRAKLSEQEIDDVRREVMLQHLSQPNIVEFRGAYEDKQNVLVMEVKKGELFDRIIEKGNYTEREAATIMR  
 QIVNVVHVCHFMGMVHDLKPENFLASKDENAKVATDFGLSIFLEEKVYKELVGSAYVVAPEVLKRSYKEDIWSAGIILYILLSG  
 VPPFWAEYTEKGIFQAILEGKLDLESAPWPSISVAAKDLIRKMLSYPDKKRITASDALEHPWMKEGGEASDKPLDNAVLIRMKQFRAMNMK  
 KKLALKVIAENLSDEEIKGLKQMFNNIDTRSGTITYEELKSGLSKLGSKLSESEIKQLMDAADVDKNGTIDYHEFITATINRHKLREE  
 NLFKAQYFDKDNGYVTREELRQALAEYQMGDEATIDEVIDDVDTNDGRINYQEFAUTMMRKGLDNDDEKEKPR

*M. truncatula* CPK29b Protein Sequence

MGHCFTKPHDRNRPISYDYGTNSPPTRNQPRPYHIAAKSDPTSYSSASSSNANASDHQPILGPRYIDMKTLYSIGKELGRQFG  
 VTYLCENATGRNYACKSISRRKLTRKEIEDVKEIMILODLSQPNIVEFKGAYEDRESVHLMELCLGELFDRITARITAKGSYSE  
 REAASIFQIMNVVHACHFMGMVHDLKPENFLASKDHKAPLKATDFGLSVFIEEKVYKELVGSAYVVAPEVLKRSYKEDIWSAGI  
 ILYILLSGVPPFWAEYTEKGIFQAILEGKLDLESAPWPSISVAAKDLIRKMLSYPDKKRITASDALEHPWMKEGGEASDKPLDNAVLIRMK  
 QFRAMNKMKLALKVIAENLSDEEIKGLKQMFNNIDTRSGTITYEELKSGLSKLGSKLSESEIKQLMDAADVDKNGTIDYHEFITATIN  
 RHKLEREENLFKAQYFDKDNGYVTREELRQALAEYQMGDEATIDEVIDDVDTNDGRINYQEFAUTMMRKGLDNDDEKEKPR

*G. max* Glyma14g40090 Genomic Sequence

ATGGGACTGGGATGTTAAGGCATTGTTGCTGAGCAAGGCCATGAAATTGACATTGCAAGACTCTGGGACTCATCTCCTGATCAT  
 ACCCCCCAACACATTCTAAACCAAGCCAACGCAATGTCGCACCTACTCATTCCAATAATAACAAACACCACATCTACACAAATA  
 GGAGCAATTCTAGGAAACCACATCGAACATACACAAATGAGATGAAGAAGGAACCTGGGAAGCGGGCAGTCGGTGTAAACAT  
 CTGTTGTTGAGAAGACGACGAAAGCAGAGTATGATGCAATCCATCTCGGTGCAAGCTGCTGAGCACAGCAGGAGATTGAGGATGT  
 AGAAGAGAGGTTATGATTCTGCAGCATCTTCGGGGCAGCCAAACATAGTGGAGTTCAGAGGGGCTTATGAGGACAAGCAGAACGTGCAT  
 CTGGTGATGGACTGTGCACTGGGGCAACTCTGACCGCATCATTGCAAAAGGAAACTACTCCGAGCGTGAAGCTGCCACTGTCATG  
 AGGCAGATGTCATGTTGCTGAGCATTGATGGCTCATGGGCTCATCGACCTCAAGGCCAGAAATTCTTGTGGCCACCAAC  
 CACCCCGATGCAGCGTAAAAGCCACTGATTGGACTCTCCATTTTTATTGGAGGAAGGTTAGTATTCTACATTGATCAAT  
 CTTATTCTCATCTTGCATATTAAAGGGTCAAGATTGGATTGAGCTTAACTGATGTTGTTGGTTAAAAGGTTGAAT  
 TACCTTCAAGAAAAAAACATTGTTCTAAGATTGATTCAACGCACTGATTGCAAGGACATCTTATATCATGTTAGCAAGTT  
 TAATAAGTGTGTCATGTTGAAATATATTGATGGTCACTTATATAGAATTAAAGAGCTTGAATAATAAGTGCAGGGAA  
 AACACGGAGTGCAGAGGACCATCTAACGACAGATTAAATAATTGGACTAAAGGTTGCTCTTCTTCTTACACAATTATAG  
 AGTACAATATATTGACTAGTGTGTCAGGTGACTTACGTGATGTTGACTTGGTACATGAAATCAAATGAAATGTTCTACAGAACCTA  
 TGCATGCACTACAAAAAATTAAAGGTCAATGTTGATAATTGGGTTCTACATTGTTGATGAAATGTTTCTACAGAACCTA  
 AAGTTAAAACCTACTTATATTATAGTTAATTGGGTTCTACATTGTTGATGTTGAGCTTAACTGAGTTATTGGGTTCTAC  
 TATGAGTATTCTAACAGAGGCTAAGTTATGTTGATGTTGAGCTTACAGGCTAACCTCTGTGTTCTACATTGATAGATGAA  
 GTGAATGAAAGCACTCTAGTAGCTTATTGGGTTGACAAGACTTCCGAGTAGCTTATTGGGTTCTTACTCTTAAACTTAATTAA  
 AACCGAAAGTTAATATGTTCATACAAACCTGTCTAACATTCCATGTTCAATAATTGGGTTGAGCTAACATTGGGTTAGTATT  
 TTTAAAAACTATATGATTGGGTTATTGTTCATGGTCAAGGTTGAGCTAACATTGGGTTGAGCTAACATTGGGTTAGTATT  
 ATATATAATTCTGGCTAACATTGGGTTGAGCTAACATTGGGTTGAGCTAACATTGGGTTGAGCTAACATTGGGTTAGTATT  
 TTGCTATTGGACATGTCGGGAGAGAATTACATTAAACGCCCCATAAGGTCACAAACAAATTCTCTAGACACGTAAGTAAACACATA  
 ACAATAATGAACTCATGAAACAACTCGTTCTCTTGGTTAACTGAGTATATAAAAGGTTGAGCTAACATTGGGTTAGTATT  
 TCTCTTGTGTTATTGTTAAGTAAACATTGTTCAATTACAATTGTTGAGTAACTGAGCTAACATTGGGTTAGTATT  
 AGACTCAAGTATTGAAACAACCAATTGAGCAACAACTTATGAAAAAAAGTGGAGGAATGATGCTTTTTGAGTAAGGAGTGGAGGACCA  
 TCCCATCCATATCCAACCAAAGGAAAGCAAGCATAAATTGAAAGCAGCAGCATAGTTAGCTGTTCACAAACTACTCTTT  
 TTTCTTTTTTTTCTCACTGCTCAACTCGACTGAGCTGAGGCTGAAACTATCATATATAAAACCAATTAAACTAATATCTCCAC  
 AAAGAAACATTCTGACATGGGCACTGCTTCAAGCAACCCAGCACAAACGAAACCAACTATGATTATTCAACCCACCCCTCAT  
 CATTATCAGCCACGCCGCACTCACACTCAGACTCAAGGAGAACACAACACTCAACTTCACCTGGTTACCCCAATCGAACT  
 CCAAAATCAGACCCATCTCCATCATCATATTGTTGATCAAGTAGCAGCACGAATATTGACAAACCATACTTGACATCAA  
 CTTTACAACCTCGAGAGGAAACTCGGGAGGGGTCAATTGGGATCACTGTTGACCGAGAAGACCAACGGGAGGAATACGCTG  
 AAGTCCATTCCAAGCGGAAGCTAAGTAAAAAGCATACTGATGATGTCAGAGGAGAAGTCTCATCTTCTGACACCTCTCGGGACAG  
 CCCAACATCGTTGAGTTCAAGGGTCTTATGAGGATGGCAACACGTCATTGGTATGGAGTTGTTGGGTGAGCTCTCGAC  
 CGCATCACTGCAAAAGGGTAGTTACTCGAGAGCTGAGGCTGTTCTATATTCAAGACAAATTGTTAATGTTGTTGTTGTTG  
 GGGGTCTGATGAGGCTTAAGGCTTAAAGCTTCTGCTGCTAATAGGATCTTCAAGGACACCTCTCAAGGCCAGATTGGATTG  
 TCCGTTCTATTGAAAGAAGGTCATCATCATTCTACACGCTTTGCAATTCTTCAATTGTTGAGTTAATGCTTATATAACCA  
 TTATCCTTGAATTATTAAAGTTAAAGTTAAACAAATTATACATTAGATGATGAGCTTAAAGACA

CTATATAACCTTTCCCTTATTTCATTATCTGGGTTCAAGTCTGATTGCTCTTCTTTCTTTAATTTCCT  
 CTTTAGAAAAAGATTGAAACGTTGCCGTCTAAACAGATTGTTGGATCCAACCTTAGATTAAGCACTGACTAAAAGAATGAT  
 AATGTATAGTATAATAAAAGAAAACTAGGTAGCTCAGCATGGATGACTTAATTAGCTACGTTGCCGAATATAATTGAGTTGAATTA  
 TAGTTGGATGAAGACTGAGTCATTGTTATTGAGACAGCGAGTAAACCATCTTCATATGCTAAAGTCAAGTCAACCG  
 AGTAAACGTTTCCCATATAAAAGGAGCAACAGAGAAAACAGTGCACAGATTGACACTGCCAGTCAAGTCAAGTCAACCG  
 CATAAAATCATGATTCCAATTGACTAGTAGAAGTGTATTTTATTTAAATAACTATTATTGTTGACACCTCTCACTCTAA  
 ATATCTCATTCACACCTACATTTCTGTATTTTTATTTCATCATATTCTACCATTTGTAATTCTCCTT  
 TTTCTCTCACTACCTGCATCTACATCTCAGTGAAGACTCTAATTGTTGACTCAGATCTCATTCAACTCTTCATTCTCTT  
 CATATTCTCTTATTCAATTATTAATCACTTATCTTGTCTCTGATATCTACCATCCCTCGGGTACCAATGCGGTGCAA  
 AAAGTTCTGTTATGTTGTTCTTGAGATGACTTGAATAGCGACTAGTCAATTGTCACAGATTGCAAAATTCGATCATT  
 AACGATTGTTGAAATCTAGTATTGACTAAATAACATCCAATTCAACAGATTGATAGTGTAGAGAAATTGTTGGAAGTG  
 CATACTATGACTCCGGAGGTGTTAACGCAAAATGAGGAGAGATAGTGTGGAGCGCAGGAATCATTATACATCTCTAA  
 GTGGGGTGCCTCATTGGGGCGTAAGTATATTACTCTGTTAATTCAAACTGCAGAAAATTAATTCAAAACATCATTGGAAT  
 TCAGTAGCCACTCGTGCACCTTGCTGGTTAAGTGAAGTCTGAAATAATTGCAAGATTGAAACACTACACGCTCTAAAGTAGTAGCA  
 GCTGAGCGCTACCTGTTGACTTAAACAAACAATGTTAGATCAATTCTGCTCCCTCACGTTGTTATTTCAGCTCATGATAG  
 ATACATTGTTAGTATTATTGTTAGTGTATTGTCAGTGTAAATTCAGTCAATCTGTTACATGCAATCAAACAT  
 CGTTGATATGTTAGTATTGTTAGTGTAAAGCAGACTATGTTAGTGTGTTTACAGACTAACTTGATTAAAGTTGACATT  
 TAGTCTCTGTTCTATATCTGGTTAGTGTAAAGCAGACTATGTTAGTGTGTTTACAGCTGCTGCAAAGGATTGATCAGGAAAATGTTGAA  
 CTATTGTTGGAGGCAAGCTGATCTGGAGAGCGCACCATGGCTTCAATTCTAGCTGCTGCAAAGGATTGATCAGGAAAATGTTGAA  
 ATGACCCTAAAGAACGCATTACAGCTGCCAGGCCCTGGTAAGTGTACTGCGTTCTCTTCTGTTCCACTGACACTCGG  
 TTGAGAATTGACCCAATTACTGCTTAGCATGAAAGTTGTTTACAGACTAACTTGATTAAAGTTGACATT  
 ACTCATTGGAACGAAACCCCTGGATGAAGGAAGCTGGTGAAGCATCTGACAAGCCTTAGACAATGCTGTTTGACTAGAAATGAAAC  
 AGTCAGAGCAATGAAAGATGAAGAAACTTGCTTAAAGGACTACCTGCTTAAAGGACTACCTGCTTAAAGGACTACCTGCTTAAAGG  
 GTGTAAGGAGATTTCACATGAGCCTTAAAGGACTACCTGCTTAAAGGACTACCTGCTTAAAGGACTACCTGCTTAAAGG  
 AAGTGTGTTAGTGTGTTAGTGTGTTAGTGTGTTAGTGTGTTAGTGTGTTAGTGTGTTAGTGTGTTAGTGTGTTAGTGTGTTAG  
 TAGAGCTGGGTGTGATCGGTTGAGTAAGCGAAACGTAAGGAGGTTAGTGTGTTAGTGTGTTAGTGTGTTAGTGTGTTAGTGTGTTAG  
 GAGAGGGTAGAAAATAATGATCATTCTCTAGTAAATAATTGTTGTTGATATGAAAGGTTAGCAGAAAACCTTCA  
 GGAAGAAAATAAGGGTTGAAACAAATGTCACAAATATGGATACTGATCGCAGTGGCACAATCATTGAGGAACTCAAATCTGATT  
 GACCAAAATTGGGATCCAAGCTGTTAGTGTGAACTTAAAGGACTACCTGCTTAAAGGACTACCTGCTTAAAGGACTACCTGCTTAAAGG  
 TAAATAGTGGTACATAATTAAATTCTTCTTCACATGTTGACATGTTGCTCAGGCTGATGTTGACAAAGTGGTACTATTGACTAT  
 CAAGAATTGATCCTGCAACCATTAACCGGCATAAACTAGAGAAGGAATTGTTAAGGCTTCAACTTGTGACAAGGATAG  
 AGTGGGTTAGTATAAGATTGTTATATTGATCATTCTTTTTTATGGAAAATGTTAATTGTTAGTGTGTTAGTGTGTTAG  
 ATATAAGTTGAAAGATTCAAACCTGCAACCTCTCCCTCCCTCTCCATCTTCACTGTTCTGGAGACTATCTTATATCTCAT  
 TGTGTTAGTCTCTGGTCTGTTAACTTAAAGGAGTGTGTTAGTGTGTTAGTGTGTTAGTGTGTTAGTGTGTTAGTGTGTTAGTGTGTTAG  
 ACTGAGTATCAAATGGGAGTGAAGCAGACTATAGTGAAGTCATCGACATGTTGACACTGATAACGTATGCTACAATTATATATA  
 TCCGTGTTATGCCCTCAATTGACTAGTGAACATTGACTATGATTGAGCTTCCGTTGAGCAGGACGGGAAATTAAATTACCAAGGAGTTG  
 TGGCTATGAGAAAGGGGATCTGGATATTGATGAGAAAGAGAAACCAATAA

#### G. max Glyma14g40090a Putative Coding Sequence

ATGGGACTGGGATGTTAAGGCATTGTTGCTCGACAAGCCCCATGAAATTGACATTGCGACTCTGGACTCATCTCCTGATCAT  
 ACCCCCACAAACATTCTAAACCAAAAGCCAAGCCAAATGCTGCACCTACTCATTCCAATAATAACAAACACACCATCTACACAAATA  
 GGAGCAATTCTAGGGAAACCACATGTAACATACACAAATGTAACGAGATGAAGAAGGAACCTGGGAAGCGGGAGTCTGGTAAACAT  
 CTGTTGTTGAGAAGACGACGAAGCGAGAGTATGCAATGCAAACTCATCTCGGTGCAAGCTGCTGAGCACCGCAGGAGATTGAGGATGT  
 AGAAGAGAGGTTATGATTCTGAGCATCTTCGGGGCAGCCACATAGTGGAGTTCAGAGGGCTTATGAGGACAAGCAGAACGTC  
 CTGGTGTGGAGACTGTTGAGCTGAGCTGGGGCGAAACTCTCGACCGCATATTGCCAAGGAAACTCTGGAGCTGAGCTGCCACTGTC  
 AGGCAGATTGTCATGTTGTTACGCTGCCATTGCGCTCATGTCATGAGACCTCAAGGCCGAGAATTCTTGTGGGACCAAC  
 CACCCCGATGAGCGCTAAAGGACTGATTGACTCTCATTGAGGATAGTGTGAGGCGCAGGAATCATTGTTACATCCTCTAAGT  
 TACTATGAGCTCCGGAGGTGTTAACGAAATTGAAAGGAGATAGTGTGAGGCGCAGGAATCATTGTTACATCCTCTAAGT  
 GGGGTGCTCCATTGGGGCAAAAGAGAGAAGCATATTGAAAGCTATTGGGAGGCAAGCTGATCTGGAGGCGCACCAGGCT  
 TCAATTTCAGCTGCTGCAAAAGATTGATCAGGAAATGTTGAAATAATGACCTAAAGAAACCCATTACAGCTGCCAGGCCCTGAA  
 CCGTGGAGAGGAAGGGTGTGAGCATCTGACAAGCCTTACGACAATGCTGTTGACTGAGAATGAAACAGTCCAGAGCAATGAAAC  
 ATGAAGAAACTGCTTAAAGGTTATGAGCAAAACCTTACGAGGAAGAAATTAGGTTGAAACAAATGTTCAACAAATATGGAA  
 ACTGTCAGGTCACATCATTGAGGAAACTCAATTGAGGATGACCAATTGGGATCAAGCTTAGTGTGAAATCAGAAATAAGCAGCTA  
 ATGGACGCTGATGTTGACAAAGTGGTACTATTGACTATCAAGAATTGACTCATGCCACCATTAACCGCATAAACTAGAGAAGGAA  
 GAGAATTGTTAAGGCTTCAACTTGTACAAGGATAGCAGTGGATATATAACAAGAGATGAGCTTAGACAAGCTTGACTGAGTAT  
 CAAATGGGAGTGAAGCAGACTATAGTGAAGTCATCGACATGTTGACACTGATAACGACGGGAAATTAAATTACCAAGGAGTTG  
 ATGATGAGAAAGGGGATCTGGATATTGATGAGAAAGAGAAACCAATAA

#### G. max Glyma14g40090b Putative Coding Sequence

ATGGGGCACTGCTTCAGCAAACCCAGCACAACAGAAATACCAACTATGATTATTACCAACCCCCCTCATCATTATCAGCCACGCCCG  
 CACTCACACTCAGACTCAGGAGAACACAACCTCAACTTCAACCTCAACCTGGTACCTCCAACTGCAACTCTAAAATCAGACCCATCT  
 CCATCATCATCATTGGTGTGATCAGTAGCAGCACGAATATTAGACAAACCATACTTGTACATCAAATCTCTTACACCTCGAGAG  
 GAACTCGGGAGGGCTCAATTGGGATCACTCGTCTTGCACCGAGAACGCCACGGGAAGGAATACGCTGCAAGTCCATTCCAAGGG  
 AAGCTAAGTAAAAAAAGCATACTGATGATGTCAAGAGGGAAAGTTCTCATCTTCAGCACCTCTCGGGACAGCCAAACATGTTGAGTTC  
 AAGGGTCTTATGAGGATTGGCAACACGTGCATTGGTGTGAGGTTGTTGGGTGGTGAAGCTTCTCGACCGCATACTGCAAAGGGT  
 AGTTACTCCGAGAGTGAAGCTGTTCTATATTGAGACAAATTGTTAATGTTGTCATGCTGTCATTGTTATGGGGTCATGCATAGGG  
 CTTAAGCTGAAAATTCTCTGCTTGTCAATAAGGATCTAAGGCACCTCTCAAGGCCACGGATTGTTGAGTGTCCGTCATTGAGA  
 GGTATAGTGTATAGAAGAATTGTTGAGTGCATACTATGAGCTCCGGAGGTTGTTAAAGGAAATGAGGAGATAGATGTGTT  
 AGCGCAGGAATTCTTACATCCTCTAAGTGGGTGCTCCATTGTTGGGCGAAAACCGAGAGAAGCATATTGAAAGCTATTG  
 GGCAAGCTTGTGAGAGCGCACCAGGCCCTCAATTGAGCTGCTGCAAAAGATTGAGCAGGAAATGTTGAGATAATGACCC  
 AAACGCATTACAGCTGCCAGGCCCTGAACACCCGGATGAAGGAAGGGTGAAGCATCTGACAAGCCTTAGACAATGCTGTT  
 ACTAGAATGAAACAGTTCAGAGCAATGAAAGAAGAAACTGCTTAAAGGTTATAGCAGAAAACCTTCAGAGGAAGAAATAAG  
 GGTTGAAACAAATGTTCAACAAATATGGGACTCTGAGCTGGCACAATCACATTGAGGAACCTAAATCTGGATTGACCAAAATTG  
 TCCAAGCTTGTGAGAACTGAGCAATGAGCTGAGCTGCTGAGTTGACAAAAGTGGTACTATTGACTATCAAGAATTG  
 GCCACCATTAACCGCATAAAACTAGAGAAGGAAGACAATTGTTCAAGGCTTCAACTTGTGACAAGGATACTGAGGATATAAACA

AGAGATGAGCTTAGACAAGCTTGACTGAGTATCAAATGGGAGATGAAGCAGTATAGATGAAGTCATCGACGATGTTGACACTGATAAC  
GACGGGAAATTAAATTACCAGGAGTTGTCATGAGAAGGGATCTGGATATTGATGAGAAAGAGAACACAATAA

#### G. max Glyma14g40090a Putative Protein Sequence

MGLGMFKALFCCSKPHEIDIADSDSSPDHTPKQHSKPKPKPNAAAPTHSNNQTTSTQIGAILGKPYVNIHQMYEMKKELGSGQSGVTY  
LCVEKTTKREYACKSISRSKLLSTQEIEDVRREVMILQHLSQGPNIIVEFRGAYEDKQNVLVMELCGGELFDRIIAKGNYSEREATV  
RQIVNVVHVCHFMGVHMRLKPENFLATNHPDAVKATDFGLSIFIEEGIVYREIVGSAYVVAPEVLKRNYGEIDVWSAGIILYILLS  
GVFWGENERSIFEIALGGKLDLESAPWPSISAACKLIRKMLNNDPKKRITAEEALEHPWMKEGGEASDKPLDNAVTRMKQFRAMNK  
MKKLALKVIAENLSEEIKGLQMFNMDTDRGITFEELKSLTKLGSKLSSEIQLMDAADVDKSGTIDYQEFITATINRHLEKE  
ENLFKAQFYFDKDSSGYITRDELROALTEYQMGDEATIDEVIDDVTDNDGKINYQEFVAMMRKGILDIDEKEKPQ

#### G. max Glyma14g40090b Putative Protein Sequence

MGHFSKPSTNEIPINYDSSPPPHYQPRPHSHSDSRRTQQPQLQPQPGYPNRTPKSDPSSSSGDQVAARIILDKPYFDIKSLYNLER  
ELGRGQFGITRLCTEKTTGRKYACKSIPKRKLSKKKHTDDVKREVLILQHLSQGPNIIVEFKGAYEDWQHVHLVMECLGGELFDRIATKG  
SYSESEAASIFRQIVNVVHACHFMGVHMRLKPENFLANKDPKAPLKATDFGLSVFIEEGIVYREIVGSAYVVAPEVLKRNYGEIDVW  
SAGIILYILLSGVPPFWGENERSIFEIALGGKLDLESAPWPSISAACKLIRKMLNNDPKKRITAEEALEHPWMKEGGEASDKPLDNAVL  
TRMKOFRAMNKMKKLALKVIAENLSEEIKGLQMFNMDTDRGITFEELKSLTKLGSKLSSEIQLMDAADVDKSGTIDYQEFIT  
ATINRHLEKEENLFKAQFYFDKDSSGYITRDELROALTEYQMGDEATIDEVIDDVTDNDGKINYQEFVAMMRKGILDIDEKEKPQ

#### **9.1.2 CNGC Sequences**

##### L. japonicus CNGC1 Genomic Sequence

ATGCCCTCAATTGACAAGATGGGTGCCGGTGTGGAAACACATGCTAACAACTGATGAATTGATGGATTCTAATTGCCGGAGG  
CTCTCATACAGGACACGGAGTGATCAATTCTATTCCGATGGTCCATTGAACCATATGAGGGAGGAACACTCTGGACATACT  
GGTCCACTCTGTAGTGTGAGAAAACACCCCTCTGGCAGATGGTCCACTATATGCTCACACTGCAGGAGCTGGAAATCATTTTCAG  
CACAGTATAGCTGTGCCAGAAAACAGTGGAGGGCAACAGACAAACAAACTTCACATTGGTACAGATGAGAATCTTGGAAC  
AACAACTATGAGAAAATGAAACACTTAAGTGTGAGGCTCTGGTACAGTGGTACAGATGAGAATCTTGGACATACTGCCCCTACTT  
ATTAAGGCTCTCAGAAAGGAATCCAAGGTTTCAGTGTGTTGATTCCAGGTGCTTCTAAAGGTGCTTCTCTAAATAGACTATTACTTCTCA  
TAAATTCTAAACAAAGACTAAATACATTGCTATAAGTATTAAATAATTATTAACATTATTAGAATTGGAAATGATCCTTA  
TTCCTTTACTTAAATACATTGCTATAACCACTCTGAACCCCTCGAACCTTCATGTTACCATGCTCATCTCGTATATTGCTTTTG  
TTGTTGATATTATTGTCTACTTTAAAGACAATAGAACATTGCTCAATTGACCATTTGACACTGTCTCATTTTGCAAACAACTTATTCTG  
AAGGACACAATGACAGACTTCATTTCTCAACCTTTCACTTGTGTTGACATATTGCTACATTCATATGCTATTAACAAATGT  
ATTGTAATGTTACAGTCCATAATTCTCTTATGGGGAGGCAAAGGTTGGAGAAAATTTCTTCTGCTTCTGCTTCAAGAATCAAGCT  
TGGAGTTATGAACCCCTCACGCTAAAGGTGACAACAAATGGAACAGTTCTGCCATGTTGCTTGTGATGGGATTTGTTGATCATT  
ATTTTCTCTTATCTATGTGAGGAAGGTGATTATTTCCTTTATTTAATTGTAACAAATTCTAGCTGTAGGAGTAGATATTAA  
TTTCCTTGCTACAATTCTTGCAAAATTACTCTATTTCCTCTCATTTATCCAGGATTCTAAGTGTATTGTTATCGACCTGACAA  
TGACAAAATACTCTTCTTACTTCGAAGCATAAAATGATGTTGATATTGTAACATTCTCCAGGTAAATTATCAGTAGCCACCTT  
CTCAGAAGGTTACCTCTGGCCCTCCCTTACATTGAAATTGCTGTAATTCTGATATTGCTGAGAATTTGTTGCAATTGTTAACAAA  
AACAGAACGCCAAGGATTCTCAGTAGGTGGCTCAGTACATGAATCACAACAAATGCCATAATTGCTTCTGAGAATCAAGCT  
GATAGATTATTAAACCTCAGTCTCTTAATGGTTAGCCTACATTTCGTTCTTGTCTCATCACACACAATTGTTGCTAGAGAATAGT  
CAGATCATGAAAGCTAAAAGCATGCTGAACATTCTCTGTTCTACTTATATCTAGCTGATAAAAGAGCCAGTTGGGTTGAGTC  
TTTGTGAGCTGATCAGTAAAGAGTAGTAGGCAATGCTATCACATGAATCATTCTCATCTCAAAGATAGGCCATACAAGGGTCT  
CTGTTTTACTTTGCTCTCTTCTGATTTTTGTAATGATGACATAGAACAATTGTTGAGGAGTGTAGGAACAATTAGA  
TGATGGAAGCAAATCATCTAAACTGATGTTGAGTCTAGCTCCAGTAAATGCTCAATAAAAGCCTTGATACAGTATTCC  
AAGTGGTATTCCCCATCATAGCTTAAATAACTCTACTAAGTGTCTTCTGAGTTAGGTTGCTTATGTTTCACTGTAATCACCG  
TGGTGGGGCTGGAGATTAGTGTGACAATCCAAAAAAATTGCTCTTAATTACGTGAAGGGTTACTTTTTGACTATTGTCGAT  
CACCACTCTACCTCAGTAAATTCTCCTCTCCTACTGTTGTTGAGGGCAAATGTTTACTAATGTAAGCTGTAGCTGATGCA  
TATAATTACTTTTATCTCAAGAACCTGCATGCAAAACTCTTTCTGAGCATAGTCATGCCACAGGCTCACCTATGTTGTTG  
AAATGAAATTAAATGAAAGACGGAGGGACATATCTCTGATGTCATCTGGTAAGACCCGATTCTAAAGCTCAAGTTGAGAGTT  
ACATTAGAAATGATATTCTCTATGAAACATTCTCATGCTGTGTTGAAAGATTGTTGAAATATTGCTATTGTTCTTGTATTCA  
TTTGTAAACTCTCTTGTCTATATCATATAATTCAAAATTCAAGTGAAGTCAAAAGATTCTCTTGTGACATGGATATGTTCTGA  
AAACATGTAACGAAGAAGAGAGCTGTGATCTGAAAAAAAGACTGGTTTATAAGGTACTCATCAAATACTTGTATGACATATGT  
GTGAAATACTACAGATAATGATACTTTGTCCTACCGACTCTCTGGATCACCAGGACAAATTCTACTAAGAATGTTCTACATGTA  
GCAGTCCTTGCAGTATGTTCCAGATTATTCAAGGTTTCTGCTCTGCTAAATTGGCAGTCTCAACTGGATTCTATTTGAGTCAGCA  
TGGGTGAATTCTGCTCATAAATCTCTCATTTTATGCTATCTGCTGTTGGATCTGCTGTTACCTTGGTTACAGGTGAGT  
AAAACAACAAATGAAGCTCTATTGAAAAGTAAAAAAACATATTGCTGCTACCAAGTGTCAAGCTTGGCTTAAATTATCACC  
TGTATGAAAAGGGAGGAAAGGTACTCTGTAACCTCTGCAATTAAAGGAAATGAGTAAAGTGTGTTGAGGTTCTTCTGTT  
TTCTGATTTCATGTATAACACAATAATTAAACAAAGGTATAGGAAATTGAAGTATGATAGTGTGTTGAGGTTCTTCTGTT  
TATAATTACATATTAGTCTGTTAGTTCTGTTAGCTGTTCTAGTGTGTTAATAAAACTGTTAGTTCTTCTGTTGAGT  
TAGATCAAACGGTCTGATGTTTATTCTCATGATTCTCACATAAGAAGATCATTCTCATAGTACATCCCACATATTATACAAACACA  
CTCTATTCTGAGAACCATAGAGCAGAAAAACATTCTCACAGTCTCGGAAACTACTTCTCTTCTCTCAATCATAGCTGCTATAGGTT  
CTGTCGTTGCTGATGAGTACAGTAAAGTCTTCAATTATTGTTAATAGAATGAAACTTAACATTCAATTACTAATTCTCC  
GATTATGAGAAATAGTTAATTGGAACAGGAAATTAACTGAGTAAATGCTTAATTAAACATTCAATTACTAATTCTCC  
TCCCTTTCTCTCCAGGGTTAATCAATGTTGCAAAATGCTGCTCATAGTCTTCTATTAAACATGGATGACCGAATTGATTGATG  
GATTCTAGGATGGGCCAGATGTCAGCTATGTTGAGAAACAATACAACATGGCAGTCTGTTGAGTCCACATCTGGTCTTCC  
GGGATATGACAGAGCTGTAGCACTACTACAGAAAATAAGTGTGTTGACTGTTGAGGATATGAGGATATGAAAGATTCAA  
ATGGGCTTCAAGTATGTGTTGACTGTTGAGGATATGAGGATATGAGGATATGAGGATATGAGGATATGAGGATATGAGGCT  
TAATAAAACGCATATGCATAC

TGTGTAATGCTAACCTCTTTATGGCAACTATGATCATGAACTTTATAGTTGACGCAAGCAGTAACTTTCTTAATTAAAG  
 ACAATACATAGTTATTAATCACAAATCCCATTAACTTCTACGAAACAATTGAGATTAATTCAGGAGGTAGTTACTGGCTTT  
 TAAATAAGTCCTACTCCATTGTTATAAGTCTTGATGGAGTATTACACTTTACAGTTAAATAGGTCCCTACTGTTATA  
 GTTTTAATAAAATAAGTCCTGAAACCCCTAATTACAACACAGAATGGCTTAGAGTTACTATAAGTATAATTGTATAAACATCCATT  
 GTGCCAGTGGAGCTTGATGGGCTTATAAAATATCAGAAGGTAGTAAGAACATGATCTCATAAACAACTTCAGGTTGAAGAGGGACATATA  
 TGCAAGCAGCCTCTGGTTCAAAAGTCAGACAAGCCTAGTTGCAAGCTGAACAAAGCTTATATGGCTCAAACAGGCTCCAAGAG  
 CTTGGTTGATAGGTTGAAGACAGCTAATCAAATTGGGTCAGGGCAAGCTGTTGATCCTCCCTTTACTTCCATCATAAGT  
 CAAGTATCATATATTGGTCTATGAGATGACATCATTACAGGGATTCTGCCTTATTCAAGAGATTGTTCAAAGCTTA  
 ATTCTGAATTGCTTAAACAAATTGGTCAGTTAGACTATTCTGCTGTCAGTCATCTGCAAGAGATAGGCTCTCCCTACTTA  
 CTCAGACAAAATACATTGGTGTCTGAAAGCAGACAGCTGGCAGAAGCTAAAGGCATCTACACCTATGGTCAGTGGTGCACAAAC  
 TAAGCAAGCATGGAGCAGATTTCAGACCTACTATAGGTCATAGTGGGCTTGCATATTGCCACTTACAGCCTTACCCAGACCTG  
 AAATAAGCTTCAAGCAAAAGTGTCAATTCTCAGTCAGCAGGCTTGGAGAACATTGAGGCAAGTTAAAGGATATTGAGGTATC  
 TAAAGGTACAATTCATCATGGCTGCATATCAAGCTTGTCTGCATTCTCAGTTGCTAGTGGCATACTGTGATGCTGATTGGG  
 GATCTGATCCTGATGACAGGAGGTCCACCTTGGCTTAATCTGCTCTGGACCTCTAAGAAGCAAACCTTGTAGCCAGGTCTAGTAC  
 TGAAGCAGAATATAGGAGCTTGCTAATACCTCAGCTGAGTTGCTATGGATTCATCTGTTACAAGAGCTGCATGTCATTACAGT  
 TCCCAGAATTTCAGTGTGATAATATGGAGCTGGTGTCTGATTCTCAGTCATGTTGCTTGCATACCCGACACAAACATATGGAGCTTGACAT  
 TTCTTGTAGAGAGAGGCTGTAATAAGTCTTGTCTCATGTTGCTTGCATGTTCTCATTGATCAGCTGCTGACCTTCAACAAAGC  
 TCTTCTCCTACTCGTTGTAAGACCTTTAGAAGCAAACCTTAATGTGACTGAGAACACTAGTTCTCACCACCTTCAGTTGAGGGGTGT  
 ATTAGGATATGTGACTCACATGTCAGTCATGGCATTGCTGACATGTCAATCTGAACTAGGATATTGATGACTCAACTTTCAAGAAATA  
 TCTCTCTAGTAACAGCTGCTACGCAAGCTCTGATTCTCATAAAATAGCTAAATGCTATTGTAACACTCAACTTTCAAGAAATA  
 CAATTCAAGTTAGAATCTAACACATATTGGAAAGCAAATGGTAAATTAAAGATCCAATAACTGTTTCACTTTCTCATTTCG  
 TAGGTGATTACAAAACATTACATTAAACATTTCAGAAGAATGGGAAAGGAGGTTGAACTTTAGAGCACATGATCAT  
 ATATGCTCTAAATATCATTCAAGGCTTAATGGACCATCATAAAATCCACAAATGGTTGATATCCTTACCAATTATACCTATT  
 TGATCTTAAACAGCAAACTGACTCTGGCGGTAACTTACCAAAATCCAAGCTTGGAGGGTCTTTTACATGGCCATATA  
 GGATGGGACTTTGCTTTGCCTCTCATTGAAACATACAGAACTTCTCAGGCTTGGACGGAGGTAGAACCTCATTACTCTTA  
 CTCAAGTCTTACTTGTGTCGCCCATGACTGTTGGTACAATGGTCTGTCATCTGTTCTTTAAATCAATTCTATTAAAGTT  
 CTTCATTGAAAATTAAAATTATGCAAGATGGGTGACGACGGCTATTCTATAAGTCTAGATGCACTCAAGTTCATATTGTCTT  
 CAATATTGGACTGATATTCTTAAGTGGGTCTAGGAAGAAGACTTTTATAAATATTATGCTATATTCTGTGATGGGAAATT  
 TCCTTGTAGTCAGTTAAATTTATCTAGTGTCTGAACTTTAACCTAACAGCTTAAATAGTGAAGGTTGATCTGATGAGTTCAAGACCA  
 GGTTGTAACACATTGATATACTTCTCCATCTCACCTACAGGAGGTAGAGATGCAACTTAGGGCCTGATGTTGAGCAATGGATG  
 AGCCACCGTCTGCCAGAAGGCTCAGAAGGTGAAATACGCAAATTCTTAAACACATTCTCTGATGAAATTCCCTATCCCTCC  
 CACAACCTTCTTATTGACTATGACTGAGCAGCTACTCTACAGCTGTATTACATATTAGCAGCTATTCAAGACTAACTTTAGT  
 TTTAAATGTGGCTATTCTGGACACAACAAACCTACATTCTTCCACTAGATGTTAGGGCTGCATAGGCTAAACAAACACTGTAA  
 CATGCTGTCATGAATCATCTTAAAGCTACTAAAAAGATTATGAAAGTTAAATCTTCTTAAACTATATTCTGGTTCTTGGCTT  
 ACCATTCACTATTGGGTATCCTAACACATCTGTTCTCTGATTCTCTGATCTTCATGTCATCAATTGAGATTTCTTGGCTT  
 ATCACTTTTACGGTTCTATAAAATGGGCCACCTGTCATGTTCTCAGTGTCTCATTCAAAATATGACTAACTTAGAATTAGTATCC  
 TGAAACTTATGGGATTAGGAATTACTATTGGGACATCTTATTAGAAGGATGTTGTCACTTTAGTGTCTTATTGTTGAAATCA  
 TATTATTACTTTCTATTCTCTTACCTTCTAAATGACACACCATTGTGTATGTTACATAAAATCCTTCCATGAATTAA  
 TTCTTGTCTCTAAAAATTATTCAATAGACAATGTACATATGTGTAGAGCTACTGATAATTAAACATAGAGCATATACTCTGAGTC  
 CTGACTGCTAAGAAAATGTTGACTATTTCACCTTATTAGGTTCTATGCTACATGAAATAATGAATCACATCACATGTAATGT  
 ACAAAATGATGCTATTGTTGGCGTGCAGGAAACTACGTCAGGCTGACGGTATAGTGGCTGCAACAAGGGGGTTAATGAAGAAATG  
 CTTCTAGAGAATTGGCGGAAGATCTCAGACAGACATAGCCTCTTCATCTCCTTAACTTGGCCTTCTCAGGCTCAGGAGCT  
 GCATACCTCAAAATTCAAAATTCTCAGCATGACTTTGAACTTCTCCTCTTCTAAATGAGGTTGATCTGCTCTTAAAGGTTAGAAG  
 TTGAAAATGAAAACCATTTGAAAGACAAAGCTGTTGATCATATTCAATGAAAGTAAACAAATGACATGTCAGGAAAGCAGTGT  
 ACAACCCCAATGTTGATGACTTAATATTCTGAGAATATTAGATATCCGAGGTTGCAATTGGCTGATGGATGAA  
 CCTATCTTACGGTCTATTGAGAGACTTAAACAGAAAGACATACATAAGGAAGTGAATTGGTACTGGGAGCTTGTAGAAAAG  
 ATGGTCTTGTGCGTGGAAATTAGAGAGCATGGAGAAGATGGAATTGGAGTCCCTATCTGAAGGAGATGCTGTGGTGAAGAA  
 CTTCTCACATGGTCTTGTGAGAACTTCTCTGTAAGCAAAGGTATGGCAAAACACTCGGTGCAAAAGATAATGGATGACATGCC  
 ATATCTTCTTACGGAGATCTGAGAATTACTACAGCAGAACATTGCTCCTACACAAAGTGGATATGTTGTTGCTT  
 TTCTTGTGAGGTTTACAGAGGGTTAACATGTTGCAAAATGTCTGCCATTGTTGATGTTGCTTACCTACTGGAGATCCCTG  
 TTCAAAACTAGGCTCTGACATAATGATCTGGCTATTGAGTGAATCACCTACTGGAGATCCCTGAGCAAACAGAATTCAAG  
 GCATGGAGATACAGGAAGAACGCTAGGCTGCTGCTAATATCTCACAATCAGATCAAACACCGAAGTCAGT

#### *L. japonicus* CNGC1 Coding Sequence

ATGCCCTCAATTGCAAAAGATGGGTGCCGGTGTGTTGAAACACATGCTCAACAATCTGATGAATTCTATGGATTCTAATTGCCGAGG  
 CTCTCATACAGGACACGGAGTGCATCAATTCTATTCCGATGGCCCCATTGAAACCATATGAGGGAGGAACCTCTTGTGGACATACT  
 GGTCCACTTCGCTAGTGTGAGAAAACCACCCCTCTGGCAGATGAGTGGTCCACTATATGCTACCACTGCAAGGAGCTGGAAATCTTCTAG  
 CACAGTATAGCTGCCAGGAAAAAGCAGTGGAGGGCAAGACACAACAACTTCAACTTTGATGGTACAGATGAGAATCTTGGAAAC  
 AACAAACTGATAGAAAAAAATGAAACACTTACTGAGGCTGGAGCTGGGAATGTGTAATGATCTTATGCACTACTTGCCTACTT  
 ATTAAGGCTCTCAGAAAAGGAATCCAAAGGTTCTGACTGTGTTGATCTTCAAGTCTTCTTATGTTGGGAGGCAAAAGGTT  
 GGAAGAAAATTTTCTCTGCTCTCATGTGTTCTGGAGGTATGAAACCTCAGCTAAAGTGTACAACAAATGAAACAAGTTCTG  
 CGCATGTTCTGATGGCTATTGTTGATCATTCTCATATTGCTATGTTGATCTGACCTTGGTCCAAATTATGTTGTTGCTT  
 CTGACAATGACAAAATACTTCTTACTTCGAACGATAATGATGTTGATATTGAAACATTCTCTCAGTTAGGTTGGCTT  
 GTTTCACCTGAATCAACGGTGGTGGGCTGGAGATTAGTGTGACAATCCAAAAAAATTGCTCTTAAATTACGTGAAGGGTTACTTT  
 TTTGACTTATTGTCGATCACCCCTCACCTGAGATAATTGACTTTGTCCTACCGACTTCCCTGGGATCACCAGGACCAATTCT  
 ACTAAGAATGTTCTACATGTCAGCTGCTCTTGCAGTGTGTTGCTTACAGGTTTGCATGTTGCTATGCTTGGGCTTCAACAAATCAGT  
 GGATTCTACATGGTACGATGGCTAATTTCGTCATAAAATCTCTCATTTTATGCTATCTGCTTGGGCTTCAACAAATCAGT  
 CTCTTGGTTACAGAGGGTTAACATGTTGCAAAATGTCTGCCATTGCTTACAGGTTCTGAGGAGGTAGAGGTTGACCTTGG  
 ATATATGACAGAGCTGACTTACTACAGAAACTAAGGTGTCAGAAAGGAAATGTCAGGCTACATAGGATTGGGACTTTGCTTT  
 ACTCTGGCGGTAACTAAACATACAGAACTTCTCAGGCTCTGGAGGGAGGCTAGAGATGCAACTTAGGGCCGTGATGTTGAGCAATGG  
 CTTCTCATGGAAACATACAGAAACTTCTCAGGCTCTGGAGGGAGGCTAGAGATGCAACTTAGGGCCGTGATGTTGAGCAATGG  
 ATGAGCCACCGTCTGGCAGAAGGCTCAGAAGGAAAGTACGTCAGGCTGACCGTATAGTGGCTGCAACAAAGGGGGTTAATGAA  
 GAAATGTTCTAGAGAATTTCGGCGAAGATCTCCAGACAGACATTAGACGCCATTCTTCAAAATTGCAAAAAGGTTGCAATT  
 TGC

CTGATGGATGAACCTATCTTAGATGCTTCGTGAGAGACTAAACAGAACATACATCAAAGGAAGTACAATTGAGTCGGGGAAAGT  
CTTGTAGAAAAGATGGCTTTGTCGTTGCGAAAATTAGAGAGCATTGGAGAAGATGGAATTGGAGTCCCTTATCTGAAGGAGATGCT  
TGTGGTGAGAAACTTCTCACATGGTATCTTGAGAACTTCTCTGTAAGCAAGAGATGGTAAAGGCTTCAGGACAGAGGTTGCTA  
AGCAACAGAACACTGTGAGATGCTAACAAATGTGGAGGCATTTCACTCCATGTCGAGACCTTGAGAAGAAGTAAACATTCTTTCACAAGA  
TTCTTGCGGAGCCCTCAGGTCAAGGAGCTCAAGGTATGAATCACCTACTGGAGATCCCTGCAGCAAACAGAACATTAGGTTGCTGG  
AGATAACAGGAAGAACGTCTAGGTCGTGCTGCTAATATCACAATCAGATCAAACACCGAACGTGCTAG

### *L. japonicus* CNGC1 Protein Sequence

MPQFDKDGVPVLLETHAQQSDEFMDNSCRRRLSYRTRSASISIPMVPIEPYEGGTHLVGHTGPLRSVRKPMSGPLYATTAGAGNHFO  
HSIAVPGKKAVERGKTOOLSTFDGTDENLWNNNNYDRKNEHLLRSOLGMCDPYCTTCPTYIKASOKGNPKVSTFDSFHNSLYGEAKGF  
GRKLFSFCSSCVPVMNPNAKVVQWNKFLAMFCILMAIFVDPLFFFYLIVRKDSNCIVIDLTMTKILLLRSENDVYVLLNILLQFRLAY  
VSPESTVVAGDLVDNPKKIALNYVKYFFFDFLFFVSPPLPQIMILFVLPTSLGSPGPNSTKVNVLHVAVILQYVPRLFPLLIGQSP  
GFIFESAWNVFVINLLI FMLSGHVVGSCWYLFGLQRVNQCLQNVCNSSIKHGCTELIDCDSRMGQMSAMWRNNTNATACLNSTS  
GSFPYG IYDRAVALLTETKVVKYVFALFWGFAQQISTLAGQNQPSYFEWEVLFTMAIIGLGLLFFALLIGNIQNFLQALGRRLLEMQLRGRDVEQW  
MSHRLRPLEGLRRKVRQAERYSWAATRVGNEEMILLENLPEDLQTDIDRRLFKFAKKVRI  
FALMDEPILDRAIRERLKQKTYIKGSRILSRGS  
LVEKMVFFVRGKLESIGEDGIGVPLSEGADCEELLTWYLENSVSVDGKVKRLPGQRLLSNRTVRCLTNVEAFSLHAADLEEVTFLFT  
FLRSPQVQGALRYEWSLAANRIQVAWRYRKRLGRARANISQSDQTPKS

### *L. japonicus* CNGC2 Genomic Sequence

ATGGATAATTTGAAAAAGATGGGTTCTGTGCTGAGAAACACATGTACAAGTATCTGATAAAACTCATCGATTATAATTCCGGAGG  
CCTGTATCAAGGACAAAGAATGTAGCAATTCTATTCCCATGATATCCATGGAGTCACATCAGAACATGAAAGTAGTCTTAAGGAACACACT  
AGCCCATTATGATGTAGTGGAGGAAAATCCCTTGATGCAAGATGAGTTATCGCTATATGGTACTCATGGAACATAGAAATCTTGCAGCAG  
ACAATGGTGTGAAAGAAAACAGTATCAGAGAACAGAACAAAAATTATACTTCCACGGCACAGGTGAGCAGGCACTGGAAATAGT  
AACAGCCCTGATAAGAAAATGAAACATGTGGAGTCAGGGAAACTGGGAAGTGTGATGATCCTTATGGTACTACTGTGCCACTGAC  
TTCAAGGCTCTGAGGAAAGAACATCAAAGTTTCACTGTGATGTTGATGTTGAGCTTTTCAATTGATCTTGTAGATATTATCCT  
AATGTTAGACATTATCTTGAATTGATGATCATTATACTTGAATTCTGTGAGCTTTTCAATTGATCTTGTAGATATTATCCT  
TGTCACTTTCACATAACCAGCATCTTCTCATGATTGTAATGTTAACAGTCCCGAGTTCTTATGGTGAAGGCAAGGGTTTG  
GGAAAAAAACTTACGTCTTTCTCGTATGTATTCCGGAGTAATGAACCTCACACTAAAGTGGTACAAAATGGAACAAATTTCG  
CCATCTTTCGCTGGTGCATTTTGTGGATCCATTGTTCTTCTTCAATTCTATGTGAGCAGGTTATTCTTCTTCTTCTTAA  
CTGCAAAATCTTAAGATTTGAGTCCAAATTCTACTGTCAATTATTTCTTGTGATTTTCAATTCTCTTCTTCTTCTTCTTCT  
TATGCAAGGACTATAATGTTTACTTCAACTGGAAACATTGAGAACACTAATTCTACTCAGAACCTAAATGATTGTATACTTCT  
GAAAATTCTTCAGGTAAATTGATTCTCACATTCTACCGCTTTAGATGTCACCCCTGCCCTAACGTTGGTAGTGTGAACCTACCAT  
ATATAAAATTAAATTGGAAGAATAAAATGAAATGATTACTTCTACGAGATGATAGGTTAAAGTAACTTATTGATAGTCTATTGCA  
GCATATCATGTACTTTGTATGCCTACTTGTGTTACCGTAAGTGTGAGATCAAAGGAAAGTAAAGAAATGGATAAGTTCATGTGTC  
TGAATCTTGAATATATTACCTAATTGCACTGACTATTCTTCTTACCATTTTATGTTGTTCTGTTGAACTTATTT  
GGGTTAACCTAGGCCTACTCTACTAAACCTGTTCTTAATAGATTATACAGTGGGTTCTTAAAGGTTTATATTGCTTCAGGTCT  
AAAGAACACAGTCAAATTAAAGGCCAAATGAAATGATCAAAACATATTCAACCCACACACTAACTTACCAAGGTTCTT  
TTGCAAGTTAGGTTGGCCTATATTCTCTGAGTCAGGTTGGGTTGGTCTGGAGATTAGTGTGATGCTTAAGAAATTGTTGTCCT  
TACTTGAAGGGTTATTCTTACTGTGTTGTTGCTCTCTCAGTAAATTCTCTTCTCAGTAAATTCTCTGTTGAAATCTTCT  
AACTATGGTTGTTAAGTACTTACAAACTCCTGCCATGATATCAATAGCAGAACATGTCAGATAATGATACTATCCATCTTACCAA  
GGAACTTGGGTACGGAGCAAATTGCTAAAGAACATTTGCGTGCAGTGTACTTGTGAGTATATTCCAGGCTATTAGGGTCT  
TGCCTCTGCTAAATGGCAGTCTCACAGGATTCTTGTAGTCATGTCATGGCAAAATTCTTCAATTATAATCTCTCATGTATATGCTT  
CTAGCCATGTTGGCTCTGCTGTTGACCTCTTGTAGTCAGTCAGGTTGGGTTGGTCTGGAGATTAGTGTGATGCTTAAGAAATTGTTGTCCT  
TGCAATGTGATATTCTTATTCTCATGTAATGATTGATGTTGATGTTGATGTTGCTCTCTCAGTAAATTCTCTGTTGAAATCTTCT  
CTTCTCTAAAGGCCAGAACATCAATTGGAGCAAATTGAGTAACTTGTGAGTAATTGTTGAGGTTCTTCAATTGATTAACATTGAGGAAATAGGAG  
CTGAAAATGAGTCATTCTCAGTATGATAGTAATAAGTGTCTAGAAATTCACTCTGGTAACATCTTAAATTGATTCTATCTTAA  
TTATTATGTTCTAAGATTCTTAAAGATGAGTACTCACTCAGAACATTGAAATTCTCAATTGAGTAAATTAAAGTTAACAGTTCTCCT  
TTTTTCTATCTTCTTCTCAGGGGTTAATGAGTAACTTACAGGATGCTCTGAGCTTAACTTGTGAGTAAATTGTTGTTGTTCTTAAGAA  
TGCAATGTGATATTCTTATTCTCATGTAATGATTGAGTCTGGCCAAACACCAGTGTGTTGAGAACAACTGAGTCAGTGGGTTGGTGAAGC  
CCTCTCTGAGGTTGATTGGATCTACGTCACTGAGTCAAGTACCTACTATAGAACAACTATTGTTGAGGAAATTATGTGACTCTC  
TTTTTGGGATTCCAGGTATGCTATTCTTCTTCTGTTGTTGTTGAGTACATTGAGTACATTGCTCTGCTTCTGTTGTTGTTGTTGTTG  
GACTATGGATTCAAGTAATGATCATGCAAGCCTTTCTGAGGTTAAAGCAGCACATAAAGTGTGTTGGAAATGAGGAAATAACTTCA  
CCACATCTATATTAGGATTTCGAACACAATAAAATCATTATAAATTACGTACCTCTGTAAGACACAAATGAGAACATTGTCGTAGCTCAAG  
AATGTACCTACATTGAGATGTCATGCAACAGCGTCACTCTCAGACCCAGGATTCTCTCTCTCTCTCATATAATCGGGGCTCTGGA  
TATGAGAACATGCAACAGTGTCAAGAGTGGAGGAGGATCTGAGCATATACAGCTGAGTCCATCATGGGGCTTAGGTT  
CTTACTTGGCCTACACATACTTGCACACTTCAATTGAGCTTAATGGAGAACATGAGCTTAAAGCTTAAATAAATACAAACAGTGAATTCCCTAGGTT  
ATAATGGATCAAATAATTACAGGAATATAGCTTAATTGGAATAATAGGGAGAACACAGTGAATTGTTGGTATCTCTAATTATCA  
CTTTTATCATATTAGCTTAATTGAACTTACACCATATGCTCTCTGTAACAACACATGAATGGTTGGTATCTCTAATTATCA  
TTTGCCTATCTTGCACACAGAACATCAGTACCCCTAGCTGGTAGCTTAACCCAAGCTATTGTTGGAGTCCTTTGCAATTGG  
CATCATAGGGTAGGACTCTGCTTTGCACTTCTTATGGGAACACATCAGAACATTGCAAGGTTGGAGAGGTTAGGATTAGT  
GCTCTCTCATACTGTGACCTTAACTCTTGTGACAATTGCTCTTATTGAGTAACTTCTCTTAAATCAAATTCTGTTAGAGTTC  
CTCTCAAGGTTAGAAGTTGAAAGAACATGCAAAACATGAGTTGGCATCTTGTGAGTAACTTCTCTTAAACACTAACAGATATAATTCC  
ATGTTCTCATATTGAGTCTGCTTGTGTTGAGATTGTTGCTCTGTTGAGTAACTTCTCTGTTGAGTAACTTCTCT  
AGTATTATATCATTCTAGTGTCTGCTGTTGAGATTGTTGCTCTGTTGAGTAACTTCTCTGTTGAGTAACTTCTCT  
TAACCTTACTAAATGCTGTTTCTGCCCTCGCCGAGCAAAGGTTGGTTAGTCCCTAACCTTGCCTAACCTTGCCTAACCTTGC  
CTCCGGAGCTGGTCAACGCCGAGCTCCGATGGCCATGGCACATGGGTTAATGAGGCCAGCTGTTATTATTAA  
TTTTTTAAGAAAACGAAAATTACTCAGTAATTAAACTCTTAACACTCAATTAAACCCCAATTAAACCTAAACTAAACTATCCCTCA  
CCACAATGCAACTAAATCACTCTTCTTAAATTAAATTAAACCCCAACCCAGAACCTCTCTCTCTCATCATCACACCCATCATC  
ATCTCTCTCTTACCTCATCCAAGCGCAGAACATTGCTTACAGACACTCCATCCAACCCCAACCCCAACCCACCTCAC  
CCCACATTCCACCACTGATTCTCTCTCAAATCGCAACTTTAACACCCATTCCCCCAATTCAACACTTACCA  
GGCCGGAGGCAACTATGAAGCCATCGATGGTTATACAAGGGTGCAGTGAAGGGATAGGGAGGAGATAACGAGAGTAGAGGGAGG  
GTCATTGAAACCCAAATCCAATTCACTGAGATCCCTCAACCCCAACCCAGATATGAAACACAACGGTGGATGCCCTCATGAAGGATGAGG  
GCCGGCGCAGAGCAGAACCTGCGCGCGCTTGAGCAACCCCTCACCGCACCAAGGCCACGCCACGCCCTGGATCTGGCTT  
TTCACTGCACTCAGATCATATTCCACCGCATCTGAGATCAATCTTCTATTGGAACATTGCAACTTACAGTCAAACACATG  
ATCTTCAACTTCTCTTATATTGTTGTTGCTCTGTTGAGTCAATTGGAACATTGTTGAGTCAAGGTTCTCTCAAGGGCTGGGAATG  
CAAAGATCGAGTACTGATTGGGCTGAGCACAGGGTTGATTGTTGAGTCAAGGTTGTTGGGAGGGGGTGGAGGATCAC

## APPENDIX

---

GTTTTGGGTGAGTAAAAACTATTTAAATTGCTTTGAAAGATGAAAAGAATTGTTGAGATTAAACATAATTGGAGATTGTGAAA  
 GATCTGGAAACTTGAGTGGATGCAGGCTGTTGAAGAAGGAAAATTAGTTATTGCAATTGAAGAGTTAATTAGAGCACCCAAATT  
 GGACTGGGAGCCCCTAGAGGGCAACGCCAGCATGTATCCGCCCTGAGGCCGGCCCTGCCCTCAGATGGGCCCTGATCTCGGAG  
 GCCCAATTGGCCAATAGGTAGTACCCAAGCTCTATAAATAGGAGGTAGTTATCAATTGTAAGGGACTTTGGCTCATTGATGAAGTA  
 ACACATAAAATTAGCAGTCTCTCTTACTCTCTCTAGACAATCTCTACCCCTAGGTACTATACTTCCATTCATGGTCAATTGAGTA  
 CCCAGAACATTGGCGCGTCTGCGGACTGTAAACTTCTACTCCATTACGTGGATTGATGTGATGAAGTTACCTCTGATTGTG  
 ATTAGGCAACTCTCTGGTTTCGATTTGATTCTGTGACTAGTGTGGTTTCGATCGAGTTGATCGATCGTTCTGGTTAGATGGAGA  
 CTCGACGCCAGAGGCAACATTACCAATGCGACAGCGGATTTCGCCCTCGGCCCTCATGTGAGCTGGACCTGGATTCTCCGGTGC  
 GAACGGCAGGAGTACAGTCGCCCTCCATCACCAACCTCCATGCCCTCACAGGTGGATCTCGGGACACTCACCAAGGAAATT  
 CACCTGCTCCGGAACAAACACGGCGGTGACGCCAGGAGCAATGCCGAGGACTTGTGCGCAGCATTGCAACATCCAGCAGCGGAAT  
 ATCTCAGGCTCAGTGTAGATTCTACCTGCGCAGCAGCAGGAGTATGGAGAGAGAGAGAGAGAGAGAGAGAGAGAGAGAG  
 CGGAAGATGTGAGGTGTCGGGATTCGGATAACATGAAACAGCTTGTAGTTCTGAGATTCTACAGCGGAGATTCCGATCGAAAGATC  
 TACTGACTTTAATACGAAATGGTATAATTGCGCGTCAAGATGCGTGAAGTGCAGGATGTTCCATCGACGTTCAATGACGCCA  
 TGGCGTGGTCACAACATTGCGCGTGGATCGATTCAAATTTCAGAGACTTCTCATCCAAGTTCTAGTGAATTCTCGGCAAATAAGA  
 ATCAGCCGGTGAATGACCTATAACATATTCTCAGCAGGAAAGGGAGTCACTGAAGAGAGTACATGGCAAGGTATAGCGCGGT  
 CGGTAAGGAGTAGGAGCAGGGACCTCGAGCTTGTCTTGTAGATTAAACAGGTTTGTGCGGGGAGGGTGAACAGCAAATTGACAC  
 GTAAGCGGCCCTCGAGGGAGAGATGGCAGCTGCTGCGCAGCAGTATATTCTCGACGCCAGGAGGAGCAGCTTCAAAAGAAGGCC  
 CGAAGTTGGAAAAGGGCAGACCGTCCGAGGAGGAGGAGGAGGAGGAGGAGGAGGAGGAGGAGGAGGAGGAGGAGGAGGAGGAG  
 GTAAGGGGAAGTCGGTATTCAAACCGACCAAGGAACAGTTGTATCCACCGCGCATGATTATGAACAAACGTCGCCCTGGCAATCTAAGT  
 CTACATGCCAGCGGGAGGAAACTGATATGGTGAACACAGATGCATCGGATATGCTCGAGGGGCAAGCGACGCAAATCTAGTGGATG  
 AGCGGAGGCCAAAGTATCAGGCCAGGGACGCCAATCCAAGAAGTGTGCGAGTTCCACCGGCCGGCATATAACGGATGACT  
 GTTGGACTTGCAGCGGAGATTGATAAGTGTGATCGGGGATATCAAGGAAATCGTCAAGGCCAGTGGCCAATGGTGGCATCAAA  
 ACAAAAGCGCAACAGCGGAG  
 ACACGTTCCGCTAACACTCAGGCCCGCTGGGAGGACATCACACCATCGTGGGGGATTGGCAGGGCTGGGAGCACTCATGCCGCG  
 GTAAGGCCATGTCGCGCTTAATTCCGTTATGAGGTCGCTTGTGATCACCCCTACATAACATCTCGATGGCGACTTGG  
 AGGGATAAAGCCTATAAGGACGCCAGTTGGTGTGAGTTAAGGATGAACAGTTCAAGCTTAAAGGGTACTCTGGATCAGGGTA  
 GTTCGGCTGATATTATCTATGGTATGCAAGTTGGGACTAATGACAATGATCTAACCTACACGGAACCTTGGTAGGTT  
 TCGCGGGGAGGAGCAAGTAATGGTGGGGGATACATTGATCTAGACACAATTGGGGAGAGCAGGAGTGTGCTAGGGTTTGAAGGTAAGG  
 ATCTGGTTCTCCAGGTGGTAGCATCTACAGTCACTGGGGAATACATTGGCAGATTGGGGGATCATCTGGCTTGTGCTGTAATTTCGACAGCC  
 TAGCGGTCAAGTATCCGCTAACACTGAGCTGGAAAGGTTGGAAAGCTGAAGGAGGACAGAAGATGGCAGGGAGGAGTGTGTTACATAATTGCC  
 ACTTGTACCGCAAGAAGAGTGTGTTGGTATAGATGTTATGAAATCTAACGCGCCGCTCGGCATGCCCATCCCCCACAG  
 TCTTCTACCTTACGACGTCGACCCCAAGTCCATCAAAACAAAGGATGGATTTCCTGAGGCCAGGCCGGGAAGTGTGTTGCATC  
 CCCACAAAAGTAACCGCAAGTCTCCCTCGCACGAAAGTACTTCGCTGGGGTTCATCCGCTACCCAGAGGACATCACCCCTCAGAG  
 ACGGGACGCCCTTCTCTTACTGGACAGAGAAGCCCAACGGGATCAGGAGTCAAGCTTGGCAGACTGACATGGAGCTGAGCTGGAG  
 AGTGGAAAAGGGCTGGGGAGCAAGAGAAAAGTCTGGGGAGCTTGGCAGGG  
 GTCCGAGGAGATCAAAAGGAGGCCAAACTCATGCCAGGCCCTCGGCCAGGAGGAGGAGGAGGAGGAGGAGGAGGAGGAGGAGGAG  
 AAGTCTAGGAGCAGCTGGCAGGCCAGGAGGAGGAGGAGGAGGAGGAGGAGGAGGAGGAGGAGGAGGAGGAGGAGGAGGAGGAG  
 CGGTTCTACCTGCCAAAGATCAGGCCAAACATTGTTACCCGAACATTGACTTGGCAGGGAGGAGGAGGAGGAGGAGGAGGAGGAG  
 AGGACTGGTTGGTCCCAGCAGTCTCCCTGATTGACCAAAACCTCTGGACAGCAGTGAAGAAGAGAGAGAGAGAGAGAGAGAG  
 AGAAAACAATGAAATGTAATTTCACATTACCTTATCTTTACTGTCACCTTGAGTTGACTTTCCGCCATTCTGCTATGTTAA  
 GGAACCCCTGCCCATGCTTATATCGCGTGGATATTGTAAGTCATATTGGAACGCTTCCGCTACACTACTCGCCCTTCC  
 CTATTCTTCGCGACCTTATCTTCGCTATTTCGCTATGATGAAATTACCGCTTACAGGATTCGCTGCTTAAATTTCG  
 AGGACTTGGTCTGGTATTCCACCAAGACTTTAGCAGTTTCTCTTAACTAGGAGAAACAGGCCCTTCAATTCTCGAGGACTTCC  
 GGGGTTTGGCCGCTGGGGCTTACATGCTTGGATCCAATGCCATTGGGGGTCCTTGGGGGGGGGGGGGGGGGGGGGGGGGGGGGGGGGGGG  
 TATTCTGGGAGACTTACCCAGCACATGCTTATGGACCGGGGATCACGTTAGACTTCCGGAGGGGTGATTCCAGGGCTCAAAGGCC  
 TTTGTGGAATGCCACAACCTTCAGGGTCCAGCAAGCCCTTGGGGATCAAGCTGCTCCACTTGTGATCGCGTAATTCTTATGT  
 CGATCGGCAATTCCGATCGTCAGGGAACTCTAGAATTGGACAGAATTCTGTAATTCTGGTTATTGATTTGCTGCTGCTGCT  
 TCTGGCGAGACTTACCCAGCACATGCTTACGGGATCCCTGAGCTGGGAGCTTGGGAGGAGGAGGAGGAGGAGGAGGAGGAG  
 GTGGAATCGGCCACACCTTCAAGGTTGGTACGGGAGCTGGGAGGAGGAGGAGGAGGAGGAGGAGGAGGAGGAGGAGGAGGAG  
 TCGGCAATTCCGATCGTCAGGGAACTCTAGAATTGGACAGAATTCTGTAATTCTGGTTATTGATTTGCTGCTGCTGCT  
 TACATTGGAGAATTGGAGAACACTCGGAAAATCTAAAGGATATCTGGCTCCGGGATTCGCTGCTTGTGACTTCTCGCCTGCGATCAA  
 CTATAAAAGTAGCGCAAGCTCAAACCATGAAACGATCAGGTAACCGCCTCCCATCAAGCTCTCTAAGTGTAGAGGCCCAATTACCAAGA  
 ACTTTAAATGCGGTAGGGCCCTCCAGTTGGGAGTAAGCTGTGCTTCCGGGGCTCCGAGCTTGGGAGGAGGAGGAGGAGGAG  
 TGCAATCTCGGAGCAGCAACCTCTGGGAGCTGGGAGCTGGGAGGAGGAGGAGGAGGAGGAGGAGGAGGAGGAGGAGGAG  
 TCCGCAAAAGCTAGCTCCACCCCGATGGCTGTTCTCTTCTCTTCTCTTCTCTTCTCTTCTCTTCTCTTCTCTTCTCT  
 ACCGGCAACATTGCACTACCCCGTAGGTCTTCTTCTTCTTCTTCTTCTTCTTCTTCTTCTTCTTCTTCTTCTTCTTCT  
 GCCGGAAAGTCATCCAACCAAGCTCCCTAGCCTCCCGAGTCGCTGCTTGTGCTGAGGATTACCTGTTGAGGAGGAGGAG  
 CGTCCCTCGTCTCGGGATGCTCAACAGAGGCGAACCTCATCTGTATGCCATTCCCTTGAGAAGTCCCTTGTGAGGAGGAG  
 GTCCCATTGTCAGATACGATGCCCTGGGATCCGAACCTGCAAAACAAATACGCTTCAATAGAATTGACTATCTTGCATAAGTAC  
 TTGGCCAAGGGTCCGCCATCCATTAGTGAAGTAGTCCACCCGCCAACCTATTAACACTCTTGTGCTCCCTGGGGGGGGGGGGGGGG  
 CCTACTAAGTCCACACCCACATGGGAAAGGCCAACGGGCCAGGGGGCTCATGTTACCAACTCTTGTGCTCCCTGGGGGGGGGGGGGGGG  
 ACTTGTGACACTCTTCGACTGCTTCAAGGAGCTTCAACATCTTCTCTGAGGGGGGGGGGGGGGGGGGGGGGGGGGGGGGGGGGGGGGG  
 AAAGACCTCCCCGATGGCTCGCGCACACTCTTCTATGTTACTGACTTCAAGGAGGAGGAGGAGGAGGAGGAGGAGGAGGAG  
 AATGGCGTCGAGAACACCAGGCCATACAAGTGTCCGTCATGAGAGTATAGTGAACGCTGCCCTCCGCTGCTGCTCCTCTG  
 ACTCTGCGAGTCCCCCGCAAGATAGATATTGGAATCCATGTTCTCCCTCTGTTCACTGAGCTGCTGCCCTTCTGCT  
 CTTGGGTACGCCAGCTTCTGAATCACACTTTGTTATTGCGGGGCTTCCGCGTCTGGCCAGCTTGGCTAGCGCTGCC  
 TCTTCTGCGGAG  
 TCTTGTGACTGGAAAGTCCCTTCACTTGTGATTTCCACCAATTGTTGAGTCCGTTCTTATCAACAAACTCTGATCTT  
 AACCTCTGACTTCTCTGCGGAGGAGGAGGAGGAGGAGGAGGAGGAGGAGGAGGAGGAGGAGGAGGAGGAGGAG  
 AACTTCAATCCGGCGATGAGAGCTTCAATTCTGCTTGGTTGTTGCTGTTGAACTCAATTTCAGAGAGCTGCTCC  
 CCTGGCCCTCTAACGTTACTCCGCCGCTGACAGATCTTCTTGTGAACTCAATTTCAGTATGAAATGCCCTGCTTCT  
 TTTATCTGTAATGCCCTGCTCTTGTGTTCAAGGGGGCAAGTTTGTGATTGATGACATCACATCCAGAGGAACTGAG  
 GAAAGGGAG  
 GCGCGGGAG  
 ATGAAGCTCTATGCCGGATTGAGGAGGAGGAGGAGGAGGAGGAGGAGGAGGAGGAGGAGGAGGAGGAGGAG  
 AAGTGAAGGAAACTTCCAGGTCAAAGATCTTAATCTGATCAAGTACCTTGTGAGCGGGTACGGTATTGATG  
 TGGTGGAGTACGTTCTCGGGAGGAAACTAGTGTGAGGAGGAGGAGGAGGAGGAGGAGGAGGAGGAGGAG  
 TGATTCAAGGAAACGCTGGCGTACCCAGCATGCAAGGAGGAGGAGGAGGAGGAGGAGGAGGAGGAG  
 CTATCTGGCGGGGGACTCGGCAGAAGTGGAGCAATGCAACGAGGAGGAGGAGGAGGAGGAGGAG  
 TGTATGCCGTGGTTCTGACGCCATTGTTGAAATGTTGACTCCGCCAGAGAAGTACGAGGAGGAGGAG  
 GCGCGAGGCCACATGGGGGAAGGTCTTGACTTGCACAAAGTGTGAGGGCGGGTTTACTGCCACCCCTCAGGAAAGATTGATGGACT

## APPENDIX

## APPENDIX

AACTGGATTACAATGGTCATCAAATTATTTCTCTGGGCTGACTCTGACATATAATCATTGATCATGTGAGGTATGAATCC  
CATATTGGAGATCCCTTGAGCACTCGAATTCAAGGTTGCATGGAGATACAGGAAAAAACGTTAACGTTAACCTCATAA

## L. japonicus CNGC2 Putative Coding Sequence

ATGGATAATTGAAAAAGATGGGGTCTGTGCTGAGAACACATGTACAAGTATCTGATAAACTCATGATTATAATTCGGAGG  
CCTGTATCAAGGACAAAAGAATGAGCAATTCTATTCCCATGATATCCATGGAGTCACATCAGAATGAAAGTAGCTTAAGGAACACACT  
AGCCCATTATGTAGTGAGGAGAAAATCCCTGTAGCAGATGAGTTATCCGCTATGGTACTCATGAACTAGAAATCTTTGCAGCAG  
ACAATGGTGTGAAAGAAAACAAAGTATCAGAGAGAAAAGAGAAAAAAATTATACATTTCCACGGCACAGGTGAGCGCACTGGAAATAGT  
AACAGCCCTGATAAAGAAAATGACACTTGTGGAGACTGGGAACCTGGAAATGTGTGATGATCCTTATGGTCACTACTTGTCCACTGAC  
TTCAAGGCTCTAGGCCAGAAAACCTAAAGTTCCACTGTATTGTATCCCAGTCTCTTTATGGTGAAGCCAAGGGTTT  
GGGAAAAAAACTTACGTCTTTCTCGTCATGTATTCCCGAGATAATGAACCCCTACACTAAAGTGGTACAAAATGGAACAAATTTC  
GCCATCTTGCCTGGCAATTGGTGGATCATTGTTCTTTCTTAATCTATGTGCAAGCAGGACTATAATGTATTCTTATCAC  
TGGAAATATGCAAGAACACTAATTTACTCAGAACCCATAATGATTGTATACTCTTGTAAAATTCTCTCAGTTAGGTTGGCCTAT  
ATTCTCCTGACTGCAAGGTGGTGTGGCTGGAGATTAGTGTGATGATCCTAAGAAAATTGTGTCCATTACTTGAAGGGTTATTATT  
CTTGACTCTGTTGTCTGGCTCTTCCCTAGATAATGATACATCTACCTTACAGGAACTTGGGGTCTCGGGGACAAATTATGCT  
AAGAATCTTTGCGTCAGTGATACCTGTCAGTGATATTCCCAAGGCTATTAGGGTCTGCCTCTGCTAATGGCCAGTCTAACAGGA  
TTCCATTGAGTCATCATGGCAAATTTCATTATAAAATCTTCATGTATATGCTGCTAGCCATGTTGGCTCTGGTACCTC  
TTAGGTCTACAAAGGTTAATCAATGTTACGAGATGCCGTCAGTAAGTCTAATATTAGTGGATGCTTAAAGTCATTGATTGGTAA  
GGTCATATTGGATATGCCAGTCTGGCCAACACAGTTGTCAGAACACAATCCAGATGCCATTGCTGTTGAAGCCCTCTCTAGT  
GGATTGATTATGGGATCTACGTCATGTCAGTACACTTACTATAGAAAACATTGGTGGAAAAAATATGTTGACTCTCTTTGGG  
TTCCAGCAAATCAGTCTTCTAGCTGGTAGCTAACCCCAAGCTATTGGTGGAGCTCTTGCATGGGCTAGGGCTAGAG  
CTCTGCTTTGCACTCTTATCGGAAACATACAGAATTCTTCAAGGCTTGGAGCAGAGGAGGCTAGAAATGCTAAAGGCCG  
GATGTTGAGCAATGGATGAGGCATGGTCGCAATTCCAGAAGATTAAAGAAGGAGATACGGCAGGGTACAGGTATAGTGGTGGCAACA  
AGGGGAGCGAATGAGAAAACACTTCTGAGAATTGCCAGAAGATTACAGATGCACATAAGCGTCATCTCTCAAATTGTTAAAGAAA  
ATTGCAATTCTCCCTAATGGATGAGCTATCTAGATGCCATTGTGAGAGACTAAAGACAGAACATACATCAATGGAAGTAGAAC  
TTGAGGCCAGGGTGGTATGTGGAGAAGATGGCTTATTGTGCGCGGAAAATTAGAGAGCATTGGAGAAGATGGAATTGAGTCCGTTA  
TCTGAAGGGGATGCTTGTGGTGAAGAACCTCAGTGGTACATGGTACATGGTAAAGCAGAGTGGTAAAAGGTTAAC  
GGACAAAGGTGCTTAGCAGAACACTGGCAAGTGCCTAACAAATGTCAGGGCTTTTCTACCCGAGCTACAGATCTGAAGAAC  
ACCTTTTATGAGAACCTGGCGAGTCTACGTTCAAGGACCTAAGGTATGAATCCCCATATTGGAGATCCCTTGAGCAACTCGA  
ATTCAAGGGTGCATGGAGATAACAGGAAAAACGTTAAGTCTGCTGATACCTCATAA

## L. japonicus CNGC2 Putative Protein Sequence

MDNFEKDGVPVLSETHVQVSDFKLIDYFNFRRVPSRTKNAISIPIISMESHQNESSLKEHTSPCLCERKNPLMQMSYPILYGTGHCTRNLQQ  
TMVVKENKVSERKTEKNTFHGTGERHWNNSNPDKKNEHLWKSGEGLGMCDDPYCTTCPTDFKASRRRNKSVSTVFDPKFRSSLYGEAKGF  
GKKLTSFFSSCIPGVVMNPHTKVVQKWNKFFAIFCFLVAIFVDPFLFFFLLIYVQODYKCILINWKIAETLILLRTINDFVYFLKILLQFRLAY  
ISPESRVRVVGAGDLDVDPFKIVVHYLKGYFILDLFVVLPLP0IMILSILPRNLGSSGANYAKNLLRAVILVOYIPRLFRRVLPFLNGQSPPTG  
FLFESSWANFIINLLMMLASHVVGCSWYLLGLQRVNQCLRDACSKSNISGCIKVIDCGKGHIGYSQSGPTVVWNNAADAIACLKPSPS  
GFDGYIGIVNAVPLTIETNLVKQKYVSYLSFWGFFQOISTLAGSLTPSYFWWEVLFAMGIIGLGLLLFALLIGNIONFQQLGQQRREMLLRAR  
DQEVOQMRHRRIPEIDLRRVQARYSWSVATRGRANEETLLENLPDLQIDIRRLFKVKKIRIFSLMDEPILDAICERLRQKTYINGSRI  
LSOGGIVEKMVFIDRKLESIGEDGIRVPLSEGDACGEELLTWYEHSSVSTDGKVRLPQORLLSSRTVKCLTNVEAFSLRATDLEEVT  
TLMFRTLRSRLRFQGPLRYESPYWRSIATRIQVAWRKKRLSLADTS

## *L. japonicus* CNGC3 Genomic Sequence

ATGGCTCAATTGATAAAAGATGAGGTGCCAATGCTGTCAAGAACACCGCCTACAACATTGATGAGCTCGAGGATTAAATGTCGGAGGTTCTCATCCAGGACCGAGTGCATCAATGCTATTCCCTATGGCTCCATGGAACCATATGATACAAAACCTAATCTCGTTGGACATACC  
GGTCCACTTCGCACTTGAGAAAAACCCCTTTGTGCAAGATGAGTGGTCAACTATATGCTACTCCACGCTGAACTGGAAATCTTTGCAG  
CATAGTATGCTGGGGGGAGAAAAAACAGCAGAGAGAACACCGATGATTTCCTACTTTGATGTTGAGATGAAATCACTGGAA  
AACAAACATGATAAAAATGAAACACTACTGAGGCTGTCAGTGGGAGCTGGGAAATGCTAATGATCCATATGTCACACTTGCCTACTTAC  
TTCAGGCTTCTCAGAAAAGAAATCCTAAAGCTCAACTGTTATGATCCAAGGTTCTTCTCTCTAAACTAGACTCATGTTGGTCA  
TAAATTATAAAAATATTCTATATTGAAATTGACTTTTTGACTGCATCATCATAAACTTTATTATAAGGTTGATTTTGT  
GCTATACATCTTACTCTAGAGTCTGTGTGATGATCTTTCTTTGAAATAATTAGATATTGTTAAATTGACTGTGCTATT  
ATGTTTCTCAGTGCCTATAATTTCATATGGCATGCTAGCCTATAATTACTCAAGGTAATTAGTCCCCTATAGGAC  
TACTTTCTGTTGAAATTCAAGGCTATCTTCAATTCTCTTCACTTCAATTAAACCAAGGAAATTTTATCATGTTGGATG  
TTTACAGTTCTATAATTCTTCTTATGGGATGCGAAAGGTTTGGAAAGAAAATTCTTCTCTCTCTCATGTTGGAGGAT  
GAACCCGCACTAAAGGTGACACATTGGAACCCAGATTCTGGAAATTTTCTTCTGGTGGCAATTGGTGTGATCCCTGTTCTT  
CTTAATTATGTGAGAAGGTATTCTTTCTTTATTAAATTAAATTCAAGGTTTAGTATTACATACTAATTCTCTT  
CTTCTATAGGGAAATTACTCTACTTCTCCCACTCATTGTCAGGATTCTAAATGATTGCTATCAACTGGACAATGACAAAAA  
CAATTGTTCACTTCGAAGCATAAATGATGTTGATATTCTCAACATTCTGCAAGGTAAATTATCAGTAACCACCTTGGAAAT  
TCCCCCTCAGCATCCCTTACATTCTGCTAATTCTATATTCTCATAGATGTTGATATTATCCTGCAACAAATAACATATAACAA  
CAACAAAGGCTTCTACTAGGTGAGGGTCTGATACATGGCAACAAATGCCATGCTGGTCTGGAGATCAAGCTAATTAGTC  
ATTTTAACTACAACCTTCTGATGGCTTGGCTTATATTCTGGTCTCTCTCTCTCTCTCTATATATATATAAAATA  
TATATGTATATATATATATAACTTTGGACTGTTCCATCCGGTTTACCTCTTACTTGATGCGATGTTTATTATCAATT  
TTACTGGTTTGAGAAGGAAATATGTTGATAAAATGTTAGCAGAAGAACTTGTAGCAACATAAAACAGGGTTAGGTTGATCGTGC  
ATCACCCGCAATTGTTACAAAGAGTAATTAGATCATTGAAAGGTCAAAGCATGCTGAAACATTCTCTTCAACTAAGTATATCTAGC  
AAATAATGAGGCTGATTGTTACAAAGATTGATTGTTGGCTGAGTCTGTTAATGCCACACAAAGAGTGGTGCAGCATGCCATCAT  
ATAGTCTTCTACATCTCAAAAGATATATTACTGGATACAGGGTTGTTTCTTAACTCTCTCTCTCTCTGTTGGTAAACCTCTG  
TTAATAGGAAACAACTGTCAGTTGGATGACTTAAGGTTACTGACTACTTGCTTCAACTTAATTAATGATGAACTCATATAGAAAA  
TTTAATAGATGGAGTGCAGAAGAAACAAATAGCTGGAGCAAGCATACTAAACATTCTCATCAGGAAACCTTTTTTAAATTGCA  
AAATCAAACCTTCATTAAGATATATGAGCATATCATGGTATCATGATAAGGATTGATATGAGTGGATATGGCTTCTCATTTAATTGCA  
TTAATAAAAGCCCTGATACAGCTTCCGCTTCAATTCTCATCATAAAGCAATAACCAATGCAATTCTCTGAGTCATCAATT  
CACTCCCTAGGTGAGAATGCAAGAATTTCAGATGAGATTCTCTTACCTTCAACTTAACATGCAATCCATTGAGCT  
TGATCATATTCAACATACAAAATATACAAGGATCAATTGTTGATACCTTGGAAATGAGGTTACTCTGTTAGGTTAGGTTAGG  
CAATGATAAAAGACTTTATTATAATGTTAATGTTAATTCTGAGTACTCTAATGGGACATAATGTTAGGTTAAATTAGTATTACT  
TACTTTTGACTTATTCTCCACCTCATTAATGTCAGTGTGAATCTGTTAGATCCGCTACCTTAATTTC

## APPENDIX

## L. japonicus CNGC3 Putative Coding Sequence

ATGGCTCAATTGATAAAGATGAGGTGCCAATGCTGTCAAGAACACCGCCTACAACATTGATGAGCTCGAGGATTTAATGTCGGAGGTTCTCATCCAGGACACGGAGTGCATCAATGCTATTCCCTATGGCTCCATGGAACCATATGATACAAAACCTAATCTCGTTGGACATACC  
GGTCCACTTCGCACTTGAGAAAAACCCCTTTGTGCAGATGAGTGGTCACTATATGCTACTCCAGCTGAACTGGAAATCTTTGCAGCATAGTATGCTGTGGGGGGAGAAAAACAGCAGAGGACACCGCATGGATGTTTCACTTTGATGGTCACTGGAA  
ACAGATGGTCACTGGGGGGAGAAAAACAGCAGAGGACACCGCATGGATGTTTCACTTTGATGGTCACTGGAA  
ACAAACAATGATAAAGAAAATGAAACACTTACTGGAGTCTGGGCACTGGGATGTAATGTCATATGTCACACTTGCCTACTTAC  
TTCAAGCCTTCTCAGAAAAGAAATCCAAAGCTTCACGTATTGATCCCAAGTCTCATATACTTCTTATGGGGATGCGAAAGGTTT  
GGAAGAAAACTCTTCTCTGCTTCTCATGTGTTCTGGAGTTATGAAACCCGACGCTAAAGTGTACAACATTGGAACCAGATTG  
GGAATTCTTCTGGTGGCAATTGTGATCCCTGTTTCTTAATTATGTAAGAAGGATTCAAATGTAATTGCTATCAC  
TGGACAATGACAAAAAACATTGTTCACTTCAAGCATAAAATGATGTTGATATTCTTCACACATTCTGCACTGGTTAGGTTGGCTTAT  
GTTTCACCTGAGTCACAGTGGTTGGTCTGGAGATTGGTGCACCATCCAAAATGCTCTTAATTACTTGAGGGTTATTGTTG  
TTGCACTTATTCTTGTATTACCTCCTACCTCAGATTGATATTGTTGCTACCAAAATCTGGGTCATCAGGGACAAATTCTACT  
AAGAATCTTCTACGTGCACTGGCAGCTTGTCAAGTATATTCCAGATTTCAGGGTTGGCTCTGCTAATTGGCCAATCTCAACTGG  
TTCATATTGAGTCAGGCTGGCAAACATTATAAAATCTCTCATTTTATGCTATCTGGCATTCTGTTGGATCTGCTGGTACACTC

TTTGGCCTACAGATGCCAACTTACCGTCTGGAGCATCAATGAAAATGCCACTGCTTGGATCCGCATCTAAATGCTTCCTT  
 TATGGGATATATGACAAGCTGTGACTTACTACAGAAACTAGGGTGGTCAACAAATATGTATGCGCTGTTGGGCTTCAACAA  
 ATCAGTACTCTGCTGGAATCAAGAGCCTAGCTTTGGGGAACTGCCTTACATAGGATCTGGACTCTTCCTT  
 TTTGGCCTCTCATGGAAAACATACAGAACATCTTCAGGCTCGCCAGGGCTAGAGATGCAACTTAGAGGCCGTGATGTTGAG  
 CAATGGATGAGCCATCGCCTACAGACCACATCTAGAGAGAGTCACTGGAGGCTGAACGATATAGTGGGCTGCAACAAAGGGGTT  
 CATGAGGAAATGCTTAGAGAAATTGCGGAAGATCTCAGACTGACATAAGACGTCACTCTCAAACATTGTTAAAAAGTTGAATT  
 TTTGCCCTGATGGATGAACTTGTAGATGCCATTGAGAGACTAAACAGAACATACATCAAAGGAAGTAGAATTGACTAGG  
 GGTGGCTTGTAGAGAAAGATGGCTTGTGCGGAAAATTAGAGAGCATCGGAGAACATGGAATTGGAGTCCATTATCGGAAGGG  
 GATGCTTGCTGAGAACACTCTCACATGGTATCTGAACATTCTCTGTAAGCAAAGATGTTAAAAAGTAAGGCTCCAGGACAGAGG  
 TTGAGAGAACAGAACAGAATTGCTAACAAAGTGGAGGATTTCACTCCGCTGAGATCTGAGAACAGTAACAATTCTTTC  
 ACAAGATTCTGGAGGCCCTCAAGTCCAAGGAGCTTAAGGTATGATTCCACTTGGAGATCCCTGAGCAAACAGAACATTGAGTT  
 GCATGGAGATACAGGAAGAACGCTAAGTGTGTAATACCTCACAAGGGCTTGA

#### *L. japonicus* CNGC3 Putative Protein Sequence

MAQFDKDEVPMLESETRAQQFDELEDFNVRFFSSRTRSASMSIPMVSMEPYDTKPNLVGHTGPLRSLLKKTPFVQMSGPLYATPAGTGMLLO  
 HSIAVAGEKTAESNTDDFSTFDGSDENHWNNNNDRKNEHLLRGQLGMCDNPYCTCPYKPSQKRNPKAFTVFDPKFHNFLYDAKGF  
 GRKLSSLCSSCPVGVMNPHAVVQHWNQIILGIFFLVAIFVDPLFFFILYVKKDSKCIAINWMTKTIVSLSRINDVVFNNILLQFRLAY  
 VSPESTVVAGDLVDHPKKIALNLYLKGYFLFDLFLVLPQIMLFVLPNSLSSGANSTKNLLRAAVLVQYIPRLFRVLPLLIGQSPG  
 FIFESAWANFIINLLIFMLSGHSVGSWCYLFLQMANSLRSWINENATACLDSASNAFPYIYDKAVALTTETRVVNKYVYALFWGFOQ  
 ISTLAGNQEPYSFYVWEVLFMIAIGSGLLFALLIGNIQNFLQALGRRLDEMQLRGRDVEQWMSHRRLPDHRRRVREAERYSWAATRGV  
 HEEMLENLPEDLQDIDRRHLFKLVKKVRFALMDEPCLDRAIRLKQKTYIKGSRILTRGGLVEKMVFVVRGKLESIGEDGIGVPLSEG  
 DACEELLTWLEHSSVSKDGKKVRLPGQRQLQSNRTVKCLNVEGFSLRAADLEEVTILFTRFLRSPQVQGALRYDSPYWRSLAANRIQV  
 AWRYRKKRLSRANTSQGL

#### *L. japonicus* CNGC4 Genomic Sequence

ATGGCCAGTTGAAAACAATGAGCATCCAACACTATTAGAAAAGTGGAGAACATCATATGGTGGAGGCCCTGCATACAAGATTCCAAGA  
 CTTGCATCCAACACACAAAGTCATCATGTTCTATCTCATTGAGTCATATGAAAAGAACATGCTTGTGAAACAAAGGAGTGGAACT  
 GGAAATCTTGAAACAGAGTATTGTTAACCGGAAACAAACACAGAGGAAAGCAACACAGGTTGATTACTCGGATAAAAAGTATGAT  
 AGAAATAATGAAAATTACTGAGATCTAGGCAAGTGGAAATTGTAATGATCTTGTTTCAACACATCGCAACTAACTCCAAGGCTCT  
 CACTCTCAGCTAGTTCTCAAAGCTTCGACTATTCTGATTCTGAGGTTAATGTTACTTCTAGCATTATGTTGATTACTTCTAGCATTG  
 ATTCTCTCATATCTCAAATATTCTCATTTGAGACATTGTTGAGGTTAATGTTGATTACTTCTAGCATTATGTTGATTACTTCTAGCATT  
 ATGTTAATATGTTGAATGTTCACAGTCCATAATGTTATGGAGATGCAAAAGGTTTGGAGAAATCATATACTTACTCTTGT  
 TCCTGGAGTCATGAACCCCTCACACTAAGTCATACAACAAATGAAACAAGGTTGGCCATTGGTGCATTTGCTTGGTGCATTTGTTGATCC  
 ACTATTCTCTTACTCTATGTGCAACGGGTATGGTAGTTCTCTTATTGTTTATAAGCTCTCGAAGTTTGGTCTATTCTCAT  
 TATATTTCTCTGACTTTTGCAAAATTACTTTGCAATTGTTCTGTTGTTGTTGATGAGGTTAATGTTGATTCTCAT  
 TTGAGCAAAGCACTGTTATAGTCAGAACAGTAAATGTTTAACTTCTGTTGTTGTTGTTGATGAGGTTAATGTTGATTCTCAT  
 TTGAGCAAAGCACTGTTCTAGCAGGAAATTAACATAACAGGCAAAATGAGCTTACTCTGTTGTTGTTGTTGATGAGGTTAATGTTG  
 CTGAGTACTGCTCTAGCAGGAAATTAACATAACAGGCAAAATGAGCTTACTCTGTTGTTGTTGTTGATGAGGTTAATGTTGATTCT  
 TAAGCATGCCGTGTCATGACATCTGAGTTACCCCCACTATTCTACAGCCACACTCATTGAAACTATTCAACCTATTAT  
 TGTTGAGTACATTCTCTTATCCACAAACTCAAGAGTATTCTATTATTTGGAGAAGAATATTATTATCATAGCTTAC  
 ACTCTTAAAGTGGATTAGGTCTATCTACCGCAAAAGCTAGGTTAGGGAGAACATGCTTACCCCTTATAAGGATTATTGGCC  
 GTATCTCTAGTCATGAGACTTTCAACACACCTCTCACGCCCATGACTAGGCATTGGAGCGTGAATTCTAGACTGAATATCT  
 CGGGGTGACCTATATGAGCGGTCTCAAAACCGGATCTAGAATTGACTCTCATATCATCTTAAAGCTTGAAGGTTAGGCTTAACCTAC  
 CCCCCAAGCTATGCGAGGGTGGACTGCTACCCCTTATAAGGAGTTATTCTCATATCTAGCATTGAAACTATTCTCAACATATA  
 CATAGCAATTGAGAAAATAAAAGTGAAGTGAATTGCAAGCTTACAGTGAATATAGATTGGTATAAGCTTATCTGTTATTGAG  
 TGTTGTTGTTGTCATGAATCAACTATTCTGAAAGCTTAGGTCAAAACACATGAATTAAAGCTTGAATCTAAATACGGTTGTTAAATT  
 TAAGTCTGATTGCTGCTTTCATCACTTAAGGTTGAATAACTGAGTTGCTTGGCAGTTAGGTTGGCTTATGTTCTCTGAGTC  
 GAGGGTGGTTGCTGAGATTAGGTGACCATCAGGAAAGAAAATCGCTCTTCATTACCTGAAAGGGTTATTGTTTATTGACCTGTTAT  
 TGTGTTCTCTCTCTCAGGAAATTCTCTGATCTGACTCTTCTCTATGAGGTTATTGCTACTGATGTTAGCTCATATT  
 AACCTAGTATACTTGTCTATCCAATTGCAATGTTGAGTCTGAGTATGAGGTTATTGCTACTGATGTTAGCTCATATT  
 TCATTCTCTTGGAGATCATGTTAGTGAATCACACATATTCTGGTCAATTCTACAGTAAAGTGTCTGTCAGTAAATTATGAGT  
 TCTTGTATTTGACATAAAAGATAAAACATGAAGATCCTGGTGGTGCATTGGAGATAACCAATTGGATTATTGGGTTTACA  
 TATGTGAGATTCAAGTTATAAGGTTCCCTCAAACATGGATTAGGGTTCTAATGGATTATATCTCTGCTATGGCAAGGTCCAGG  
 GAGGGGGCCGACGGGACCAACTTCTGAGTCTAGGAAATCTTGCATTGGTCAAGAGGTTATTCCACAGCTCGAACCTGTGACCCGAGA  
 GTCACATGCCAGCAACCCCTACCATGGAGCAAAAGGCTACATGCCAGGAAAGAAGCTTGTAGGGTTGATGAGGTTCCATCGTAATT  
 TGTTGTCAGGACTCTCTGGTCTGCAAGGTAGTGAAGAAATGCAATTCTGATGTTCTTCAATTGTTCTTCAATTCTGCTTCAATT  
 AAAAACCTTCTCACTTGAACACTGCTGACATGACATATGTTAGTGAATATGTCAGATAATGTTATTGTTGTTGCTTACAGAATT  
 AAATGTGCTGAGAACATGTGCTGTCATGACATATGTTAGTGAATATGTCAGATAATGTTATTGTTGTTGCTTACAGAATT  
 GGAGCAAATTGCTAAGAACCTCTGCGTGGTGTACCTAGTGAACATACCTCCAGATTTCAGGTTCTCTGCTCAATT  
 CAGTCCCAACAGGATTCTATTTGAGTCGGCTGGGCAATTCTTAAATTATCTCTCATATGCTTGTAGCAGTGTGTTGGC  
 TCTTGTCTGAGCTTCTCTGGTCTGCAAGGTAGTGAAGAAATGCAATTCTGATGTTCTTCAATTGTTGCTTACAGAATT  
 ATGATATAAAATATATAATTAACTTACCGAGTCTCTGCAACTATTATGAGCTACCTGAGTACCTGAGTAACTGTTGCTATGACCAATCA  
 GGGTGGGCTCTCCATAATGAAGTTGATTCTCTCAATAGGTTAAATATCTCTTAACTGCGGAGATAAGATCCTAAACATCTGTTG  
 TGGATGATATATAATAATATGTTAGGTTATTGATCTGCTTGTGAGTGGATTCTCTGCTTAAATTCTGCAATT  
 TTCGTAGCCATGTGATCAAGATTAGACGGTTCAAAATTAAAGGATTTAGGTGTTAGCATCAATCTCTTAAACTTAATTGTCAGAT  
 TTCGATCAGATGGTTATGAGTCAGTGCAGTAAATTAGGAAATTAAAGCTGAGTAACTGAGTAACTCCAAATCCGAGATTATGGCTAAATG  
 AAGTGTGCTGTCATATGTTAGTGTGAAATTGAGCTTCTGCAACTATTGTTACTGCAATTGTTGAAATTCAACCATCC  
 AAGTTGTTATTCTCTTGGGTTGAATGAAGGAGGTTAGAATGAGGTTATTGCTAGTAACTGAGTAAAGGTTATTGATCAATT  
 TTCTCTCTCTGAGGGTTAATCTGAGTTAGGTTAACTGCTGCAACAGTCTAGTGTACCTGGATGCTGAGATTCAATT  
 GATTGACCATGATAGAAACTATCTCAAGGGCCCAATCAGAACAGTGGAAACAACATACAGTGTATTGTTGTTGGGTTCCCTTC  
 CACTGGTTCTTGGATTATGGGATCTATGGCAATGCTGCGCTTACTACAAAAACAGACATGGTACCAATTGTTGTTGTTGGGTTCCCTTC  
 TTGGGGATTCCAGGTATGCTTCTTATTATTTATAATTATGTTCTCTTCTGAGTTAGTGTACATATTGTTGTTGTTGTTGGGATCA  
 GATGAACTAGTGTAAAGCTTGTGATGCCCGCAGCAACTCTATTGTCATGTTAGTGAATGAGGTTATTGATCAATT  
 TATGTTAGTCTAGTATAATTCTAGGAAATTGAGTACTAGAAGGAAATATAACAAATCAT  
 AAAGATTTAACCTTGGGATGAAGCTATTGAGTAGTACACTAGAAGGAAATAAAAGAATTGTTGATAAGGTTATTCTAACGGAAACAC  
 TGACAAATCTCGAGTTCAATGCACTCGATCAATTACTACACTGTTAGTATTCTGGTGGCTCCCTCCTCAATGTACATTGCA

## APPENDIX

CGAATTCCGAGGCATAAAATCCAACAGATGTGATGGTTGGATGGACAAACGGCTTACATTCAACCAATTAAAACAAACACT  
TAGTCACATAGGAACCTCAACTGTTGACATGACTCCTTTCAGATAATATCAGTTTCCACCTAATAACCAGGGATCAACTACTAAC  
ATTGTTAGATAATGCACATGAATGGCTAATATCTCAACAAATTATAACAATATATGATTTTGACAGCAAATCAGTACTCTGGCTGTTAA  
TCTAACACCAAGCAATTGTTGTTGAGGACTATGCCACATTGGATTGGACTCTTGTCTTTGACTCTCATGGAAA  
CATGCAGAATTCTTCAAGGTCTGGACGGAGGTAGAATCTTCAACTAGGAAACTTTAAGTAAACTTGATCATCAATGGTTATAG  
TGTGTTATATGTTGATATATTCTTCAACCCCTTACAGGAGACAAGAAATGCAACTTAGACGACGTGAGTTGAGCAATGGATG  
GATACAGACGATTACCGAAGACTAAGAAGGTTAAAGCTCTTATTCTTCACTTGTGATTGATTTCTGATTCAAGGCC  
TTGAGTGTAACTCCCACCCCCATCCCTCAAACCTCTTGTGACAATGTATGTTAGAAGTCTCTGCTCTAGACGCAAGGACT  
GTTTGATGATGACTAGATAACTCTGCAAGGTTATTTGAGTTGAATAGGAAAGGATAATTAAATTCTTGTACAGTCTGGGTATTCTTAGC  
TGTGTTATTTCTTCAAGGTCTGGACGGAGGTAGAATCTTCAACTAGGAAACTTTAATCTTCACTTGTGAGTCTAGCTAATAATGAAATTGAT  
CGTCATAATGAAAGATCTGCAAGACATCTTACTGGGATCTTAAATTCTTCACTTGTGAGTCTAGCTAATAATGAAATTGAT  
CCAATGTCAGTAATGAAAGAAACCCGGCTTGTGCTAAGTAAGAACTCGCTCGAGTCTGTGAGATGAAAAACCCCGCTGAGAG  
CTAGTTAGCCCCACCAAGATGTGGGTGATCCCAACTCAAAGAGGATTGCCCTCGAGGAGGAACTTGTATTAGACCAAAATAAGA  
GCAATCTATAATAGCATGAGTTATGAAATTGATGCTATTCTCATTCTGATAGTCTAGGTTATTAGTGTATGAAATATCAGAT  
CAAGCACAACATATAAGTCATACATAATGTTGATGCAAGGAGAGTAAGGCAAGGCTGAAACCGTACTTGGCTGCGACACGGGGGTG  
AATGAAAGAAATGCTTATGGTGAATCTCCAGAAGACTCCAAAGAGACATTAGACGTCACCTCTTCAATTGTTAAGGAAAGTAAGCAGT  
AGAATACTTTATAATCACACATAATGTCAGCTTGTGACCTTGAGTTAATATGTTAGGTTAGCTTAAACGTTAAACGTTAAACGTC  
GCCAACCTGTTATTTGAAATTCTGATTTCTTGTCTTGTGAACTGCTAAACTGGCTTAAGTCTAGGTTAAACGTTAAACGTC  
TTGAGGAAAATTAAATGATCTTGTGAGGATCTATAACTTGCAGGTTGATTCTCCGTGATGGATGAGCTATCTAGGCTGAGAGACTAAAA  
CAAACATACATACAAGGAAGTAGAGTTCTGACAACAGGTGGTCTGTAGAGAAGATGGTATCTGTGGCGTGGAAAATTGGAGAGC  
ATTGGAGAAGATGAACTAGAGTTGACATTCTGAAAGGTGACGTTGAGTTGAGAAGACTCTGACATGGTATCTGAGCATTCTGTC  
AGCAGGATCTAACATGCACTTAAAGGACTTGTGAACTTGTGAACTTGTGAACTTGTGAACTTGTGAACTTGTGAACTTGTGAACT  
TTGAGTATAACAAACAAACAAAGCTTACCTTCAACTAGGCTGGCAATTCTGAGGTTGAGCTTGTGAGTGGGAAATTAAACTTCA  
GGACAAGGGTTGCTCAGCAGTAAACAAAGTGTGAACTTACAAATGTCAGGAGCATTCTGGGGCCGAGCCTAGAGAAGTCACA  
CTTCTGTTACAAGATTCTGACAGTCCTGTTGCAAGGAGCCTTGAGGTCATTCCCTGTTCTGTATCTGGATTAGGTTAGGGCGT  
TCAGCATAATCTTGTGACCAATTAGTGAATACAATAATGAATAACTAAGACAACAGGCTTGGCGCAACAGTAAGTTGTTGTC  
TGACTTTGAGTTACCGGCTCTAGTAATAACACTAAGTTGCTTCTTACAATAATGAAAGACTAATGTCATAAGACACAACAGTTC  
TATCTCAGTCTCATATTGTTAGAATAGCATTACATGTGTTTAAACACTAGGATTCAACTTCCATTTGAGTGGCTCATTTCA  
AGAGAAGGGGAATTTCACAGGTGAAAGCTAACATTCTGTTTACATCCATGGATGACATAACTTGGGCTCATTTCAATTGTTAGGTT  
ACTTTAGGTATGAAATCACCATATTGAGATCCCTGAGCAACACGATTAGGTTGATGGAGATACAGGAAGAAACGTC  
CTCATTGTCATTATCAGGTTG

### *L. japonicus* CNGC4 Putative Coding Sequence

ATGGCCAGTTGAAAACAATGAGCATTCAACACTATTAGAAACTGAGGAACAATCATATGGTGGAGCCCTGCTACAAAGATTCCAAAGA  
CTTGCATCCAACACACAAAGTCATCATGTTCTATCTCATTGAGTCATATGAAAAGAAACTAGTCTTGTAACAAAGGAGTGGAACT  
GGAAATCTTGCACAGAGTATTGTTAACCGGAAACAAACCCAGAGGAAAGCAACACAGGTTGATTACTCGGATAAAACTATGAT  
AGAAATATGAAATTACTGAGATCTAGGCAAGTGGATTGTAATGTCATCTGTTACCCACATACGCAACTAACCTCAAGCTCT  
CACTCTCAGCTAGTTATCCTAACCTGGCTGACTTCTGATTGCAAGTCTTCAATACTGTTATGGAGATGCAAAGGTTTGCAGAAAT  
CATAAATTCTTCACTCTTATGTCCTGGAGTCATGAACCCCTCACACTAAAGTCATACAAACAATGGAACAAGGCTTGGCCATT  
TTGGTTGCAATTGTTGAGTCACTTCTTCTTACTCTATGTCACCTGGCAACGGGATTGTTAATTGTTAGGCTATCAATTGGAGATTGACA  
AAAGCACTTGTATAGTCAGAAGCATAAATGTTTATATTCTTAAACATTCTGTCAGTTAGGTTGCTTATGTTCTCTGAG  
TCGAGGGTGGTGGTGGAGATTAGTGCACATCCAAAGAAAATGCTCTTACCTGTCAGGGTTATTGTTATTGACCTGTT  
ATTGTTGTTCTCTTCTCAGATAATGTTATTGTTGTCCTACAGAATCCATGAGGGGACCAAATTATGCTAAGAACCTTCTGCGTGC  
GTGATCCTAGTGAATACATTCCAGATTTCAGGTTCTCTCTGCTAATTGGCAGCTCCAAACAGGATTCTGAGTGGCCT  
TGGGCAATTATTATTCATCTCATATGTCCTGGAGTCAGGCTTGTGGCTTCTGTCAGGGATTCTGGCTGAGGGTT  
AATCAGTGTGTTAGAAATGCTGCCACAGTTCTAGTGTACCTGGATGCTTGTGAGATTCTGGATTGACCATGATAGAAACTAT  
CTCCAAGGGCCCAAATCAGAACAGTGGAAACAACAACAGATGCTATTGCTTGGGGTCTCCACTGGTCTGGATTATGGG  
ATCTATGGCAATGCTGCTCTTACACAAACAGACATGGTACCAAATATGTTATTCTCTATTGGGATTCCAGCAAATCAGT  
ACTCTGGCTGTAATCTAACACCAAGCAATTGTTGTCGGAAAGTCTTACTATGGCACCATTGGATTGGACTCTGCTATTGCA  
CTTCTCATGGAAACATGCAAGATTCTTCAAGGCTTGGAGGAGACAAAGCAACTAGACGACGCTGATTGAGCAATGG  
ATGAGATACAGCATTACCGAAGACTAAGAAGAGAGTAAGGAGGAGCTGAAACGGTATCTGGCTGCGACACGGGGGGTGAATGAA  
GAAATGTTATGTAATCTTCAAGAGATCTCAACAGACATGGTACCTCTCAATTGTTAAGAAAGTCGATTATTTCC  
CTGATGGATGAGCCTATCTAGATGCAATTGCGAGAGACTAAACAAACTACATACATACAAGGAAGTAGAGTTCTGAAACAAGGGGGT  
CTGGTAGAGAAGAGTGGTATTGTCGGCGTGGAAAATTGGAGAGCATTGGAGAAGATGGAAGTAGAGTCTCATTATCTGAAAGGTGACGTT  
TGTGGTGAAGAACTTCTGACATGTTCTGAGCATTCTCTGTCAGCACAGATGGGAAAAAAATTAAACTTCCAGGACAAGGGTGC  
AGCAGTAGAACATAAAAGTGTGTTAACAAATGTTGAGGACATTCTACTGGGGCCGAGCCTTAGAGAAGTCACACTTCTGTT  
TTCTGCAAGTCTCGTGTCAAGGAGCCTTGAGGTATGAATCACCATATTGGAGATCCCTGCGACACACGCAATTGAGTGA  
AGATACAGGAAGAAACGTCAAAATCGCGTCATTGTCATTATCAGGTTGA

### *L. japonicus* CNGC4 Putative Protein Sequence

MASSENNEHPTLLETEEQSYGEPLHTRFQRLASNTQSASCISIESYEKETSLVKQRSGTGNLLQOSICLTGNKPEESNTGSIYSKNDYD  
RNNEKLLRSRQVGCNCDFCFTTYATNSKASHSOLVPKASTISDSKFHNAYGDAKGAFARNHNSFYSYPGVMNPFHTKFIQQWNKVLAIFC  
LVAIFVDPLFFFLLYVQDRFNClAINWRLTKALVIIRSINDFIYFFNVLQFRLAYSPESRVVGAGDLVDPKKAIALHYLKGYFFIDLF  
IVFPLPQIMLLVLVLPESMRGANYAKNLLRAVILVQYIPRLFRFLPLLIGQSPSTGFIFESAWANFIINLLIYMLASHVVGSCWYFLGLQRV  
NQCFRNACHSSVPGCLRFIDCGIDHDRNYLQGPKSEQWNNTDAIACWGSPTGSTSLDYGIYGNAPLTTKDMVTKYVFSLFWGFFQOIS  
TLAGNLTPSNFVWEVLFTMATIGLGLLFLALLIGNMONFLQGLGRRRQEMLRRRDFEOWMRYRRLPEDLRRRVROAERYTWAATRGVNE  
EMLMVNLPELDLQRDIIRHLFKFVKKVRLFSLMDEPIldaicerlkqattyiqgsrvlnkgglvekmvfvargklesigedgt  
CGEELLTWYEHSSVSTDGKKIKLPGQGLLSSRTIKCLTNVEAFSLRAIDLREVTLLFTRFLHSPRVQGALRYESPYWRS  
RYRKKRQNRRAHSSLG

## L. japonicus CNGC5 Genomic Sequence

## APPENDIX

GTTGAACTGTGGTCCGGATAAGAGTATATGGTGTGCGGAAATATTAAATTAGAGGAATGGAAAAGACAACGTGAACTACTTGC  
TACCTTGATCTTATGAACCTGTGATACTATGTCACAAATTGTCAGGCTCAACAGGCTGAAATCTAACAGCACATGAAT  
CATTTATAGCTCTAACAAATATGTTCTTGTGATCTTCATACAGCAAATCAGTAATCTAGCTGGAAATCTAACAGCACATGAAT  
GGAGATCCTTTTACTATGTCATGGGATTGGGACTCTGGCTTTTGCACATTCTCATGGAAACATACAGAACATTCTCACAGGCTCT  
TGGCGGAGGAGTAGAACTAACCTAATGTCAGGAGTTTTAAATTAAACATTGTCAGTGTGCAACTTGTGATGTTTATTGGTCAATATG  
TGTGATATTAACTTCTATCCCTTACAGGAAGCTGGAAATGCAACTTAGAGCTGTGATGTTGACCATGGATGAGGCCATCGGGCCT  
TACCACTAGACCTGAGAAGGTAAAAATTCCCATTCTCTCATGACTCATATCCACAGTCACAAAGCATGTCAACTGCTGATCTCAA  
GTCATTGGTTGTCACCTCCCACCCCTCCAGAACCTGTTATTGACATTATACATAGTCTCTGTGATGGGCAATTACTGATCCG  
AGACACAAAGTTCTGTTTGATGACTTGCTAACAAATTAGCAGCTCTGAAGAATATTAAATTAAAGAGGCATAGGGATGATTG  
GAATTCTTTTCTATGTCCCCCAAATATGTTCTGGTTTTGTGATTTAAATATAATTAAACTACTGTGATATTGTTGATGCA  
TAATCTGCAAAATATGTAATTGATATTCTCAGCATATCTCTCATCTAATGGGAGTGGTATACAAACAGTGATATTACATA  
AAAGGAAAACGTTTAAATTCTACCACCTGGTAGCTCTCCAGGCACTCTAGTCTCCATTAAATTAACTCTGTGACATATACG  
GTGCATTTTTAATCTGTGTCATATACTCATGTCTTAAATCATAGTATACGATGCACTTTAAATTGAGATTCTTAATCTAGTCT  
CCATATATGAGGAACACTCTTCTTATAGCATGTCGTAGGCCTCAAAGCTAACAGCTGCACTGTATATTGTCATTT  
TTAGTCATTGATCACATTGATCATACATTGTCACAGTAATAGATAATATGTCATGCAAGGAGAGTAAGACAGGCTG  
AACGGTAAATTGGGCTGCAACAAGGGGGGTGAATGAAGAAATGGTTATGGAGAATCTGCAGAGATCTGCAGAGAGACATTAGACGCC  
ATCTCTTCAGATTGTTAGGAAGTATGTCATACATCTGCAACTAAATGACTTAATTAATTACAAACATTGTCATGTTACACCTTA  
AGTAGATTAAATCATGTTGTTAGATGCTAGATAAGCTTCAAGGCAATCTCAGTCACCATGGTCACTTAAGATTGGTTTCTTAGGTCT  
CTACTTGTAAACCTTCTAGACTGAGTAGAAGTTAAATGTAACATTCTTGAAGGAAATCTTAATGTCATCTTCATCATGAGTTAAA  
CCATGATATATGAAAGGCCAAAGTATGTCACAGCATTCTGAAACTTCTGTAATGATGATATGATTTAACCTGCGTGTA  
TACCTCATACAAATTATGTCCTTAATCCAAAGATCTAAATTATCTGCAGATTGCAATTTCCTGATGGATGTGCCCATCTAGACG  
CTGTAATGAGAGACTAACAGACAAAACATACATTAAGGAACCTAAAGGAACTAAATTGAGTCAGGGCAGTTGATAGAGAAGATGTT  
TGGCGGAAAATTGGAGAGCATTGGAGAGGATGGAACCTAGAATGCCATTATCTGAGGGGAGCCTGTGTTGAGAAGAACATTGACATGGT  
ATCTGACACATTCTCTGTAAGCTCAGTATAACAAACTCTGTCACAGCAGGATGCTGTTTCAACATATTAAATTGCAATA  
GTCAGCAACTTGGGCACTGCAAATAAGCAACAGCATGGTCATTGATTCAATCTGGTGCAAGATGTTAGAAAAGTAAGGCTTCTGG  
CAGAGGTTGGTTAGCAACAGGACAGTAAAGTGTGACAAATGTGGAGGCATTTCACTCTGCGCCGACCTTGAAGAAGTCACGATA  
CTTTCAACAGATTCTGGGAGCCCTCAGGTCAAAGGAGCTTAAGGTAATTCTTATCTACTATCAGTATTAGGGTTCAGCATA  
AATAAAAAATGAAAATAAGCAACACAGAACATAATACCTGCAACACTTTTATATTCAAAATTCTCACAGATGGTAACATTGGTCAGC  
TATAACTCTTGTGAATGTTCTGTGATGAGGTTCACTTGGGATTCAGTGAAGAAGTTGTGCTATTGTTATCTTACATTGATATTAAACCA  
CTAATATCTTAAAGATGTTGAGATTTCAGCAGTCAAAGCTTAATTGTTGATATTCTAGTGGCCACATGTTCAATTGATAATTG  
GTGTTTTAGGATTAAGATGCCATTGGAGATCCTGGCCGAAACCGCATTCAAGTGTGATGGAGATATAGACAGAACGCTGAGTC  
GTGTTAATTCTCAGTAACAACTAACATTGTA

## L. japonicus CNGC5 Putative Coding Sequence

## L. japonicus CNGC5 Putative Protein Sequence

MANFKNDEVPMILAETKARARPGDGFPSKFQRLVTRTQSASTISVPLSSMEQEYEGDTSVIRHTGPLQSQRNAPLQMOSGPLKATPGTANL  
LQQHIIIGIGNRAEERKTENFAFRSTGPNYWDNNHDRKNEHLLRSGQLGMCNDPYCTTCPTYFNASQQRKPKPSTIFDHKFHNVLGYDAK  
GFARKLYLFCCSYFPGVNMNPHTKV1QQWNKFLAIFCLIAIFVDPFLFFFLLYVQDYKCIVINWAMTIGLVLRSINDFVYLLNIFLQFKL  
AYVSPESTVVAGDLVDPHKPRIARHYLRGYFLIDLIVFVPLQOIMILTVLPNTLWGANCHAKNLLRAAILOVOYIPKLFRFLPILLIGOSPTG  
FIFESARANFVINLLIFMLASHVVGSCWYLFGQLQRVNQCLRDAKSNTICGMKFIDCGRGRGLNGNTSNQWKNNNTDAINCNPSSDGFF  
PYGIYELAVPLTIEVNVNKYVYSLFWGFFQOISTIAGNQVPSVFVWEVLFMTMSIMGLGLLLFAILIGNIQNFLQALGRRKLEMQLRGDRV  
EQWMSSHRLRPLVDRRRVQAERYNWAATGVNEEMVMNLPEDLQRDIRRHLFRFVKEIRIFSLMDVPILDACERLQRQTYIKGSKILS  
OGSLLIEKMFVVRGKLESIGEDGTRMLPSEGADCCEELMTWYLEHSSVSSEDRGKVRLLPGQRLVSNRTVKCLTNVEAFSLAADLEEVTL  
FTRFLRSPQVOGALRYESPYWRSLAANRIOVAWRYROKRLSRVNSSVTTH

## 9.2 List of Figures

Figure 1. AM development.	4
Figure 2. Common SYM signalling pathway.	7
Figure 3. Overview of <i>Lotus</i> TILLING populations and SL lines analyzed during the AM screen.	11
Figure 4. Schematic overview of AM development.	12
Figure 5. Venn diagram illustrating quantities of putative AM mutant lines.	13
Figure 6. AM phenotypes of putative mutants.	15
Figure 7. Genomic, cDNA and protein domain structures of the <i>L. japonicus</i> CPK29 variants.	20
Figure 8. Restriction analysis of cloned 5'-RACE products.	21
Figure 9. Amino acid alignment of CPK29a and CPK29b of <i>L. japonicus</i> .	21
Figure 10. Expression patterns of Lj CPK29 versions by promoter-GUS fusions.	22
Figure 11. Subcellular localization of Lj CPK29a and Lj CPK29b in <i>N. benthamiana</i> leaves.	23
Figure 12. <i>M. truncatula</i> CPK29 gene structure.	24
Figure 13. Agarose gel fluorography visualizing Mt CPK29 variants amplified from cDNA.	24
Figure 14. Multiple Sequence Alignment of legume and <i>A. thaliana</i> CPK29 protein sequences.	26
Figure 15. Phylogenetic tree of the CPK29 cluster.	28
Figure 16. Phylogenetic tree of CPKs.	28
Figure 17. Schematic domain structure of plant CNGCs.	32
Figure 18. Wild-type and <i>brush</i> plants after early temperature shifts.	34
Figure 19. Root and shoot lengths and nodulation phenotypes after early temperature shifts of wild-type and <i>brush</i> seedlings.	35
Figure 20. Nodulation phenotypes of wild-type and <i>brush</i> roots.	36
Figure 21. Plant growth and infection threads of wild-type and <i>brush</i> plants after temperature shift two weeks post germination.	37
Figure 22. Wild type-like roots of <i>brush</i> mutants.	38
Figure 23. Infection threads of wild type-like <i>brush</i> roots.	38
Figure 24. Nodulation phenotype of wild type-like <i>brush</i> roots.	39
Figure 25. SSR mapping marker positions on contigs of <i>L. japonicus</i> chromosome 2.	40
Figure 26. F2 genotypes and corresponding F3 progeny phenotypes.	41
Figure 27. Fine mapping of <i>brush</i> .	42
Figure 28. Annotations of candidate genes and positions of SSR and SNP markers between G179 and G173 on CM0435.	43
Figure 29. F4 plants grown at 18°C and 26°C.	44
Figure 30. Diagram showing percentages of F4 phenotypic categories at 18°C and 26°C.	45
Figure 31. Chart of root lengths of F4 plants grown at 18°C and 26°C.	45
Figure 32. Phenotypes of F5 plants and their corresponding genotypes.	47
Figure 33. Phenotypes of <i>brush</i> backcross progenies.	48
Figure 34. Root systems of <i>brush</i> backcross mutants resembled the <i>brush</i> root phenotype.	49
Figure 35. Analysis of nodulation and root lengths of <i>brush</i> and <i>brush</i> backcross mutants.	50

Figure 36. Illustration of the gene structure of <i>CNGC1</i> .....	51
Figure 37. Hairy-roots of <i>brush</i> mutants transformed with <i>CNGC1</i> .....	52
Figure 38. White bumps of brush hairy roots after attempted complementation with <i>CNGC1</i> .....	53
Figure 39. The <i>L. japonicus</i> CNGC1 amino acid sequence in comparison to CNGC1 sequences in the analyzed SL lines and the <i>Arabidopsis</i> CNGC19 and CNGC20. ....	55
Figure 40. Expression patterns of <i>CNGC1</i> in roots and nodules visualized by <i>ProCNGC1-GUS</i> staining. ....	56
Figure 41. Alignment of amino acid sequences of the five CNGCs. ....	57
Figure 42. Phylogenetic tree showing the five CNGC clusters of <i>A. thaliana</i> with the identified <i>L. japonicus</i> and <i>M. truncatula</i> CNGCs. ....	59
Figure 43. Model for the evolution of CPK29 with two alternative first exons. ....	65

### 9.3 List of Tables

Table 1. Summary of putative M3 AM mutant lines.....	15
Table 2. Overview of phenotypes of F3 plants and their F4 progeny.....	44
Table 3. EMS-induced mutations of <i>CNGC1</i> TILLING lines and their nodulation ability.....	54
Table 4. Nodule number and genotype of SL1484-1 individuals.....	54

## Acknowledgements

I would like to express my sincere gratitude to my PhD supervisor Prof. Martin Parniske for giving me the opportunity to conduct my PhD thesis in his lab and for fruitful discussions, support and constructive advice.

Many thanks go to all former and present members of the 3<sup>rd</sup> floor Genetics and especially the Parniske lab for creating an inspiring and cooperative working environment.

I would like to say thank you to Meritxell Antolín Llovera, Aline Banhara Pereira, Andreas Binder, Joana Bittencourt Silvestre, Myriam Charpentier, Ana Cosme, Griet Den Herder, Matthias Ellerbeck, Martin Groth, Simone Hardel, Stefanie Kiebart, Regina Kühner, Jayne Lambert, Makoto Maekawa-Yoshikawa, Katharina Markmann, Martina Ried, Sylvia Singh, Naoya Takeda and Katalin Tóth for useful discussions, help at any time and having a good time in the office and in the lab.

I am grateful to Axel Strauß for his help with the statistics and to Andreas Brachmann for his collaboration in the sequencing and mapping projects.

My kind thanks are due to  
Johanna, Birgit, Carina, Helena, Martina, Sarah and Vera  
for the long-lasting and cordial friendship.

I warmly thank my parents, Karin and Hermann, my sister Julia  
as well as my whole family for their loving encouragement.

And last but not least: thank you, Jürgen, for your love and support!

## Curriculum Vitae

KRISTINA HAAGE

### **Personal Data**

Date of birth                    1980  
Place of birth                    Ulm

### **Higher Education**

1999 – 2001                    Grundstudium Biologie/Diplom, Universität Konstanz  
2001 – 2005                    Hauptstudium Biologie/Diplom, Technische Universität München  
                                    Major Subject: Genetics. Minor Subjects: Botany and Bioinformatics  
March 2005                    Diplom Biologie  
Nov. 2005 – present           PhD student at the Ludwig-Maximilians-Universität München, Institute of  
                                    Genetics of the Faculty of Biology, in the lab of Prof. Dr. Martin Parniske.  
                                    Title: The *Lotus japonicus* Temperature-Sensitive Root Development and  
                                    Nodulation Mutant *brush*.

**Peer-reviewed Publications**

Takeda, N., Haage, K., Sato, S., Tabata, S., and Parniske, M. (2011). Activation of a *Lotus japonicus* subtilase gene during arbuscular mycorrhiza is dependent on the common symbiosis genes and two cis-active promoter regions. *Molecular Plant-Microbe Interactions* **24**, 662-670.

Perry, J., Brachmann, A., Welham, T., Binder, A., Charpentier, M., Groth, M., Haage, K., Markmann, K., Wang, T.L., and Parniske, M. (2009). TILLING in *Lotus japonicus* identified large allelic series for symbiosis genes and revealed a bias in functionally defective ethyl methanesulfonate alleles toward glycine replacements. *Plant Physiology* **151**, 1281-1291.

Yu, Z., Haage, K., Streit, V.E., Gierl, A., and Ruiz, R.A. (2009). A large number of tetraploid *Arabidopsis thaliana* lines, generated by a rapid strategy, reveal high stability of neo-tetraploids during consecutive generations. *Theor Appl Genet* **118**, 1107-1119.

**Review Article**

Haage, K., Groth, M., Kosuta, S., and Parniske, M. (2007). Arbuscular mycorrhiza mutants in *Lotus japonicus*. In 13<sup>th</sup> International Congress on MPMI (Sorrento, Italy).